Strengthening Mechanism and Bio-degradability of a Silk-based Polymer Composite

By

Mei-Po Ho

Supervised by

Prof. Alan Kin-Tak Lau

Assoc. Prof. Hao Wang

A dissertation submitted for the award of

DOCTOR OF PHILOSOPHY

Centre of Excellence in Engineered Fibre Composites
Faculty of Engineering and Surveying University of
Southern Queensland Toowoomba, Queensland,
Australia
February 2012

Certification of Dissertation

I certify that the ideas, experimental works, results, analysis and conclusion reported in this dissertation are entirely my own effort, except where otherwise acknowledged. I also certify that the work is original and has not been previously submitted for any award, except where otherwise acknowledged.
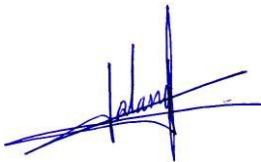
22/2/2012

_____   _____

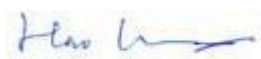Signature of Candidate   Date

Endorsement:

22/2/2012

_____   _____

Signature of Chief Supervisor   Date

22/2/2012

_____   _____

Signature of Supervisor   Date

Abstract

Silkworm silk fibre is one kind of well recognized animal fibres for bio-medical engineering and surgical operation applications because of its mechanical, biocompatible and bio-resorbable properties. Recently, the use of natural fibre as reinforcement for bio-polymers to enhance the stiffnesses of scaffolds and bone fixators has been a hot research topic. However, their mechanical and biodegradable properties have not yet been fully understood by many researchers, scientists and bio-medical engineers although these properties would govern the usefulness of resultant products.

Considering the increasing demand and potential use of biodegradable and bioresorbable polymers in coming centuries, elevated environmental awareness of the general public in reducing carbon footprints and non-naturally decomposed solid waste, as well as foreseeable drawbacks of using metallic materials for biomedical engineering, a comprehensive study on the mechanical and materials properties of a silkworm silk fibre reinforced Polylactic acid (PLA) composite is conducted through experimental and theoretical approaches in this project.

Current study aims at investigating various properties of degummed and non-degummed silkworm silk fibres and, the effect on the mechanical and thermal properties and biodegradability of their reinforced PLA composites.

An extensive review is provided to introduce the properties of the natural fibres and degradable polymers. Some critical issues including poor wettability, biodegradability and bonding properties at the fibre/matrix interface and, damage of the fibre during the manufacturing processes which are the main causes of the

reduction of the composites" strength are addressed. Furthermore, different manufacturing processes and their suitability for natural fibre composites, based on the materials, mechanical and thermal properties of the fibres and matrics are discussed in detail. The potential applications on the degradable fibre reinforced polymer composites are also addressed.

Following the comprehensive review, results obtained from preliminary experimental studies are given. The hybridization of a glass fibre reinforced composite is achieved by using short silkworm silk fibre as a medium to enhance its cross-ply strength. The comparison on the tensile and impact properties of the glass fibre composite reinforced by the short silkworm silk fibre with a neat glass fibre composite sample is conducted. Experimental results indicated that the higher Young"s modulus and ductility index (DI) of a silkworm silk fibre reinforced glass fibre composite was obtained as compared with the neat sample. Moreover, the visual examination on drop-weight test samples proved that the impact resistance of the silkworm silk fibre reinforced glass fibre composite was better than that of the neat sample as well. Nevertheless, as the non-fully biodegradable issue rose from the ultilization of glass fabrics and resin, the combination of the silkworm silk fibre and a biodegradable polymer- PLA is chosen for the following study.

Mechanical properties of different silkworm silk fibres including Bombyx mori, twisted Bombyx mori, and Tussah silk fibres were investigated. Their ultimate tensile strength, elongation at break, and Young"s modulus were examined by performing a uniaxial tensile test on a single fibre. The apparent diameters of the silkworm silk fibres were measured for stress-strain analysis. Based on the

experimental results, it was found that Tussah silk fibre has a relatively high extensibility as compared to Bombyx mori silk fibre.

When producing a biodegradable silkworm silk fibre reinforced PLA composite, hydrophilic sericin has been found to cause poor interfacial bonding with most polymers and thus, it results in affecting the resultant properties of the composite. Besides, a sericin layer on fibrils surface may also cause an adverse effect toward biocompatibility and hypersensitivity to silkworm silk fibre for implant applications. Therefore, degumming should be done for sericin removal. Different degumming processes and their influences on silkworm silk fibre are discussed. The effectivenesses of degumming parameters including degumming time and temperature on Tussah silk by using boilibg water are discussed. Based on the results obtained, it was found that the mechanical properties of Tussah silk are affected by the degumming time due to the change of fibre structure and fibrils alignment. It was also found that the degumming time has a little effect on the thermal properties and the secondary structure of the fibre.

Besides, silkworm silk fibre was degummed by different concentrations of $NaHCO_3$ (Sodium Bicarbonate) solution to study its tensile properties. Measurement of weight loss, tensile property test and differential scanning calorimetric (DSC) analysis were conducted to elucidate the effect of $NaHCO_3$ to the fibre. Experimental results revealed that the disruption of hydrogen bonds (water effect) dominated the effect of the fibre at low $NaHCO_3$ concentration. Increasing the concentration of $NaHCO_3$ resulted in increasing the pH level and thus, distorted the binding force between fibrils of the fibre. DSC analysis revealed that the fibre degummed in the solution over 5 wt% $NaHCO_3$ requires

higher energy for melt and thermal decomposition from their crystalline states. However, using NaHCO$_3$ would minimize the risk of damage of silkworm silk fibrils as compared with commonly used strong alkali solutions for degumming. A microbond test of the composite was conducted to investigate the bonding effect of the silkworm silk fibre with/ without the sericin layer. The results showed that the fibres degummed by both processes increased the interfacial shear strength.

A novel biodegradable composite for biomedical engineering applications was developed by mixing chopped silkworm silk fibre and PLA through the injection moulding process. A study on the mechanical properties and biodegradability of a silkworm silk fibre reinforced PLA composite was conducted. It was found that the Young‟s and flexural moduli of the composite increased with the use of silkworm silk fibre as reinforcement while their tensile and flexural strengths decreased. This phenomenon is attributed to the disruption of inter- and intra-molecular bonding on the silkworm silk fibre with PLA during the mixing process, and consequent reduction of the strength of the composite.

Bio-degradability tests showed that the silkworm silk fibre altered the biodegradable properties of the composite as compared with a pristine PLA sample. The initial storage modulus of the composite increased while its glass transition temperature decreased as compared with the PLA sample. Besides, the coefficient of linear thermal expansions (CLTE) of the composite was reduced by 28%. This phenomenon was attributed to the fibre-matrix interaction that restricted the mobility of polymer chains to adhere to the fibre surface, and consequently reduced the Tg and CLTE. As compared with the composite, it was found that the degraded composite exhibited lower initial storage modulus, loss

modulus and tan delta (Tan(δ)) but the Tg had higher than that of a non-dergraded sample.

A linear, elastic and isotropic theoretical model to evaluate the differential stress between a core fibre and a sericin layer with different thicknesses of the layer is firstly introduced in this report. The influence of moisture absorption during the early degradation stage, on shear stress between the fibre and the sericin is also discussed.

Finally, concluding remarks and the suggestions for the further study in the development of the silkworm silk fibre reinforced PLA composite for fracture bone fixator are addressed.

Acknowledgement

Foremost, thank God almighty for His mercies and grace throughout my life, "*I can do everything through him who gives me strength.*" (Philippians 4: 13). Thanks for my fellow brothers and sisters in Christ for their endless support and encouragement. The contributions of many people in different ways have made the completion of my PhD study. Please accept my regards and blessings to all of those who supported me in any respect, especially to the following.

I am deeply grateful to my chief supervisor, Prof. Alan Kin-Tak Lau for enlightening me the first glance of research. I would like to offer my sincerest gratitude to his excellence guidance, encouragement and especially patience assisted me from the initial to the final stage of my PhD"s life. I could not have had a better and friendlier supervisor. Thanks Alan!

I am indebted to Prof. Hao Wang, my associate supervisor who motivates and guides me through the difficulties. I would like to express my thankyou for his extensive discussion of my research and great support in all stages of my stay in the Toowoomba.

Besides, I would like to express my warm thankyou to Prof. Debes Bhattacharyya, his broad-minded thinking have expanded and inspired my research. His insightful comments have been very helpful for this study.

Last but not least, I would like to thanks my family: my dearest parents, my lovely sisters and brother, for their unconditional support throughout my life. Their patient love has enabled me to complete my PhD

Publications

I. Publications arising from the thesis

International Journals

1. **Ho MP**, Wang, H., Chung, Y.W. and Lau, K.T. (2012). Tensile and thermal properties of $NaHCO_3$ treated silk fibres. Fibers and Polymers. Submitted.

2. **Ho, M.P.**, Wang, H., and Lau, K.T. (2012). Effect of silk fibre to the mechanical and thermal properties of its bio-degradable composites. Applied Polymer Science. Accepted.

3. **Ho, M.P.**, Wang, H., and Lau, K.T. (2012). Interfacial bonding and degumming effects on silk fibre/polymer biocomposites. Composites Part B: Engineering. Accepted.

4. **Ho, M.P.**, Wang, H. and Lau, K.T. (2012). Effect of degumming time on silkworm silk fibre for biodegradable polymer composites. Applied Surface Science, 258, 3948-3955.

5. **Ho, M.P.** and Lau, K.T. (2011). Design of an impact resistant glass fibre/epoxy composites using short silk fibres. Materials and Design, 35, 664–669.

6. Lau, K.T. and **Ho, M.P.** (2011). Recent Research Trend in Natural-fibre Composites. JEC Composites Magazine, 67, 6-7.

7. **Ho, M.P.**, Wang, H., Lee, J.H., Ho, C.K. and Lau, K.T. (2011). Critical Factors on Manufacturing Processes of Natural Fibre Composites. Composites Part B, Available online 15 October 2011.

8. **Ho, M.P.**, Lau, K.T. and Wang, H., Bhattacharyya, D. (2011). Characteristics of a Silk Fibre Reinforced Biodegradable Plastic. Composites: Part B, 42, 117–122.

9. Lau, K.T., **Ho, M.P.**, Au-Yeung, C.T. and Cheung, H.Y. (2010) Biocomposites: their Multi-functionality. International Journal of Smart and Nano Materials, 1(1), 13–27.

10. Cheung, H.Y., Lau, K.T., **Ho, M.P.** and Mosallam, A. (2009). Study on the Mechanical Properties of Different Silkworm Silk Fibers. Journal of Composites Material, 43(22), 2521-2531.

11. Cheung, H.Y., **Ho, M.P.**, Lau, K.T., Cardona, F. and Hui, D. (2009). Natural Fibre-reinforced Composites for Bioengineering and Environmental Engineering Applications. Composites: Part B, 40, 655–663.

II. Publications arising from other research projects

International Journals

12. Chan, M.L., Lau, K.T., Wong, T.T., **Ho, M.P.** and Hui, D. (2011). Mechanism of Reinforcement in a Nanoclay/ polymer Composites. Composites Part B: Engineering, 42(6), 1708-1712.

13. Chan, M.L., Lau, K.T., **Ho, M.P.**, Cheng, A. and Wong, T.T. (2008). New Equipment and Approaches for Fabrication of uniformly-Dispersed Nanoclay Cluster/Epoxy Composites. Polymers and Polymer Composites, **16**, 555-559.

14. Chan, M.L., Lau, K.T., **Ho, M.P.**, (2008). Preliminary Study on a High Strength Nanoclay/Epoxy Coating for Ocean Engineering Applications. Advanced Materials Research, 47 – 50, 1217-1220.

Conferences

15. **Ho, M.P.**, Wang, H. and Lau, K.T. (2012). Thermal Properties and structure conformation on silkworm silk fibre. Australia"s Composites Conference 2012.

16. **Ho, M.P.**, Lau, K.T. and Wang, H. (2011). Effect of Degumming on Tussah silk Fibre. Proceeding of the 19th International Conference on Composite Materials. M13-6-AF2055.

17. **Ho, M.P.**, Lau, K.T., Wang, H., Bhattacharyya, D. (2011). Mechanical Properties of an Injected Silk Fibre Reinforced PLA Composite. Processing and Fabrication of Advanced Materials XIX, 885-894.

18. **Ho, M.P.**, Wang, H., Ho, C.K. and Lau, K.T. (2011). A Study on the Dynamic Mechanical Properties of Silk Fibre Composites. The 20th International Symposium on Processing and Fabrication of Advanced Materials (PFAM XX).

III. Awards and Honors

1. The Best Paper Award in the 20th International Symposium on Processing and Fabrication of Advanced Materials (PFAM XX) 2011.

2. Research Awards for Graduate Research Excellence 2011.

3. The Best Paper Award in the 3rd International Conference on Multifunctional Materials and Structures (MFMS 2010).

Table of Contents

CHAPTER 1 INTRODUCTION

CHAPTER 2 LITERATURE REVIEW

CHAPTER 3 PRELIMINARY STUDY

CHAPTER 4 PROPERTIES OF DOMESTIC AND WILD SILKWORM SILK FIBRES

CHAPTER 5 EFFECT OF DEGUMMING ON SILKWORM SILK FIBRE

CHAPTER 6   PROPERTIES OF A SILKWORM SILK FIBRE REINFORCED PLA COMPOSITE

CHAPTER 7   THEORETICAL ANALYSIS

CHAPTER 8   CONCLUDING REMARKS AND SUGGESTIONS FOR FUTURE STUDY

APPENDICES

List of Figures

Chapter 4

Chapter 6

Chapter 7

List of Tables

Chapter 6

Chapter 1

Introduction

1.1 Research Background and Significance

Degradable polymers are generally believed as substances that will decompose in a natural environment. However, a case of lawsuits between October 1990 and June 1992 regarding misleading and deceitful environmental advertising using the term "biodegradable" raised the discussion and necessitated claiming of the term (Narayan & Pettigrew 1999). Besides, the industries need the tools to ensure the credibility of claims for current and future generations of degradable polymer. Thus, there is a need in the society of evident to the American Society for Testing of Materials (ASTM) and International Standards Organization (ISO) that common test methods and protocols for degradable polymers. The ASTM and ISO define degradable plastics as "a plastic designed to undergo a significant change in its chemical structure under specific environmental conditions resulting in a loss of some properties that may vary as measured by standard test methods appropriate to the plastic and the application in a period of time that determines its classification" (Narayan & Pettigrew 1999). The standards measure biodegradability under different environmental/disposal conditions which plastic

may also be designated as photodegradable, oxidatively degradable, hydrolytically degradable, or those which may be composted. In particular, biodegradable plastic materials are of interest for the use in packaging, agriculture, medicine, and other areas. The ASTM and ISO define biodegradable plastics as "a degradable plastic in which the degradation results from the action of naturally-occurring micro-organisms such as bacteria, fungi and algae" (Narayan & Pettigrew 1999).

Recently, biodegradable polymers have continued attracting attention worldwide. Within the period of 2005 and 2009, the global market for the demand of biodegradable polymers was doubled in size. The total consumption of this type of polymers has been forecasted to grow at an average annual rate of nearly 13% from 2009 to 2014 in the major global markets for materials" consumption. Among all countries in the world in 2009, Europe had the largest growth in the range of 5 to 10% on the use of biodegradable polymers as compared with 2008. The trend of this growth has been continuing. North American consumption of biodegradable polymers has grown significantly in recent years. In Japan, there has been some growth in biodegradable polymers use as a result of the promotion from the government and the industry. In China, high growth is due to an increase in production capacity. In other Asian countries, the demand on biodegradable polymers is expected to increase greatly in the next several years (Mohan 2010).

Biodegradable composites are generally believed as one of the key materials in coming centuries. They are generally composed of biodegradable fibre and biodegradable polymer, and manufactured by various processes. Their properties can be tailor-made to satisfy varied product requirements for specific applications. Major applications for biodegradable composites are for disposable product, bio-

engineering and tissue engineering applications.

1.1.1 Environmental Concern

Petroleum is a fossil fuel which is estimated to last for another 50–60 years at the current rate of consumption. Preservation of non-renewable petroleum-based materials especial for petroleum-based polymers is a critical topic because of the increasing environmental consciousness in the society. The advantages including more cost-competitive with petroleum-based products and the reduction of greenhouse gas emissions motivate using biodegradable polymers nowadays. Besides, an excessive use of petroleum-based polymers inducing a huge amount of solid waste disposals causes to a serious depletion of landfill capacities. The severe government"s plastic waste control legislation and the growing interest among the customers in sustainable and environmentally friendly products drive the retailers and manufacturing companies to trend towards developing more sustainable materials for alleviating the impact of global warming. Therefore, the awareness of increased waste problems and their impact on the environment has awakened a new interest in the area of developing degradable polymers. In order to solve the crises of resource and environment, different types of fully biodegradable composites are being developed recently, as substitutions for non-biodegradable petroleum-based plastics, and even metallic components.

1.1.2   Engineering Concern

Bio-engineering is usually defined as a basic research-oriented activity closely related to biotechnology and genetic engineering which are used for the modification of animal or plant cells, or parts of cells, to restore their function or repair their damage regions, or to develop new microorganisms for beneficial ends (Bronzino 1999). Concerning the implementation of technology in bio-engineering, biomaterials are mainly used in the applications of directing, supplementing, or replacing the functions of living tissues in the human body (Black 2006).

The term of "Bio-composite" is a new and advanced bio-material and being used for bone repairs and implant development recently as a replacement for traditional metallic materials such as stainless steel and titanium. Although stainless steel and titanium provide sufficient strength and rigidity to align the bone and control motion while healing of bone fracture, they are too stiff as compared with the properties of nature bone. The Young"s modulus of steel typically falls into the range of 100 to 200 GPa while the bone is only 6 to 20 GPa. Therefore, metallic implant plate carries the majority of load which leads to that stress-shielded once delay bridging. Moreover, the incompletely healed bone is susceptible to refracture after the removal of a metallic implant plate. This weaken bone also suffers serious bone loss (osteoporosis) including intracortical porosity, cortical thinning and correspondingly greater loss of mechanical properties (Flahiff, Blackwell & Hollis 1996; Claes 1989). The need of the second surgery for removing a metallic fixator, corrosion of the fixator inside the human body and bone atrophy associated with rigid metallic fixation devices increase the probably

of bone infection (Burns & Varin 1998). Moreover, the postoperative radiotherapy as well as X-ray for diagnostic imaging on healing bone is interfered by the metallic implant plate. It is because the presence of metallic plates changes the local dose distribution and these changes result from backscattering effects which cause the overdosage in front of and underdosage behind the plates (Tams, Rozema & Bos 1996). To overcome the disadvantages of using traditional metallic bone implant plates, silkworm silk fibre reinforced polylactic acid (PLA) composites, based on their inherent mechanical, biocompatible and bioresorable properties have found to be a desirable versatile bio-material for bone implant plate.

Silkworm silk fibres as sutures for human wound dressing have been used for centuries (Wang 2008). Recently, regenerated silk solutions have been used to form a variety of biomaterials, such as gels, sponges and films, for medical applications (Vepari & Kaplan 2007). Silkworm silk fibre has also been exploited as a scaffold biomaterial for cell culture and tissue engineering in vitro and in vivo (Wang 2006). However, this topic is in need of further study and clarification as no thorough study, particularly on the correlation between the properties such as thermal properties, mechanical properties, and degradation properties of the silkworm silk fibre and its reinforced PLA composites have been conducted to date.

1.2 Objectives

Considering the increasing demand and potential use of biodegradable and bioresorbable polymers in coming centuries, as well as foreseeable drawbacks of using metallic materials for bone plate development, a comprehensive study on the mechanical and materials properties of a silkworm silk fibre reinforced PLA composite is conducted through experimental and theoretical approaches in this project. The objectives of this project are:

1. To develop a methodology for producing a silkworm silk fibre reinforced PLA composite;

2. To in-depth study the influence on the mechanical properties of the silkworm silk fibre degummed by different degumming solutions and

3. To investigate and validate the bio-degradation, mechanical properties and thermal properties of the composite.

This research project aims at contributing a novel concept of using a biodegradable silkworm silk fibre reinforced PLA composite for the target of fracture bone repair. In this report, a literature review on recent research related to bone fracture and bone repair methods is firstly addressed. An elaborate discussion on existing methods for bone repair and material selections is also discussed. Natural fibre including plant-based fibre and animal-based fibre is a hot topic for industries and bio-medical applications. Their properties and characteristics are addressed and compared too. A preliminary study focuses on using silkworm silk fibre as interlaminar reinforcement. According to the groundwork analysis of the natural fibre and biodegradable composites

applications, detailed studies including mechanical properties and thermal properties of the degummed silkworm silk fibre were undertaken. Further studies including mechanical, thermal and biodegradability and the fracture surface analysis of the silkworm silk fibre reinforced PLA composite are under investigated. Last but not least, a conclusion and discussion about the silkworm silk fibre reinforced PLA composite is proposed.

1.3 Scope of Thesis

This project focuses on the study of the mechanical and thermal behaviours of a silkworm silk fibre reinforced PLA composite and investigates its potential for bone fixation. Several topics are included in this report:

- Review on the requirement for the development of bone fixator by using biodegradable polymers;

- Feasibility study on the use of silkworm silk fibre as interlaminar reinforcement for a glass fibre reinforced composite;

- Characterizations and material properties of silkworm silk fibre;

- Properties and failure mechanisms of degummed silkworm silk fibre;

- Mechanical performance and biodegradability of a silkworm silk fibre reinforced PLA composite.

1.4 Outline of Thesis

This thesis is divided into 8 chapters, which are described as below:

- Chapter 1 is an introduction sesction which provides the background, objectives and scope of this study;

- Chapter 2 provides an overview on the bone fracture and healing techniques. Besides, the properties of natural fibres, degradable polymers and their composites are addressed. A review on the manufacturing processes of the composites including the importance of pre-treatment processes of raw materials and intrinsic challenges on natural fibre for manufacturing are conducted;

- Chapter 3 is the preliminary study on the mechanical properties of the silkworm silk fibre reinforced glass fibre composite. Silkworm silk fibre was used as interlaminar reinforcement to eliminate the risk of delamination of the glass fibre composite;

- Chapter 4 studies the properties of Bombyx mori, twisted Bombyx mori and Tussah silk fibre;

- Chapter 5 discusses the mechanical, thermal and interfacial bonding properties of silkworm silk fibre degummed by different methods;

- Chapter 6 characterizes the mechanical and thermal behaviours of the silkworm silk reinforced PLA composite. A comprehensive investigation including in vitro degradation, mechanical, dynamic mechanical and

thermal properties are discussed;

- Chapter 7 theoretically analyses the bonding and stress transfer properties of a silk fibre reinforced polymer system with and without a sericin layer;

- Chapter 8 concludes the outcomes from this project and provides suggestions for future study.

Chapter 2

Literature Review

2.1 Overview

Elevated environmental awareness of the general public in reducing carbon footprints and non-naturally decomposed solid wastes has resulted in an increasing use of natural fibre and biodegradable polymers, and their composites. The properties of natural fibre reinforced composites are generally governed by the pre-treatment process of fibres and the manufacturing process of composites. Due to the complexity of fibre structures, different mechanical performances of the composites are obtained even with the use of the same fibre types with different matrices.These properties can be tailored for different applications by properly selecting suitable fibres, matrices, additives and production methods. The wide range of applications has been developed using these natural fibre reinforced composites.

2.2 Natural Fibre

Natural fibre is a type of renewable sources and a new generation of

reinforcements and supplements for polymer materials. Briefly grouping different categories of natural fibres, they can be divided based on their origin, derivations of plant, animal and mineral types which are shown in detail in fig. 2.1, (Ballie & Bader 1994; Bledzki, Sperber & Faruk 2002; Mohanty, Misra & Drzal 2005; Pickering 2008). These renewable fibres have been applied as substitutions for glass fibre and other synthetic polymer fibres for various engineering applications.

The remarkable advantages of natural fibres compared with those conventional inorganic man-made fillers enhance their commercial and research potentials. Natural fibres normally are abundantly-renewable resource so that their cost is relatively low as compared with synthetic fibres. With the consideration of environmental consciousness, natural fibres are biodegradable so as they can alleviate the problem of massive solid wastes produced and relief the pressure of landfills if they are used for replacing other non-degradable materials for product development. Besides, according to their inherent properties, natural fibres are flexible for processing due to their less susceptible to machine tool damage and health hazards during the manufacturing and etc. Moreover, natural fibres possess many advantageous characteristics such as desirable fibre aspect ratio, low density and relatively high tensile and flexural moduli (Xie et al. 2010). Table 2.1 summarizes the mechanical properties of natural and man-made fibres. In order to meet the requirement for suiting with the different potential applications, table 2.2 provides the detail information on the properties of hard and soft tissues in human body as reference.

Fibres

Q

...

Naturalfibres | Manrnade-fibres

Plant-based | Anirnal-based | Mineral

(cellulose or ligpocellulose) | (Protein)

Asbestos Fibrous
brucite
Wollastonite
Inorganic whiskers

Wood | Cane, @:'ass & reed | Stalk | Leaf | Bast (Stern) | Seed | Fruit | *WooV* hair | Silk

Hardwood
Softwood

m

Bamboo
Bagasse
Esparto
Sabei
Phra ites
Communis
Canary @:'asS
Elaphant @:'ass

Wheat
Maize
Barley
Rye
Oat
Rice

Sisal
Abaca
Henequen
Pineapple
Palm
Harakeke flax

Flax
Hernp
Jute
Ramie
Kenaf

Cotton
Kapok
Milkweed
Rice husk

Coir

Larnb'swool
Goathair
Angora wool
Cashmere
Yak
Horsehair
Feather
Down

Tussahsilk
Mulberry silk
Spider silk

Figure 2.1. The classification of the fibre.

Table 2.1. Mechanical properties of natural and man-made fibres.

Fibre	Density (g/cm^3)	Elongation (%)	Tensile Strength (MPa)	Young"s modulus (GPa)	Ref.
Natural fibre					
Cotton	1.5-1.6	7.0-8.0	287-597	5.5-12.6	(Black 2006)
Jute	1.3	1.5-1.8	393-773	26.5	(Black 2006)
Flax	1.5	2.7-3.2	345-1035	27.6	(Black 2006)
Hemp		1.6	690		(Black 2006)
Ramie		3.6-3.8	400-938	61.4-128	(Black 2006)
Sisal	1.5	2.0-2.5	511-635	9.4-22.0	(Black 2006)
Coir		30.0	175	4.0-6.02	(Black 2006)
Viscose (cord)		11.4	593	11.0	(Black 2006)
Soft wood kraft	1.5		1000	40.0	(Black 2006)
Kenaf		1.5	930	53	(Claes 1989)
Nettle		1.7	650	38	(Claes 1989)
Abaca			430-760		(Claes 1989)
Oil palm	0.7-1.55	3.2	248	25	(Claes 1989)
Pineapple		2.4	170-1627	60-82	(Flahiff, Blackwell & Hollis 1996)
Banna		3	529-914	27-32	(Flahiff, Blackwell & Hollis 1996)
Wool		25-35	120-174	2.3-3.4	(Flahiff, Blackwell & Hollis 1996)
Spider silk		17-18	875-972	11-13	(Flahiff, Blackwell & Hollis 1996)
Bombyx mori silk	1.33	19.55	208.45	6.10	(Burns & Varin 1998)
Twisted Bombyx mori silk		20.57	156.27	3.82	(Burns & Varin 1998)
Tussah silk	1.32	33.48	248.77	5.79	(Burns & Varin 1998)
Man-made fibre					
E- glass	2.5	2.5	2000-3500	70.0	(Black 2006)
Aramid	1.4	3.3-3.7	3000-3150	63.0-67.0	(Black 2006)
Carbon	1.4	1.4-1.8	4000	230.0-240.0	(Black 2006)

Table 2.2. Mechanical properties of hard and soft tissues in human body.

Fibre	Tensile Strength (MPa)	Young"s modulus (GPa)	Ref.
Hard tissue			
Cortical bone (longitudinal direction)	133	17.7	(Tams & Rozema 1996)
Cortical bone (transverse direction)	52	12.8	(Tams & Rozema 1996)
Cancellous bone	7.4	0.4	(Tams & Rozema 1996)
Enamel	10	84.2	(Tams & Rozema 1996)
Dentine	39.3	11	(Tams & Rozema 1996)
Soft tissue			
Articular cartilage	27.5	10.5	(Tams & Rozema 1996)
Fibrocartilage	10.4	159.1	(Tams & Rozema 1996)
Elastic cartiage	3		(Flahiff, Blackwell & Hollis 1996)
Ligament	29.5	303.0	(Tams & Rozema 1996)
Tendon	46.5	401.5	(Tams & Rozema 1996)
Skin	7.6	0.1-0.2	(Tams & Rozema 1996)
Heart valves	0.45-2.6		(Flahiff, Blackwell & Hollis 1996)
Arterial tissue (longitudinal direction)	0.1		(Tams & Rozema 1996)
Arterial tissue (transverse direction)	1.1		(Tams & Rozema 1996)
Intraocular lens	2.9	5.6	(Tams & Rozema 1996)

2.2.1 Plant-based Fibre

By grinding the bark of the plant, its cell wall can be separated into different sub-sections as shown in fig.2.2 (a). The schematic representation of the cell wall of a natural plant is shown in fig. 2.2 (b). The cell wall consists of a hollow tube,

which has four different layers: one primary cell wall and three secondary cell walls and a lumen. Each layer is composed of cellulose embedded in a matrix of hemicellulose and lignin. The lumen is an open channel in the centre of the macrofibril. The microfibril is composed of crystalline regions and amorphous regions alternately, as shown in fig. 2.2(c) (Baillie 2004).
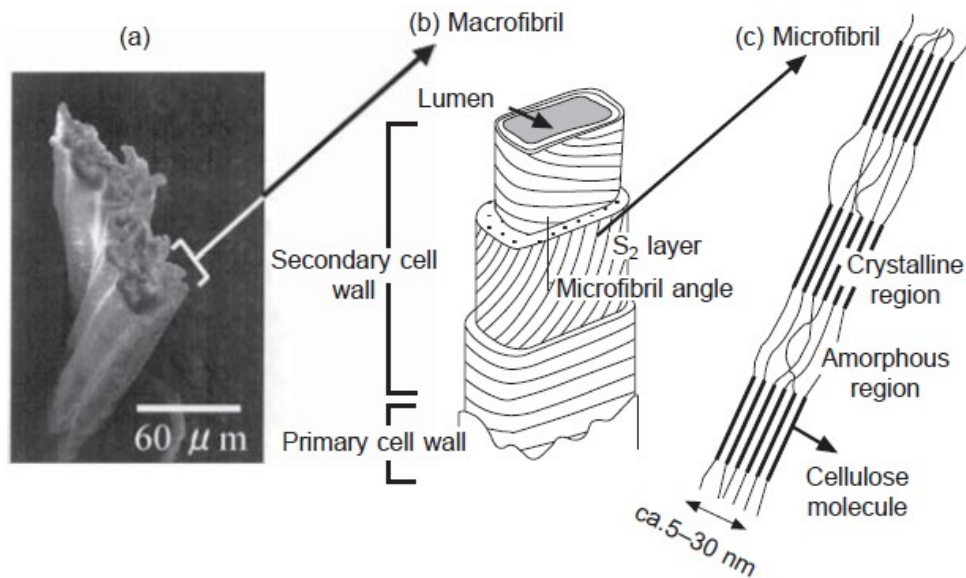
Figure 2.2. (a) Scanning electron micrograh of a kenaf bark fibre, and schematic representations of (b) macrofibril and (c) microfibril of natural plant (Baillie 2004).

The age of the plant, climate conditions and fibre processing techniques influence the structure of fibre as well as their chemical composition. The primary constituents of plant-based fibre (lignocelluloses) are cellulose, hemicelluloses and lignin. Cellulose contributes the strength which contains alcoholic hydroxyl groups so that it is hydrophilic in nature (Baillie 2004). The moisture content of plant-based fibre reaches 8–12.6% (Mohanty, Misra & Hinrichsen 2001). The basic chemical structure of cellulose in all fibre is the same but they have different degrees of polymerisation whereas the cell geometry of each type of cellulose

15

varies with the fibre. These factors contribute to the properties of the green fibre. Fig. 2.3 indicates the properties and their dependence on chemical constituents (Baillie 2004).
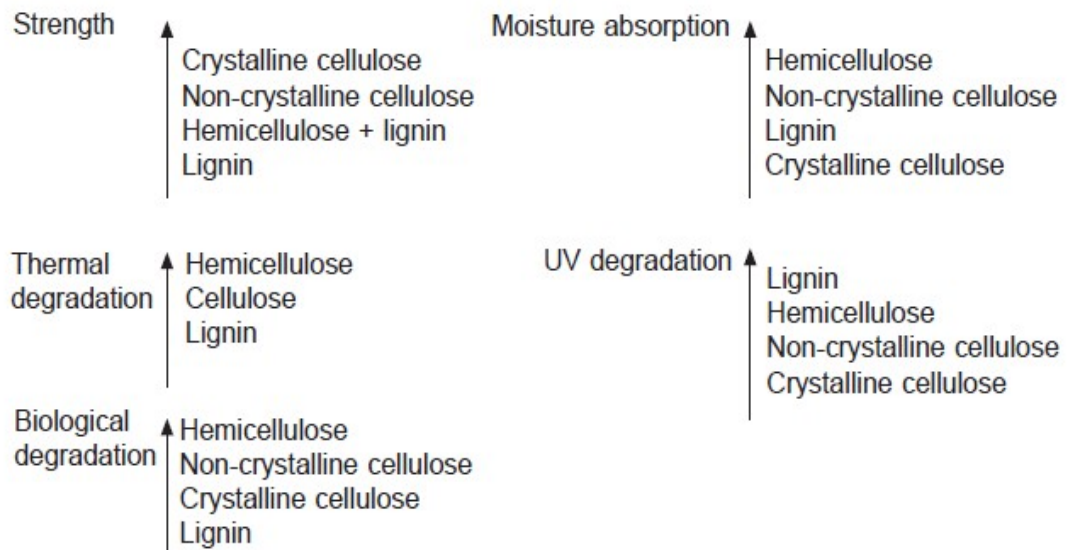
Figure 2.3. Properties of cellulose fibre and their dependence on chemical constituents (Baillie 2004).

2.2.2 Animal-based Fibre

Animal-based fibre generally is comprised of proteins such as collagen and keratin. It can be divided into three categories, animal hair, avian fibre and silk. Animal hair fibre is defined as the fibre which is taken from animal and hairy mammals. Examples of animal hair are sheep's wool, cashmere, alpaca hair, horse hair. Sheep‟s wool is mainly composed of α-keratins, a protein which is formed by a horny layer of the epidermis and of the epidermal appendages such as hair. Wool

16

is a multi-component fibre which consists of about 170 different protein molecules and these protein molecules constitute the morphological components of wool (Zahn, Hles & Nlenhaus 1980). The diameter of wool fibre is in the range of 20 to 40 mm and the cross-section is elliptical (Simpson & Crawshaw 2002). Wool fibre is typically divided into three morphological components including cuticle, cortex and cell membrane. The microfibrils in the cortex represent approximately 50-60% by mass of the cortex material. The bonding between the microfibrils and their embedding matrix within the cortex and the presence of the organized helics within the microfibrils dominate the mechanical and water absorption properties of wool fibres (Feughelman 1997).

Avian fibres are feather fibre. Chicken feather, which contains approximately 91% protein (keratin), 1% lipids, and 8% water is one of the examples of avian fibre. The diameter of chicken feather fibre is found to be in the range of 5–50 μm (Kock 2006). Its" tensile strength varies indirectly with moisture content. The tensile strength of feather rachis conditioned at 100% relative humidity is 106 MPa. The tensile strength of feather rachis conditioned at 0% relative humidity is 221 MPa (Kock 2006). The Young's modulus increases markedly along the length of the rachis, with the highest values at the feather tip. X-ray diffraction measurements show more keratin molecule orientation further out along the rachis. Moreover, the fibre located closer to the bird is smaller in diameter and has lower physical properties compared with the fibre which is far from the rachis (Barone & Schmidt 2005). It is obvious that flight feather fibre exists in a hollow form while down fibre is in solid. In terms of the purpose of fibre-reinforcement, the use of down fibre appears much better than that the use of flight fibre.

Silk fibre is a type of fibre collected from dried saliva of bugs or insects during the preparation of cocoons. Silks are generally defined as protein polymers that are spun into fibres by some Lepidoptera larvae such as silkworms, spiders, scorpions, mites and flies (Altman et al. 2003). Spiders have six or seven sets of glands including major and minor ampullate, flagelliform, aggregate, cylindrical, aciniform and piriform for production of fibres with different amino acid composition. These silks serve as (1) orb-web Frame, (2) prey capture, (3) wrapping, (4) joint and attachment, (5) reproduction, (6) vibrational sensor and (7) dispersion. The mechanical properties of the dragline silk are highly influenced by the composition of amino acids, insect size, diet conditions, body temperature and drawing speed (Saravanan 2006). Some spider silks exhibit over 200% elongation (Wang 2006). Compare with kevlar fibre, the tensile strength of spider silk is a factor of four less than kevlar fibre (3.4-4.1 GPa), but the energy used to break the silk is about three times greater ($1x\ 10^5 Jkg^{-1}$) (Bonino 2003). However, the predatory nature of spider silk causes it difficult to handle, the production of spider silk fibre is relatively low compared to silkworm silk fibre hence (Altman et al. 2003).

2.2.3   Silkworm Silk Fibre

Arthropods including spider and silkworm have evolved to produce a variety of task-specific silk-protein-based fibres. However, Silkworm silk fibre is different to the spider silk fibre as only one type of silk generated by individual silkworms but individual spider can generate 6-7 types of silk fibre for different purposes Moreover, draglines produced by spider silk are insufficient to support any

industrial process. The glue-like proteins are generally absent in the spider silk. Therefore, silkworm silk fibre is found to be the most potential material for industrial and biomedical engineering applications.

The silkworm cocoon is built at the end of the larval stage and protects the pupa during metamorphosis to an adult moth. It contains silk protein, known as silk fibroin which is stored in the glands of insects and spiders as an aqueous solution. It is understood that the water is acting as a plasticizing agent, keeping the protein malleable (Atkins 2003). Silk protein is usually produced within specialized glands after biosynthesis in epithelial cells, followed by secretion into the lumen of these glands and prepared to spin out as filament (Altman et al. 2003). During the spinning, the concentration of silk protein in the solution is gradually increased, and thus the shear and elongational stresses are formed and acted on the fibroin solution in the gland. Elongational flow orients the fibroin chains, and the fibroin in liquid form is converted into partly crystalline, insoluble fibrous filaments in the solid form (Hoppenfeld & Murthy 2000). The bulk of the polymer chains in the crystalline regions are oriented parallel to the fibre axis (Atkins 2003). Silkworm silk fibre is a semi-crystalline natural fibre and can be characterized using X-ray and electron scattering techniques (e.g. crystallinity, crystalline and amorphous orientations). Many of the crystalline phase-related parameters correlate with the tensile mechanical characteristic of silkworm silk fibre (Fakirov & Bhattacharya 2007).

The speed of spinning controls the mechanical properties of fibre (Shao & Vollrath 2002). As silkworm silk fibre can be obtained naturally by spinning through the spinneret of the moving silkworm head by accelerating and

decelerating its head. The silkworm produces strong but relatively brittle fibres through faster spinning speed, whereas slow speed lead to weak, more extensible fibres. The silkworm silk fibre is an inhomogeneously distributed polymer blend material (John & Thomas 2009). The core fibres are encased in a sericin coating, a family of glue-like proteins that hold two strands of fibrils together to form composite fibres and a silkworm cocoon case (Jiang, Liu & Wang 2006). This glue –like protein is called sericin which is amorphous in nature and acts as binder to ensure the structural integrity of the cocoon. Fig. 2.4 shows a single strand of silk fibre. A fibre itself is a bundle of several fibrils with a diameter of 1μm. A fibril contains 15nm wide microfibrils. These microfibrils are packed together to form the fibril bundle and several fibril bundles produce a single strand (Fakirov & Bhattacharya 2007).
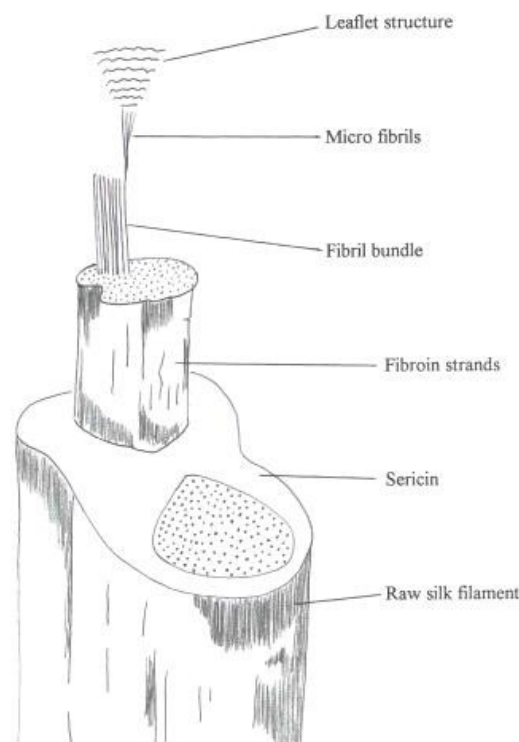
Figure 2.4. Structure of raw silkworm silk fibre (Sonthisombat & Speakman 2004).

The reeling long (300-1200m) of continuous fibre from the cocoon certainly contributes to its success as textile fibres. However, a long and continuous fibre can only be reeled after removing an adhesive sericin coating. Silk fibres including silkworm silk and spider silk contain assembled anti-parallel β-pleated sheet crystalline structures. Silks are considered as semi-crystalline materials with 30– 50% crystallinity in spider silks, 62– 65% in cocoon silk fibroin from the Bombyx mori silk, and 50– 63% in Tussah silk (Lewin 2006). Fig. 2.5 shows the cross section, longitudinal view and perspective of silk fibre.
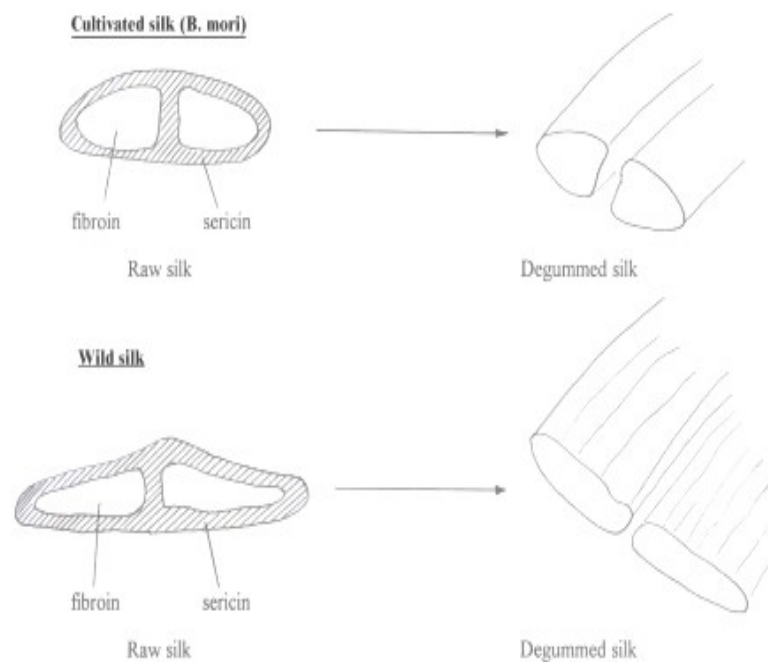
Figure 2. 5. Cross section and longitudinal view of silk filaments (Sonthisombat & Speakman 2004).

2.3 Biodegradable Polymers

Conventional plastics such as polyethylene (PE) and polypropylene (PP) are used for many years. With time and the rapid development of science and technology, the mechanical property, stability and durability of conventional plastics have been improved continuously. However, these long lasting plastics seem inappropriate in application for a product which has short product life cycle, such as plastic plates and forks. These plastics persist for hundred years in a landfill after disposal. Therefore, advantages as disadvantage, high durable property of these plastics increase the environmental burden. Moreover, these plastics are often disposed and stained with food residue; increase the complexity of plastic recycling. The cost of recycling plastics is thus increased. As the public starts focusing on the huge environmental accumulation of these long lasting plastics and pollutions may be induced during and after the life cycle of the plastics (such as manufacturing and disposal processes), and fitting the modern society, the study on naturally-degradable polymers with short life cycle is needed.

Biodegradable polymer was first introduced in 1980s (Vroman & Tighzert 2009) which was designed to degrade upon disposal by the action of microorganisms. In general, polymers are solid, non-metallic compounds with high molecular weight. They are comprised of repeated macro-molecules, and have varying characteristics. Material usage and final mode of biodegradation are dependent on the composition and processing method employed (Kolybaba et al. 2003).
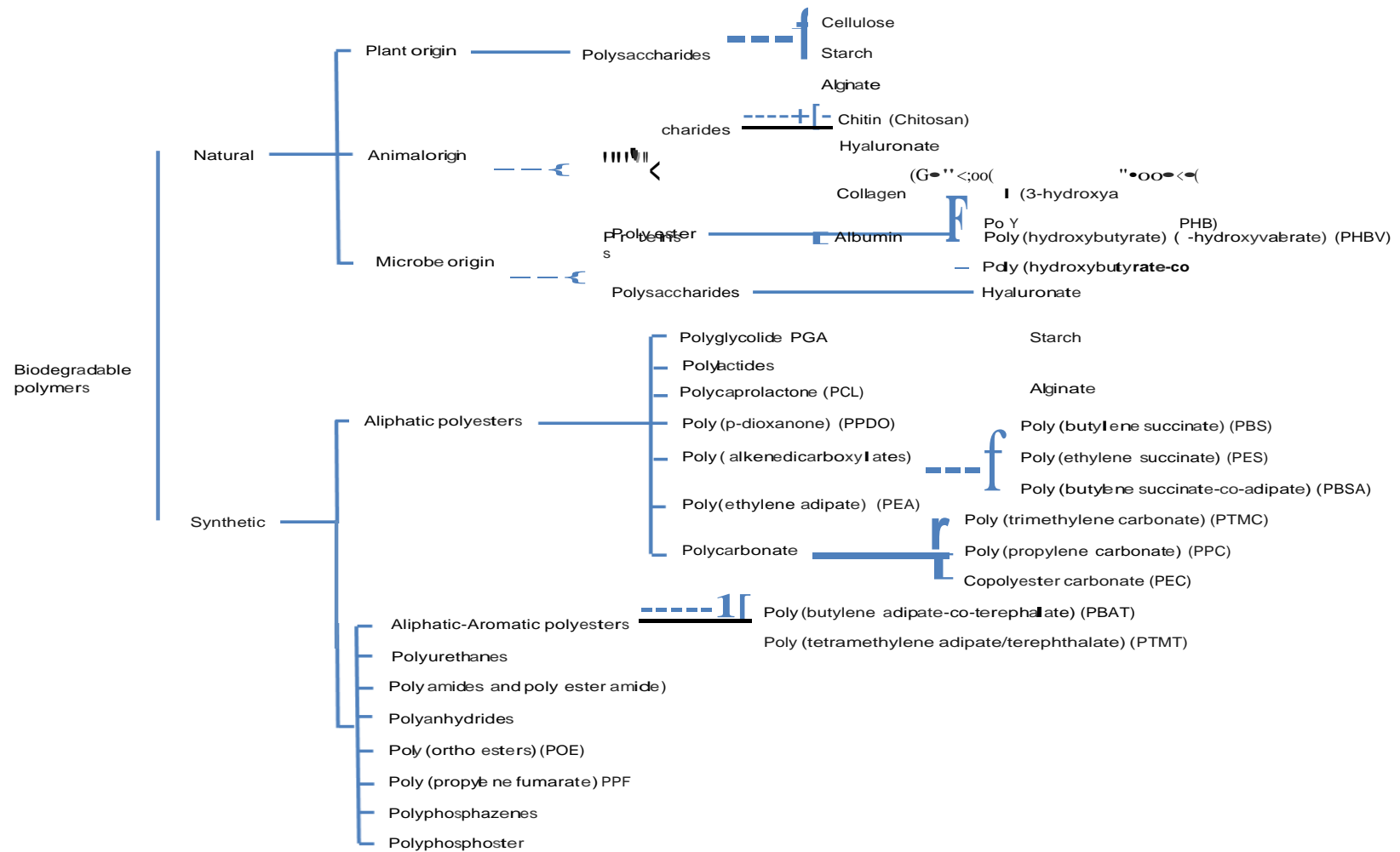
Figure 2.6. Natural and synthetic biodegradable plastics (Ikada & Tsuji 2000).

Biodegradable polymers are capable of undergoing decomposition in which the predominant mechanism is the emzymatic action of micro-organisms. These polymers can be also classified on the basis of the origin, that is, naturally occurring or synthetic in fig. 2.6 (Ikada & Tsuji 2000).

Natural polymers are available in large quantities from renewable sources, while synthetic polymers are produced from non renewable petroleum-based resources. Nowadays, degradable polymers are used in various forms including films, moulded articles, sheet, etc. The potential applications of biodegradable applications include (1) film such as plastic shopping bags and bin bags, (2) cling wrap, (3) flushable sanitary products, (4) sheet and non woven packaging, (5) bottles and container, (6) loose fill foam and (7) bio-medical applications. Among these biodegradable polymers, aliphatic polyesters constitute the most attractive family have been studied extensively. Table 2.3 summarizes the properties of aliphatic polyesters. Polyesters play a predominant role as biodegradable polymers due to their potentially hydrolysable ester bonds.

Poly (lactic acid) (PLA) or called polylactide belongs to the family of aliphatic polyesters derived from α-hydroxy acids which is mainly obtained from starch and sugar. Since PLA is compostable and derived from sustainable sources, it is viewed as a promising material to reduce societal solid waste disposal problems (Lim, Auras & Rubino 2008).

Table 2.3. The properties of aliphatic polyesters.

Examples	Crystallinity	Glass transition Temp.	Melting point	Modulus	Loss Strength (month)	Loss Mass (month)	Processing temp	Ref.
Poly (butylene succinate) (PBS)		-45 to -10	90-120	0.4-0.6			160-200	(Matuana & Balatinecz 2001; Zulkifli et al. 2009)
Poly (ethylene succinate) (PES)		-45 to -10	90-120				160-200	(Matuana & Balatinecz 2001; Zulkifli et al. 2009)
Polyglycolide (PGA)	45-55%	35-40	200	12.5Gpa	1-2	6-12		(Zulkifli et al. 2009)
Polycaprolactone (PCL)	67	-60	55-60	0.19		24-36		(Zulkifli et al. 2009; Chaivan, Pasaja & Boonyawan 2005; Serizawa, Inoue & Iji 2006)
Poly L-lactide (PLLA)	~37	60-65	170-180	4.8	~6	12-24		(Zulkifli et al. 2009; Chaivan, Pasaja & Boonyawan 2005)
Poly DL-lactide (PDLLA)		55-60		1.9	1-2	12-16		(Zulkifli et al. 2009)
Polydioxanone PDS, PPDO	high	<20	2.1	1.5	1-2	6-12		(Kazayawoko 1999; Zulkifli et al. 2009; Huda, Drzal & Misra 2005)
Poly (3-hydroxybutyrate) (PHB)	80	5	173-180	0.9-4				(Huda & Huda 2005; Serizawa, Inoue & Iji 2006)
Poly (trimethylene carbonate) PTMC						3-4		(Zulkifli et al. 2009)

PLA belongs to the family of the polyester and is generally linear (without strong entanglement, branching between the chains). The structure of the molecule influences its mechanical and thermal properties (PLA 3051D: T_g ~55-65°C, T_c ~ 150-165°C and tensile strength ~48MPa) (NatureWorks 2005), which are quite similar to other polyesters (such as PET). The thermal properties are however a bit

lower, due to the absence of the benzoic cycle (chain more free to move). Its chemical properties and water resistance are weakened by the presence of the carbonyl group (C=O), which allows hydrolysis degradation. Like most of the polymers, the different macromolecules (chains) are bonded together by hydrogen bonds (Van de Waals forces). Most important mechanical and thermal properties (crystallinity rate, Tg and Tm) are then influenced by the concentration and disposition of different enantiomers (L- and/or D- lactic acid). Indeed, the chains made of a unique basic element can align each other easier in a configuration favoring inter chain bonds. Thus the lowest T_g is found in racemic mixing of L- and D- enantiomers while the highest properties are obtained by stereo complex PDLA and PLLA blends (respectively using the D- and L- enantiomers) and reach a maximum with a ratio of 50:50. However, a high-molecular PLA cannot be directly synthesized from the molecule of lactic acid, mainly because of the generation of water during the condensation process (leading to the degradation of the PLA formed and formation of only low-molecular oligomer). In general, three different ways can be followed to solve this problem:

1. Addition of chain-coupling agents during the condensation process;

2. Dimerization the oligomer into cyclic lactide, distillation of solution to take out the water condensed and then production of the PLA by ring-opening polymerization;

3. Azeotropical dehydration during the condensation process, removing the water during the process by change of pressure.

Like most polymers, PLA is hydrophobic. It can only absorb 1wt% water and undergo hydrolytic degradation, making it biodegradable and environmentally friendly. PLA normally undergoes three main degradation processes: (i) chemical hydrolysis, (ii) enzymatic degradation and/or (iii) microbial degradation (Amnat & Tokiwa 2004). During the chemical hydrolysis, the water molecule attacks the double bounding C=O of PLA. PLA is degraded in the scheme as bulk degradation (same as PGA, PLGA and PCL). Therefore, the ingress of water is faster than the rate of degradation and the degradation takes place throughout the whole of a sample. The enzymatic degradation occurs mainly in the amorphous region of the polymer and seems to attack preferentially the ester bonds of L-lactic acid (cleaving the polymer) (Altman et al. 2003).

In order for PLA to be processed in large-scale production lines through injection moulding, blow moulding, thermoforming, and extrusion, it must possess adequate thermal stability to prevent degradation and maintain molecular weight and properties. PLA undergoes thermal degradation at temperatures above $200^{o}C$ ($392.8^{o}F$) by hydrolysis, lactide reformation, oxidative main chain scission, and inter- or intra-molecular trans-esterification reactions. Its homopolymers have a glass transition and melt temperature at about $55^{o}C$ and $175^{o}C$, respectively. They require processing temperatures over $180^{o}C$. At this temperature, unzipping and chain scission reactions lead them to loss the molecular weight, as well as thermal degradations. Consequently, PLA homopolymers have a very narrow processing window. The rheological properties of PLA, especially its shear viscosity, have important effects on thermal processes, including injection molding, extrusion, film blowing, sheet forming, fibre spinning, and thermoforming. PLA melts are shear thinning, similar to polystyrene. Its working temperature is dependent on the

melt viscosity, which is, in turn, dependent on the weight-average molecular weight of PLA, the amount of plasticizer, the shear rate, the type of melt processing, and the amount of work put into the polymer. Under the same processing conditions, semi- crystalline PLA has a higher shear viscosity than amorphous PLA. As the temperature increases, the shear viscosity would be decreased for both types of PLA. The PLA melt was characterized as a pseudo plastic, non-Newtonian fluid (Antroine, Davies & Baley 2010).

2.4 Manufacturing Processes of Degradable Natural Fibre Reinforced Composites

2.4.1 Selection Criteria

Suitable manufacturing processes must be utilized to transform materials to a final shape without causing any defect. For the selection of a suitable process to fabricate biodegradable composites, design and manufacturing engineers would mainly focus on numbers of criteria, such as desired mechanical and thermal properties, size and shape of resultant composites, processing characteristics of raw materials, the production speed and the manufacturing cost. The size of the composite is a dominating factor for the preliminary assessment on a suitable type of manufacturing processes to be used. For a small to medium sized component, injection or compression moldings is preferred due to their simplicity and fast processing cycle. However, for large structure, it is typically manufactured by open moulding or autoclave processes.

The complexity of shape of a product also influences the type of manufacturing processes choosen. Filament winding is the most suitable method for manufacturing composite pressure vessels and cylinders. Recent development has also used carbon fibre wrapped on the surface of forged Aluminum cylinders to form ultra-high pressure tanks. Besides, pultrusion is mainly used for producing long and uniform cross-section parts. In some extent, an optic fibre can be integrated into the pultrusion process to produce self-structural-health monitored composite structures. The shape of the parts being made is highly dependent on the shape of the die. Somehow, several stages of heat control are needed to cure composite parts. Depending on the performance of composite products, suitable raw materials (thermosets/thermoplastics), high/low viscosity, processing temperature should be chosen with an appropriate composite fabrication technology. However, in certain extent, the criteria of selecting the right manufacturing processes for degradable natural fibre reinforced composites are quite different with that for traditional polymers. The properties of natural fibre reinforced composites are highly depended on the length, orientation, diameter and content of the fibre. Moreover, the surface condition of the fibre also plays a key role as it would affect the bonding interface between the fibre and surrounding polymer. Removal of a surface coating of fibre (like silk and coir fibres) or pretreatment of fibre (like hemp) by using chemical process may be needed to ensure a good bonding is resulted.

Theoretically, high tensile strength could be achieved by increasing the amount of fibre used. However, it may not be done by using certain manufacturing process such as injection moulding processs, as the expansion (swelling) of fibre in wet condition could cause a sucking effect. Therefore, for high fibre content

reinforced composites, compression moulding is prefered for a simple form fabrication.

2.4.2   Processing of Raw Materials

Natural fibre always cannot be wetted completely by following the general manufacturing processes as they are not designed for wetting fibre with tight-packing fibrils. The viscosity of polymers is normally too high for impregnation. Better fibre pre-impregnation allows a better fibre wetting and thus enhances the mechanical interlocking between fibre and polymer (Gonzaleza, Cervantes-Uca & Olayob 1999).

A noteworthy weakness in natural fibre reinforced thermoplastic composites is their poor interfacial bonding properties between fibre and matrix. The interfacial adhesion between them plays an important role in determining the performance of the composites. As silk proteins are stored in the silk gland and transported down the spinning duct in a lyotropic liquid crystalline state in silkworm silk glands, the molecules of the silk protein must be amphiphilic, which is having a combination of hydrophobic and hydrophilic blocks or groups. When producing silk fibre reinforced composites, hydrophilic characteristic of silk fibre was found to cause poor interfacial bonding with polymer. This is mainly due to their dissimilar hydrophobicity as the surface of fibre is hydrophilic while organic polymers are generally hydrophobic, they are incompatible and prevent efficient fibre–matrix bonding. Therefore, debonded fibres dilute the matrix content and act as flaws which reduce the effective cross sectional area of reinforcement, and finally poor

mechanical strength is resulted. Moreover, the formation of fibre agglomeration, due to the inter-fibre hydrogen bonding which prevents thorough dispersion of fibres during the manufacturing process weakens the strength and affects the appearance of the composites (Keener & Stuart 2004; Matuana & Balatinecz 2001; Saheb & Jog 1999). In such case, the use of silk fibre could not provide any advantage to the composites (Kazayawoko 1999; Matuana & Balatinecz 2001). Thus the treatment of natural fibres for adhesion improvement is a critical step in the development of the composites. Different treatments such as pre-impregnation, surface modifications, chemical reactions and plasma have been studied for interfacial shear strength improvement in order to develop composites with better mechanical properties (Matuana & Balatinecz 2001; Saheb & Jog 1999; Gonzaleza, Cervantes-Uca & Olayob 1999; Mohanty & Drazal 2002; Zulkifli et al. 2009).The comprehensive study on the surface treatment and the change on the mechanical properties of silk fibre is discussed in Chapter 5.

2.4.3   Moulding Processes

2.4.3.1   Injection moulding

Injection molding of composites is a process that forces a measured amount of mixture which contains molten polymer and fibre into mould cavities. Many studies have been conducted on the potential of using natural fibres as reinforcement for renewable polymer to make a composite through injection moulding (Serizawa, Inoue & Iji 2006; Huda & Huda 2005; Huda, Drzal & Misra 2006; Huda, Drzal & Misra 2005; Huda et al. 2006; Birgitha 2007) The original

thermoplastic used by this process was designed for polymer pellets. For the manufacturing of short fibre reinforced composites, the pellets with chopped fibres are fed individually through a funnel-shaped feed hopper into a heated compression barrel with a rotating screw ("screws" for twin-screw extruder). The purpose of heating the barrel is to transform the solid pellets into viscous liquid which can be drove through the sprue nozzle and finally forced into the matched-metal closed mould cavities. The mould is tightly clamped against injection pressure where the polymer solidifies, freezing the orientation and distribution of the fibres. The composite is then removed from the closed mould after it is sufficiently cooled to be ejected to form a part of desired shape. As the mixture is required to move toward to the sprue nozzle, molten polymer is pressurized by the screw mechanism. The function of the screw is to (1) generate heat by viscous shearing to melt the polymer, some heat that is used for melting pellets evolved from the friction in between pellets, barrel and screw (Birgitha 2007), (2) apply the shear force to mix the polymer and fibre and (3) act as a piston to force the mixture of fibres and molten polymer through sprue nozzle into a matched-metal closed mould. It has been reported that as the temperature increases, the shear viscosity of biodegradable polymers would decrease which makes the flow easier. Besides, as the shear rate increases, the viscosity of the polymer melts would also be decreased significantly. This change of viscosity is caused mainly by the breaking of PLA molecule chains due to the strong shear forces and temperature (Qi & Milford 1999).

Fibre that is used in the injection moulding is usually chopped into short fibre according to the critical fibre length criterion in which the stress should be fully transferred from the polymer to the fibre and the fibre can be loaded to its full

capacity assuming a good interfacial bonding is resulted. However, the traditional injection moulding process limits the fibre length that solidifies in the final part since the high shear rates in the barrel and the passage of fibres through narrow gates and openings in the mould which cause significant fibre attrition. Therefore, the fibre length in practice is normally shorter than the predicted fibre length because of the fibre attrition. It causes the fibre length below the critical length as expected, the fibres shorter than the critical length would not be able to carry their maximum load effectively. In an extreme case, the problem raised from the length effect with the poor fibre-polymer bonding properties, the fibre rather acts as a defect in the material. Nevertheless, if the fibre length is beyond the pre-determined critical length, it will carry an increasing fraction of the applied load and may fracture prior to the failure of the polymer. Therefore, it is necessary to carefully determine the critical length of the fibre before injection action is performed. On the other hand, increasing fibre content would theoretically improve the stiffness and the strength of resultant composites. However, in practice, the traditional injection modeling process would limit the amount of fibres to be injected because of fibre cluttering, narrow gate and sprue and, viscosity of the fibre/ polymer mixture. Another main issue is the volume expansion of the fibre after mixing with the liquid form of polymer.

Residual stress and fibre orientation with respect to the depth are also the critical issues which affect the modulus distribution of the injection moulded composites. Residual stress is an internal stress which occurs as a result of the rapidly cooling of molten polymer in the absence of external forces. In general, the residual stress distribution shows tensile stresses at the surface and core regions and compressive stress at the intermediate region, which is well-known as the characteristic

residual stress distribution in injection-moulded parts (Kim, Lee & Youn 2002). Many researchers have studied the residual stress distribution of composites made by the injection moulding process (Qi & Milford 1999; Kim, Lee & Youn 2002; Lee et al. 2001; White 1985). (1) High pressure gradient, (2) non-uniform temperature profile caused by inhomogeneous cooling of polymer melt, (3) orientation of polymer chains and (4) the difference in thermal expansion coefficient between polymer and fibres, are the common phenomena which residual stresses may be introduced in injection moulded polymers or composites during filling, packing, and cooling stages.

When the flow is ceased, the molecule orientation starts to relax while solidification process subsequently occurs before this process is completed. It would impede the relaxation of the molecular orientation which is then frozen in, the residual stress is therefore formed inside the part. Residual stress in a pure thermopolymer and its fibre reinforced composites cause an earlier fracture of the composites which affect the quality of products seriously. Stress distribution along the flow path is influenced by the pressure history of the molten mixture at the beginning of the injection moulding process to the end of filling up the mould cavity. Various features of the stress profiles are explained by the influence of the pressure decay rate in the injection moulding process (White 1985). These residual stresses also result in warpage and shrinkage of final products and may cause the reduction of mechanical properties. Therefore, the dimensional accuracy and properties of the final products are highly related to the residual stress distribution in the molded part (Kim, Lee & Youn 2002). For natural fibres, as their moisture absorption characteristics, impurities and voids formation inside injection moulded composites may be resulted as high temperature is used during

the process and cause water molecules trapped inside micro-fibrils to be gasified.

Fibre orientation in an injection moulded short fibre composite is experienced variation with respect to the thickness direction as well as the in-plane direction. It induces the mechanical properties of the composite such as modulus and tensile strength may vary in the thickness direction according to the corresponding orientation status. For the range of fibre concentrations encountered commercially, fibres do not appear to have any direct effect on the polymer orientation. As the fibre concentration increases, however, the polymer orientation becomes dominated by the orientation of the fibres (Folkesa & Russell 1980). During the injection moulding process for the composite, a complex molten polymer flow field is generated and fibres are therefore oriented. The orientation of the fibres will be fixed until the polymer is solidified. Convergent flow results in high fibre alignment along the flow direction, whereas diverging flow causes the fibres to align at 90° to the major flow direction. Shear flow produces a decrease in alignment parallel to the flow direction and the effect is pronounced at low flow rates. In generally, the fibres align in the direction of shearing and also in the direction of stretching. The shear flow near the mould walls aligns the fibres in the direction of the injection flow and this layer is called the skin. Below the skin layer, the molten mixture continues to experience shear and fibres orient along the shear lines. Finally, the core layer is formed as the fibres are swayed by the bulk deformation of the flow in the mould which usually has an elongated component, causing the material to stretch in and out of the paper direction aligning the fibres. This skin core structure shown in fig. 2.7 is a common microstructural observation. However, the skin core structure is less significant in the small sample with low fibre volume fraction.
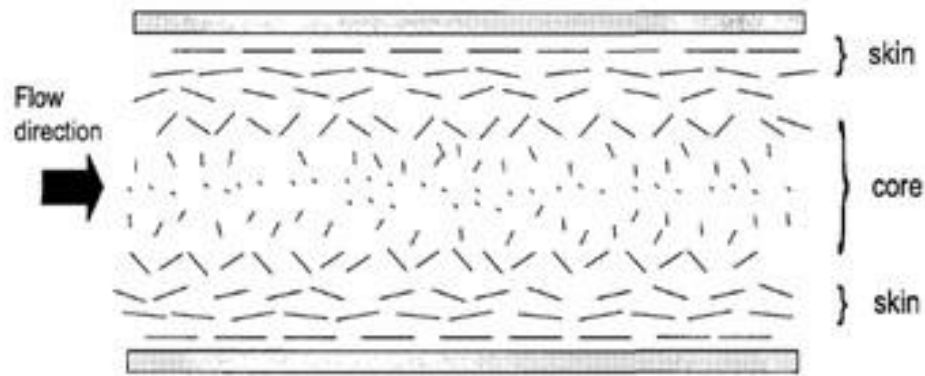
Figure 2.7 Influence of flow on fibre orientation: Skin – fibres are mostly aligned along the flow direcion; Core – fibres are mostly aligned perpendicular to the flow direction.

There are numerous issues that should be concern in the injection moulding process to obtain optimal properties of resulting natural fibre composites and avoid the generation of residual stress which cause warpage, stress cracking, and long-term deformation. Process, material and geometric parameters should be optimized to minimize these problems happen. Process parameters include the melt temperature, injection and screw speeds, injection pressure and the mould temperature that can be controlled on the injection units. Increasing mould temperature results in a decreasing overall stress level, while the compressive stress region is shifted onto the surface (White 1985). For biodegradable composites, the machine temperature of biodegradable polymer, such as PLA composites are made by using injection moulding process should be restricted in the range of 150°C to 210°C depending on the type of PLAs and their crystallinity from diverse manufacturers. Especially, under the same processing conditions, semicrystalline PLA has a higher shear viscosity than that of amorphous PLA (Qi & Milford 1999). The geometric parameters also play a key role on the residual

stress elimination. The shape and size of mould cavity, the locations of injection gates and the vents that allow air to escape, are the examples of geometric parameter which not only affect the residual stress, but also the air trapping and stress concentration.

2.4.3.2   Compression moulding

Many studies have been conducted on the feasibility of using natural fibres as reinforcement mixed with renewable polymers to form a new class of biocomposites through the compression moulding process (Serizawa, Inoue & Iji 2006; Huda & Huda 2005; Huda, Drzal & Misra 2006; Huda, Drzal & Misra 2005). This process is a combination of hot-press and autoclave processes. For autoclave process, thermoplastic prepregs are laid up on a mould in a desired sequence. An entire laminate is then bagged under vacuum and placed inside an autoclave. The laminate is then heated up following a preset heat-pressure cycle and a resultant composite is formed after curing (Mallick 2008). However, for the hot-press processing, a close mould may or may not be necessary (Ruihua & Lim 2007). With the use of close-moulds, the precut and weighed amount of fibres (in the forms of chopped, mat or stitched) are stacked together and placed inside a pre-heated mould cavity. For natural fibre, the fracture of some fibres may occur before resin films are molten if excessive pressure is applied.

Sheet molding compounds (SMCs) and bulk molding compounds (BMCs) are traditional initial charges for compression molding process. The charges usually cover 30-70% of the female mould cavity surface (Mallick 2008). The mould is

closed and then pressurized before temperature is applied. The compounds are molten to form the shape of the cavity. Afterward, the mould is opened and the part is ejected. As the fibre can be gently placed inside the mould and no shear stress and vigorous motion are applied, the damage of the fibre can be kept as minimal. In this case, long fibre can be used to produce a biocomposites with higher volume fracture. For the natural fibre composites, short fibres or fibre mats could be pre-mixed with the compounds for compression moulding, it would act as reinforcement to reduce the shrinkage of final products.

2.4.3.3   Hot pressing

Hot press is favorable for simple flat samples as only two hot plates are needed to compact fibre and polymer together and then heat is applied subsequently. However, the viscosity of the polymer during the pressing and heating processes is a concern as it is not easy to be controlled, in particular for thick samples. The viscosity of molten polymer should be low enough to impregnate into the space between fibres and high enough to avoid spurting out.

As natural fibres are made by microfibrils, it also takes time for wetting them. Therefore, the controls of viscosity, pressure, holding time, temperature in relation to the types of fibres and polymer, thickness and size of samples are critical to produce quality composites. Several minor defects such as residual stresses, voids, warpage, fibre breakage, sink marks and scorching would cause the reduction of the mechanical properties of the composites. Therefore, process, material and geometric parameters should be optimized to minimize any possible defects.

Besides, the processing temperature of biodegradable polymers is normally below 200°C to avoid the degradation of the polymers. If the product is thick enough, it is too long to transfer the heat from the surface to the core and thus causes the generation of residual stress. Therefore, throughout study on the temperature gradient is essential to avoid overheating on the surface or sub-temperature in the core to melt the polymers.

The required temperature and pressure for the moulding process may be varied depending upon the thermal and rheological properties of the polymer. Flow of the material is required to expel air entrapped in the mould as well as in the charge. Void morphology in the sample has a negative effect on the flexural modulus and strength, but a clear positive effect on the beam stiffness (Hagstrand & Bonjour 2005). During the moulding process, a complex heat transfer and a viscous flow phenomenon take place in the cavity (Kim, Choi & Kim 1995). For a good moulded part, a rapid mould-closing speed is desirable since it avoids the possibility of premature gelation and produces most uniform flow patterns regardless of the charge thickness (Mallick 2008).

Material parameters, for example, increasing the filler content also acts as a heat sink within inside the material as it would decrease the total amount of heat liberated (Mallick 2008). The initial charge shape, size and its placement location in the mould are crucial parameters for the properties of resultant product. The amount of flow in compression moulding is small but critical to the properties and the quality of final parts as the flow controls the orientation of short fibres. In order to control the moulding process smoothly and effectively, an optimized fibre which possesses high-surface energy and low expansion should be used so as to

lead to a better wetting and impregnation (Comte & Merhi 2006).

A slight excess of material is usually placed inside the mould to ensure it is completely filled. It is possible to have varying degrees of flow of fibres and/or of melt in compression moulding, the fibres are initially randomly oriented. Based on the past experience, it was found that the tensile properties of natural fibre reinforced composites decrease when the set mould temperature and flow velocity decrease. Most of natural fibres are normally distributed randomly at the beginning and finally aligned toward the polymer flow direction for flat plate molding (Kim & Jeong 1997; Jendlia & Meraghni 2004).However, as the mixture becomes fluid in the mould it deforms and the deformation changes the orientation of the fibres. Orientation distributions can be extremely complicated. The fibre can retain at randomly orientedin some location, whereas others may have high degree of alignment toward the flow direction.

Increasing the fibre content also leads to enhance the anisotropy of final moulding products (Dumont, Orge'as & Corre 2003). A low-viscosity paste may flow rapidly and cause air entrapment (Comte & Merhi 2006). Different temperatures inside moulded parts would generate different degrees of residual stresses, particular at thick sections. Thus, the temperature distribution and rate of cooling are important factors to determine how these stresses relax during cooling status (Kim & Jeong 1997).

The geometry of moulding parts is also crucial as it would affect the flowing behaviour and fibre orientation. Fibre content inside the rib and around the sharp turning sections is normally much lower than that of other flat sections. It was also found that the larger the rib thickness, the easier the flow (with the fibres)

into the ribs. A small lead-in radius would reduce the flow or increase the flow resistance into the ribs (Christensen & Hutchinson 1997). High pressure loss at the entrance of the rib is due to viscous friction. This pressure loss would result in fibre-polymer separation in these areas which in turn weakens the structural integrity of resultant parts and leads to increased sink-mark depth. For the curing process concerned, the material at the center of the rib sub-structure cures relatively slower than other flat-plate sections. The fibres are dense near to the top surface and around the rib corners, whilst a resin-rich area appeared just below the top surface at the center (Kim, Choi & Kim 1995). High pressure is required for molding parts that contain deep ribs and bosses (Mallick 2008). Thick structures are not easily produced by this technique because of heat conduction. The charge surface temperature quickly attains to the mould temperature and remains relatively uniform compared with the centerline temperature. The centerline temperature increases slowly until the curing reaction is initiated at the mid-thickness of the part. For thin parts, the temperature rise is nearly uniform across the thickness and the maximum temperature in the material seldom exceeds the mold temperature. When the SMCs is placed at the room temperature on the hot mould, the surface of the SMCs is soften and make them forming a resin-rich lubricating layer. Thus, for the purposes of modeling, the flow field can be divided into two regions: the core, which occupies most of the flow domain: and a thin lubricating layer. This is shown schematically in fig. 2.8 (Abrams & Castro 2003). For a thin part, the extensional deformation becomes more uniform and approaches the same flow pattern observed at fast mould-closing speed (Mallick 2008). For a thick part, high molding temperature should be avoided. Since the surface temperature first attains to the resin gel temperature, curing begins first at the surface and progresses inward. Curing occurs more rapidly at high moulding

temperature but the peak exotherm temperature also increases. Residual curing stresses in the moulded part are reduced as the thermal gradient remains nearly constant across the thickness through preheating (Mallick 2008).
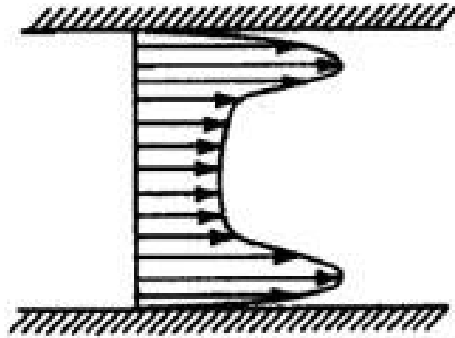
Figure 2.8. Transverse velocity profile for "Preferential flow" (Abrams & Castro 2003).

2.4.3.4   Resin transfer molding (RTM)

Liquid composite moulding processes encompass resin transfer molding (RTM), vacuum assisted resin transfer moulding (VARTM), structural reaction injection moulding (S-RIM), co-injection resin transfer moulding (CIRTM) and other subsets where the basic approach is to separately inject the liquid resin into a bed of stationary preforms. The RTM process has become a popular composite manufacturing process due to its capability for high volume production and cost effectiveness. Many studies have been made on the potential of natural fibres as reinforcement with renewable polymers as polymer through RTM (Sreekumar, Joseph & Unnikrishnan 2007; Willians & Wool 2000; Ferland & Trochu 1996; Kim & Daniel 2003; Ikegawa 1996; Warrior et al. 2003). In the RTM process, dry

fibre perform (impregnating) or porous fibrous preform is placed into the mould cavity. Two matching mould halves are clamped tightly to avoid leakage of molten polymer during injection process. Then, using dispensing equipment, a pressurized molten polymer is injected into the heated mould using single or multiple inlet ports in the mould (depending on the complexity of the shape of a final product) until the mould is filled with polymer. After cooling, the part is then removed from the mould (Sreekumar, Joseph & Unnikrishnan 2007). Post-curing normally is needed to ensure the resin is fully cured.

In the RTM process, the molten polymer injection pressure, temperature of the mould, permeability of the fibre mat, preform architecture and permeability, polymer viscosity, gate location and configuration, vent control and preform placement techniques are the major processing variables. In general, higher injection pressure and mould temperature would shorten the manufacturing cycle time due to the viscosity of resin is low. However, an excessive injection pressure may cause deformation of the mould and wash-out of the fibre preform. Besides, an excessively high mould temperature may induce pre-mature resin gelation and cause short shot. All of the process variables are interrelated and have effects on the mechanical properties of final products. These processing variables have significant effects on different aspects, such as fibre wetting out and impregnation, injection gate design, "dry patch" and void formation (Kang, Jung & Lee 2000).

For natural fibre reinforced composites, small clearances may exist between the fibre preform and mould edges because of loose edge fibre bundles, poor fitting size, or deformation of the fibre preform in the RTM process. The clearance results in a preferential polymer flow path during the mould filling stage. This

edge flow can disrupt the uniformity of the flow pattern and cause incomplete wetting of the preform. This phenomenon intensifies with the decrease of preform permeability. At the early stage of the injection process, the velocity difference is very high and then gradually reduced. It is due to the gradual increase in flow resistance which leads to smaller difference in velocity. Edge flow is introduced due to the clearance between the preform and the mould edge. The presence of edge flow leads to the interruption of flow uniformity and the polymer near the edge has a tendency to flow much faster than in the main area due to lower resistance. Edge flow is less sensitive to injection pressure variations but fibre concentrations have a dramatic influence. The deployment of preforms which is larger than the mould can eliminate the problem. "Quasi-one-dimensional steady" flow is preferred in order to achieve successful mould filling with complete impregnation and proper ventilation (Richardson & Zhang 2000).

For fast polymer flow without increasing injection pressure, resin can be injected using multiple injection gates. However, with improper injection schemes, the front of polymer flow becomes complicated and numerous air bubbles may be formed where the flow fronts merge (Kang, Jung & Lee 2000). Because of the high flow resistance, slow flow and impregnation, the molten polymer has a tendency to flow along the channel of least resistance under injection pressure and therefore the effect is intensified. Consequently both the values of mould filling distance differences between the centre and edge and the arrival time of edge flow at the bottom are substantially increased. The edge flow has an adverse effect on the mould filling process which leads to the formation of dry spots and spillage (Rodriguez, Giacomelli & Varzquez 2004). Due to aforementioned problems, it would induce a difficulty to assure full wetting inside the preform because of the

inconsistence of the natural fibre's geometry and the inhomogeneous fibre architecture. Such inhomogeneity leads to non-uniform permeability of the fibre preform, which in turn causes the velocity of the polymer varing from point to point at a micro scale. The capillary pressure, which also prevails at this length scale, exacerbates the spatial variation of the resin velocity. The resulting microscopic perturbations in the resin flow front allow voids to form (Kang, Lee & Hahn 2000).

While the average velocity field of the polymer may appear smooth, the local velocity can vary considerably from point to point at the micro scale. The reason is that the fibre preform has a non-uniform microstructure, and hence its local permeability and the local capillary pressure may differ between inside and outside fibre tows (Kang, Lee & Hahn 2000). It has been shown that there is a marked increase in voidage in the areas where flows meet and this is correlated to a deterioration of mechanical properties. The void content within a composite material produced by RTM will depend on the void content of the polymer prior to injection and the extent of void formation and growth during mould filling and cure. In general, vacuuming of the mould and injection pot is required prior to the injection process starts.

2.5 Potential Applications

2.5.1 Ecological Applications

Recent increase in the prices of petroleum-based products, strict governmental

regulations and taxation systems on carbon footprints and well-educated young generation on the acceptance of adopting green products have driven the growth of developing materials with the use of natural resource to another peak.   It therefore creates a new business model for all engineering enterprises to re-invest their capital including human resource. The application of natural fibre reinforced composites and natural-based resins for replacing existing synthetic polymer or glass fibre reinforced materials is huge. Automotive and aircraft industries have been actively developing different kinds of natural fibres, mainly on hemp, flax and sisal, and bioresins systems for their interior components. High specific properties with lower prices of natural fibre reinforced composites are making it attractive for various applications. According to Lucintel, a leading global management consulting and market research firm, the global natural fibre composites market reached to US $2.1 billion in 2010. This market is expected to grow with a CAGR (compound annual growth rate) of 10% over the next 5 years (2011-2016) (Black 2006).

Nowadays, new construction materials using natural fibre are well suited for anisotropic and specially tailored lightweight structural components parts such as interior panels inside cars, partitions (or called "dividers") inside airplanes and coats and other secondary structures with low temperature servicing condition. Table 2.4 summarizes the potential applications of natural fibre reinforced composites in automotive, electrical & electronics, sports and leisure items, construction, aircraft and household products & furniture industries (Flahiff, Blackwell & Hollis 1996; Claes 1989; Burns & Varin 1998; Wang 2008). Besides, as natural fibre is formed by several thousands of microfibrils together which is an ideal structure for energy absorption including sound wave energy, so it is good

for using its inherent advantage for developing noise barriers and impact resistance structures. Moreover, eco-friendly measures taken by the electronic industry is another major growth driver for these composites in electrical and electronics applications. Recently, a major research focus on natural fibre composites, mainly on the plant-based fibre is on their fire resistance properties. The result has found that using natural fibres as supplement and/or reinforcement of thermoplastics, the amount of Carbon Monoxide provided during fire is less than that of their host materials (Rakotomomalala, Wagner & Doring 2010).

Table 2.4. Common applications of natural fibre reinforced composites.

Potential application	Examples
Automotive	Door panels, seat backs, headliners, dash boards, car door, Transport pallets, trunk liners, Decking, rear parcel shelves, spare tyre covers, other interior trim, spare-wheel pan, trim bin
Aircraft	Interior paneling
Construction	Railing, bridge, siding profiles
Household products and furniture	Table, chair, fencing elements, Door panels, interior panelling, Window frames, door-frame profiles, food tray, partition
Electrical & electronics	Mobile cases, laptops cases
Sports and leisure items	Sports and leisure items: Tennis Racket, bicycle, Frames, Snowboards

2.5.2 Bio-Medical Applications

The drawbacks of the traditional metallic material motivate the study for a new material for bio-engineering. These drawbacks include (1) osteoporosis causes of

stress-shielded effect, (2) increasing in the risk of refracture by drop in mechanical properties of recovered bone, (3) second surgery in order to avoid corrosion and infection, (4) radiotherapy impediment. Hence, fibre reinforced composites as replacement for the traditional metallic materials are becoming popular for the application of bone fixators.

2.5.2.1 Bone Fracture and Fixator

A bone fixator for bone repair used in orthopedics is a medical device for supporting damaged biological structures. Typically applying to a long bone, the main mechanical functions of bone fixators are (1) to transmit forces from one end of a bone to another and (2) to hold fracture bone ends together. It can protect the area of bone fracture and maintain the proper alignment of the bone fragments throughout the healing process. Knowledge of biomechanics including the bones response to different types of loads and their fracture patterns is a fundamental to diagnose the fracture of the long bone. After the assessment of morphological characteristics of fracture, the physician can assess the validity fracture therapy and fracture healing.

Fracture is an indication that the stresses within a structure excess the specific strength of material in the region of a failure (Pierce et al. 2004). Bone is weakest in shear, followed by tension, and compression (Tencer & Johnson 1994). These properties in bone are also time-dependent (viscoelasticity). Subsequently, when the load applied is high, a greater amount of energy is stored within the bone, resulting in a more severe fracture (Autefage 2000). Most long bone fractures are subjected to a combination of applied loads that produce a complex fracture

pattern (Tencer & Johnson 1994). Bone fractures, in general are divided into five major types, which are shear, tension, compression, bending and torsion. Such fracture types can happen individually or overlapped. A summary of bone fracture patterns is shown in fig. 2.9.

Appearance	Fracture Pattern	Load	Common sites	Energy
	Transverse	Bending	Long bone diaphysis	Low
	Spiral	Torsion	Long bone diaphysis frequently tibia and humerus	Low
	Oblique-transverse or butterfly	Compression + torsion	Femur, tibia, humerus	Mod
	Oblique	Compression + Bending + Torsion	Tibia-fibula, forearm	Mod
	Comminuted	Variable	Varible	High
	Diaphyseal impaction, metaphyseal compression	Compression	Intercondylar humerus, femur, tibial plafond	Variable

Figure 2.9. Summary of long bone fractures (Autefage 2000).

A bone fixator appears in the forms of pin, rod, screw and plate used to anchor fractured bones while healing. Nowadays, bone plate, is also called "osteosynthesis plate", is the most common internal fixation devices used in orthopedic surgery. All plates are classified into four groups (1) Neutralization plate, (2) buttress plate, (3) condylar plate and (4) compression plate according to their functions (Thakur 1997). Among all these plates, compression plate is the

most popular method for internal bone fixation. This plate is a narrow rectangular shape (or strip) with a curved cross-section that fits onto the bone surface contour. The plate is attached by screwing in such a way to create compression at the fracture site (Hoppenfeld & Murthy 2000). The primary roles of compression plate are:

1. To compact the fracture bone by forcing the interdigitating spicules together of the bone and increase the stability of the construct;

2. To reduce the spacing between the bone fragments to avoid bridging of new bone;

3. To protect the blood supply and

4. To utilize friction at the fracture surfaces to resist the tendency of the fragments to slide under torsion or shear (Thakur 1997).

Fibre reinforced composites for bone implant can be categorized into non-resorbable, partially resorbable, and fully resorbable. Fig. 2.10 is the summary of various applications of different polymer-based biomaterials. The advantages of these implants are not only limited to the mechanical properties which can be tailor-made to fit to the properties of the human bone. These polymeric implants are also possible to combine physiologically active components which accelerate or facilitate tissue healing (Rokkanen, Bostman & Hirvensalo 2000).

Dental Implant
CF/C, SiC/C

penial Post
CF/C, CF/Epoxy,
GF/Polyester

Arch Wlrn & Brackets
GF/PC, GF/PP,
GF/Ny!on, GF/PMMA

penial Bridgllf

UHMWPE/PMMA
CF/PMMA, GF/PMMA
KF/PMMA

Dental Restorative Materfal
Silica/BIS-GMA
HA/2.2"(4-methacryloxydiethoxyphenyl)

Bone Replacement Material
HAIPHB, HAIPEG·PHB
CFIPTFE, PET/PU, HAIHDPE
PET/PU, HA/PE, Blo Giass/PE,
Bio-Giass/PHB, Blo·Giass/PS, HAIPLA

Spine Cage. Plate, Rods.
Screws and Disc
CF/PEEK, CF/Epoxy, CF/PS
Bio-Giass/PU. Bio-Giass/PS.
PET/SR. PET/Hydrogel

Vascular Graft Cells/PTFE,
Cells/PET PET/Collagen,
PET/Gelatin PU/PU-PELA

Abdominal Wall Prosthesis
PET/PU, PET/Collagen

Finger Joint
PET/SR, CRUHMWPE

Total Hip Replacement
CF/Epoxy, CF/C, CFIPS, CF/PEEK,
CF/PTFE, CF/UHMWPE, CF/PE,
UHMWPEIUHMWPE

Intramedullary Nails
CF/LCP, CF/PEEK
GF/PEEK

Tendon / Ligamont
PET/PHEMA, KF/PMA, KF/PE
CF/ PTFE, CFIPLLA, GF/PU

Bone Cement
Bone part cles/PMMA, Titanium/PMMA,
UHMWPE/PMMA, GF/PMMA, CfJl>MIVIA•
KF/PMMA, PMMA/PMMA,
Bio-Giass!Bis-GMA

Cartilage Replacement
PET/PU, PTFE/PU, CF/PTFE
CF/C

Bone plate & Screws
CF/PEEK, CF/Epoxy,
CF/PMMA, CF/PP, CF/PS
CF/PLLA, CF/PLA, KF/PC
HA/PE, PLLA/PLDLA,
PGA/PGA

Total Knee Replacement
CF/UHMWPE
UHMWPE/UHMWPE

External Fixation
CF/ Epoxy

CF carbon fibers, C: carbon, GF: glass fibers, KF: kevlar fibers, PMMA: Polymethylmethaaylate, PS-polysulfone, PP: Polypropylene, UHMWPE: uHra-high.fllolecular weight polyathylene, PLDLA: poty(L-OL-llactide), PLLA: poly (L-lactic acid), PGA: polglyoolic acid, PC: polycarbonate, PEEK: polyetheretherl<elone; HA: hydroxyapatite, PMA: potymelhyllacryllate, BS-GMA: bis·phenol A glycidyl methacrylate, PU: pollyurethane, PTFE- polytetrafluoroethylene, PET: polyethyleneterephthallate, PEA: poltethylacrylate, SR: silicone rubber, PELA: Bloc!(Oll-i)Oiymer of lactic acid and polyethylene glycol, LCP: liquid crystalline pollymer, PHB: polyhydroxybutyrate. PEG: polyethyleneglycol PHEMA: poly(20hydroxyethylmethacrylate)

Figure 2.10. Various applications of different polymer-based biomaterials (Ramakrishna, Mayer & Wintermantel2001).

2.5.2.2 Bone repair

The three main phases of the fracture healing are overlapped and in generally, classified as (a) inflammatory phase (10%), (b) the reparative phase (40%) and (c) the remodeling phase (70%). The inflammatory phase lasts approximately 1 to 2 weeks. The reparative phase usually lasts several months. The finally stage of fracture healing is remodeling phase, which requires months to years for completion. Radiography is used to identify the healing process. During the inflammatory phase, the fracture line becomes visible as the necrotic material is removed. The fracture line then begins to disappear which starts in reparative phase and finally no longer visualized in the remodeling phase (Hoppenfeld & Murthy 2000). For biomedical applications, protein based natural fibre such as silkworm silk, feather and spider silk fibres are suggested rather than other type of plant based natural fibre. The researchers have found that silk is a kind of material which can promote the process of healing (Schneider et al. 2009; Wang 2006).

2.5.2.3 Requirements for biodegradable bone fixator

In general, several critical issues are guided on choosing appropriate natural fibre composites for biomedical and bioengineering applications,

1. Biodegradability: "Biodegradable" is prompted by the American Society for Testing of Materials (ASTM) and the International Standards Organization (ISO) to come up an official definition for biodegradable as follows: "capable of undergoing decomposition into carbon dioxide, methane, water,

inorganic compounds, or biomass in which the predominant mechanism is the enzymatic action of microorganisms, that can be measured by standard tests in a specified period of time, reflecting available disposal condition" (DiGregorio 2009);

2. Bioresorbability: It is referred to a material that upon placement within the human body starts to dissolve (resorbed) and is slowly replaced by advancing tissue (such as bone) (Ramakrishna, Mayer & Wintermantel 2001). Degradation and resorption of polymers in the human body generally occurs when the polymer chains are broken down through hydrolysis. The molecular weight of the material drops which is followed by the loss of mechanical strength and finally, loss of mass. The fixator loses its form in the second stage. The fixator breaks into particles as debris, which is rided by macrophages. Depending on the size of the particulates, they are phagocytosed for debris elimination and the byproducts are excreted by the kidneys and lungs (Ambrose & Clanton 2004).

3. Biocompatibility: The material must not disturb or induce un-welcoming repose from the hoist, but rather promote harmony and good tissue-fixator integration. An initial burst of inflammatory response is expected and is sometimes considered essential in the healing process (Teoh 2004);

4. Sterilizability: the material must be able to undergo sterilization. Sterilization techniques include gamma, gas (ethylene oxide (ETO)) and steam autoclaving (Teoh 2004);

5. Functionability: It is mainly dependent on the ability of the material to be shaped to suit a particular function. The material must therefore be able to be shaped economically using engineering fabrication processes (Teoh 2004);

6. Manufacturability: The manufacturability of the material that hinders the actual production of the medical devices (Teoh 2004) and,

7. Mechanical and thermal properties: The material needs to suffer the most of the loads during the bone repair. For an example, as the bending modulus of long bone is about 120-210MPa and Young''s modulus is 10 – 18GPa. The material should have similar modulus to (or larger than) bone to be repaired. Moreover, the material must suffer the human body temperature (Teoh 2004).

Chapter 3

Preliminary Study

3.1 Introduction

The prevailing utilization of light and strong structural materials has led to an increasing demand to the engineering industry on developing different types of advanced composites. Thus, the development of simple and low cost woven glass fibre composites with an improvement on their tensile and impact properties is suggested. As discussed in chapter 2, natural fibre is a high potential reinforcing material into polymer for the development of various structural or non-structural components. The main advantages of using this fibre instead of traditional materials like steel and concrete include its light in weight properties, high strength to weight ratio and good resistance in fracture in general (along their fibre direction(s)). Besides, natural fibre can be treated as the inter-laminar reinforcement for fabric type composites. Therefore, the hybridization of a glass fibre reinforced composite is achieved by using short silkworm silk fibres as a medium to enhance its cross-ply strength.

3.2   Ecological Application: Silkworm Silk Fibre as Inter-laminar Reinforcement

The composites which are made by strong fibres (carbon, glass or aramid) and soft polymer (epoxy, polyester, Vinyl-ester and others), can produce their properties are very strong in tension, and also good in energy absorption. Woven fibre is the most common type of reinforcement to make glass fibre reinforced polymer composite due to its simplicity in composites" lay-up process and strength estimation by using simple classical lamination theories. However, there are some drawbacks which hinder the attraction of using these composites such as (1) weak in the out-of-plane direction as compared with their in-plane direction (Gibson 1994) and (2) high energy consumption is required during the manufacturing process. Compared with other isotropic materials, the mechanical properties of laminate composites are behaved anisotropically. Residual stresses may also be easily induced during the manufacturing process due to differential coefficients of thermal expansion (CTE) between fibre and matrix.

Since the fabrics have to be laid up one-by-one with being isolated by a layer of matrix (described ideally), the out-of-plane properties are dominated by the properties of matrix and its bonding efficiency with glass fibres. To improve the out-of-plane properties of the composites with minimizing the cost involvement, low cost short silkworm silk fibres would be a good material to be used, like z-pins as inter-laminar reinforcement.

Crucially, the advantage of a well designed hybrid composite is the combination of the properties of their respective constituents and even the addition of qualities that neither their constituent possesses. Therefore, the short fibre inter-laminar

reinforcement technique, as a method which is simpler, cheaper and unnecessary of imposing an extra complicated process in existing manufacturing process is proposed.

The hybrid composites ars classified as sandwich type, intra-ply type and inter-ply type. Fig. 3.1 illustrates the classification of the fibre hybrid composites. Sandwich-type hybrid composites normally consist of two or more different types of layers to form light weight structures. Typically, this type of structures is used to sustain bending loads (the core is made by a light material such as foam while the skins are made by high strength fibre composite materials) (Saha & Banerjee 1996; Subhash & Michael 1996).

Intra-ply is defined as the layer of fabric weaved by different types of fibres (Fua et al. 2002; Manders & Bader 1981), its purpose is to design a composite with the strengths are different in both longitudinal and lateral directions. The common practice is to weave carbon fibres in 0° direction (main loading direction) and glass fibres are in 90° direction to form a fabric. Inter-ply fibre hybrid composite is often called "inter-laminar reinforcement composite". This type of hybrid composite is clarified as only one type of fibre made up of individual piles, but specific type of material is dispersed in between the plies to improve their out-of-plane properties.

(a)

(b)   (c)
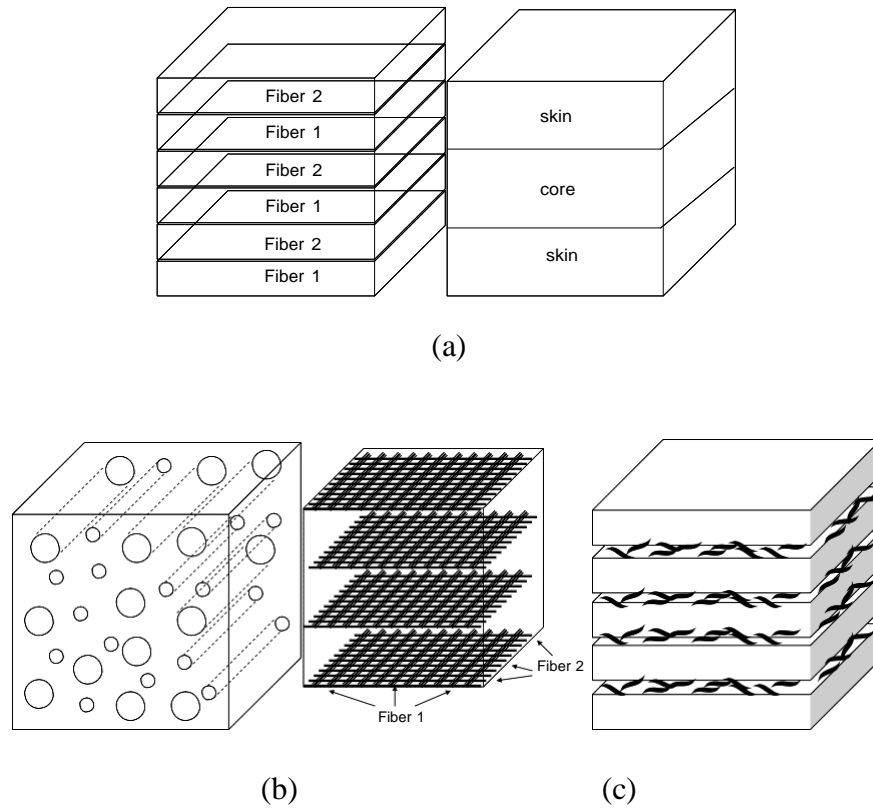
Figure 3.1. (a) Sandwich type, (b) Intra-ply type and (c) Inter-ply type.

In general, the failure mechanisms of short fibre reinforced polymers are in semi-elastic failure, fibre pullout or short fibre breakage which effect in increasing the energy absorption capability. By using the similar principle in long fibre reinforced polymer composites, it could enhance the fracture toughness of the composites as the short fibre can be used to reinforce the strength between different plies and also absorb energy during foreign object impact (Walker, Sohn & Hu 2002). As aforementioned, for fabric reinforced composites, the mechanical properties are mainly governed by the properties of matrix, it therefore by appropriately adding short fibres can improve the bonding strength between the plies and thus, the out-of-plane properties of the composites (Lin & Jang 1990).

Although many research have been conducted by using carbon, glass or kevlar fibres as short fibre reinforcements for laminate composites, their raw materials cost and pre-processing time are concerns to most composite manufacturers, particularly in the consideration of producing composites with good out-of-plane and impact properties.

Natural fibres including plant-based, such as hemp, sisal and bamboo, and animal-based such as spider silk and silkworm silk, are commonly used as reinforcements for many polymer-based materials (Arbelaiz & Fernandez 2005). It has been proved that the mechanical properties of natural fibre reinforced polymer composites are much better than pure polymers (table 3.1). Therefore, they are potential candidates for serving the purpose of reinforcing laminate composites. Moreover, compared with other type of artificial inter-laminar short fibre, natural fibre such as silkworm silk fibre which is natural available.

Table 3.1. Comparison of natural fibre reinforcement materials with E-glass.

Properties	E-glass	Flax	Jute	Hemp	Sisal	Silk	Coir
Density (g/cm^3)	2.57	1.40	1.46	1.48	1.33	1.23-1.34	1.25
Tensile strength (MPa)	3450	800-1500	400-800	550-900	600-700	157	230
Tensile Modulus (GPa)	72	60-80	10-30	70	38	103	6
Moisture absorption (wt %)	None	7	12	8	11	7	10

Many researchers attempted to use short fibre to reinforce composites made by woven fibres in order to increase their fracture energy (Singh & Partridge 1995; Zhihang & Santare 2008; Park & Kim 1997;). However, few of them focused on the tensile and impact properties of these composites reinforced by short natural fibres to form a hybrid composite. Among numerous natural fibres, silkworm silk fibre is a natural protein fibre which is biodegradable and highly crystalline with a well-aligned structure. Moreover, silkworm silk fibre has a high extensibility among natural fibres. This chapter focuses on the development on a hybrid composite that is low cost, light weight with improved tensile modulus and inter-laminar properties, and possesses adequate strength and elongation at break for different engineering applications. In this work, woven glass fibre and chopped silkworm silk fibre were used to fabricate the hybrid composite. The mechanical properties of the hybrid composite compared with a neat woven glass fibre/epoxy sample were studied. The optimized fraction of the short silkworm silk fibre and fabrication method of the composite in order to achieve the maximal strength is also discussed.

3.2.1 Experimental Set-up

Plain weave glass fabrics (style AF218) were supplied from COLAN AUSTRALIA. Epoxy resin AA0341 A and Hardener AA0341 B supplied by CHEMATCO LTD were used (mixture ratio = 4:1) to form matrix for the composite. Tussah silk fibre supplied by Ocean Verve Ltd. was used as inter-laminar reinforcement. The silkworm silk fibres were cut equally into 6 mm to prevent them were stressed plastically during fabrication process. Composite

samples were made by hand lay-up process followed by vacuum bagging as shown in fig. 3.2 and fig. 3.3. Short silkworm silk fibres were distributed evenly on the surface of each layer after resin had applied. A total of 7 plies of glass fabrics were used to make the hybrid composite. Table 3.2 shows the density (g/m^2) of silkworm silk fibre and the thickness of samples with different weight percentages of silkworm silk fibre.
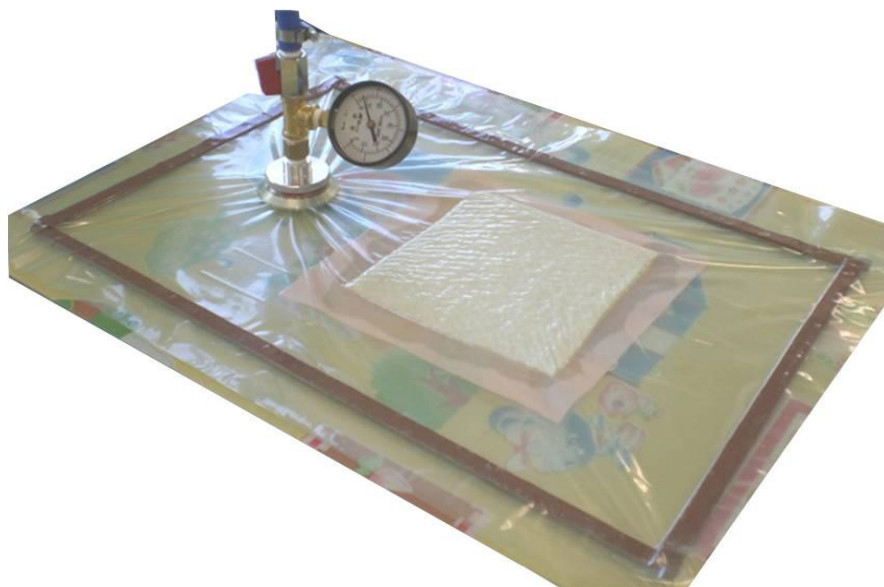
Figure 3.2. Setup of hand lay-up fabrication of silkworm silk fibre/ woven glass fibre reinforced composites.

1. Platform
2. Release film
3. Sealant tape
4. Peel ply
5. Perforated release film
6. Breather cloth
7. Composite
8. Vacuum valve
9. Vacuum hose
10. Bagging film
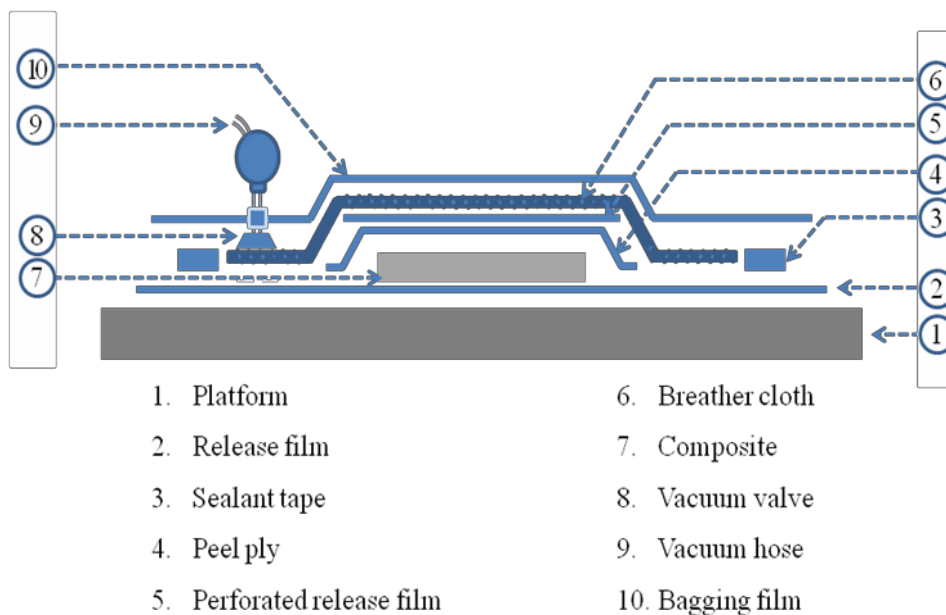
Figure 3.3. Set up of sample"s fabrication.

Table 3.2. Density of the short silkworm silk fibre and the thickness of samples.

Specimen Type	GFR	GF with 0.6% silkworm silk fibre	GF with 0.5% silkworm silk fibre	GF with 0.4% silkworm silk fibre	GF with 0.3% silkworm silk fibre
Density (g/m2)	0	28.571	22.857	17.143	11.429
Thickness (mm)	1.565	1.711	1.706	1.771	1.768

3.2.2   Mechanical Properties

Hand lay-up for composites fabrication has been widely used for many years. The advantages are not only limited to simple principles to teach, but also low cost tooling, if room-temperature cure resins are used. The choice of suppliers and material types is widely. High fibre volume fraction can be achieved and long

fibre can be used as compared with the use of spray lay-up technique. However, the quality (including mixing, fibre orientation, laminate quality) is very dependent on the skill of workmanship (practically, low resin/high fibre content cannot usually be achieved). Resins used in the fabrication need to be low in viscosity to be workable by hand. This resin is commonly used in fabrication because it has higher tendency to penetrate clothing but, have higher potential to be more harmful to the worker than higher molecular weight products.

3.2.2.1 Tensile test

The tensile property test was carried out under an ambient condition. Tensile property test is an evaluation process for characterization of mechanical and materials performance, especially strength, modulus and ductility of materials. The test was conducted by using MTS Alliance RT/50 with the cross-head speed of 1 mm/min. An extensometer was used for measurement of a small change in linear dimension. All samples were cut into the dimension of 200mm x 25mm for making testing samples as shown in fig. 3.4. To avoid any stress concentration induced at both ends of the samples during testing, four 25mm x 25mm plastic taps were glued on both end sections of the samples. The extensometer with a gauge length of 50 mm was attached to the centre of specimens to measure the strain response. The testing procedure was followed according to the ASTM D3039.
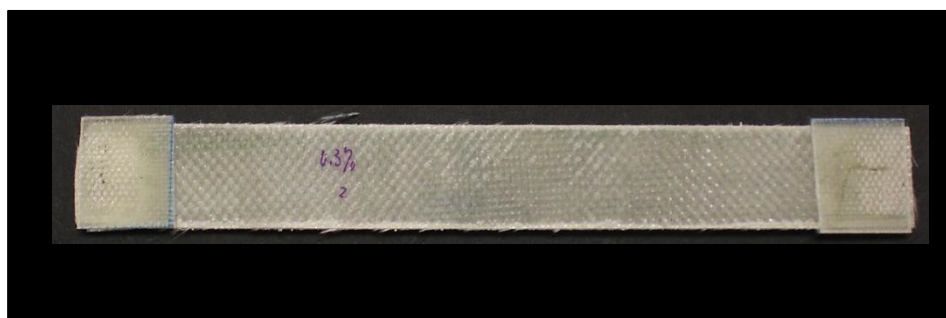
Figure 3.4. Silkworm silk fibre/ woven glass fibre reinforced composite for tensile testing.

Fig. 3.5 is fractured samples captured after the test. The Young's modulus of the hybrid composites is defined as the slope of the stress–strain curve in their initial linear-elastic region. It is observed in fig. 3.6 that the tensile strengths are found to increase with the increase of the content of short silkworm silk fibre. However, for the samples with less than 0.5 wt% of silkworm silk fibre, their strength is lower than that of a neat (glass fibre/epoxy) sample. The highest tensile strength was reached for the sample with 0.5 wt% of silkworm silk fibre, over 16% increase of strength as compared with the neat sample.

In terms of the Young"s moduli of the samples, fig. 3.7 shows that the Young"s modulus increases dramatically when silkworm silk fibres were added into the glass fibre composite. With the use of 0.3 wt%, 0.4 wt%, 0.5 wt% and 0.6 wt% of the silkworm silk fibres, the increase of the Young"s moduli are 15%, 51%, 40% and 15% respectively. In this figure, it is obvious that the Young"s modulus decreases when the amount of silkworm silk fibres increase beyond 0.4 wt%. Fig.

3.8 shows the fracture surface of the sample with 0.4 wt% of silkworm silk fibres and it also indicates that the silkworm silk fibres could be effectively used to link up two plies together. Glass fibre breakage is obviously seen at the top (tow) of the figure and silkworm silk fibres penetrated through the top and bottom plies.
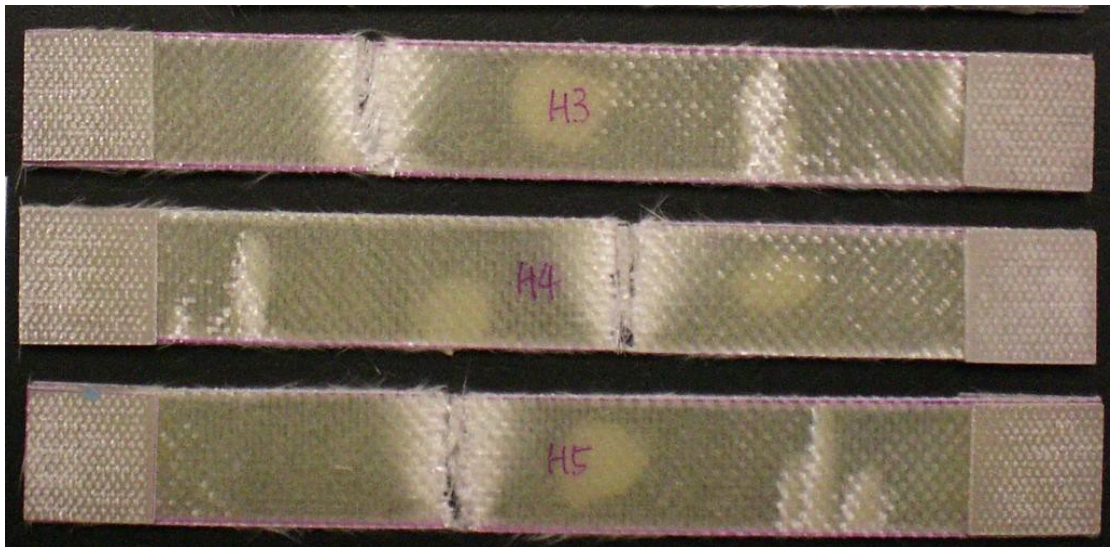
Figure 3.5. Fractured samples.
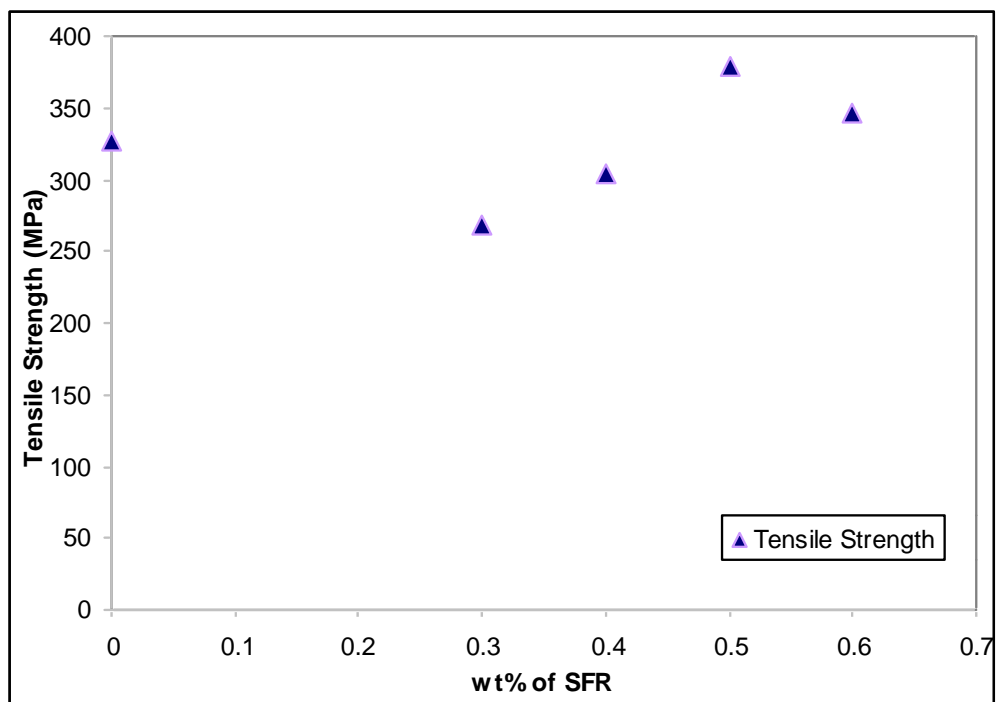
Figure 3.6. Tensile Strength (MPa) versus content of short silkworm silk fibre composite samples.
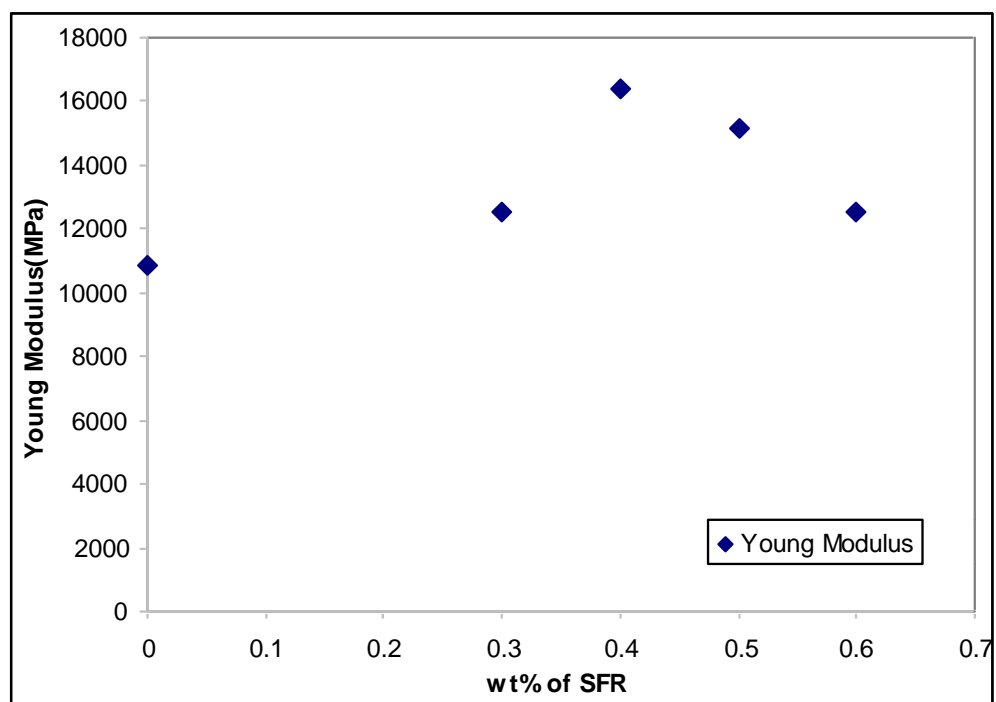
Figure 3.7. Young"s modulus (MPa) of the composites versus content of short silkworm silk fibre composite samples.
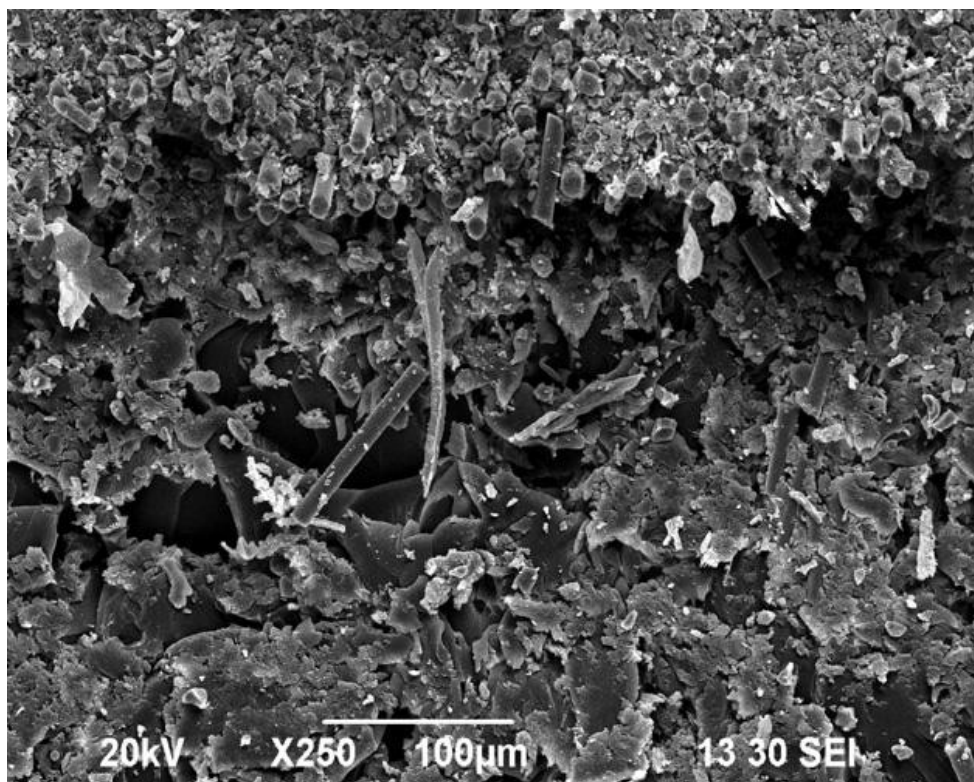
Figure 3.8. SEM micrograph shows that short silkworm silk fibres link two ply of glass fabric.

Based on the results shown, it can be seen that increasing the amount of silkworm silk fibres to a certain percentage may cause the reduction of the amount of matrix filling the gap between plies which eventually caused the poor mechanical properties of the samples. Fig. 3.9 shows the adverse effect on the elongation at break of the samples with different wt% of silkworm silk fibres. Therefore, their failure mechanism may be governed by three key factors, they are (i) bonding strength between the matrix and glass fibre; (ii) bonding strength between the matrix and silkworm silk fibre and (iii) bridging strength between glass fabrics by the silkworm silk fibres.
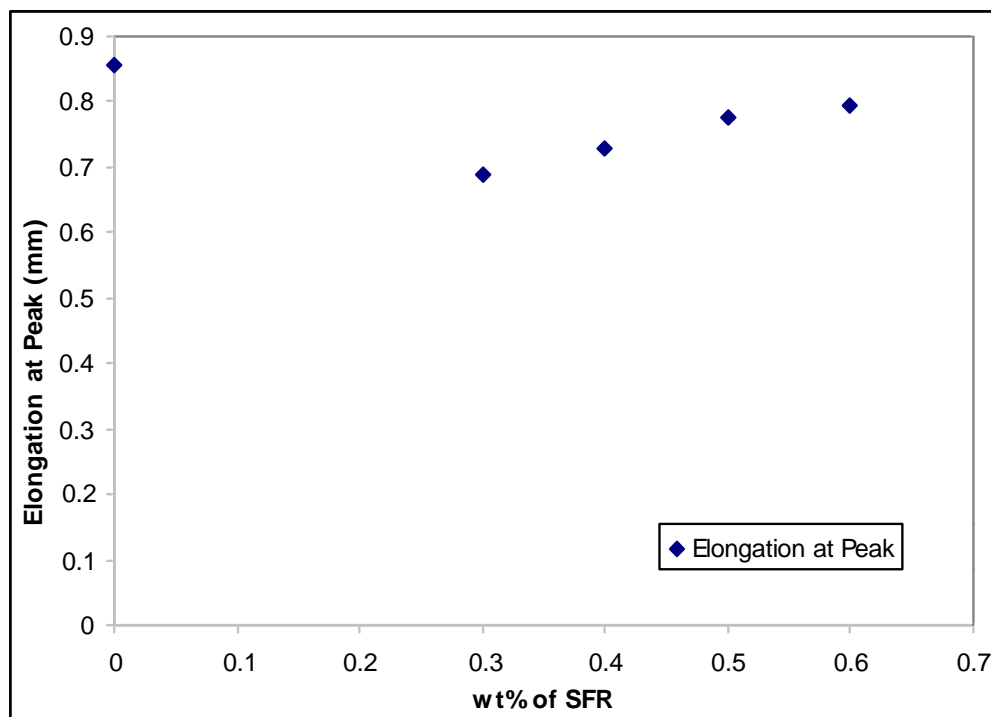
Figure 3.9. Elongation (mm) at breakversus content of short silkworm silk fibre composite samples.

Principally, a composite sample with high tensile strength reflects that the stress transfer properties between the fibre and matrix were improved. It was because the silkworm silk fibres can act as the stress transfer media between the woven glass fibre and the matrix, and perhaps, from one ply to another. Some silkworm silk fibres, during the layup process may cross through the fabrics to form a network joining two fabrics together. Besides, more tortuous paths of crack growth for increasing fracture surface area of the composite containing short silkworm silk fibre is another reason for enhancing tensile strength. Such short fibre bridging effect implies that unbroken in-plane randomly oriented short silkworm silk fibres link to the opposite fracture surface at the bridged zone. Therefore, more energy is needed to produce the crack propagation. However, a

problem is raised in fibre reinforced polymer composites is the formation of resin rich regions inside the composites. It may not only lead to the low fracture toughness of the composites but also to other undesirable effects toward the mechanical properties.

As mentioned, short silkworm silk fibres were used to form a hybrid composite in this project and their aim is to overcome poor inter-laminar strength across plies (Youjiang & Dongming 1995). During the layup process, vacuum bagging technique was used to remove excessive air inside the composite. This technique also allows proper pressure applied onto the top of the composite in order to ensure the thickness was uniform. As shown in fig. 3.6 and 3.7, the Young"s modulus and tensile strength decrease for the silkworm silk fibre content exceeds 0.6 wt%. It indicates that the silkworm silk fibres acted as a small composite unit on its own with an inner structure prone to be broken by stress transferred from the matrix at the maximum strength. Thus, they formed internal flaws which in turn acted as a crack initiator of the composite (Khan & Ganster 2009).

3.2.2.2 I-Zod impact test

The impact test was conducted by using INSTRON DDYNATUP 9250HV. Instron impact test was used to characterize the impact performance of various materials and components. The impact test utilizes drop weight style in the impact testing systems to obtain the impact properties including force-time curve, force-displacement, fracture energy and propagation energy. All samples were cut to the final dimension of 100mm x 100mm for testing. The drop height was set at 0.8 m

from the top surface of specimens. The mass of striker was 15.98 kg.

Fig. 3.10 shows the fracture of the impact test's sample. Fig. 3.11 shows the relationship between force and displacement of testing samples during the impact process. Fig. 3.12 shows the load and energy curves captured from the impact test and the results are summarized in table 3.3. It shows that increasing the amount of silkworm silk fibres in the composite results in increasing the maximum load, the crack initiation energy (Em), the propagation energy (Ep), absorb energy (Ea) proportionally. Ductility index (DI) has been proposed by Beaumont et al. which is the ratio of the propagation energy to the initiation energy for a sample under impact (Beaumont, Riewald & Zweben 1974). According to the table 3.3, most of the hybrid composites show higher DI value than a control neat sample. However, the DI value is not proportional to the total fracture energy which is same as the finding from Lin et al. (Lin & Jang 1990).
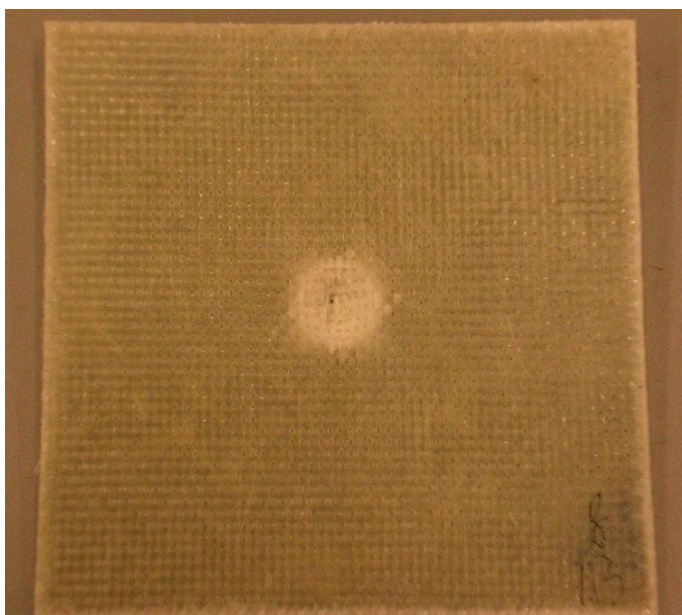
Figure 3.10. Silkworm silk fibre reinforced woven glass fibre composite after impact test.

Table 3.3. Impact data for control glass fibre and short silkworm silk fibre reinforced glass fibre composites.

Sample	Pmax (kN)	Em (J)	Ep (J)	Vi (m/s)	Ea (J)	Ei (J)	DI
GFR (Control)	2.633	9.194	3.641	1.235	14.713	15.224	0.324
GF with 0.3% silkworm silk fibre	2.683	9.405	5.335	1.233	14.724	15.243	0.568
GF with 0.4% silkworm silk fibre	2.729	10.116	5.511	1.24	14.805	15.498	0.543
GF with 0.5% silkworm silk fibre	2.895	10.752	5.695	1.233	14.854	15.283	0.493
GF with 0.6% silkworm silk fibre	2.727	9.95	4.658	1.239	14.357	15.316	0.474

Pmax is the Peak load, Em is the crack initiation energy, Ep is the propagation energy, Vi is the impact velocity, Ea is the absorbed energy, E I is the total impact energy and DI is the ductility index, T is the total time of the impact test.

Therefore, it is proved that the short fibres could play an important role in absorbing impact energy through their elastic-deformation and bridging plies together. However, when the content of silkworm silk fibres exceeded 0.5 wt%, it is found that the maximum propagation energy decreased significantly. This may be due to the difficulty in wetting up the silkworm silk fibres and glass fibres as the viscosity increased during the manufacturing process, and thus, induced more voids inside the composite.
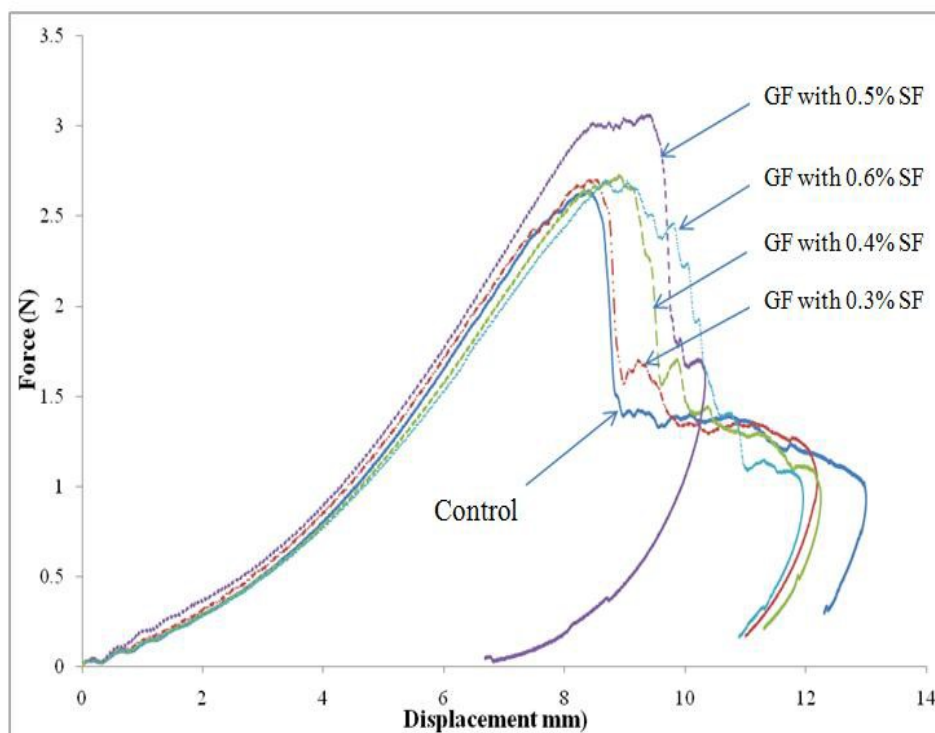
Figure 3.11. Froce- displacement curves for the impact test samples.

In fig 3.11, it is found that DI increases by 75% for the composite with silkworm silk fibre content of 0.3wt%. This result shows that the hybrid composite can absorb more impact energy as compared with the neat sample, i.e. more incident energy can be dissipated into the hybrid composite (Lin & Jang 1990).
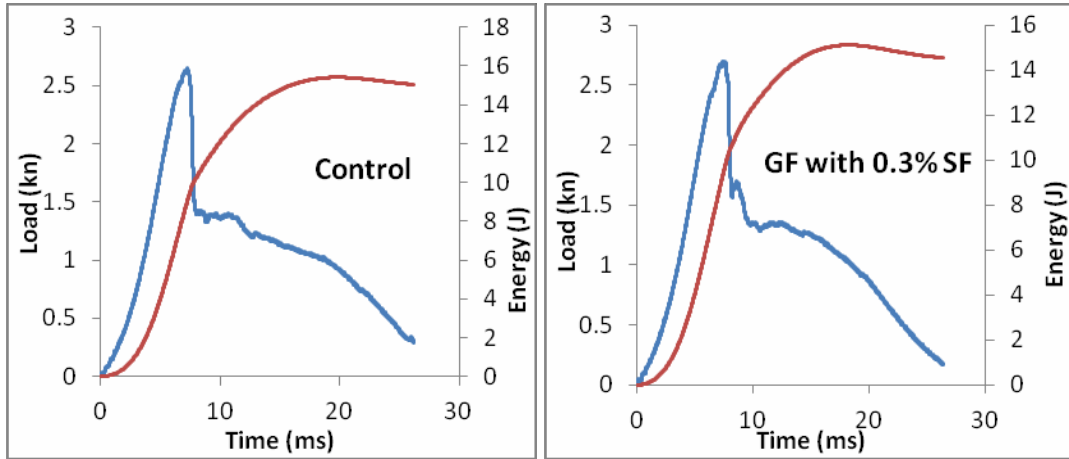
(a)

(b)
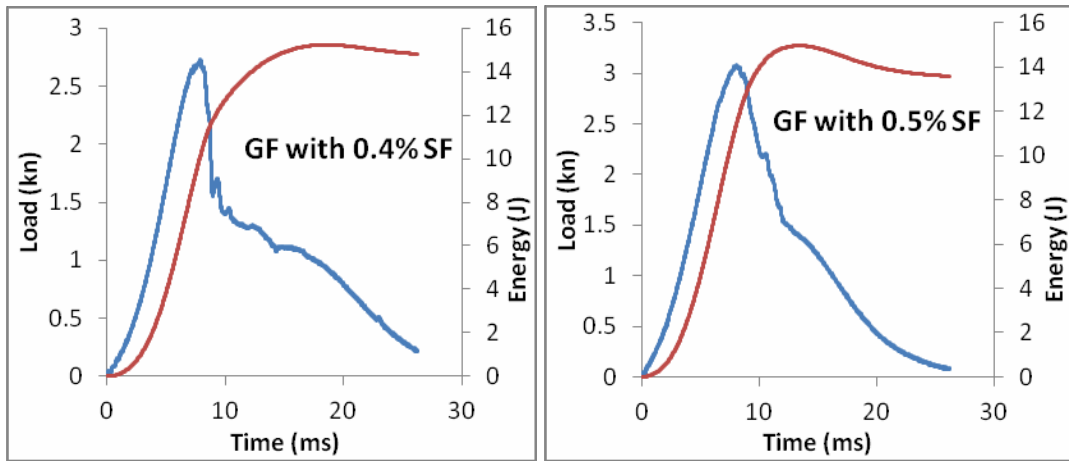
(c)

(d)
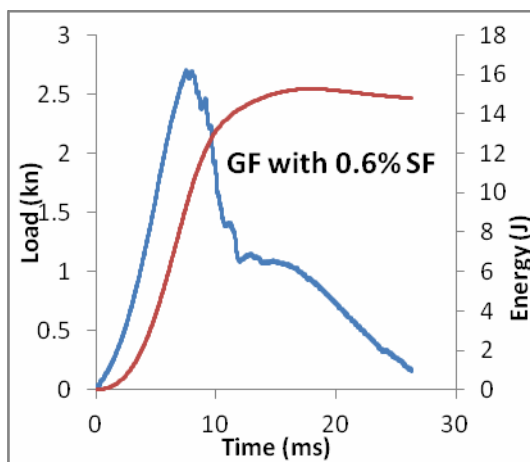
(e)

Figure 3.12. Load and energy history curves of the composite containing short silkworm silk fibre (a) control sample (0 wt% short fibre), (b) Glass fibre with 0.3 wt% short silkworm silk fibre, (c) Glass fibre with 0.4 wt% short silkworm silk fibre, (d) Glass fibre with 0.5 wt% short silkworm silk fibre & (e) Glass fibre with 0.6 wt% short silkworm silk fibre.

The composite was constructed of woven fibres which are stacked together with chopped silkworm silk fibres. The goal of using silkworm silk fibres is to produce strong inter-laminar properties of the composites. The improvement of delamination by chopped silkworm silk fibres can be detected with an analytical tool called C-mode scanning acoustic microscopy (C-SAM). The model of C-SAM used is Sonix L/HF – 200. The scanning area is 152 mm x 152 mm. This instrument incorporates a reflection, pulse-echo technique that employs a focused transducer lens to generate and receive the ultrasound signals from beneath the surface of the sample (NASA-Electronic 2005). Fig. 3.13 shows the C-scan images of neat sample and a testing sample with 0.5 wt% of silkworm silk fibres after impact. It is obvious that penetration damage appears in the sample without being reinforced by silkworm silk fibres while the hybrid composite shows no penetration damage and only slight delamination appeares.
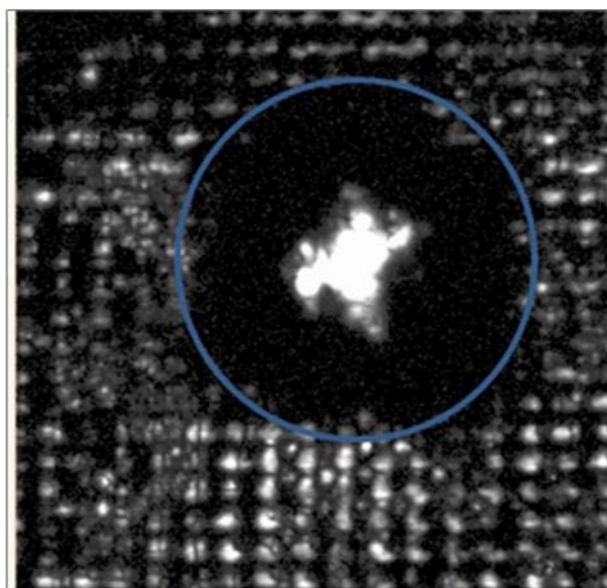
(a)
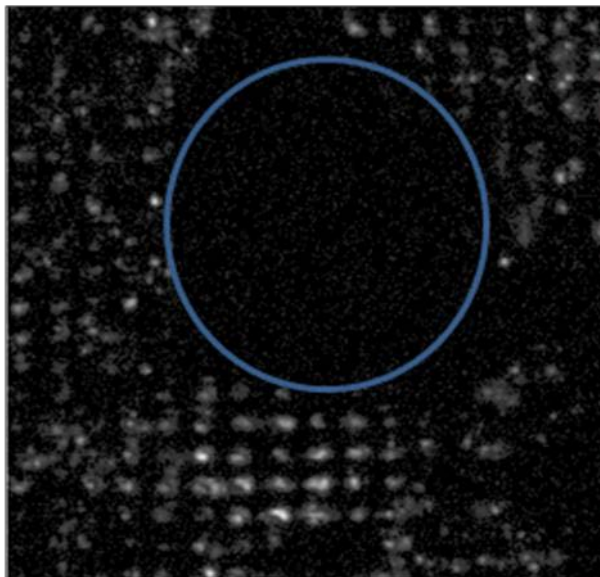
(b)

Figure 3.13. C-scan of (a) neat sample, (b) 0.5wt % short silkworm silk fibre reinforced glass fibre composite.

Optical microscope is an instrument utilized visible light, to obtain an enlarged image of a small object. Generally, it consists of a light source, a condenser, an objective lens, and an eyepiece, which can be replaced by a recording device. Fig. 3.14 (a) & (b) are taken by the optical microscope which show short silkworm silk fibres are placed in between two ply of glass fibre. These silkworm silk fibres are also attached to the woven glass fibre.
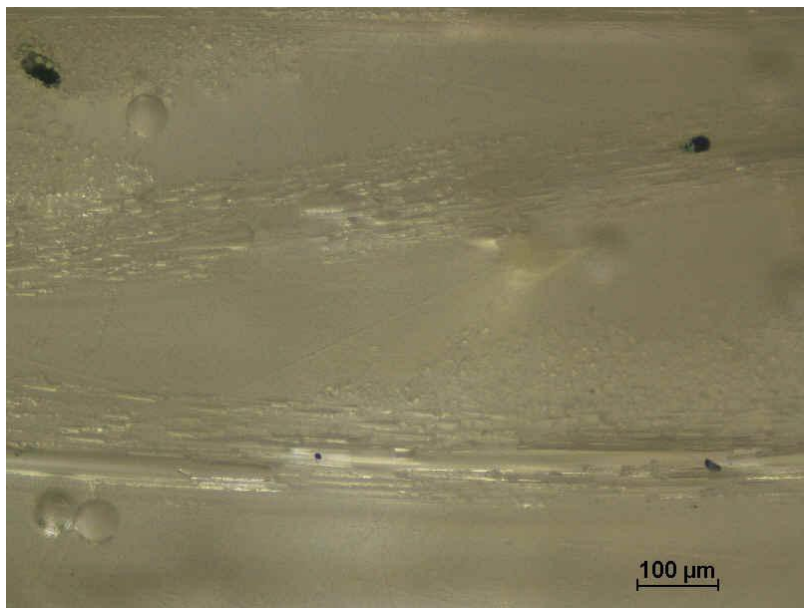
(a)
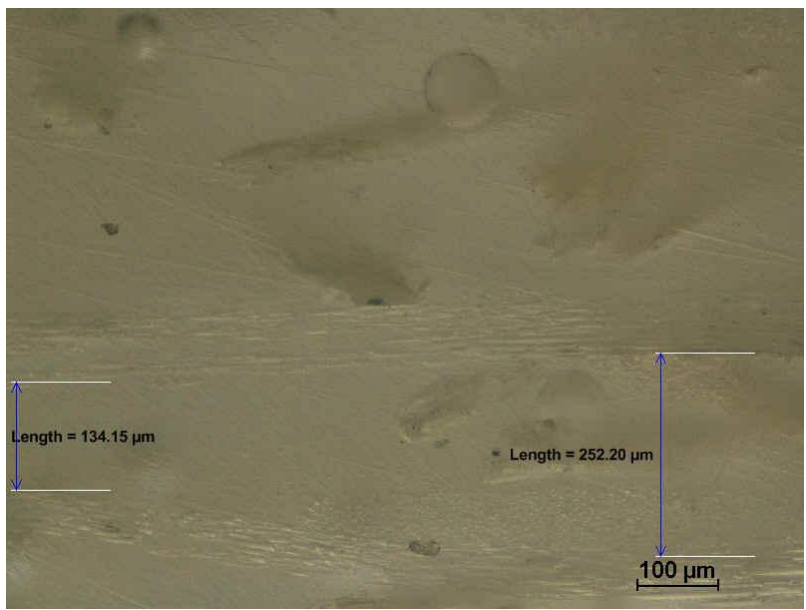
(b)

Figure 3.14. (a) & (b) **S**hort silkworm silk fibres are placed in between two ply of glass fibre and attached to the woven glass fibre taken by the optical microscope.

The hybrid composite for combination of two types of fibres results in reduction of the effects of their less desirable properties and consequently balances of their

pros and cons properties in their inherently constitutional composite materials. Short silkworm silk fibres were introduced into a woven fibre reinforced polymer composite to form the hybrid composite which possesses better Young"s modulus and impact resistance properties. The mechanical properties enhancement of the hybrid composite was due to the silkworm silk fibre acted as a media for stress transfer from one ply to another. Based on the results shown, it indicated that the maximum Young"s modulus and ductility index (DI) of the hybrid composite increased by 50 % and 75 %, respectively as compared with the neat one. Furthermore, the visual examination on drop-weight test samples proved that the impact resistance of the silkworm silk reinforced composite was better than that of the neat sample. According to the results obtained, it was found that the addition of 0.5 wt% short silkworm silk fibre into glass fibre composite was shown to be the advisable reinforcement content to achieve better tensile and impact strengths.

Chapter 4

Properties of Domestic and Wild Type of Silkworm Silk Fibres

4.1 Introduction

In this chapter, mechanical properties of Bombyx mori, twisted Bombyx mori, and Tussah silk fibres were investigated. Their ultimate tensile strength, elongation at break, and Young"s modulus were examined through the uniaxial tensile test on a single fibre. Scanning electron microscopy(SEM) was used to observe the morphology of two different types of silkworm silk fibre, and to measure their apparent diameters in order to determine the cross-sectional area of the silkworm silk fibre for stress-strain analysis. Weibull analysis was also used to quantify the tensile strength reproducibility of the silkworm silk fibre.

4.2 Different Types of Silkworm Silk Fibres

One of the most common silks in the world is Bombyx mori silk which is raised domestically. Domesticated silk moth needs to be bred under human, captive

conditions. It means that the life of Bombyx mori moth is dependent on human for food, water and shelter. Other than domestic silk, there are over 500 species of silkworms that look after themselves in the wild. The examples of the silkworm moth are shown in fig. 4.1.

Figure 4.1 A Bombyx silkmoth surrounded by different types of cocoons. Clockwise from top: four strains of Bombyx, Dupion Bombyx cocoons, Tensan, Eri, Tussah, Polyphemus, and Cecropia (Cook 2006).

Domesticated Bombyx mori silkworm is usually white toned and more reproducible. Wild silkworms live naturally in tropical or semitropical forests and eat all kinds of leaves from different trees, which are rich in tannin, so, their fibre is beige to brownish toned. The shape of the ordinary Tussah silk fibre is in a flat

triangular form. Moreover, the fibre is fine, high ductility and strong. The ability of light reflection itself makes the whole fibre shiny. This section is aimed at characterizing the tensile properties of domesticated and wild silkworm silk fibres that originated from different spinning conditions.

4.3 Experimental Set-up

Raw silkworm silk fibres with two different silkworm-raising processes, cocoon producing and spinning conditions were tested in this study: (i) Bombyx mori; (ii) twisted Bombyx mori; and (iii) Tussah silk fibres. For silkworm silk fibre obtained from cocoon, a degumming treatment is needed to remove the sericin coating from cocoon structures to obtain long continuous fibres.

The determination of the stress-strain relationship requires the measurement of cross-sectional area of tested samples. Therefore, before the tensile testing, SEM was used to observe the morphology of the Bombyx mori and Tussah silk fibres, as well as to examine their fibre diameter in average. SEM is a microscope that uses electrons rather light wave to form an image. It employs vary number of possible modes or techniques for micro characterization. The SEM used in this report was the model JEOL JSM-6490 SEM. A nonconductive sample was coated by a thin gold in order to be observed by SEM. Coating is used because it can prevent any charge-up on sample‟s surface. The nonconductive sample might build up negative charge on the sample surface and deflect the incident electron beam so that the image would be ruined. Moreover, the gold coating layer can increase a secondary electron emission.

The mean or apparent fibre diameter was estimated from SEM images taken at five different regions along the length of each fibre. Two different orientations (0° and 90°) were used to estimate the apparent diameter of silkworm silk fibre.

A tensile test was then performed to compare the mechanical properties of the cocoon spun Bombyx mori and Tussah silk fibres. Samples were randomly selected from a bundle of fibres and 10 contiguous experimental samples were used from each of the selected fibre. This sampling method can avoid high intrinsic scatter of the test data for the similarity of the tensile properties of consecutive samples, which is commonly used for spider and silkworm silk fibres. Silkworm silk fibre was cut gently into short fibre fractions in the length of 70mm in order to make sure that the fibre was not stressed plastically during the process.

Every chopped fibre was mounted and taped across a hole, which is 30mm long, of a rectangular cardboard which was fixed in an Instron mechanical testing machine. The fibre gauge length was 30mm between the two grips of the machine. The cardboard was then cut along the dotted lines and separated into two parts to ensure tensile loading was completely transmitted to the fibre during test as shown in fig. 4.2. All tests were conducted at a rate of 1 mm/min under ambient condition of 22^oC and 45% humidity.
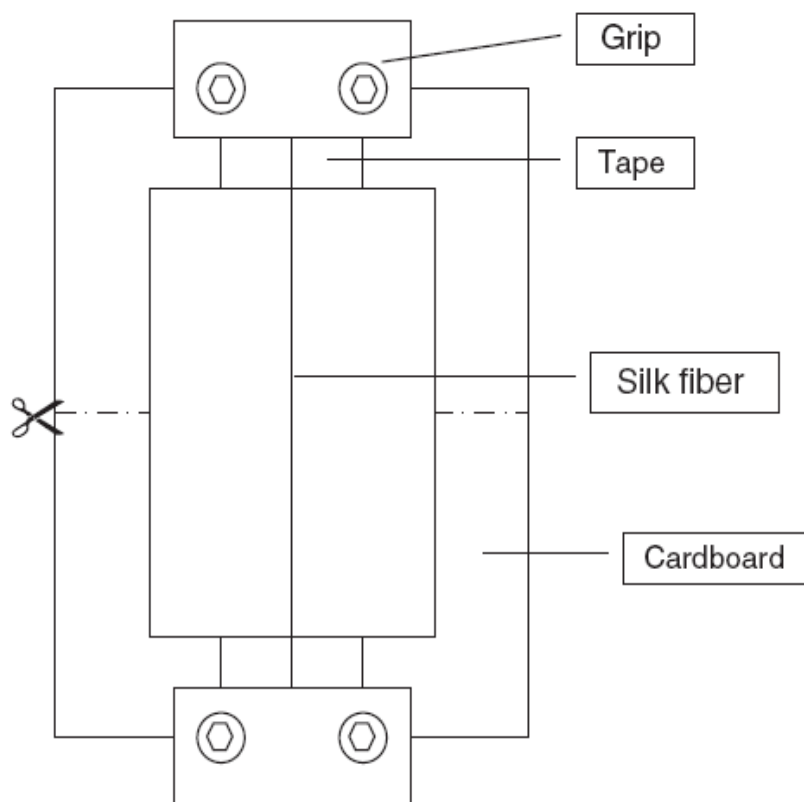
Figure 4.2. Experimental set up for tensile test of silkworm silk fibre (Rigueiro et al.

1998)

4.4   Results and Discussion

Due to the different silkworm-raising processes, cocoon-producing and spinning conditions of Bombyx mori and Tussah silk fibres, and the requirement of fibre cross-sectional area for converting the load-extension data into stress-strain analysis, the technique of SEM was used to observe the morphology of fibre surface and to measure the apparent diameters of different types of silkworm silk fibre. The anisotropy of silkworm silk fibre was calculated by the ratio of the diameter at 0° (or 90°) to the diameter at 90° (or 0°) orientations, i.e., the larger

82

diameter to the smaller diameter according to the measurement. Table 4.1 shows the averaged diameters of the six Bombyx mori and Tussah silk fibres at different orientations and the anisotropy results of each fibre. Fig. 4.3 and 4.4 show some of the selected micrographs of different silkworm silk fibre orientations.

Table 4.1. Geometrical parameters of Bombyx mori and Tussah silk fibres.

Fibre samples	Fibres	Diameter at 0° (µm)	Diameter at 90° (µm)	Anisotropy
Bombyx mori silk	1	328.3	243.2	1.35
	2	261.5	200.0	1.31
	3	312.3	228.2	1.37
Tussah silk	1	77.2	109.9	1.42
	2	63.4	86.5	1.36
	3	120.1	102.0	1.18
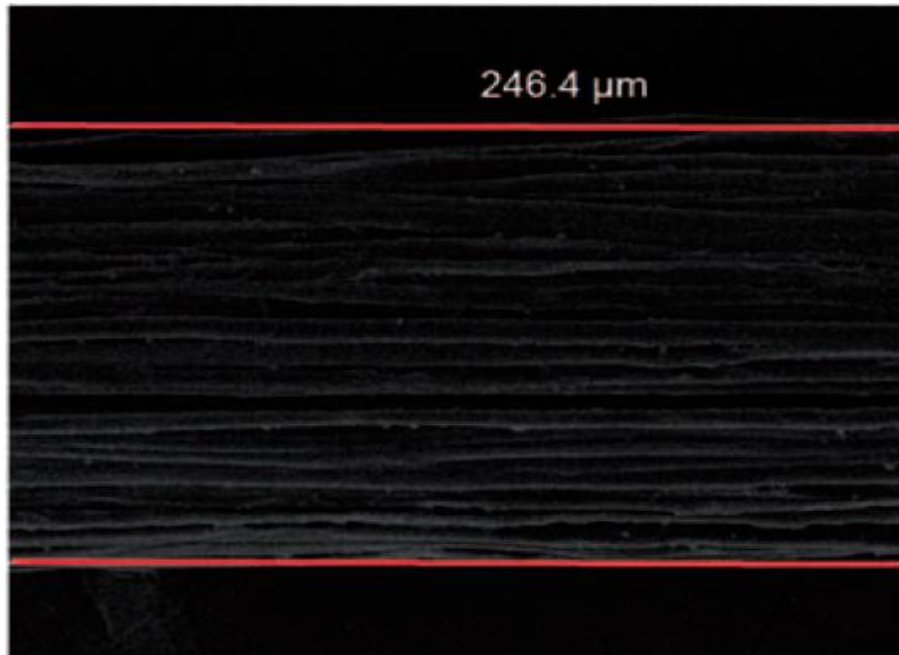
(a)
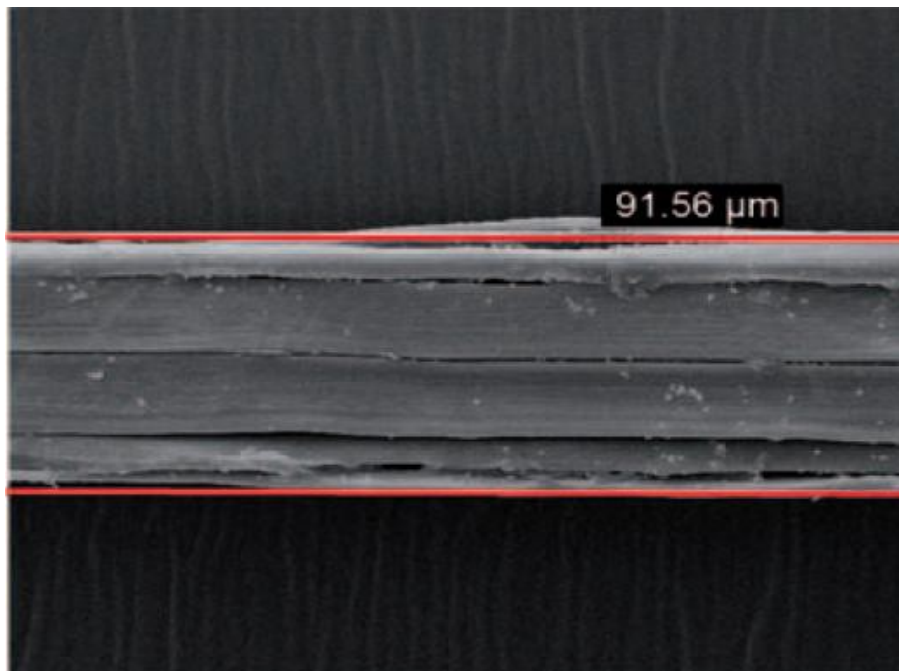
(b)

Figure 4.3. Appearances and diameters of (a) Bombyx mori silk fibre and (b) Tussah silk fibre (on the right) at 0° orientation.
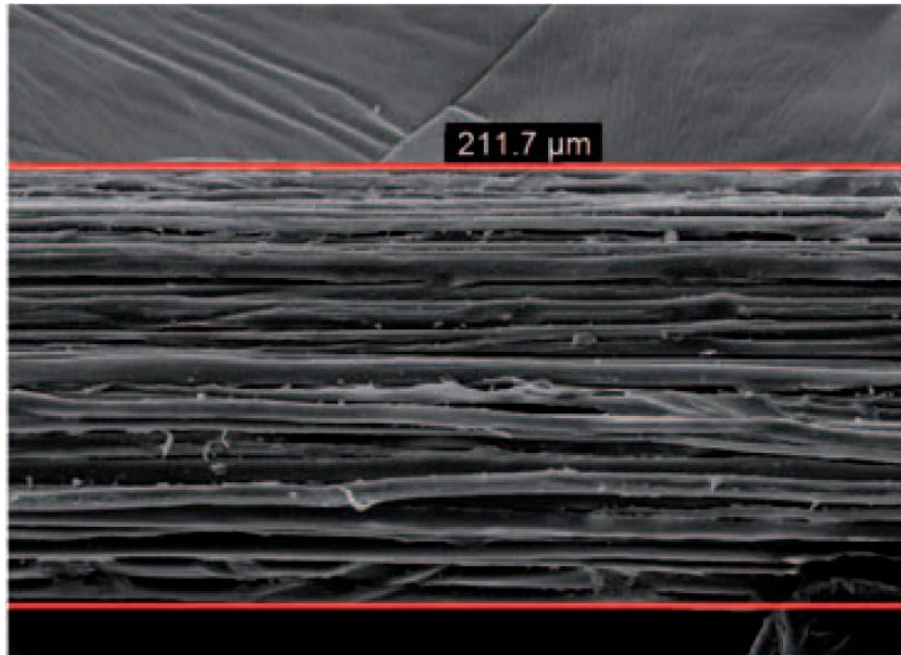
(a)
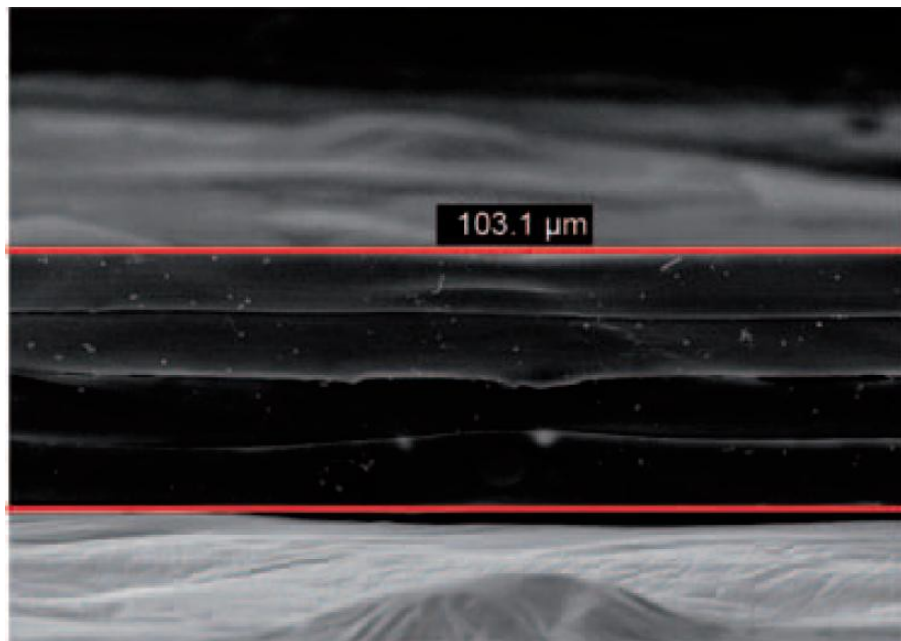
(b)

Figure 4.4. Appearances and diameters of Bombyx mori silk fibre (on the left), and Tussah silk fibre (on the right) at 90° orientation.

Dunaway et al. (Dunaway et al. 1995) have addressed that elliptical or oval cross sections can be treated as circular with a few percent of the actual value under three conditions: (i) by averaging at least four measurements of a fibre‟s apparent diameter which is equal to an „equivalent diameter‟ of the circle; (ii) by taking at equal intervals of fibre rotation through a 180° range to measure the apparent diameter; (iii) by keeping the axial ratio of the cross section less than 1.5 which is equivalent to the anisotropy as shown in the above table.

In table 4.1, the anisotropy of Tussah silk fibre is in the range of 1.18 to 1.42 whereas for Bombyx mori silk fibre, its anisotropy is in the range of 1.31 to 1.37 which is more consistent than that of the Tussah silk fibre. The cross sections of the two different silkworm silk fibres can be assumed as circular as the values of anisotropy are smaller than 1.5. The apparent diameter is calculated by collecting five different data on each fibre at different orientations and regions. After averaging the results, the apparent diameters of Bombyx mori and Tussah silk fibres are 260 and 85 µm, respectively, which can then be further used for converting the mechanical properties data. Furthermore, Bombyx mori and Tussah silk fibres have entirely different appearances for their fibre and fibrils. As seen from fig. 4.3 and 4.4, Bombyx mori silk fibre has a larger apparent diameter, about triple to that of the Tussah silk fibre and this may be the reason for their differences in mechanical properties.

The tensile test was performed on 30 samples obtained from two different types of silkworm silk fibre under three different conditions, they were Bombyx mori, twisted Bombyx mori, and Tussah silk fibres. Samples from each condition were collected by picking the adjacent part of the same origin fibre and 10 samples

were tested to maintain the reliability of the averaged results.

4.4.1   Force- Displacement Results

Force displacement curves were capturd during the test and they are shown in fig.
4.5, for comparing their mechanical behavior.
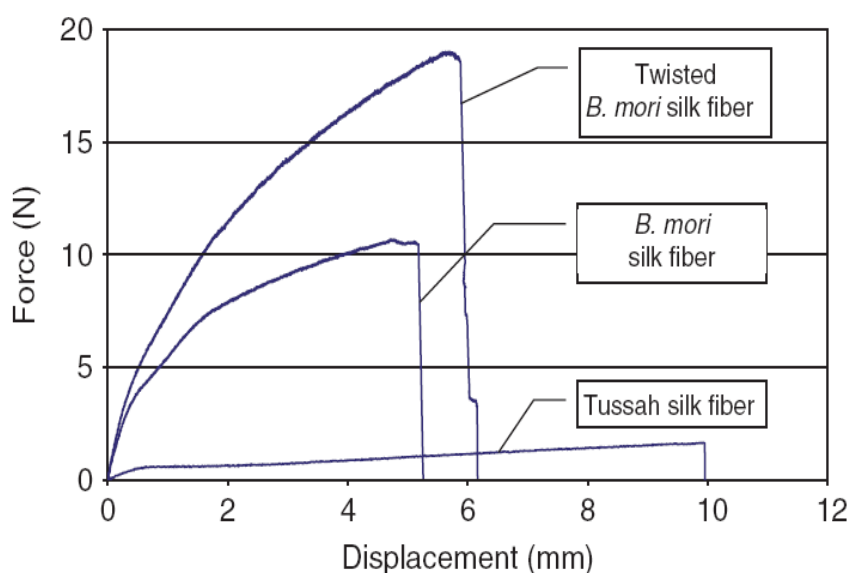
Figure 4.5. Force-displacement curves of Bombyx mori, twisted Bombyx mori and
Tussah silk fibres.

The force-displacement curves show that silkworm silk fibres with different
silkworm raising processes, cocoon-producing, and spinning conditions exhibit a
completely different tensile property. Bombyx mori fibre supports a much higher
loading (about 10 N) than the Tussah silk fibre, which can withstand a loading of

only about 2 N. Whereas for twisted Bombyx mori silk fibre, with a cross-sectional area of double to that of the single one, it is doubtless that it can bear an even higher loading. It takes about 19 N, only almost a double to that of the single Bombyx mori silk fibre which is mainly because the majority part of loading goes as tensile loading and a small portion of loading overcomes the friction among the twisted fibres.

In addition, for the extensibility, Tussah silk fibre has a greater elongation of about 89% than the Bombyx mori silk fibre, and the twisted Bombyx mori silk fibre exhibits a slightly larger elongation than the single one with about 17% increment. Shao and Vollrath have pointed out that force-drawn silkworm silk fibre was comparable to Nephila spider dragline silk (Shao & Vollrath 2002). With slow spinning speed, Bombyx mori silk fibre could obtain a large breaking elongation but became weaker; whereas with faster spinning speed, it could have a breaking energy approachable to Nephila spider dragline silk, but the silk became more brittle due to the loss of extensibility. This shows that distinct feeding habits, cocoon spinning environment, and speed etc. on Bombyx mori and Tussah silk fibre have a great effect upon their overall mechanical properties.

On the other hand, as seen from the SEM micrographs, Bombyx mori silk fibre has a larger apparent diameter but with a smaller cross-sectional area of each filament (i.e., less necking of each filament during tensile loading can be obtained) than Tussah silk fibre, so it may be incontestably concluded that Bombyx mori silk fibre can bear a higher loading but has a relatively lower extensibility than Tussah silk fibre.

4.4.2   Stress-Strain analysis

After obtaining the apparent diameters of Bombyx mori and Tussah silk fibres from the SEM micrographs, load-extension data can then be converted into stress-strain analysis. The mechanical properties (ultimate tensile strength (UTS), elongation at break and Young˝s modulus (E) of Bombyx mori, twisted Bombyx mori, and Tussah silk fibres are listed in table 4.2.

Table 4.2. Mechanical properties of bombyx mori, twisted bombyx mori and Tussah silk fibres

Fibre sample	UTS (MPa)	Elongation at break (%)	E (GPa)	Density (g/cm^3)	Cost (US$/kg)
Bombyx mori silk	208.45 (10 N)	19.55	6.10	1.33	23.62
Twiated Bombyx mori silk	165.27 (19	20.57	3.82	---	---
Tussah silk	248.77 (2N)	33.48	5.79	1.32	24.34

(http://www.silk-online.net/)

According to table 4.2, Tussah silk fibre exhibits the highest ultimate tensile strength and percentage of elongation at break of about 250MPa and 33%, respectively. It has a similar Young˝s modulus of around 6 GPa (only 5%

decrement) to Bombyx mori silk fibre. On the other hand, Bombyx mori silk fibre indicates 16% and 42% decrement of ultimate tensile strength and percentage of elongation at break, respectively, compared to the Tussah silk fibre. Twisted Bombyx mori silk fibre shows the worst stress-strain properties among the three sets of samples due to the friction in between the two single Bombyx mori silk fibres as stated in previous section. It has 34%, 39% and 34% decrement of ultimate tensile strength, percentage of elongation at break, and Young"s modulus, respectively, compared to the Tussah silk fibre. Moreover, it has 21% and 37% decrement of ultimate tensile strength and Young"s modulus, respectively, and only a 5% increment of extensibility compared to the single Bombyx mori silk fibre.

From the SEM micrographs, it is concluded that apparent diameter of the Bombyx mori silk fibre is triple to the diameter of Tussah silk fibre, and the diameter of twisted Bombyx mori silk fibre is assumed to be double than that of the single fibre. Therefore, although single and twisted Bombyx mori silk fibre can bear a higher tensile loading, when analyzing the data into stress-strain curves as shown in fig. 4.6, Tussah silk fibre indicates the highest ultimate tensile strength.
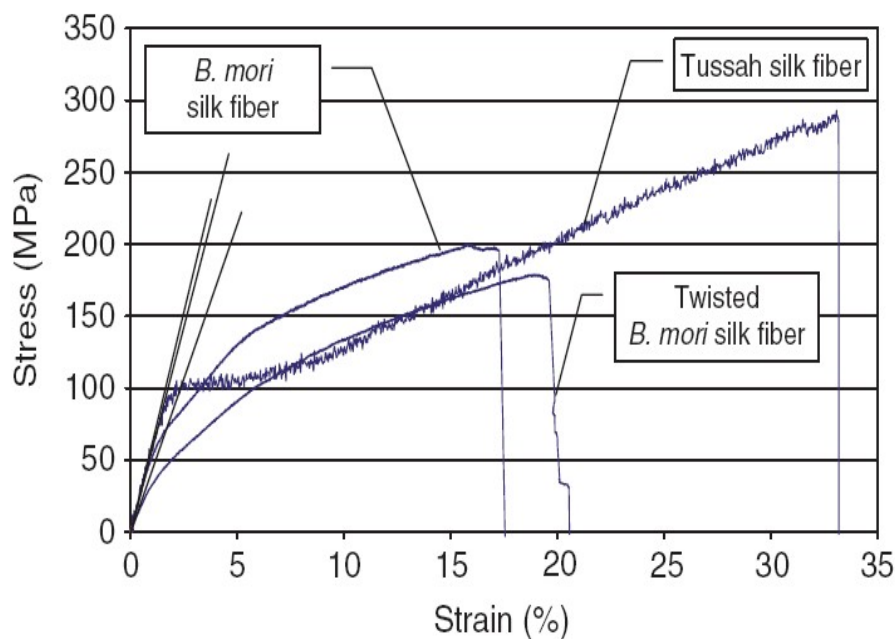
Figure 4.6. Stress-strain curves of Bombyx mori silk, twisted Bombyx mori and Tussah silk fibres.

The apparent diameter of Bombyx mori silk filament is much smaller than that of the Tussah silk filament which can be accounted for less extensibility, so, single and twisted Bombyx mori silk fibres show only about 20% elongation at break. Rigueiro et al. have explained that silk fibre is made up of both crystalline and noncrystalline regions in which the interconnected and well-aligned region would account for the stiffness of the fibre, whereas the disordered region would account for the ability of elongation at break (failure) (Rigueiro et al. 1998). The behavior of the fibres under tensile loading is generally accounted for the changes on molecular level as well (Robson, Lewin & Pearce 1998). When a tensile load is applied, initial deformation occurs primarily in amorphous region. When the load is applied continuously, inter-chain bonds are broken, more and more randomly

arranged or disordered chains are further extended, and the load will then begin to be taken up by the crystalline region. Due to the high proportion of crystalline structure in domesticated Bombyx mori silk fibre, the stress-strain curve is approximately parabolic and slightly convex to load axis up to break. A relatively high proportion of amorphous structure in wild Tussah silk fibre can be accounted for its pronounced yield plateau and a distinct concave curve up to break. Besides, when the two different types of silkworm silk fibre are applied in engineering applications, their density and cost can be of minority concern as the density and cost in table 4.2 shows similar values of around 1.4 g/cm^3 and 24 US\$/kg (Rigueiro et al. 1998), respectively,

4.4.3 Weibull Analysis

Weibull analysis is emphasized particularly for failure analysis invented by Waloddi Weibull in 1951. Nowadays, Weibull analysis is a leading method in the world for fitting and analyzing life data. This analyzing method is performed by fitting a statistical distribution to life data from a representative sample of units and interpreting the plot, then forecasts and predicts failure. It can work with extremely small samples, even only two failures for engineering analysis. In the Weibull data plot, three main parameters that define the distribution curve can be determined including the Weibull modulus (β), the characteristic life (η), and the starting point of the curve (σ_0) (Dodson 2006; United Aircraft Corporation. Pratt & Whitney Aircraft Division 1975). Rigueiro et al. have accomplished different Weibull analyses on forced reeling and cocoon spun Bombyx mori silk fibres, and

spider dragline silk (Rigueiro et al. 1998; Rigueiro et al. 2000; Rigueiro et al. 2001). In this section, Weibull analysis was performed on the single and twisted Bombyx mori and Tussah silk fibres to compare the reproducibility of these silkworm silk fibres. The statistical distribution plots of

$$\ln\left[\ln\frac{1}{1-F}\right] \tag{4.1}$$

against ln(tensile strength), where F is the probability measure of sample failure and the tensile strength is in the unit of MPa in fig. 4.7, and the Weibull parameters of the three different sets of fibre samples are listed in table 4.3.
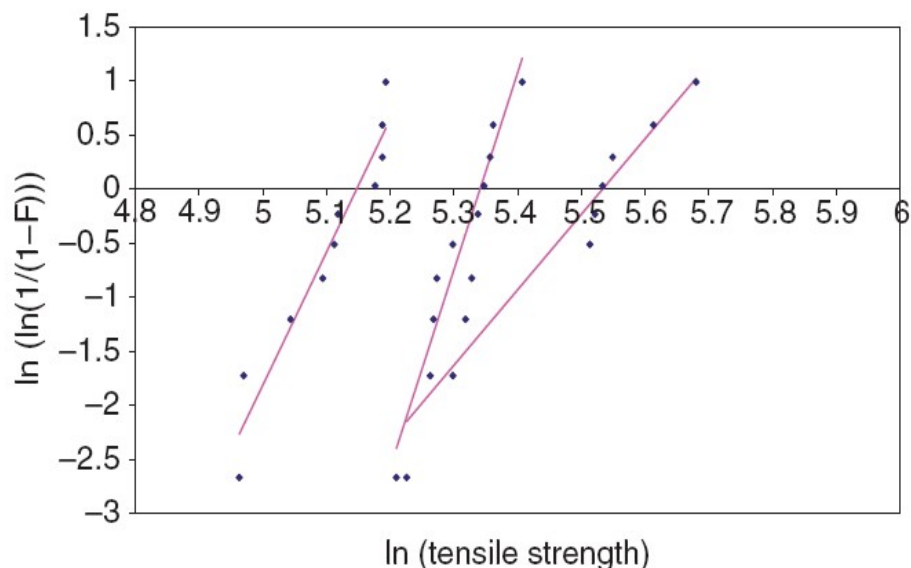
Figure 4.7. Weibull analysis of twisted Bombyx mori, Bombyx mori and Tussah silk fibres (from the left to the right of the graph).

Table 4.3. Weibull parameters of Bombyc mori, twisted Bombyx mori and Tussah silk fibres.

Fibre samples	Total number of samples	β	η(MPa)
Bombyx mori silk	10	13.46	216.16±4
Twisted Bombyx mori silk	10	12.30	171.90±3
Tussah silk	10	6.98	252.91±2

In fig. 4.7, Weibull plots of three different types of silkworm silk fibre follow the Weibull statistic as they are in straight lines. The Weibull modulus indicates the reproducibility of tensile strength of materials, with higher value of slope gives a higher reproducibility and reliability in engineering context. Single and twisted Bombyx mori silk fibres have the values of Weibull modulus of around 13 and 12, respectively, whereas Tussah silk fibre has the value of around 7. It means that wild Tussah silk fibre accounts for a relatively poor reproducibility than that of the domesticated Bombyx mori silk fibres. It can be concluded that except for harsh degumming process which may decrease the reproducibility of tensile properties of silkworm silk fibre, different silkworm-raising processes, cocoonproducing, and spinning conditions of the fibre may also be the factors to different reproducibility.

The characteristic life is always estimated by reading the x-axis value for the 63.2%, intercepting the y-axis value on the Weibull modulus, which is elucidated as the average tensile strength of different silkworm silk fibres. As seen from the plots, the values of the characteristic life (the average tensile strength) of single

and twisted Bombyx mori, and Tussah silk fibres are 216.16$\pm$ 4, 171.90$\pm$3, and 252.91 $\pm$2 MPa, respectively. Although degumming treatment decreased the reproducibility of tensile properties of silkworm silk fibre, the value of average tensile strength remained. Therefore, it may be concluded that the degumming treatment does affect the microstructure of the silkworm silk fibre but it has little effect on the molecular order in the fibre.

Since silkworm silk fibre has a great variability in appearance and dimension for different species of silkworms, the appearances and apparent diameters of the Bombyx mori and Tussah silk fibres were examined for converting experimental data into stress-strain analysis. The specific Tussah silk fibre exhibits a better ultimate tensile strength and extensibility whereas the stiffness values of both of the species are almost identical. This may be due to the distinction of silkworm raising processes, cocoon producing, and spinning conditions of the fibre. Besides, Weibull analysis showed the single and the twisted Bombyx mori silk fibres have a better reproducibility of tensile properties than the Tussah silk fibre, and it may be mainly due to the degumming treatment which has an effect on the microstructure of the fibre. Although different species of silkworms produce different types of silkworm silk fibre, with completely diverse set of properties, they can be applied to various applications according to their distinct properties or even tailor-made to suit some specifications. Therefore, silkworm silk fibre has become a promising biomaterial for engineering and biomedical applications recently, and attracted attention of researches in developing novel materials and composites with the use of this special type of protein.

Chapter 5

Effect of Degumming on Silkworm Silk Fibre

5.1 Introduction

In Chapter 4, the results prove that Tussah silk demonstrates higher ultimate tensile strength and elongation which is suitable for various industrial and engineering applications as compared with Bombyx mori silk.

Hydrophilic sericin enclosed the silkworm silk fibre which protects the fibre vary from microbial degradation, animal digestion, and other damages. These protections include: (1) oxidation resistant, (2) antibacterial, (3) UV resistant and against light damage etc (Osnat & David 2007). However, when producing silk fibre reinforced polymer composites, a sericin layer has been found to cause poor interfacial bonding with polymer because this layer hinders the bonding between the fibre and matrix inside the composites, and thus the efficiency of stress transfer from the matrix to the fibre would decrease substantially. It results in affecting the mechanical properties of the composites.

Moreover, high tensile strength with low rates of degradation of silk fibres makes it a promising candidate for tissue engineering applications (Panilaitis & Altman 2003). However, almost biomaterials derived from a non-autologous source will

elicit some level of foreign body response (FBR) following implantation in vivo (Altman, Diaz, Jakuba, Calabro, & Horan, Silk-based biomaterials, 2003). Hypersensitivity is a type of FBR which produced by the normal immune system (Altman, Diaz, Jakuba, Calabro, & Horan, Silk-based biomaterials, 2003; Kurosaki, Otsuka, Kunitomo, Koyama, Pawankar, & Matumoto, 1999) There are many factors which can influence the level of FBR, including composition, implantation site, size, geometry, surface topography of the biomaterials and etc. Silk fibre has been found to be a potential allergen causing type I hypersensitivity and sericin is considered to be the main inhalant allergen and antigenic properties in silk sensitive persons. Once the patient is sensitized to sericin, plasma cells in the human body secrete antibodies immunoglobulin E (IgE), some antigens binds IgE variable regions, degranulation of cell occurs, histamine and other vasoactive substances are released and It would cause systemic anaphylaxis, localized reactions and asthma (Kurosaki et al. 1999; Meinel & Hofmann 2005; Panilaitis & Altman 2003). Therefore, the removal of sericin of silk fibre is a crucial process for it to be applied for real life applications.

5.2 Effect of Degumming Time on Silkworm Silk Fibre

Sericin is insoluble in cold water. However, it is hydrolyzed by the breakages of long protein molecules to smaller fractions, which are easily to be dispersed or dissolved into hot water (Mondal & Trivedy 2007). Although the sericin layer accounts for less than 8% of the total material of the silk (Fu et al. 2011), a long and continuous fibre can only be reeled from the cocoon after the adhesive sericin coating is soften or eliminated. Therefore, the sericin layer is removed as waste

material from core fibre during raw silk production such as reeling mill and the other stages of silk processing.

Preprocessing of silk commonly known as "degumming" is an essential process to obtain an ideal fibre because of its compositions. Silk degumming process is scouring the sericin and some impurities from silk fibre. The principle of degumming process using water or other degumming agents such as soap, alkali, synthetic detergents, or organic acids hydrolyze the sericin, breakage the peptide linkage of amino acid into small molecules and dissolving the sericin into the water finally. However, degumming may weaken at least one type of non-covalent interactions of core fibre, such as hydrogen bond and Van der Waal's force (Jiang et al. 2006). This factor associated with degumming could affect the tensile properties of silkworm silk because of the change of the microstructure of core fibres (Altman, Diaz, Jakuba, Calabro, & Horan, Silk-based biomaterials, 2003; Shao & Vollrath, 2002). However, it has not been well understood that how the boiling water affects the performance and the morphology of Tussah silk fibre during the degumming process.

5.2.1   Experimental Set-up

Tussah silk fibre was supplied by Ocean Verve Ltd., Hong Kong. Silk fibres were separated carefully from a bundle of fibres. Special care was taken to avoid stretching the fibre plastically during the whole experiment process. Extracted silk fibres were cut into 200 mm and placed in a 100mL breaker for the preparation of degumming treatments, and sufficient distilled boiling water was added to

completely immerse the fibres into the water. The beakers with the fibres were heated in a hot water bath for 10 minutes, 30 minutes, 45 minutes and 60 minutes respectively. Afterward the hot water treated fibres were washed with cold distilled water and dried immediately at 80°C for 4 hours. Raw silk fibres were referred to as an untreated sample dried by 80°C for 4 hours similar to other hot water treated fibres.

As the water disrupts hydrogen bonds of fibres which would promote the substitution of protein–protein hydrogen bonds by water–protein hydrogen bonds and thus reduce the mechanical properties of the silk fibre (Perez-Rigueiro, Viney & Elices 2000), undesirable change of the fibre diameter would occur to hinder the effect of degumming. Therefore, drying up the fibres before the experiments was crucial and all the tests were performed immediately after the fibres had been removed from an oven.

The experimental set up is modified from Section 4.2 in order to avoid stretching of the fibre and the sliding during the testing. Each sample was mounted on cardboard frames by tapes and removed any slack without stretching the specimen. Fig. 5.1 shows the experimental setup for the tensile test for this study.
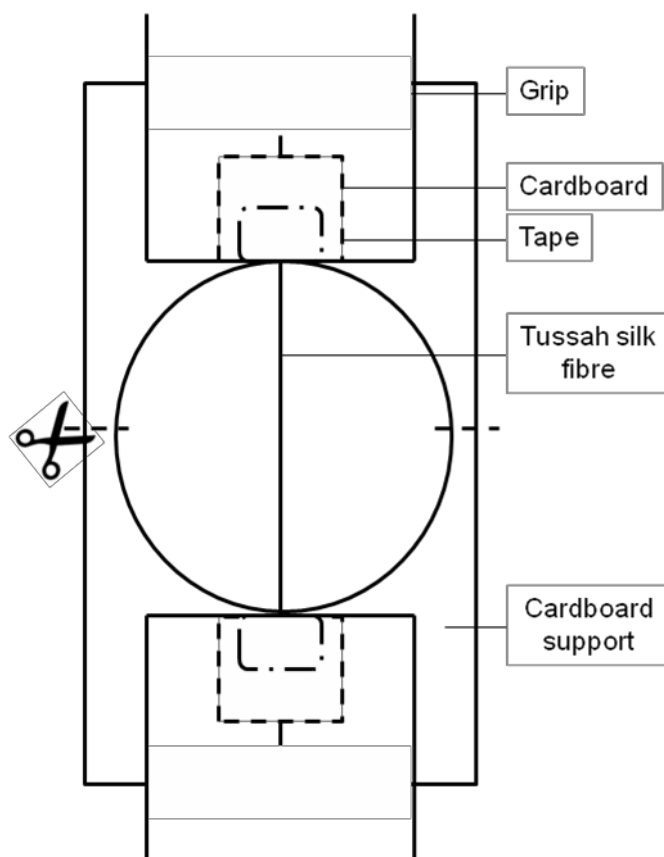
Figure 5.1. Experiment setup for the tensile property test for silk fibres.

The cardboard frame was cut with scissors through the discontinuous line as shown in the figure before starting the experiment. The diameter of center hole was 100 mm. All samples must be well aligned to the loading direction to avoid any mis-measurement of the strength of fibres.

All measurements were carried out on the MTS Alliance RT/10 materials testing machine at a crosshead speed of 60 mm/min and under standard environmental conditions (20 ^{o}C, 60% relative humidity). The samples were tested according to ASTM D 3822. The diameter of silk fibre samples were characterized by using

optical microscope (Olympus SZ-PT). Some samples were further coated by gold for SEM (JEOL Model JSM-6490) imaging.

Differential scanning calorimetry (DSC) curves were obtained with a thermal analysis instrument at a heating rate of 10 ^{o}C/min and a nitrogen gas flow rate of 50 mL/min. approximately 6-10 mg of samples obtained at different degummed parameter was sealed in aluminium pans. The experiments were performed in nitrogen atmosphere.

Thermogravimetric analysis (TGA) was performed with a Perkin-Elmer TGA-7 with heating rate of 20.0 ^{o}C/ min up to 600 ^{o}C. The experiments were performed in nitrogen atmosphere. Silk fibre is normally stable up to 140 °C and the thermal decomposition temperature is greater than 150 °C.

Fourier transforms infrared (FTIR) spectra were obtained from spectrometer (Perkin Elmer16 PC FTIR spectrophotometer) in the spectral region of 2000-600 cm^{-1}). Before testing, the fibre was mixed with KBr powder and cold-pressed into a suitable disk for FTIR measurement. For all measurement, the thickness of specimen was controlled at 5 um.

5.2.2   Results and Discussion

5.2.2.1 Tensile properties

Table 5.1 summarizes the results obtained from tensile test including average F_p (load) and ε_p (elongation) at the elastic limit point of all samples (extracted the

results from 10 samples at each type of heat-treated fibres).

Table 5.1. Load and Elongation at break of the Tussah silk fibres pre-treated at different temperatures.

Degummed time (min)	0	15	30	45	60
Load (N)	0.35	0.38	0.24	0.23	0.18
Elongation(mm)	5.6	5.9	4.9	4.7	3.8

The representative tensile load-displacement curves of Tussah silk fibres are given in fig. 5.2. The tensile test was processed with the gauge length of 100 mm. Tussah silk fibres which were degummed for 15 minutes in the hot water show a better load carrying capacity as compared with other samples. Ping et al. has suggested that the degumming process has two principal quantitative effects on the load-displacement plot including initial slope and the elastic limit (i.e. yield point) (Jiang et al. 2006). For the sample degummed for 15 minutes, the initial slope is steeper as compared with the result of the control samples. However, for the samples degummed over 15 minutes, their initial slope and the elastic limit (i.e., yield point) are lower than that of the controls. Based on the results of all curves, it is clear to see that for the fibres degummed over 1 hour caused the substantial decrease of their elastic region (by 50% as compared with the sample degummed for 15 minutes) because of the damages of the fibres.
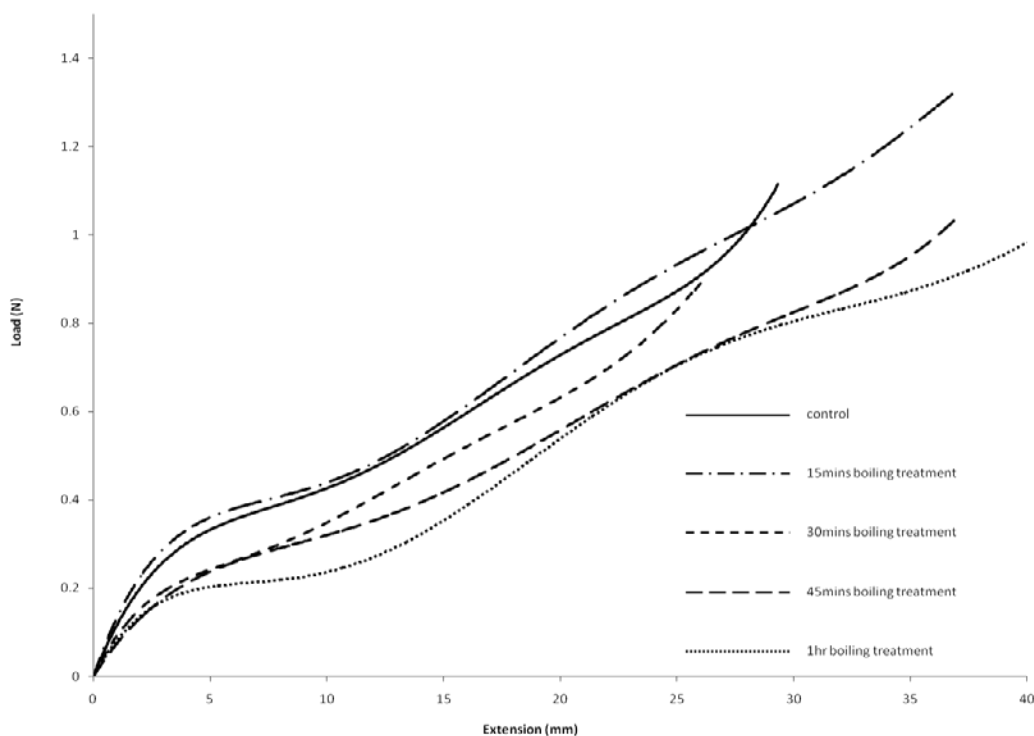
Figure 5.2. Load-displacement curves of control and degummed Tussah silk fibres.

After obtaining the load-displacement results, nominal strains of the samples were calculated. Nominal stress was also obtained by dividing the applied load to the cross sectional area of each fibre as the diameter was measured directly under the microscopy. The graphical representation of the relation between stress and strain was obtained as stress- strain curve thereafter. Similar to spider dragline silk, the Tussah silk fibre exhibits three regions with turn in its stress-strain curve. These regions include an initial linear elastic region (A), a yield region (B), and a hardening region (C) which are clearly shown in fig. 5.3. Fig. 5.4 shows the stress-strain curves of all samples. This type of sigmoidal "rubber like" shape of the stress- strain curves obtained from the experiment which is well matched with the result obtained from Zhang et al. (Zhang et al. 2010).
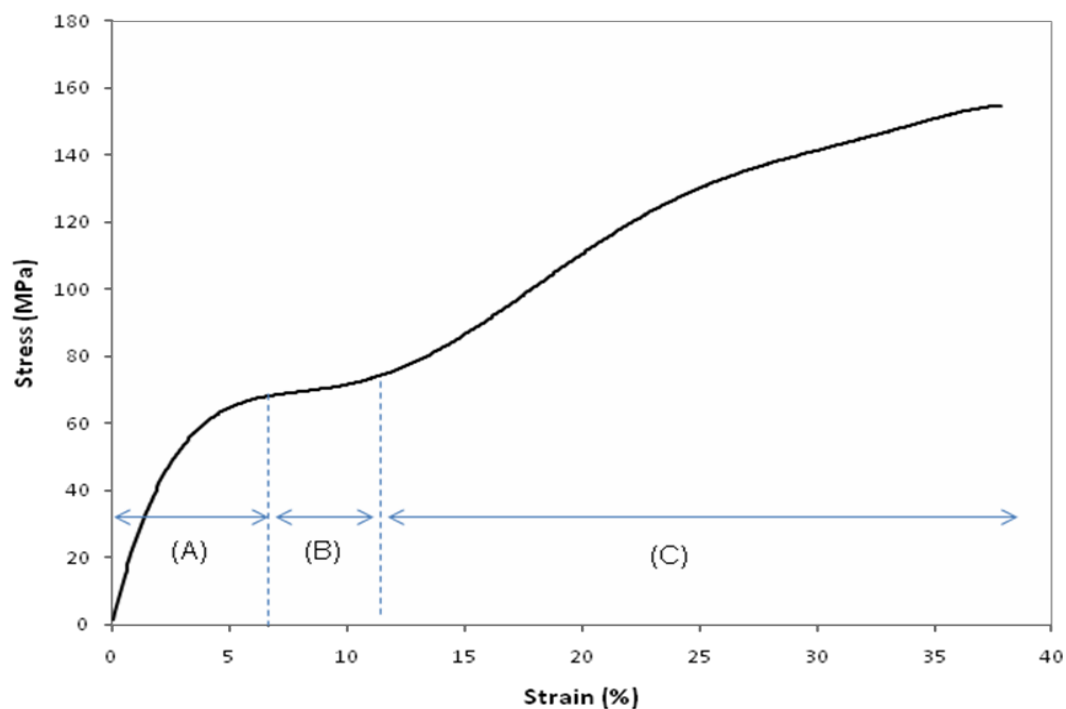
Figure 5.3. Stress-strain curves of ordinary Tussah silk fibre as (A) initial linear elastic region, (B) a yield region, and (C) a hardening region.
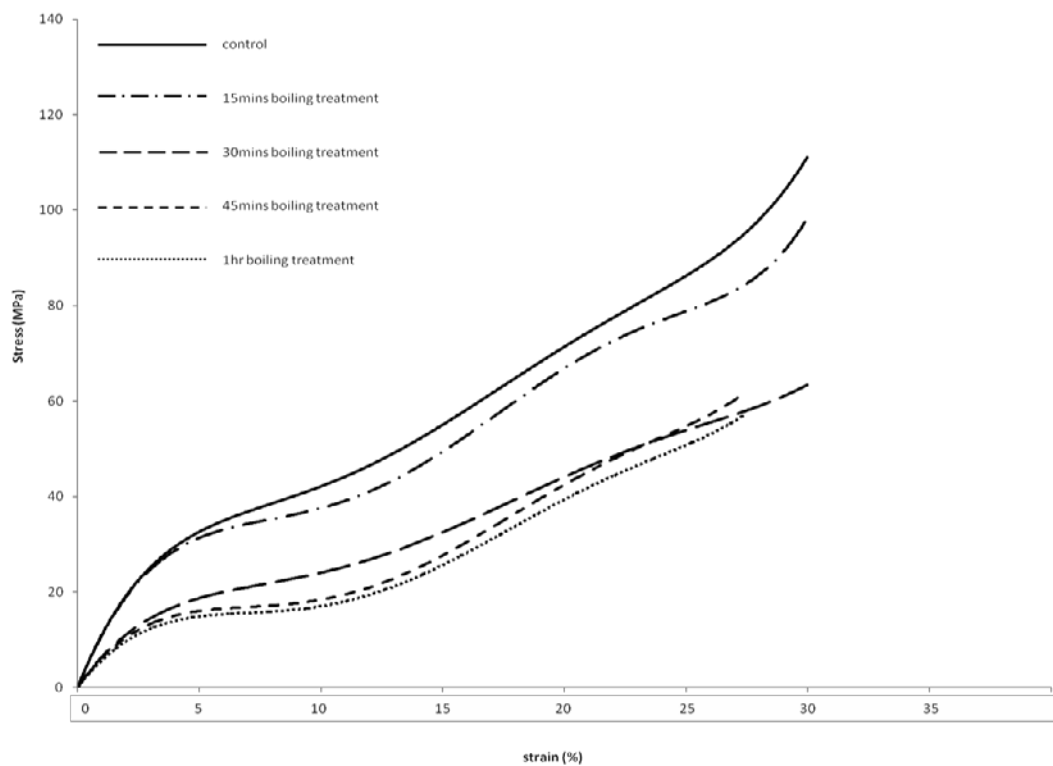
Figure 5.4. Stress-strain curves of Tussah silk fibres degummed at different time period.

Table 5.2 is the summary of the mechanical property parameters of the samples including elastic modulus E (initial modulus), slope of yield region, slope of hardening region, the strain at the proportional limit, the tensile strength and the strain at break. The relationship between the mechanical properties of the samples and the degumming time are listed in table 5.1 & 5.2. Based on the influences on the degumming time, samples which heat-treated for 15 minutes are the best among the degummed samples in term of the tensile strength. Moreover, from the tables, it is shown that fibres degummed for 15 minutes are more compliant and have better tensile strength, initial modulus, slope of yield region and strain at breaking than that of other degummed samples.

Samples being degummed over 15 minutes, their initial tensile modulus, slope of yield region, slope of hardening region, strain at the proportional limit, tensile strength and strain breaking and yield points for degummed samples start to decrease gradually and drop dramatically when the degumming process is taken over 30 minutes. According to the results shown, it can be concluded that by increasing the time for degumming until heat-treated 15 minutes, maximum tensile properties reach but start to decline when the samples degummed over 15 minutes.

Table 5.2. Summary of the tensile stress, strain, modulus of the samples.

	Initial modulus (GPa)	Slope of yield region	Slope of hardening region	Strain at the proportional limit	Tensile strength (MPa)	Strain at breaking
Control	102.86	5.714	32	5.3	156.293	28.05
Degumming after 15 minutes	112	20	30	4.5	159.837	34.127
Degumming after 30 minutes	55	5.714	6.67	4	124.081	28.838
Degumming after 45 minutes	51.43	5	6.67	3.7	106.982	27.489
Degumming after 60 minutes	45.71	0.333	6.67	3	104.922	22.625

Certain factors whereby explain the influence of degumming on the tensile properties of single silkworm silk fibre including 1) sericin removal, 2) molecular changes and 3) bonding breakage.

Focusing on the amino acids residues, the amino acid sequence of polypeptides plays a very important role in the solubility and crystallization of silk fibres (Tanaka 2002). Silks are belonged to a group of high molecular weight organic polymers with several low molecular components (sericin). The Tussah silk is classified as group three (unstable structure) as partial sequence of H-fibroin is not disclose regular polyalanine repeat. The H-fibroin of Tussah silk fibre is made up of 80 tandemly arranged repeated where there are alternative appearances of the poly (L-alanine) region and the Gly-rich region (Michal & Frantisek 2001; Zhang

et al. 2010; Yang & Bochu 2009). The repetitive organization and the presence of high content of short side chain amino acids are preserved in the Tussah silk polymer system. The amino acid composition of Tussah silk fibroin is characterized by an abundance of alanine (Ala), glycine (Gly), and serine (Ser) and significant amounts of asparagine (Asp) and arginine (Arg). In particular, glycine in Tussah silk is 26 residue % and alanine is 44.2 residue % (table. 5.3) (Richard 1955).

Basically, alanine is hydrophobic and glycine is amphiphilic which induces the hydrophobic fibres. On the other hand, most of amino acids in sericin protein have strongly polar side groups, such as hydroxyl, carboxyl, and amino groups (Yu & Michael 1998). Serine and threonine are the carbohydrates can be covalently linked to its –OH group while aspartic acid and glutamic acid contain free carboxyl group makes it acidic and hydrophilic. The residues serine (Ser), threonine (Thr), aspartic acid (Asp) and glutamic acid (Glu) in sericin are consequently causing the hydrophilic property of sericin (Zhang, Berghe & Paul 2011). Therefore when the Tussah silk fibres are boiled in the hot water, sericin will be dissolved but fibre will not. The hydrophobicity of chain segments inside Tussah silk fibroin macromolecular is quite different from that of common type of a domestic Bombyx mori fibre.

Table 5.3. Composition of fibroins of the Tussah silk (Richard 1955).

Amino- acid residue	Tussah silk (residue %)
Glycine	26.6
Alanine	44.2
Serine	11.8
Tyrosine	4.9
Aspartic acid	4.7
Arginine	2.6
Valine	0.6
Glutamic acid	0.8
Tryptophan	1.1
Phenylalanine	0.5
Isoleucine	0.4
Leucine	0.4
Histidine	0.8
Proline	0.3
Threonine	0.1
Lysine	0.1
Cystine	---
Mean residue weight	83.5

Tussah silk is regular stretches of 12 or more consecutive alanine residues interrupted by glycine-rich regions (fig. 5.5). It is easily to form hydrophobic interactions between the chain segments and promote the formation of β-sheet structure as the hydrophobicity of poly-alanine blocks inside Tussah silk fibroin is stronger than Bombyx mori silk fibroin as Bombyx mori silk fibroin is made up of Gly-X (X equal to Ala or Ser) repeats inside. (Tao, Li & Zhao 2007).

Bombyx mori fibroin

==GAGAGSGAGAGSGAGAGSGAGAGSGAGAGSGAGAGSGAGAG==YGAGVGVGYGAGYGAGAGAGY==GA GAGSGAASGAGAGSGAGAGSGAGAGSGAGAGSGAGAGSGAGAGSGAGAGSGAGAGSGAG AGSGAGAGSGAGV==GSGAGAGSGAGAG==VGYGAGAGVGY==GAGAGSGAASGAGAGSGAGAGS GAGAGSGAGAGSGAGAGSGAGAGSGAGAGSGAGAGSG==

Antherara pernyi fibroin

==AAAAAAAAAAAAAGSGAG==GSGGYGGYGGYGSD==SAAAAAAAAAAAAAGS==SAGGAGGG YGWGDGGYGSD==SAAAAAAAAAAAAA==

Figure 5.5. Typical amino acid sequence of repetitive core of Bombyx mori fibroin and A. pernyi fibroin. The highlighted are definite β-sheet forming segments. The accession number for Bombyx mori fibroin is P05790 which Tussah silk fibroin is O76786 (Tao, Li & Zhao 2007).

Glycine and alanine predominate in silk fibroin. In particular, the glycine in Tussah silk is 26 residue % and alanine is 44.2 residue % (Richard 1955). Therefore, Tussah silk fibre is predominantly hydrophobic as alanine is hydrophobic and the glycine is amphiphilic. On the contrary, residues serine, threonine, aspartic acid and glutamic acid are the main components of sericin. Serine and threonine are carbohydrate that can be covalently linked to its hydroxyl (–OH) group. While aspartic acid and glutamic acid contain free carboxyl group making it acidic and hydrophilic. Sericin is therefore hydrophilic and comprised of more random structures (Zhang, Berghe & Paul 2011; Tanaka 2002). Removal of sericin layers on the fibre surface would contribute significantly to the change of cross sectional area and subsequently the tensile properties of the fibres. The level of degumming is mainly depended on the treatment time. At the beginning of degumming, the water starts to dissolve the sericin on the fibre surface and

cause the decrement in the diameter of the fibre. The strength of the fibre being degummed for 15 minutes increases because of the decrease of the cross sectional area. As load-bearing capacity of sericin is very small compared to that of fibre, removal of the sericin represents not only the decrement in the cross sectional area, but also the increment in the effective cross sectional area. Another effect on sericin removal for the reasons of the increase strength of the degummed Tussah silk fibre for 15 minutes is their filaments are twisted in nature. After degumming, the filaments of fibre, due to the missing of binding agent (i.e. sericin) would potentially align towards the loading direction. Thus, the friction in-between the filaments were reduced and the load bearing capacity increases because of the alignment of the fibre to the loading direction. In such case, the fibre can take a large portion of tensile load instead of friction. Nevertheless, this scenario is totally reverted when the degumming time increases. As the sericin which acts as the glue to bind up all fibre filaments together, degumming would cause the removal of sericin and thus the fibres are in a loose pack form. The scattering of the fibre would increase its diameter. It can be seen that fibres heat-treated after 15 minutes had less strength as compared with the control sample because of fibre scattering.

Molecular change is one of the consequences of degumming which infers the tensile properties of control and degummed silk fibres. In the secondary structure, the repetitive primary sequence in hydrophobic residues of silk fibre composing of short side chain amino acids dominate the anti-parallel β-sheet structure. These structures permit tight packing of stacked sheets of hydrogen bonded anti-parallel chains of the protein (Kim et al. 2004). In a silk fibre, strong crystalline regions which provide tensile strength are interspersed by, the soft and more flexible

amorphous peptide chains which are responsible for the elasticity of silk and also help with the distribution of stress (Bini, Knight & Kaplan 2004; Mathur & Gupta 2010). Under tensile loading, the amorphous chains are extended, and the crystalline networks are rotated during the stretching and shrinking to produce a strongly preferred molecular orientation which is parallel to the fibre axis. Moreover, once the fibre extended physically, partly amorphous chains in the fibre would be crystallized as a rigid and highly oriented network (Gosline et al. 1999). Therefore, amorphous structure also contributes the strength because of the crystallized amorphous region.

Heavy chain and light chain fibroin inside a silk fibre with a single linkage called disulfide bridge convey the fibre with its remarkable mechanical behavior (Plaza et al. 2008). The heavy chain of silk fibre is comprised of crystalline and amorphous regions but is mainly composed of β-sheets (Kim et al. 2004). However, Excessive heating period would affect the fibroin heavy chain (Jiang et al. 2006). Besides, the water molecules damage and scissor the chain scission occurring in the amorphous component preferentially (Plaza et al. 2008) but, crystallites can also be deteriorated in an extreme case (Garside & Wyeth 2007).

The degumming effect will damage the amorphous structure as the first place after removal of sericin. It can be seen that the strains of the fibres drop dramatically after being heated over 45 minutes. Futhermore, the low tensile strength of degummed silk may probably reflect the damage of both amorphous and crystalline structures.

The structure of Tussah silk fibre is a semicrystalline polymer of natural fibrous protein mainly consisting of the two important phases: (1) highly β-sheet crystals

contribute strength and rigidity and (2) non-crystalline form consisting of microvoids and amorphous structures contribute elasticity. The main secondary crystal structure of Tussah silk was found to be predominantly antiparallel β-sheet similar to spider major ampullate silks but also with certain amount of α–helix which is distributed throughout the silk fibre (Fu et al. 2011). The β-sheets of Tussah silk fibre form the basis for the tensile strength and toughness of the material, and it stacks by hydrophobic interactions, and interact bilaterally with alanine side chains which are formed through hydrogen bonds between adjacent peptide chains (Tao, Li & Zhao 2007).

There are specific interactions among the blocks and, between the chain-ends and larger hydrophilic blocks. The β -sheets structure of Tussah silk fibre is depicted as the formation of poly-ala structure with the placement of successive alanine residues on alternate sides of a backbone. Each chain can then be interlocked with an adjacent chain via hydrophobic interactions. Thus, the strength of interactions between the β -sheet structure of these proteins predicts the tensile strength of the silk (Hayashi, Shipley & Lewis 1999). Besides, the dimension of the chain axis and hydrogen bond are similar for all types of silks, while difference is in the inter-sheet spacing. As most natural fibres owe their strength from hydrogen bond, hydrogen bond plays an important role in the secondary, tertiary, and quaternary structures of proteins. However, degumming weaken at least one type of non-covalent interaction. This interpretation is consistent with the fact that water act as a plasticizer. Water penetrates the amorphous regions and interrupting the inter- and intra- molecular hydrogen bond so that the displacements of protein chain segments and stress relaxation are increased and thus easier to respond any driving force for microstructural change consequently (Perez-Rigueiro et al. 2001;

Sahoo, Toh & Goh 2010). Heating the fibre up to 100°C only provides a thermal energy equivalent to 3.1 kJ/mol, which is below the range of typical hydrogen bonding energy. Therefore, this way is unlikely to disrupt the pattern of hydrogen bond of silk fibre significantly in the dry condition (Perez-Rigueiro et al. 2001) but is likely to affect the structure of the silk fibre by immersion it into the water during the heating duration. During degumming, the effects of water with heat disrupt the hydrogen bond and disorder the structures. Hydrogen bond becomes weak and loses its strength when heated. The existing peptide bonds, salt linkages and hydrogen bonds of the silk fibre tend to break down once the temperature exceeds 100 degree. As the crystalline units cross-link the protein chains in the fibre via hydrogen bond, disrupting the hydrogen bond would decline the load bearing of the fibre. Fibroin has a high degree of crystalline due to stacked β - sheets. In a stretched fibre, the external force propagates along the fibre axis by straightening the disordered protein chains (amorphous region) and subjecting the crystalline regions to a tensile loading along the β-strand axis. Accordingly, as the crystalline units cross-link the protein chains in the fibre via hydrogen bond, disrupt the hydrogen bond would decline the load bearing of the fibre (Mondal & Trivedy 2007).

5.2.2.2 Weibull analysis

Weibull distributions for the strength of the Tussah silk fibres are shown in fig. 5.6 .The data is scattered for both the undegummed and degummed Tussah silk fibres. The reason for scattering of the Tussah silk tensile data is the intrinsic to the most of the natural fibres. Moreover, difficult and imperfect measurement of

the fibre diameter and the roughness of the fibre surface would also reduce the reproducibility of the strength of the silk fibre. Among all the samples, the data for degummed 30 minutes are more dispersed. It may be due to the impurity non-uniform sericin on the surface is removed unequally and, boiling water started attacking the fibre at the same time. Therefore, after degummed 30 minutes the portion of the sericin removal was not equal to all fibres and thus induced the stress data dispersive.
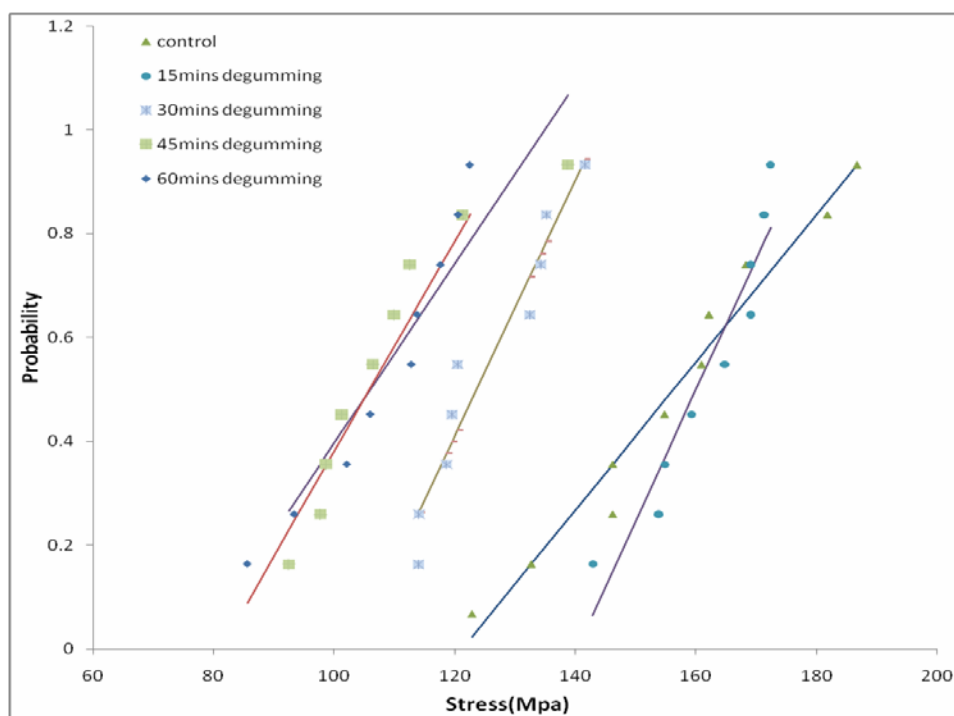
Figure 5.6 Weibull distributions for the strength of the Tussah silk fibres.

5.2.2.3 SEM imaging

The temperature of the water used for degumming must be high enough as it is used to degrade and remove the sericin layer from the fibres. The fibre would be

damaged as all the sericin from the silk fibre as the protective surface coating is removed. Therefore, increasing the time of degumming will increase the damage of the fibre. As the boiling water disrupts the hydrogen bond of the fibre, it would promote the substitution of protein–protein hydrogen bond by water–protein hydrogen bond. The decrement in tensile strength of degummed silk probably reflects this damage. Another reason is contributed from the sericin removal. Hydrophilic sericin envelops fibre. Notwithstanding sericin is insoluble in cold water, it is easily hydrolyzed in hot water, whereby the breaking down the long protein molecules into the smaller fractions which are easily dissolved in hot water (Mondal & Trivedy 2007). The removal of sericin is found from the SEM micrographs.

The surface morphology of heat-treated silk fibres according to different degumming time was investigated by SEM. The SEM micrographs are illustrated in fig. 5.7(a)-(e) and fig. 5.8(a) - (e). Fig. 5.7a, the ordinary Tussah silk fibre is not circular in cross section but its shape is in flat triangle. A Tussah silk is bonded and comprised of many fibre strands. Each fibre strand itself is a bundle of several fibrils and the periphery of the silk fibre strands coagulate many sericin particles irregularly (Jiang 2011). In addition, the Tussah silk fibre obtained directly from the spinneret of silkworm is free from calcium oxalate crystals at micrometer size but these crystals are usually observed on the undegummed cocoon silks. These micrometer-sized calcium oxalate crystals are the type of an excretion by the silkworm and it can be shown in fig. 5.9 which is same as the finding from Fu et al. (Fu et al. 2011).
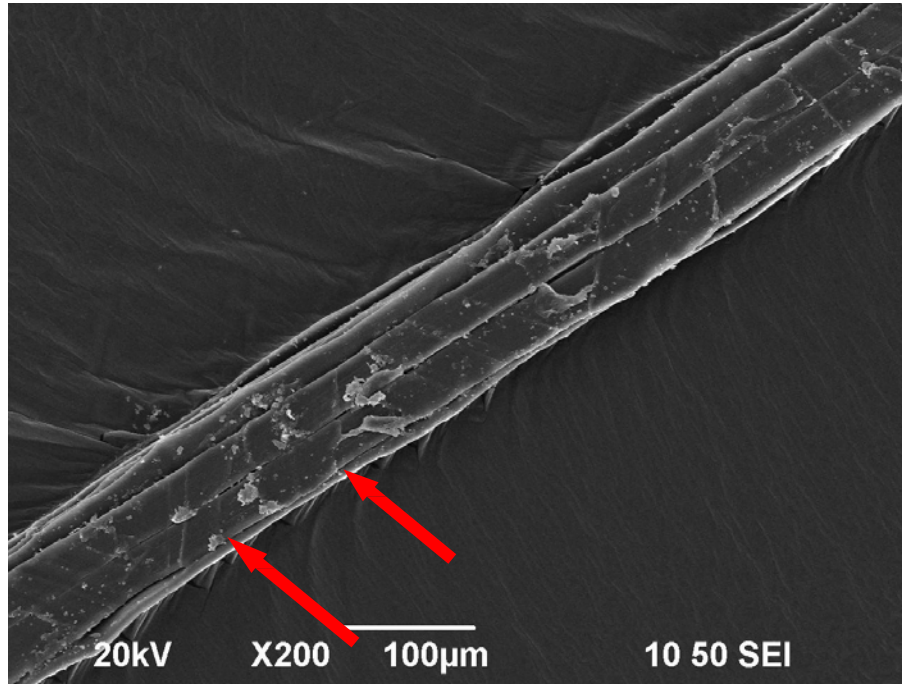
(a)
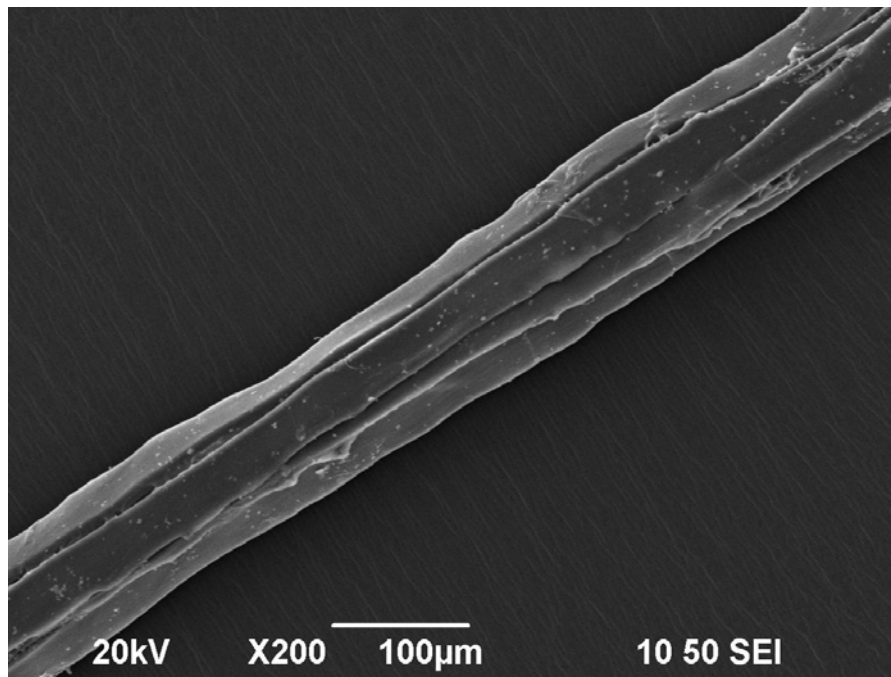
(b)
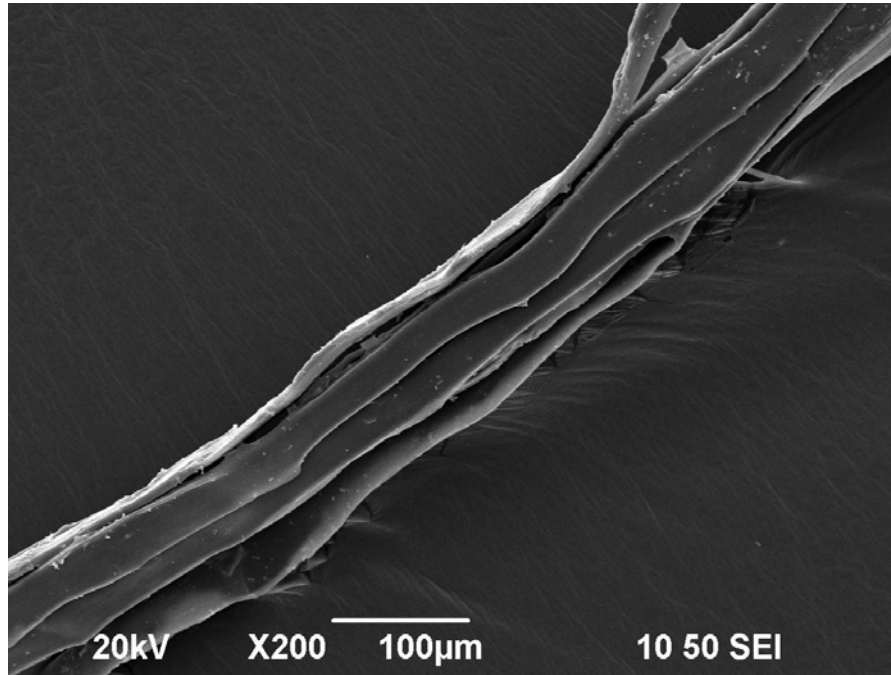
(c)
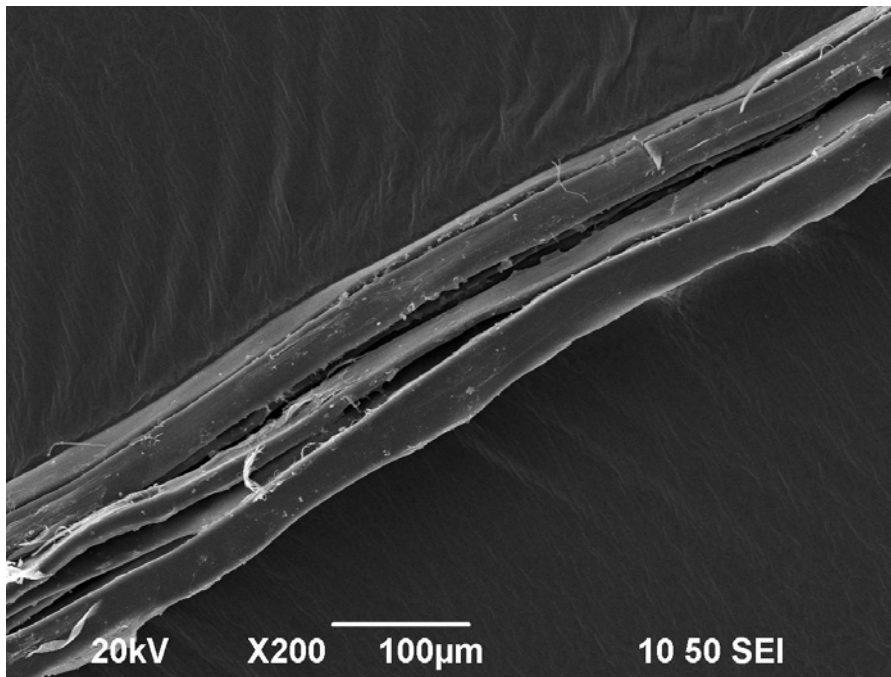
(d)

(e)

Figure 5.7. Surface of Tussah silk fibres degummed for (a) 0 minute (control sample), (b) 15 minutes, (c) 30 minutes, (d) 45 minutes, and (e) 60 minutes.

For the control samples which were not treated with hot distilled water as shown in fig. 5.7(a) & 5.8(a), the surface characteristic of the Tussah silk fibre is fairly rough. This rough surface was clearly evident to large amount of sericin coating (indicated by arrows in fig. 5.7(a)). The sericin appears as some partially non-uniform coating on the surface of the fibres and various granulas and impurity deposits are visible in the vacant spaces in-between the fibres. Different surface morphologies and fibre damages of the raw silk fibres and degummed silks in various conditions were observed according to the SEM micrographs. The micrographs of samples degummed for 15 minutes show good degumming result and no sign of destruction or damage on the silk fibres surfaces (fig. 5.7b and 5.8b). The fibres surfaces are greatly smooth, which show that only very shallow

longitudinal striations (indicated by arrows in fig. 5.7(e)) attributable to the
fibrillar structure for the truly degummed silk fibres.

(a)

(b)
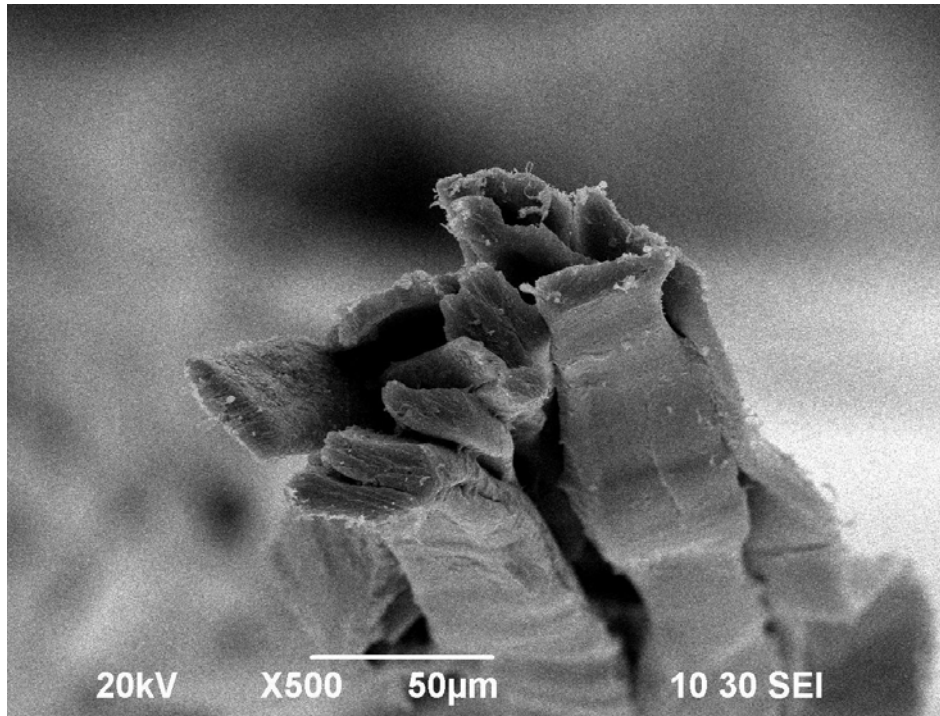
(c)
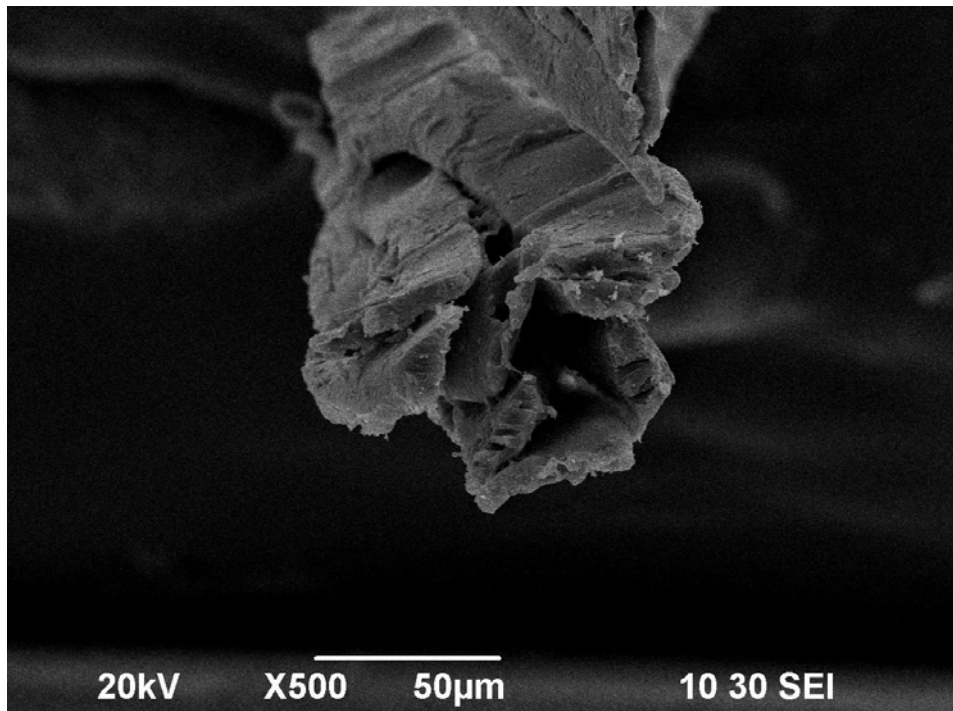
(d)
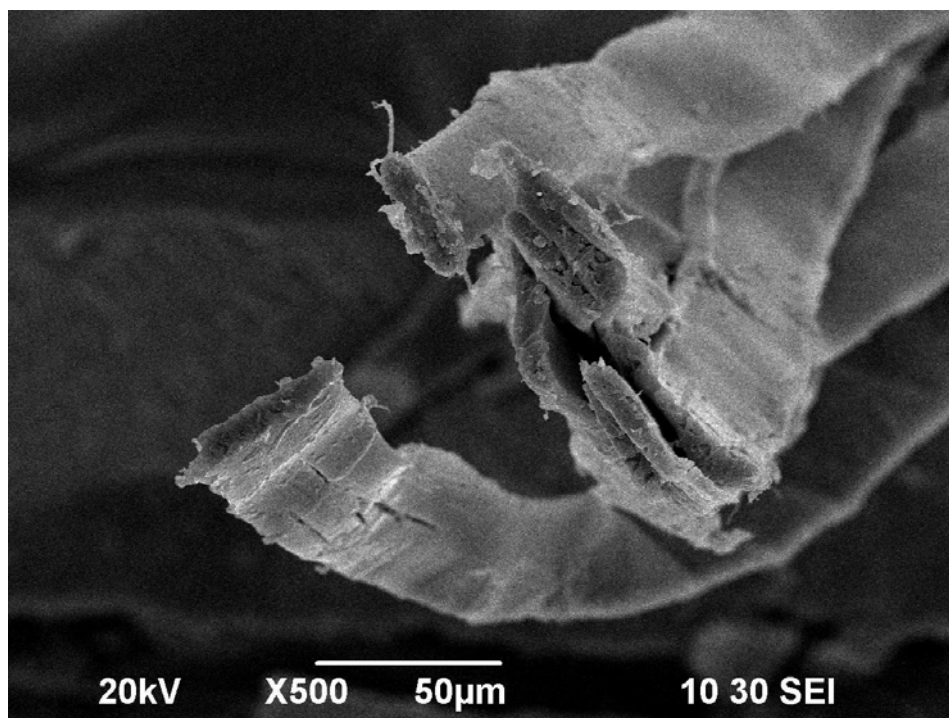
(e)

Figure 5.8. SEM images of Tussah silk fibres degummed for (a) 0 minute (control sample), (b) 15 minutes, (c) 30 minutes, (d) 45 minutes and (e) 60 minutes.

Boiled sample which degummed for 30 minutes were free from non-uniform coating, any granulas and impurity. In some parts of the fibre, sericin layers are dissolved and fibres are separated from the main fibre axis leaving the clean fibre surface to appear. Fig. 7 c-e and 8 c-e show the surfaces of silk fibres degummed for 30 minutes, it is found that the sericin are almost completely removed from the fibre surfaces but some surface damages are observed.
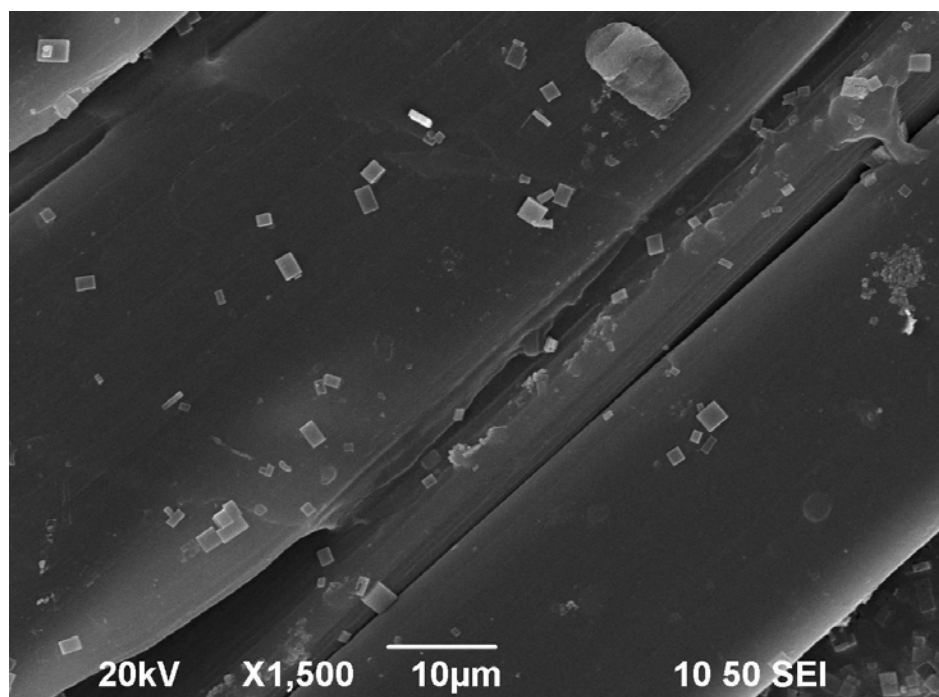
Figure 5.9. Micrometer-sized calcium oxalate crystals on the surface of Tussah silk fibre.

The cases of fibrillation get even worse as much more damages were observed for 60 minutes heat-treated. The higher magnification of SEM examination of the tussah silk fibres are showed that the individual silk fibre strands are split off (fig. 5.10(a)). Fibrillation of some fibre threads also occur (fig. 5.10(b)). Moreover, based on fig. 5.7(a-e), it is found that the fibre diameters increase gradually when extended the degumming time. It is mainly because the binder (sericin) is dissolved and removed so that the fibres disperse.
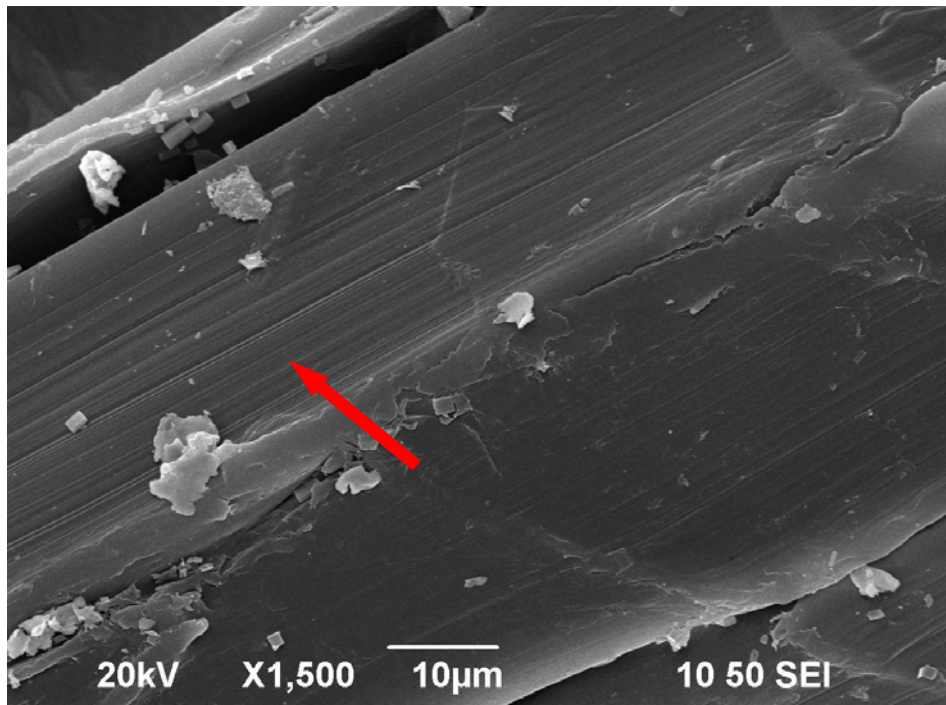
(a)
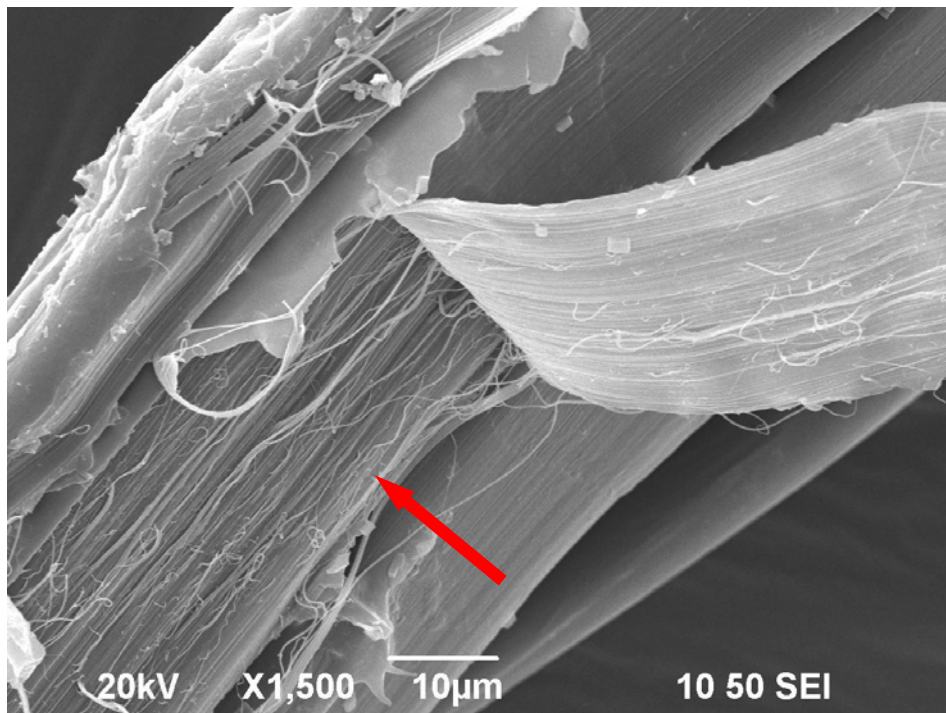
(b)

Figure 5.10. (a) & (b) Defects of the degummed Tussah silk fibres indicated by arrows.

5.2.2.4 Thermal and structural conformation

DSC curves of Tussah silk fibre degummed for different time durations as compared with control sample are shown in fig. 5.11.
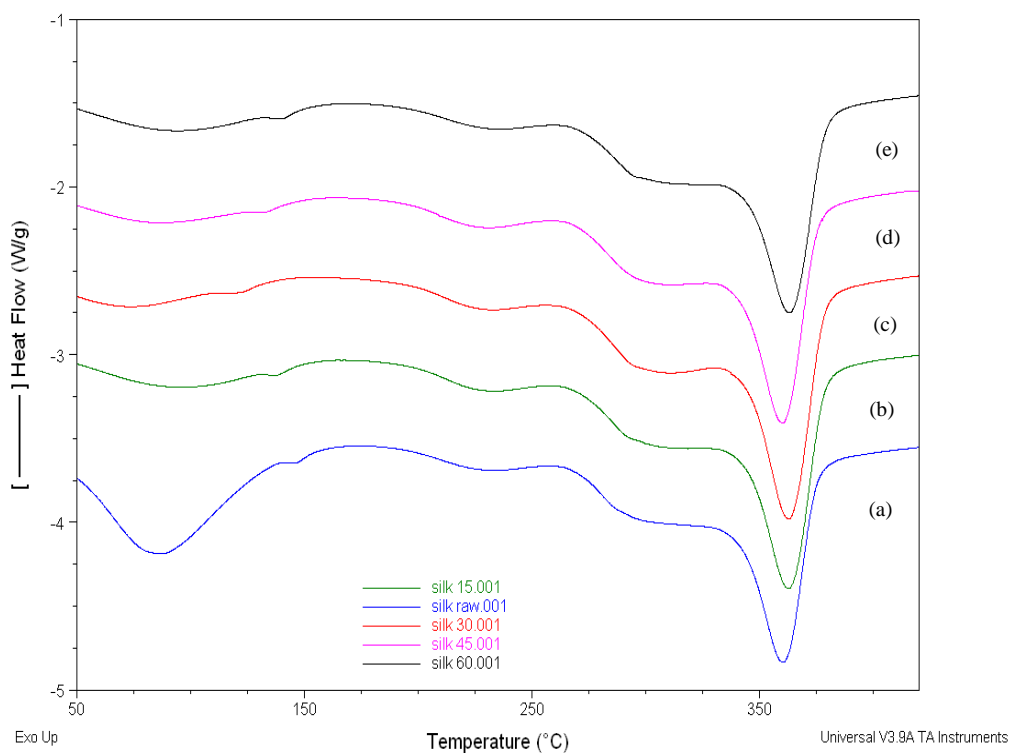
Figure 5.11. DSC curves of Tussah silk fibres degummed for (a) 0 minute (control sample), (b) 15 minutes, (c) 30 minutes, (d) 45 minutes and (e) 60 minutes.

The change of thermal behaviour seems to have little influence in respect to the degumming time (Jiang et al. 2006). Silk fibre shows two broad and large endothermic peaks around 100°C, due to the loss of moisture, at about 365°C, attributed to the thermal degradation of a well-oriented β-sheet crystalline

124

conformation. The endotherm at 225°C was attributed to the molecular motion within the α-helix crystals, while the exotherm at 270°C could be attributed to the crystallization during heating by forming the β-sheet structure from a random-coil conformation. The broad and major endotherm at 365°C was due to the decomposition of fibroin molecules with unoriented β-sheet conformations.

The thermogravimetric curves of silk fibre are shown in fig. 5.12. Different types of silk fibres exhibit different thermal degradation behaviours as it is related to the polymorphs of crystalline structure and amino acid composition. Thermal decomposition of Bombyx mori fibre took place in a single step, but Tussah silk fibre underwent several steps (Kurosaki et al. 1999). According to TGA results, the curves of thermal decomposition of all samples can be divided into three subsequent regions, characterized by evident different mass loss rates. The initial weight loss below 110°C was attributed to the evaporation of water, and was followed by nearly constant weight from 110°C to 170°C. On the other hand, little loss in mass was observed in the second stage range from 170°C to 275°C, it could be attributed to the loss of other low temperature volatile species. The third loss from 275°C to 390°C was associated with the breakdown of side chain groups of amino acid residues as well as the cleavage of peptide bonds of Tussah silk fibre (Freddi et al. 1997; Kweon & Park 2001; Kweon, Um & Park 2000)
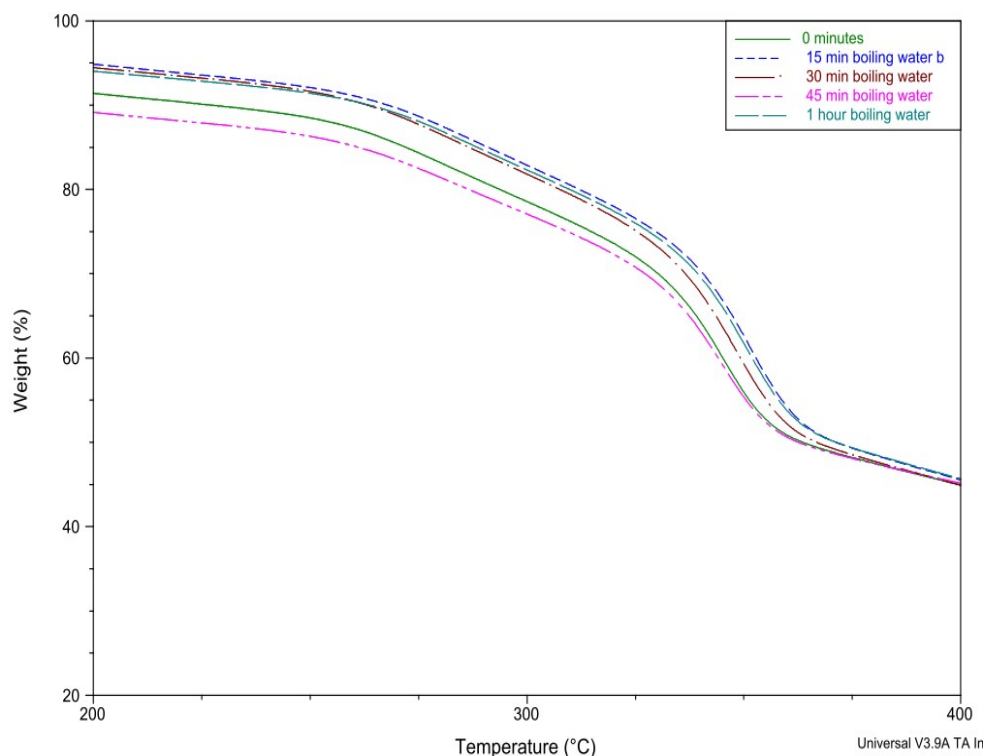
Figure 5.12. Thermogravimetric curves of the silk fibres degummed for (a) 0 minute (control sample), (b) 15 minutes, (c) 30 minutes, (d) 45 minutes and (e) 60 minutes.

Concerning the differential weight loss (dW/dT), DTG curves provide clear evidence for the aforementioned degradation steps (fig. 5.13). The maximum degradation temperature of each step is obtained at about 200°C, 280°C & 350°C, respectively. However, both of the thermal decomposition and DTG curves of the fibres are not changed significantly from those undegummed fibre samples, indicating that the hot water treatment seems to have little influence toward the thermal decomposition behaviour. Therefore, the results obtained from TGA and DSC are matched. The beginning of weight loss occurred within the same temperature range of the endo/exo transitions recorded by the DSC trace (Motta, Fambri & Migliaresi 2002).
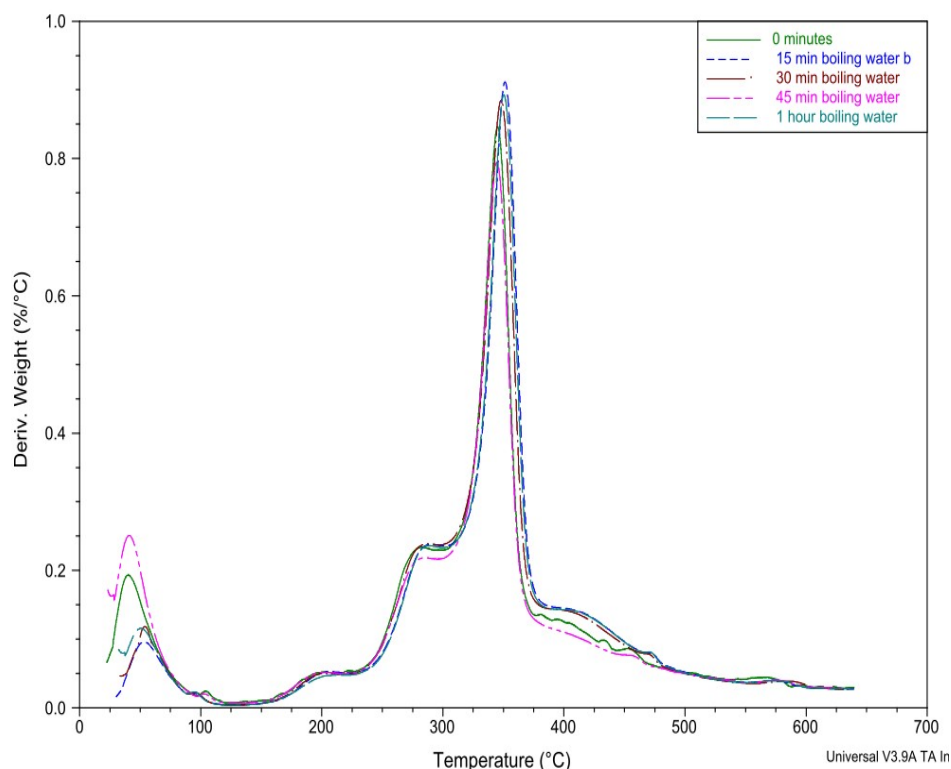
Figure 5.13. DTG curves of the Tussah silk fibres degummed for (a) 0 minute (control sample), (b) 15 minutes, (c) 30 minutes, (d) 45 minutes and (e) 60 minutes.

To examine the structural change of silk fibre degummed by hot water, the secondary structure of all types of silk fibre samples were investigated. The amide bands of FT-IR spectra are known to be sensitive to the molecular conformation of silk fibre (Freddi et al. 1997). Fig. 5.14 shows the FTIR spectra of all silk fibres degummed for different time durations. All samples show strong bands at 1516 cm-1 (amide II), 1235 cm-1(amide III), 965 cm-1(amide IV), and 695 cm-1(amide V), assigned to the β-sheet, and 1651 cm-1(amide I) and 621 cm-1(amide V), assigned to α-helix. However, the above data show the similar FTIR spectra imply that the molecular conformation of degummed fibres does not change significantly and they assume to both of β-sheet structure and random coil α-helix conformation (Li et al. 2003).
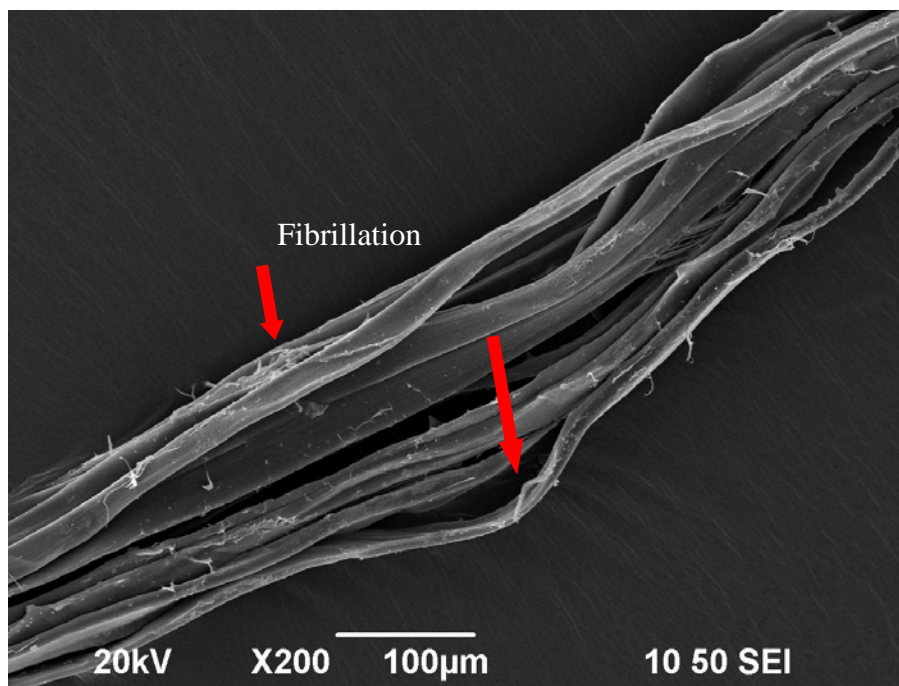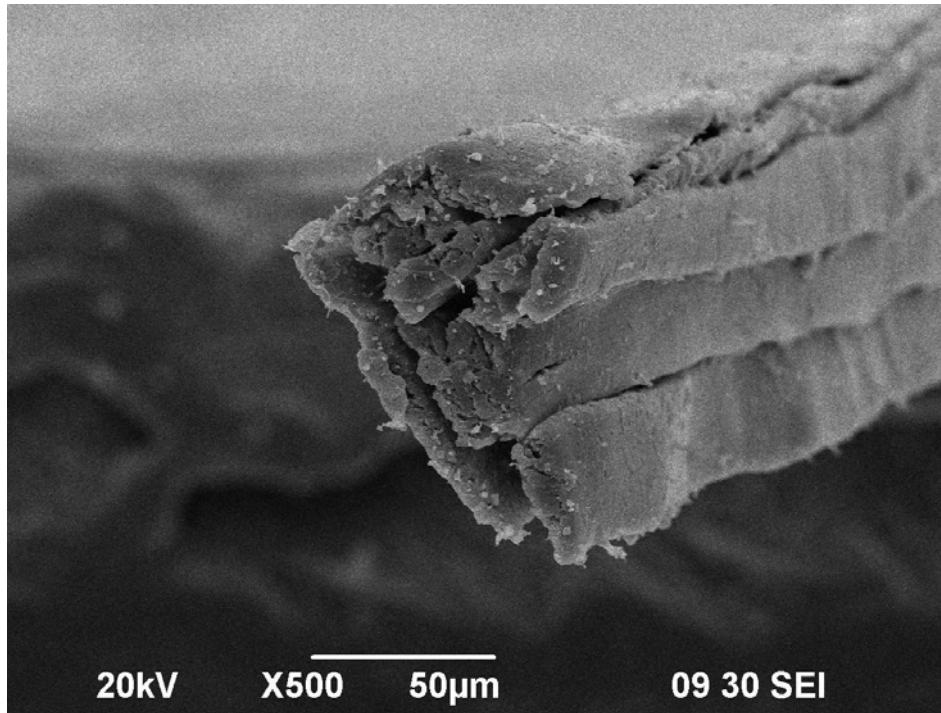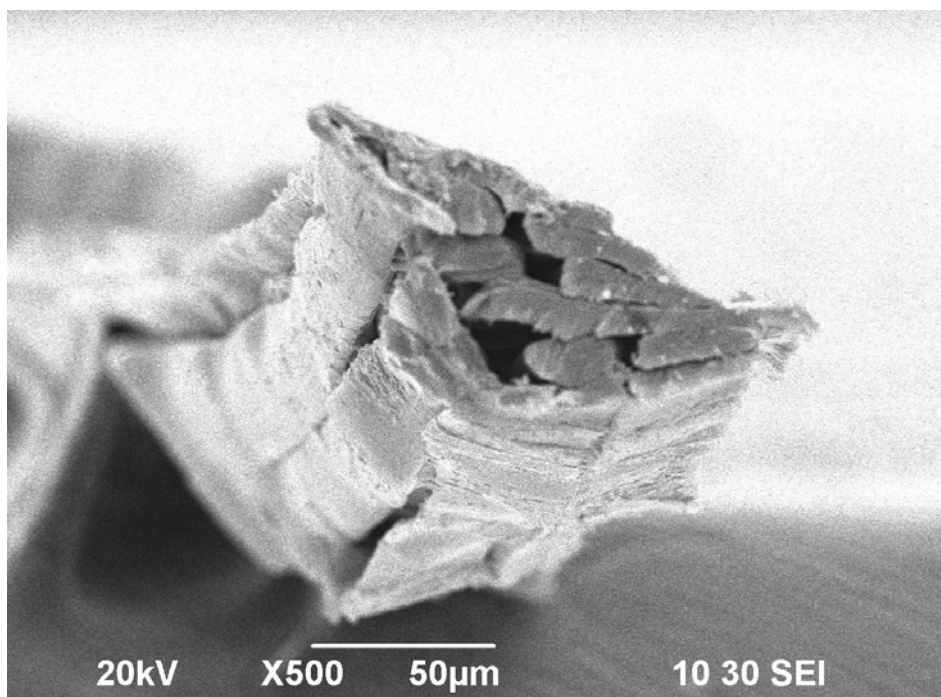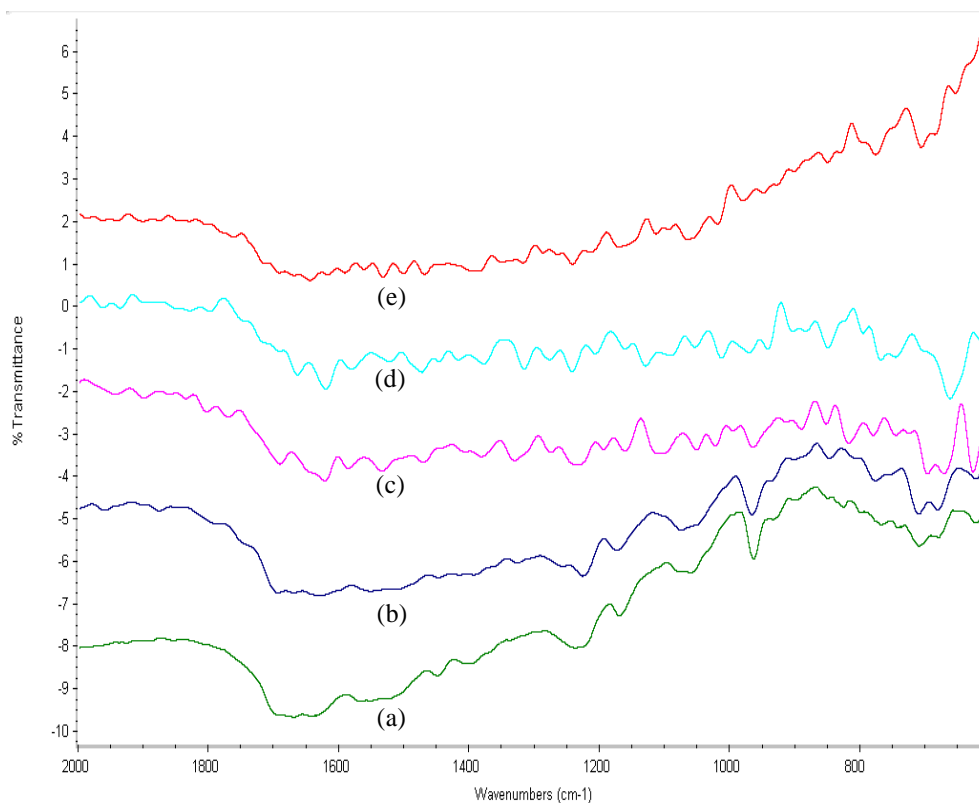
Figure 5.14. FTIR spectra of Tussah silk fibre degummed for (a) 0 minute (control sample), (b) 15 minutes, (c) 30 minutes, (d) 45 minutes and (e) 60 minutes.

As discusse in previous section, the tensile properties and the surface characteristics of the fibre are affected by the degumming time. Based on the results shown in this chapter, it is proved that only little influence on the thermal properties and FTIR spectra of the silk fibre treated for different degumming times.

To sum up, preprocessing of silk fibre commonly known as degumming is an essential process. Silk degumming process scours the sericin and some impurities from the surface of the silk fibres. Through the measurement of the mechanical properties and surface morphology of the samples, the results show that using boiling water to degum Tussah silk fibre for 15 minutes can achieve better tensile

strength, stain and modulus. As the major amino acids groups in sericin are hydrophilic, hot water degumming treatment can dissolve the sericin into the water. Three major factors that would influence the tensile properties of a silkworm silk fibre during the process of degumming are:

1) Sericin removal,

2) Molecular changes and

3) Bonding breakage.

From the SEM analysis, the micrographs show that all the impurities are removed and no damage on the surfaces is found after degumming. Degumming could affect the tensile properties of silkworm silk. However, through the measurement of the thermal properties, secondary structure and surface morphology of the samples, the results show that that the degumming time has a little effect to the thermal properties and the secondary structure of the silk fibre.

5.3 Different Surface Treatments on Silkworm Silk Fibre Degumming

During the degumming process, sericin is hydrolyzed, and solubilized in degumming agents and media. Silk degumming may cause up to 25% weight loss, which is dependent on the source and sort of silk and the chosen treatment. After removing sericin, the luster of pearls appears on the surface of silk fibres and

good surface brightness and excellent elasticity of the silk fibres are resulted (Mahmoodi, Arami & Mazaheri 2010). Several degumming processes have been developed and under investigated such as extraction with boiling water (discussed in Section 5.2), enzymatic degumming, and degumming in boiling acidic solutions, soap or alkaline solution (Section 5.3.1.1). The effect of degumming directly influences the properties of silk fibre.

Traditionally, the recommended degumming method for silk fibre is carried out by soap or soda ash method [Sodium carbonate (also known as washing soda or soda ash) (Arai, Freddi & Innocenti 2004; Jiang et al. 2006; Khan et al. 2010; Ki et al. 2007; Robson 1999; Tsukada, Freddi & Massafra 1998). In this degumming method, a weight loss of 25–30% would normally occur, which indicates a complete removal of sericin (Robson 1999). Sericin is swollen and emulsified by the soap and finally, removed from the fibre. Nevertheless, the presence of soap and alkalis in the wastewater of degumming process raise an issue of pollution (Mahmoodi, Arami & Mazaheri 2010). Besides, the degumming cycles of the soap ash bath is limited because of acidity of sericin hydrolysis products accumulating in the bath (Khan et al. 2010).

The application of enzymes in textile industries has been increased recently. Various studies have been dealt with the removal of sericin by using different types of enzymes including protease and lipase as degumming agents (Arai, Freddi & Innocenti 2004; Freddi, Mossotti & Innocenti 2003; Khan et al. 2010; Mahmoodi, Arami & Mazaheri 2010). Enzyme degumming involves the proteolytic degradation of sericin, using the specific proteins with minimum effect on fibre. When the substrate molecule fits into the active sites of the enzyme"s

molecular structure to form an enzyme–substrate complex, this complex is then broken and yields an end product and the original enzyme molecule is reproduced. Enzymes treatment operates under mild conditions and low temperatures which can reduce the energy consumption. However, the lower performance of enzyme degummed silk including difficult to handle and high cost limited the application of enzymes on the silk industry (Freddi et al. 1997).

Using acidic agents such as tartaric acid and citric acid for silk fibre degumming and finishing was approved for silk‟s physical property enhancement (Freddi, Allara & Candiani 1996; Gulrajani & Chatterjee 1992; Gulrajani, Sethi & Guptha 1992). It has been pointed out that the action of organic acids is generally milder and less aggressive than that of an action by alkali solution. Freddi et al. have found that the high performance on degumming is achieved by tartaric acid in terms of sericin removal efficiency and of intrinsic physico-mechanical characteristics of silk fibres (Freddi, Allara & Candiani 1996). Yang et al. have studied critic acid for degumming and found that the dry and wet resiliency of finished silk was remarkably increased with citric acid treatment (Yang & Li 1993). However, same as alkaline treatment, acid also causes the damage on the fibre surface (Sasithorn & Luepong 2010). Fig. 5.15 shows that there is a non-uniform removal of gum (indicated by white arrows) from interlacing regions of fibres degummed by succinic acid (Jiang et al. 2006).
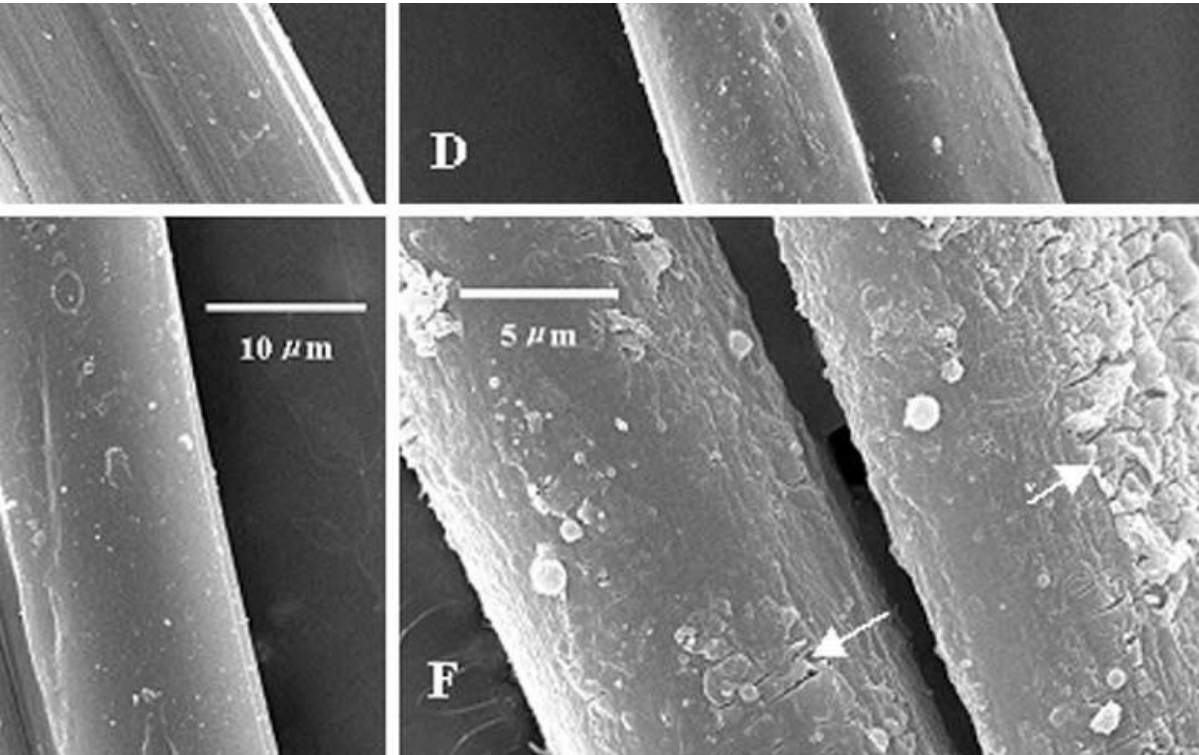
Figure 5.15. Scanning electron micrographs illustrating silk fibre degummed by succinic acid (Jiang et al. 2006).

The surface modifications of fibres by using compatibilizer or coupling agent for effective stress transfer across the interface were explored (Matuana, Balatinecz, Sodhi, & Park, 2001). The compatibilizer is a kind of polymeric interfacial agent or polymers with functional groups that graft onto the chain of polymers. Besides, the coupling agent is a chemical substance which is able to react chemically on both natural fibre and polymer matrix during processing to form or promote a strong bond at the interface as bridges in order to improve the mechanical properties of resultant composites. The nature of bond formed between a specific coupling agent and fibre depends strongly on the characteristics of fibre surface to which the coupling agent is adhered (Matuana, Balatinecz, Sodhi, & Park, 2001). Tetrafunctional organometallic compounds based on titanium, silicon and Zirconium are the common coupling agents nowadays (Saheb & Jog, Natural Fiber Polymer Composites: A Review, 1999).

These coupling agents are usually used to bind organic and inorganic materials together. Cyanuric chloride is one of the most effective and widely applicable coupling agents to attach synthetic or natural polymers such as polysaccharides to proteins (Usui & Matuhasi 1979). Gotoh et al. have found that cyanuri chloride as coupling agent improved the interaction between silk fibre and Polyethylene glycol (PEG) and the result indicated that the PEG molecules covalently bonding to silk fibre narrowed the spacing of the inter-chain periodicity and promoted the formation of the inter-chain β-sheet (Gotoh, Tsukada & Minoura 1993). Furuzone et al. used coupling agent to prepare a covalent linkage between silk fibre and hydroxyapatite (HAp) (Furuzono, Kishida & Tanaka 2004).

Plasma treatment is a new environmentally-friendly technology which can alter the surface properties of polymers and textile materials, without interfering in their bulk properties. Chaivan et al. have studied the utilisation of SF_6 plasma treatment for improving in hydrophobic property of silk fibre. A reproducible and significant increase in the hydrophobic property compared with the untreated sample was obtained (Gonzaleza, Cervantes-Uca, & Olayob, Effect of fiber surface treatment on the fiber-matrix bond strength of natural fiber reinforced composites, 1999). Fang et al. have found a numerous of advantages of oxygen plasma for silk fibre surface modification. It includes enhanced color yields, excellent pattern sharpness and more grooved surface. Besides, the hydrophilicity of silk fibre was remarkably improved after being treated with plasma (Fang et al. 2008). CF_4, CHF_3, C_2F_6, and their mixtures in plasma modification of polymers and textiles have been reported to be effective in imparting water repellency to fibres efficiency of the surface treatment (Li & Jinjin 2007). However, the cost of the plasma treatment restricts the usage of the technique in the industries widely.

Alkaline processing is one of the most common chemical treatments in the industry which is aimed at increasing the surface roughness of natural fibre that results in enchancing mechanical interlocking (Gonzaleza, Cervantes-Uca, & Olayob, Effect of fiber surface treatment on the fiber-matrix bond strength of natural fiber reinforced composites, 1999). When the silk fibre is degummed by an alkaline solution, non-covalent bonds of silk fibres are then modified and thus to cause the swell of the fibre. The swelling effect of the fibre is mainly governed by the difference of osmotic pressure arising between the fibre and the solution to form the protein salts (salts-Donnan membrane effect) (Hitchcock 1954; Higa, Taniokaa & Kira 1998).

Several alkalis such as NaOH (Sodium hydroxide) or Na_2CO_3 (Sodium carbonate) are commonly used nowadays for degumming. However, these strong alkali treatments impose a relatively harsh irritation to silk fibres (Yamadaa et al. 2001; Jiang et al. 2006). Fig. 5.16 shows the surface of a silk fibre degummed by Na_2CO_3. Individual longitudinal strands are clearly seem, white and black arrows indicate the positions and corrosive dents of the fibre, respectively (Jiang et al. 2006).
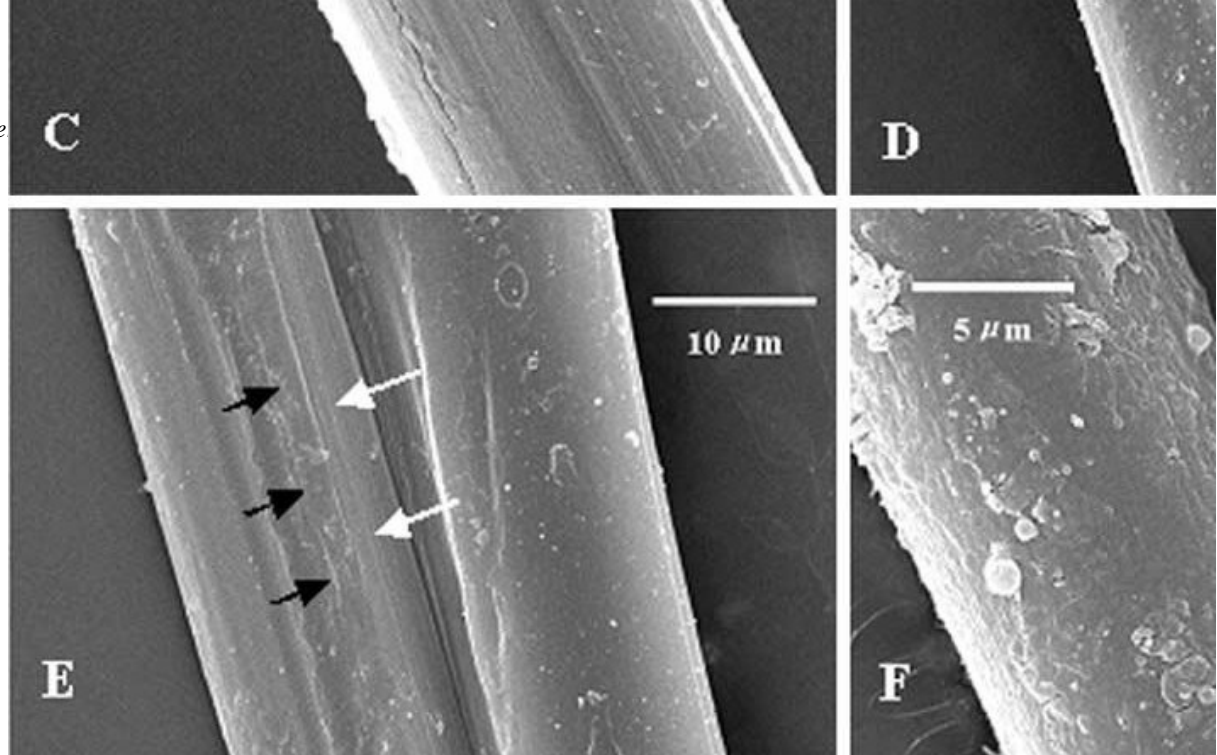
Figure 5.16. Surface of Bombyx mori silk fibre degummed by Na_2CO_3 (Jiang et al. 2006).

$NaHCO_3$ is suggested as a relatively weak alkali solution (~ pH 8-9) for silk fibre degumming. In this section, the properties of silk fibre after being degummed by different concentrations of $NaHCO_3$ for a set period of time are studied.

Tussah silk fibres were treated carefully to avoid stretching plastically during the whole experiment process. Different concentrations (0%, 0.5%, 1%, 1.5%, 2%, 5%, 10% and 15%) of $NaHCO_3$ solution were used to investigate their influence to the properties of the silk fibres. Before degumming, all fibres were cut in 30cm in length and then placed into an oven at 80°C for 8 hours. Afterward, the silk fibres were immersed into a beaker with degumming solution individually. All beakers with fibres were then heated in a hot water bath for 1 hour at 100°C for degumming. Subsequently, degummed fibres were rinsed under distilled water and dried immediately in the oven at 80°C for 4 hours.

The weights of fibres before and after degumming were measured to calculate the

weight loss. Fig. 5.17 illustrates the weight change of degummed fibres by different concentrations of $NaHCO_3$ solution. The weight of the fibres decreases and the weight loss increases sharply with the concentration from 0.5 % to 2%. Afterward, it keeps in a steady increment. The weight change of the fibres implies that the amount of residual sericin on the fibre surface decreases with an increase of the concentration of $NaHCO_3$. High moisture condition would dissolve sericin which is a key element bundling and enveloping fibres together. This layer is insoluble in cold water but easily hydrolysed and whereby the long protein molecules are broken down into small fraction. As a result, it is easily dispersed or dissolved in hot water (Mondal & Trivedy 2007).
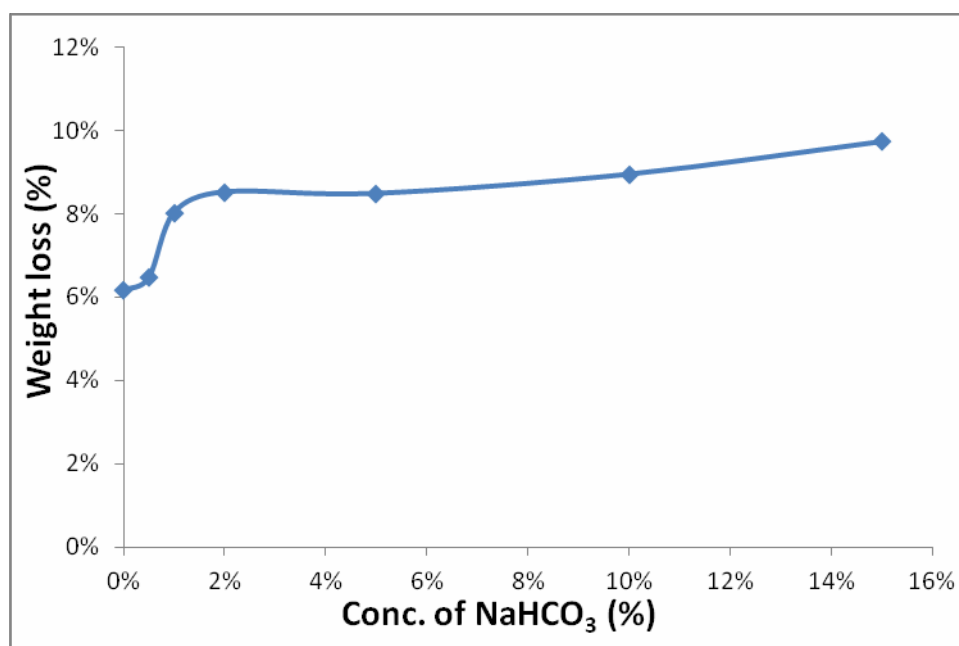
Figure 5.17. Weight change of silk fibre degummed at different concentrations of $NaHCO_3$.

Tensile property test was then performed by using MTS Alliance RT/10 with the crosshead speed of 60 mm/min at standard environmental conditions (20°C, 60% relative humidity). In fig. 5.18 and 5.19, the tensile properties, in terms of the maximum force and elongation at break of the silk fibres degummed by different concentrations of $NaHCO_3$ decrease sharply with an increase of the concentration up to 2%. The tensile properties of degummed silk fibre steadily decrease with the concentration of $NaHCO_3$ over 2%. Degumming the silk fibres by using alkali solution would cause hydrolysis of the peptide linkages and decrease their tensile properties. However, the degree of hydrolysis is dependent on the pH level of the degumming solution. Compared with the tensile properties of silk fibres degummed by water and strong alkaline solution (Jiang et al. 2006; Perez-Rigueiro, Viney & Elices 2000), $NaHCO_3$ exhibits that there is no severe detriment to the tensile properties of the silk fibre.
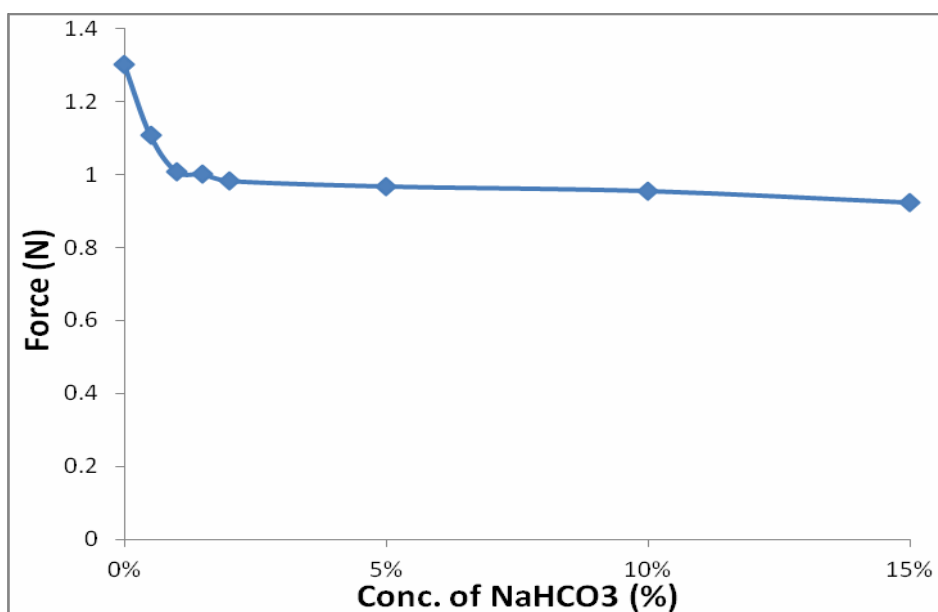
Figure 5.18. Force-Concentrations of $NaHCO_3$
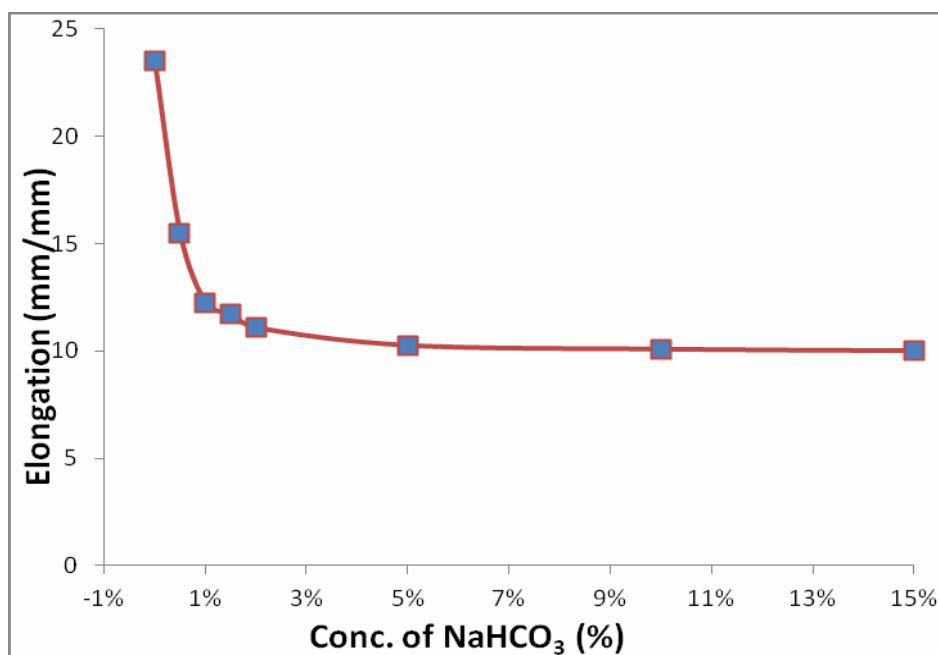
Figure 5.19. Elongation -Concentrations of $NaHCO_3$

An opposite effect between the hot water and alkaline treatments is the factor whereby explains the results of the tensile test. When the fibre is immersed into low concentration of $NaHCO_3$ solution, water molecules would influence the properties of fibre. These molecules disrupt hydrogen bonds initially and present in the amorphous phase. Thus, water-protein hydrogen bonds are formed and deteriorate the fibre"s tensile properties (Perez-Rigueiro, Viney & Elices 2000). When increasing the $NaHCO_3$ concentration, non-covalent bonds of silk fibres are modified and conformation occur. The increment of the concentration of $NaHCO_3$ and thus swell of the fibres. The swelling effect of the fibre is mainly governed by the difference of osmotic pressure arising between the fibre and $NaHCO_3$ solution and thus the protein salts are formed (salts-Donnan membrane effect) (Hitchcock 1954; Higa, Taniokaa & Kira 1998).

Further applying the heat, water is eliminated and removed by the immersion in the solution contributing to the formation of new hydrogen bonds in the amorphous phase of the fibre. The cohesive forces of the fibre are therefore weakened which induce the splitting up of the fibres (Bowes & Kenten 1950). Therefore, the reaction between the fibre surface and Na^+ increases. When the concentration of $NaHCO_3$ increases, the effect of the alkaline treatment overcomes and replaces the effect of water and thus the degradation of the tensile properties becomes less severity.

Table 5.4. Heat of fusion of $NaHCO_3$ treated fibres.

Concentration of $NaHCO_3$ solution	ΔH_f (J/g)
Raw	128
0%	106.8
1%	116.7
5%	154.8
10%	140.1
15%	141.6

DSC analysis by using TA instrument DSC Q100 was then conducted to study the fibre"s thermal properties. All fibres were weighted and then heated from 5°C to 425°C at a heating rate of 10°C/min. The flow rate of nitrogen gas was set to be 60 ml/min. The thermal properties of fibres degummed at different $NaHCO_3$

concentrations are shown in fig. 5.20. Three peaks at 100 ^{o}C, 230 ^{o}C and 340 ^{o}C are noticed on the DSC curves. As the heat of fusion can be calculated from the area under an absorption peak, the values of ΔH_f for a raw silk fibre as compared with 0%, 1%, 5%, 10% & 15% NaHCO$_3$ degummed silk fibres, respectively are shown as table 5.4. The results show that the values of ΔH_f increase dramatically when the concentration of NaHCO$_3$ increases up to 5%. It reflects that the fibre degummed by the high concentration of NaHCO$_3$ requires higher energy to melt and thermal decomposition from their crystalline state.
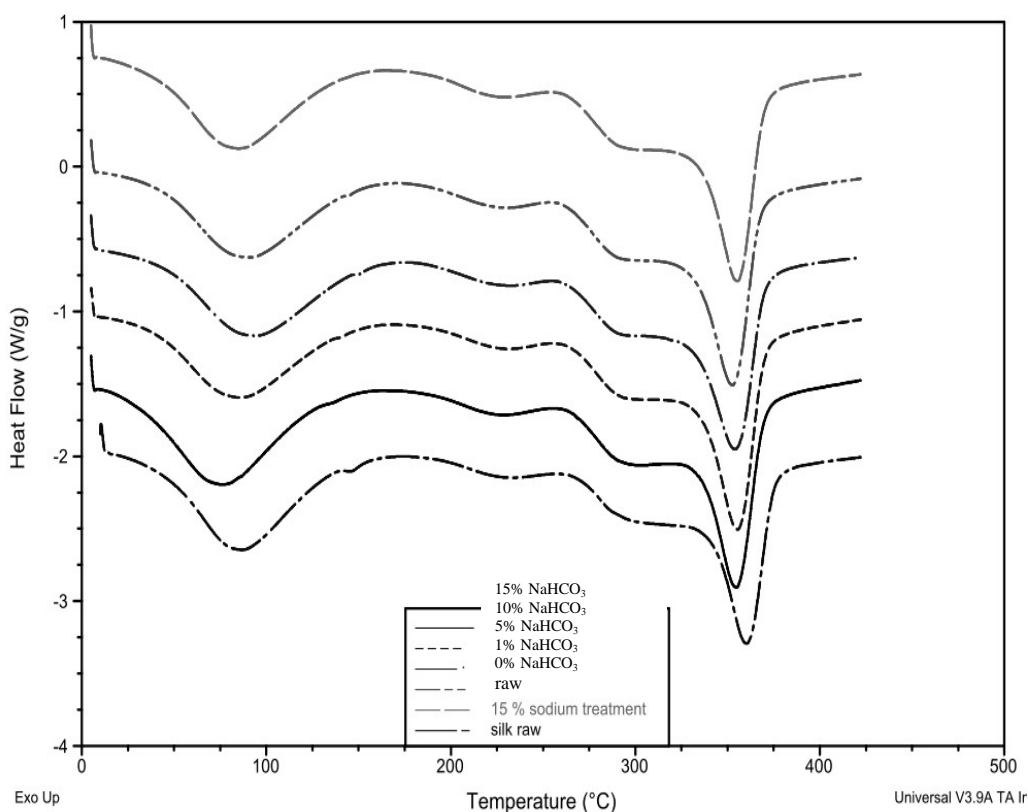
Figure 5.20. DSC thermograms of Tussah silk fibres.

The summary of the mechanical performance of the silk fibre degummed by different agents is shown in table 5.5. Significantly, the degumming process using, soap, succinic acid and enzymes may cause unwanted degradation of fibre (Kearns, MacIntosh & Crawford 2008). Chemically treated fibres showed a considerable decrease in the tensile strength and this decrease was attributed to dimensional change, the substantial bond breakage, degradation of protein chain and partial harmful damages of silk molecules during the treatment (Khan et al. 2010). However, the extent to which these properties are affected may be dependent upon the method and the period of degumming time used (Freddi, Mossotti & Innocenti 2003). As succinic acid is a strong acid (pH=2.88) (Jiang et al. 2006) but citric acid is a weak acid, succinic solution attacked the fibre after the sericin coating removed but citric acid would only have a little or no effect on the fibre. Besides, the strain % of silk fibres was noticeably increased for all degumming method except enzymes treatment. The decrement in the tensile properties of enzyme degummed silk fibre confirms that silk fibres are susceptible to proteolytic attack (Arai, Freddi & Innocenti 2004). The initial modulus of silk fibre was decreased and the elongation at break was increased after degumming with different treatments suggesting the silk fibres become soft and stretchable after degumming treatment (Khan et al. 2010).

Table 5.5. Change of the mechanical properties of silkworm silk fibre degummed by different degumming solutions as compared to its raw silk fibre.

Degummed samples	Tensile strength (%)	Young's modulus (%)	Elongation at break (%)	Ref.
Bombyx Mori silk fibre				
Distilled boiling water	-44	-50	44	(Jiang et al. 2006)
Succinic acid	-38	-28	39	(Jiang et al. 2006)
Sodium carbonate	-18	-34	28	(Jiang et al. 2006)
Urea	0	-44	33	(Jiang et al. 2006)
15% soap	-41	-13	33	(Khan et al. 2010)
15% citric acid	20	-11	47	(Khan et al. 2010)
30% citric acid	0	-17	28	(Khan et al. 2010)
Protease	-20	--	-34	(Arai, Freddi & Innocenti 2004)
Tussah silk fibre				
Enzymes	-16.1	--	--	(Ravisankar 2011)
Acid	-34.6	--	--	(Ravisankar 2011)
Distilled boiling water	3	9	21	
NaHCO$_3$	9	--	-34	

5.4 Microbond Test

After degumming silkworm silk fibre, a microbond test was processed in order to

prove the improvement on surface bonding between the silkworm silk fibre and the matrix. To date, the micobond, pull-out, fragmentation and microindentation tests have been widely used to elaluate the interfacial shear strength for both thermoset and thermoplastic composites. In this section, the micrbond test method was used (Miller, Muri & Rebenfeld 1987). A small amount of PLA in a liquid form was dropped onto the fibre surface. After the droplets were cured, they form elliptical concentric microdroplets around the silkworm silk fibre. The silkworm silk fibre sample at one end with taped cardboard was then suspended at a load cell of a mechanical machine. Two rigid plates as a jaws of microvice were positioned just above the droplet to grip it and the system was submitted to tension at a rate 1.5 mm/min. Assuming the silkworm silk fibre is circular,the interfacial shear strength, τ was calculated from:

$$\tau = \frac{F_d}{\pi d l_e}$$

(4.2)

Where F_d is the debonding force, d is the diameter of silkworm silk fibre, and l_e is the fibre embedded length. The diameters of the silkworm silk fibre were depended on the degumming process. The embedded length were measured by the optical microscopy. Table 5.6 shows the results of the interfacial shear strength between silkworm silk fibre and PLA according to equation (4.2). The interfacial shear strength increases of silk fibre reinforced PLA samples degummed by different methods. As the hydrophilic sericin was removed, the compatibility, in term if bonding strength between the silkworm silk fibre and PLA increased.

143

Besides, the degumming treatments increase the damaging of the fibre surface and thus increasing the friction and enhancing the mechanical interlocking between the fibre and PLA.

Table 5.6. Evaluation of the interfacial shear strength between silkworm silk fibre and PLA (equation (4.2)).

	Degumming process		
	Raw	Boiling	NaHCO$_3$
τ (MPa)	20.1	37.8	30.1

Chapter 6

Properties of a Silkworm Silk Fibre Reinforced PLA Composite

6.1 Introduction

To overcome the disadvantages of using traditional metallic bone fixators, silkworm silk fibre reinforced PLA composites, based on their inherent mechanical, biocompatible and bioresorable properties have been found as a desirable bio-material for bone plate fixation. This chapter is a further study and clarification on the silkworm silk fibre reinforced PLA composites, particularly on the correlationship between thermal, mechanical and degradation properties.

6.2 Injection Moulded Silkworm Silk Fibre Reinforced PLA Composite

PLA pellets used in the current study were a neat grade commercialized by Cargill-Dow under the brand name NatureWorks®PLA Polymer. Same as chapter 4 and 5, silkworm silk fibre with the average fibre diameter of 100 μm was supplied by Ocean Verve Ltd Hong Kong (fig. 6.1). The inherent body structure of

silkworm silk fibre is composed of two cores of fibre which exists in a paired of organ. The fibre itself is a bundle of several fibrils with a diameter of 1μm and one fibril contains 15nm wide microfibrils (Fakirov & Bhattacharya, Handbook of engineering biopolymers: homopolymers, blends and composites. Cincinnati (OH): Hanser, 2007; Lee Y. W., 1999). As the silk fibre is comprised of many small bundles of fibrils, there is no doubt that the wetability of its resultant composites is the key to ensure good bonding or complete chemical bonding between all fibres and matrix is achieved.

Figure 6.1. Tussah silk fibre.

All samples were made by Hakke MiniLab twin-screw micro-extruder which is shown in fig. 6.2. It includes three main components: (1) Continuous extrusion with force feeder (2) Minijet and (3) Mould.

Figure 6.2. Hakke MiniLab twin-screw micro-extruder.

Before mixing the fibre with PLA, degummed fibre were chopped into 5 mm in length in order to avoid coiling with the screws and stretching the fibres plastically either co- or counter rotating during injection process. These fibres were pre-placed inside an oven for drying to minimise excessive water/moisture content into them before the process. The optimal fibre content, in terms of mouldability inside the PLA environment was 5 wt% based on our preliminary study. A uniform temperature of 180°C was maintained at all zones inside the machine so as to ensure that PLA was in a processing temperature condition, and also this temperature is below the degradation temperature of the fibre. The screwing speed and the mixing duration were set as 100 rpm and 10 mins, respectively. The first run of the extrusion was discarded and the strands of an extrusion mixture were then directly collected by a pre-heated injection cylinder for further injection moulding. The mixture was then transferred to a Thermo

Hakke small scale injection moulding machine. The injection cylinder and the mould were pre-heated to desirable temperatures of 200°C and 45°C, respectively.

The samples were made in a dumbbell shape according to ASTM D3039 and in regular plates with the size of 90 mm x 10 mm (fig. 6.3) for the tensile property and flexural strength tests, respectively. The samples of pristine PLA and silkworm silk fibre reinforced PLA composite are shown in fig. 6.4.
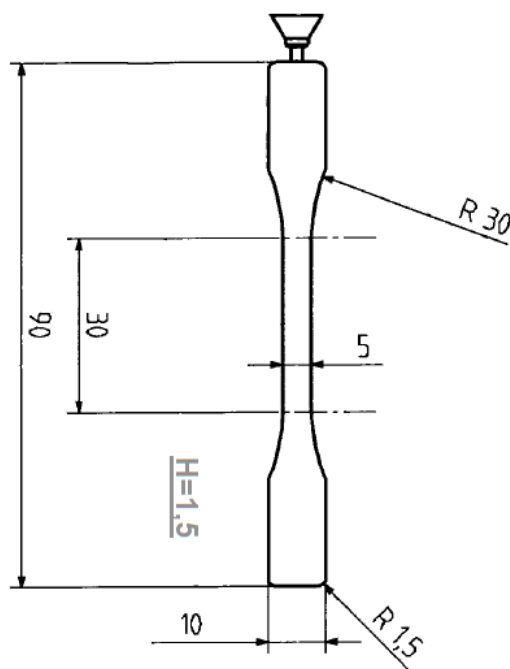
Figure 6.3. Geometry of the sample.

(a)

(b)

Figure 6.4. Sample of (1) PLA and (2) silkworm silk fibre reinforced PLA composites.

6.3 Physical and Mechanical Properties

The density of the fibres was determined by pycnometry. The density is simply defined as mass divided by volume (g/cm^3). Water was used as reference liquid at 23 ^{o}C.

Table 6.1 summarizes the results from the density measurements. The results show that the density of the composite sample decreases by 1.6 % as compared with the pristine PLA. It is a reasonable finding as the density of the silkworm silk fibre is lower than that of the PLA. Based on the principle of the "Rule of Mixture", the density of the composite is lower depending on the amount of silkworm silk fibre to be added. Moisture content in the silkworm silk fibre is also an affecting factor as voids may be formed during the moulding process. Entrapment of air within the space between fibrils may also be an issue. In reality, light weight and controllable porosity are desirable parameters for composite bone fixators as it can reduce their deadweight and control the rate of bioresorption inside the human body.

Table 6.1. The density measurement of the pristine PLA and the silkworm silk fibre reinforced PLA composite.

	Density (g/cm^3)
Pristine PLA	1.26
Composite	1.24
Change of percentage (%)	-1.6

The tensile property test was carried out under an ambient condition. Tensile property test is an evaluation process for characterization of mechanical and materials performance, especially strength, modulus and ductility of a specimen. MTS RT-50 (50kN) testing machine was utilized for the test in the current study. Silkworm silk fibre reinforced PLA samples were made in a dumbbell shape according to ASTM D3039 for the tensile property and flexural strength tests, respectively. Grip separation was set to 48 mm in length and the crosshead speed was adjusted to 1.5 mm/min for the tensile test. Extensometer was used for measurement of a small change in linear dimension.

During a flexural strength test, tensile stress in the convex side and the compression stress in the concave side were produced. Then the shear stress along the midline was generated. Flexural strength properties obtained in this test mainly included the modulus of elasticity in bending, flexural stress, and flexural strain. The samples were tested according to the ASTM D(7264)790 by the MTS (RT-50) testing machine. The default radii of the loading nose and supports were 5.0. The crosshead speed of the flexural strength tests was 0.946 mm/min. Fig. 6.5 shows a tailor-made supporting fixture for flexural test.

Izod impact strength of un-notched samples was tested instrument according to ASTM D256. The measurements were performed at ambient conditions, a temperature of 25°C and a relative humidity of approximately 40%. The impact energy was divided by the width of the specimens to yield impact strength (J/m). 10 samples of each type of materials were tested.
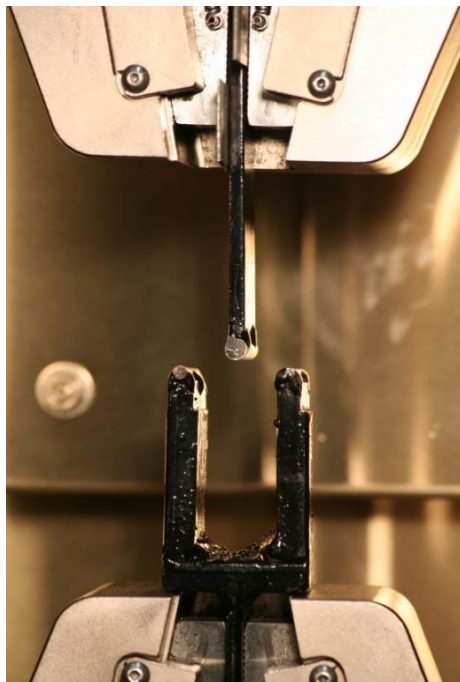
Figure 6.5. Tailor-made supporting fixtures for flexural test.

Average impact strength of about 156.3 J/m was found for the pristine PLA samples that did break during the testing compare with 110.7 J/m of silkworm silk fibre reinforced PLA composite. The impact strength of the composite was significantly lower than that of the pristine PLA samples. The reduction of the impact strength was because silkworm silk fibres in the polymer matrix acted as stress concentrators. Consequently, the stress concentration occured which decreased the crack initiation energy. Fig. 6.6 & 6.7 show the stress-strain curves obtained from the experiments. In these figures, they show that the tensile and flexural strengths as well as ductility of the silkworm silk fibre reinforced PLA samples as compared with the pristine PLA.
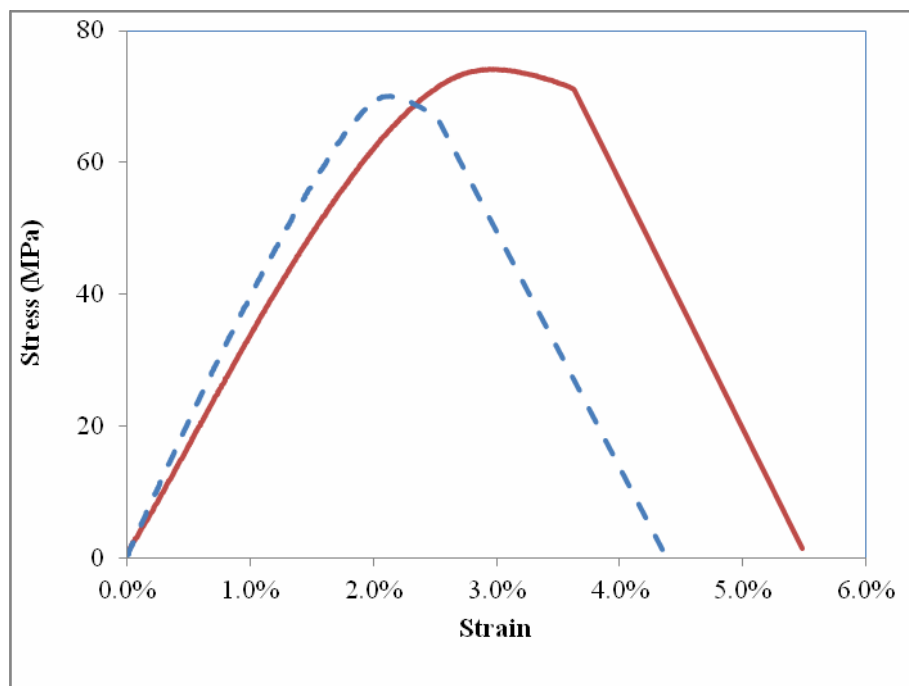
Figure 6.6. Tensile stress-strain curves of (i) pristine PLA – solid line and (ii) silk reinforced PLA composite – dashed line.
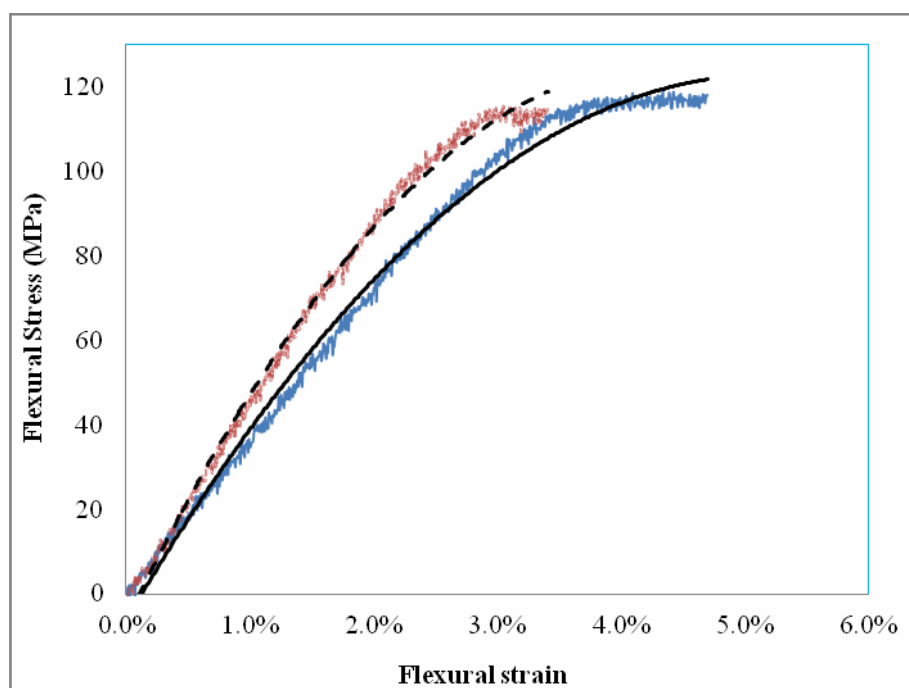
Figure 6.7. Tensile stress-strain curves of (i) pristine PLA – solid line and (ii) silk reinforced PLA composite – dashed line.

Table 6.2 shows the tensile, flexural and impact properties obtained from the tests for PLA and the composite samples. According to the results shown, the Young's modulus and flexural modulus of the composites increase by 27% and 2%, respectively as compared with a pristine PLA sample. It can be seen that the chopped silkworm silk fibres can play a role of effectively enhancing the tensile modulus of PLA. However, the enhancement in flexural modulus is small.

Table 6.2. Experimental results extracted from the tensile property and flexural strength tests, and impact resistant.

	Young's Modulus (GPa)	Tensile Strength (MPa)	Strain at Break (%)	Flexural Modulus (GPa)	Flexural Strength (MPa)	Flexural Strain at Break (%)	Mean Impact Resistant (kJ/m$^{2)}$)
PLA	3.21 (0.08)	70.73 (2.4)	5.5 (1.7)	3.98 (0.23)	109.4 (14.5)	4.1 (0.75)	156.3 (13)
Silkworm silk fibre reinforced PLA composites	4.08 (0.05)	70.6 (1.1)	3.8 (0.5)	4.06 (0.20)	97.41 (21.8)	2.9 (0.99)	110.7 (7)
Percentage increase	27.1%	-0.2%	-30.9%	2.0%	-11.0%	-29.3%	-29.1%

The major factors affecting the mechanical performance of short fibre reinforced composites include fibre-matrix interface, fibre length, fibre content and fibre orientation. Bsed on our pervious study, 5mm is the most optimal silkworm silk fibre length for injection moulding which can prevent the fibre from being coiled

with the screws or stressed plastically. Fibre content is another factor in influencing the tensile strength but it is limited by the restriction of the injection molding and the sample size. At low fibre content (5%) of silkworm silk fibre reinforced PLA composite sample, the matrix is not restrained by enough fibres and highly localized strain occurs in the matrix, causing the bond between matrix and fibre to break. Therefore, the debonded fibres dilute the matrix content and act as flaws which reduce the effective cross sectional area and, finally poor mechanical strength is resulted.

Fibres, due to their surface contour can provide mechanical interlocking, if they align along the loading direction, it allows good stress transfer when the composite is under tensile loading. To assess the alignment of fibres during the manufacturing process, small and thin dumbbell shaped composite samples were made by the injection moulding (Fu & Bernd 2009). A microscopy was used accordingly to observe the fibre orientation through the image analysis technique. According to fig. 6.8, most of the fibres are well aligned along the sample"s axis (i.e. the loading direction), only a small amount of obliqued fibres. Notwithstanding fibre length, fibre content and fibre orientation would affect the properties of the composite, interfacial bonding between silkworm silk fibre and PLA plays a decisive role on expressing the phenomenon on the increment in the modulus but decrement in the strength. In order to illustrate the relation between the mechanical properties and fibre-matrix interfacial bonding of the composite, the sequences of the loading of fibre and surrounding matrix of the composite with the interfacial bonding are discussed.
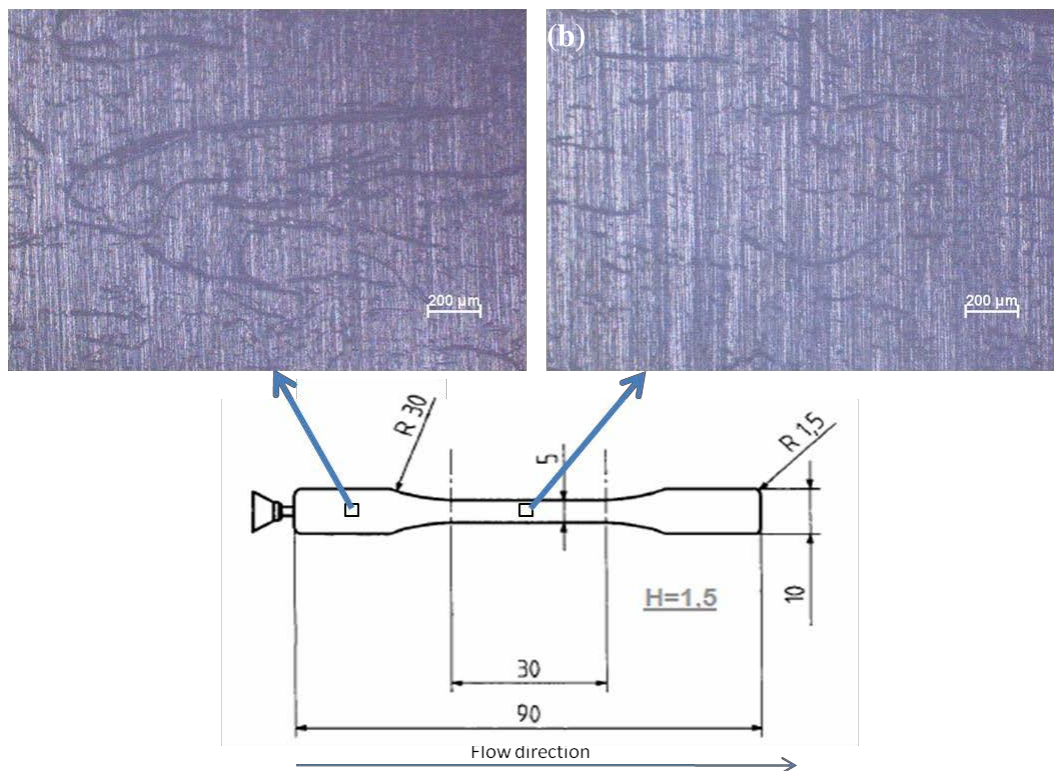
Figure 6.8. Micro graphs of cut-off view (along the longitudinal direction of the sample) of the silkworm silk fibre reinforced PLA composite with 5 vol% silkworm silk fibre: (a) wide section and (b) narrow section.

During the tensile loading process, matrix supposedly takes load a bit earlier than that of the fibre at the very beginning stage. Continuously increasing the load may cause fibres and matrix to share the load and fibres take higher load subsequently through the stress transfer by surface friction of the fibres. Modulus is determined at low strain levels where the fibre-matrix interfaces under very low shear force. Therefore, as the modulus is a property of material at low strain and is not very sensitive to the fibre-matrix interface, thus the modulus of composites is higher than that of a pristine PLA. At the certain level of load applied at that time the strain increases into the non-elastic region, debonding between the fibre and matrix happens as the shear force with the normal force at the bonding region may

overcome the surface frictional force. The strength of composites is a direct indicator of the strength of interfacial bonds since the applied stress is more efficiently transferred through the interface (Facca 2007; Fu & Bernd 2009). The interfacial debonding limits the stress transfer through the interface and thereby, as all fibres are debonded, areas with the fibres exist like a cavity without any reinforcement which cause the ultimate strength decreases consequently.

Therefore, poor bonding between the fibre and the matrix would dominate over other factors of strength reduction. Sericin and the hydrophilic characteristic of the silkworm silk fibre as the reasons for poor bonding are discussed as follows. A small gap is observed between the fibre and the matrix on the fracture surface of the composite (fig. 6.9). Silkworm silk fibre used for this project was collected as in an "as-it-is" form, which was degummed by boiling water from the supplier. This degumming procedure removes the more soluble components of sericin, but does not clean all the sericin as both sericin and fibre core are protein. Thus partial sericin would remain on the surface (Craven, Cripps & Viney 2000). Sericin hinders the bonding between the fibre and matrix, and the efficiency of stress transferred between resin and fibre decreased from the weak interfacial regions thus. Moreover, the fibre used in this project was not undergone any chemical treatment with compatilizer, modifier and/or other bonding agencies due to our target application is for the development of bone implants (no excessive chemical treatment of natural materials is allowed), it is therefore expected that a weak bonding between them was still the case here.

(a)

(b)

158
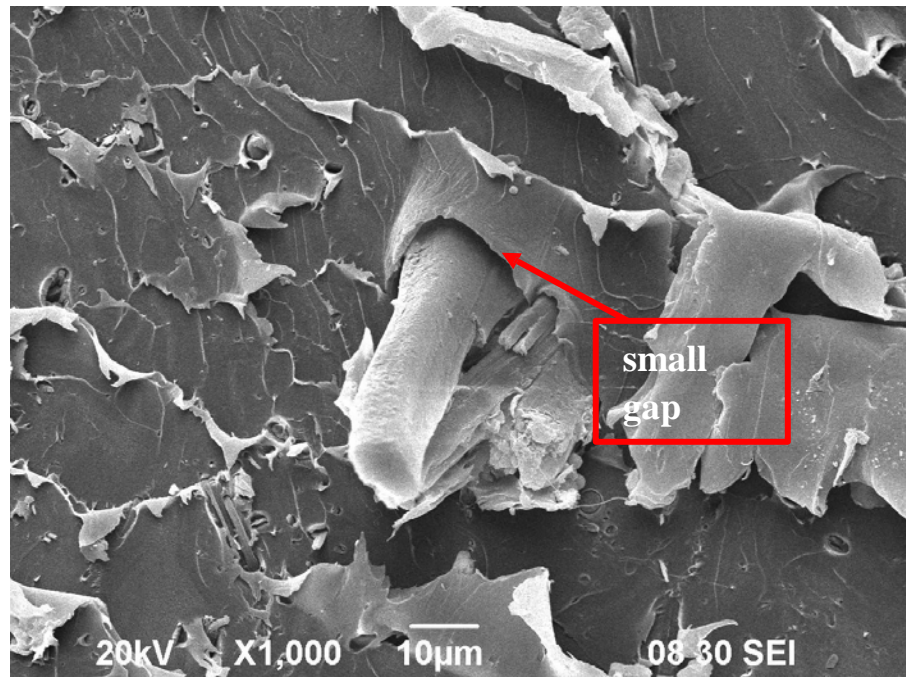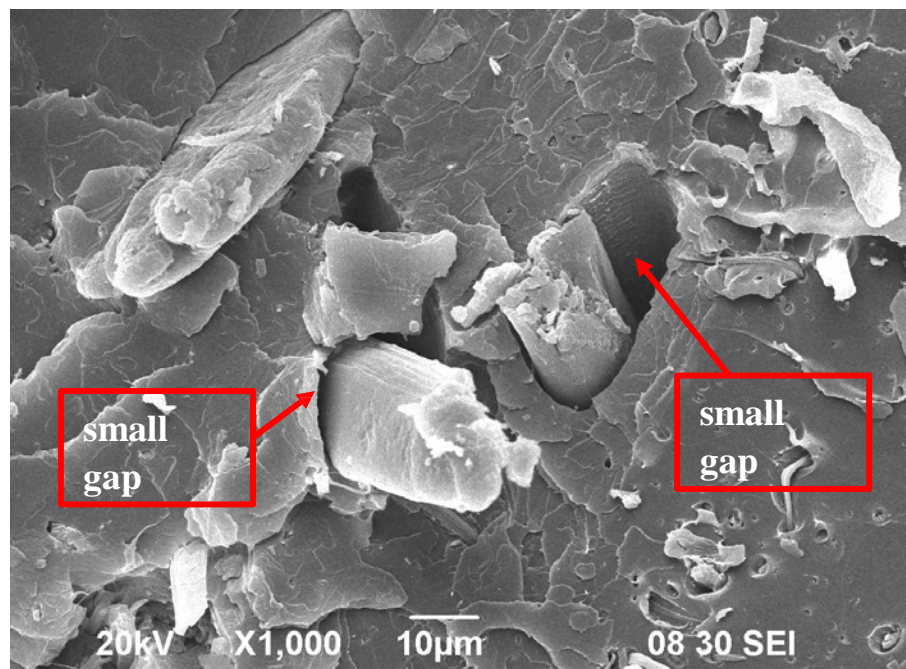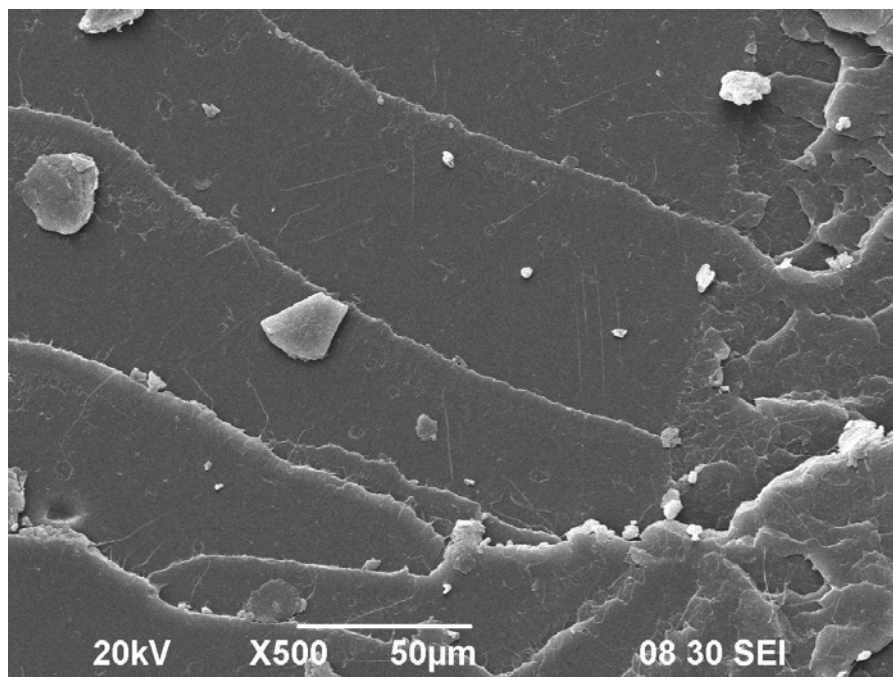
(c)

Figure 6.9. Scanning electron micrographs showing the fractured surfaces of (a) & (b) silk reinforced PLA composites with the fibre pull out compare with (c) pristine PLA.

Natural silkworm silk fibre contains hydroxyl groups which is called hydrophilic. In this composite system, one (fibre) is in hydrophilic while another is hydrophobic (matrix) properties, their interface cannot be assumed to be securely (chemically) bonded together due to the inherently poor compatibility and thus induce poor bonding and limit the load transfer through the interface. Therefore, the tensile strength of the composites would not be improved by the addition of silkworm silk fibre. However, mechanical interlocking still exists due to the roughness of the fibre and this kind of weak bonding dominates the reasons for diminished strength and strain The roughness of the fibre is basically formed during the spinning process of cocoon, two strands of fibrils which contain

numerous silk filaments with different diameters bundled together to form the fibre.

Non-uniform cross sectional area along the fibre"s axis may also casues the reduction of mechanical strength due to the induction of stress concentration zone. Fig. 6.10 shows the silkworm silk fibre acts as a crack initiation in the composites.
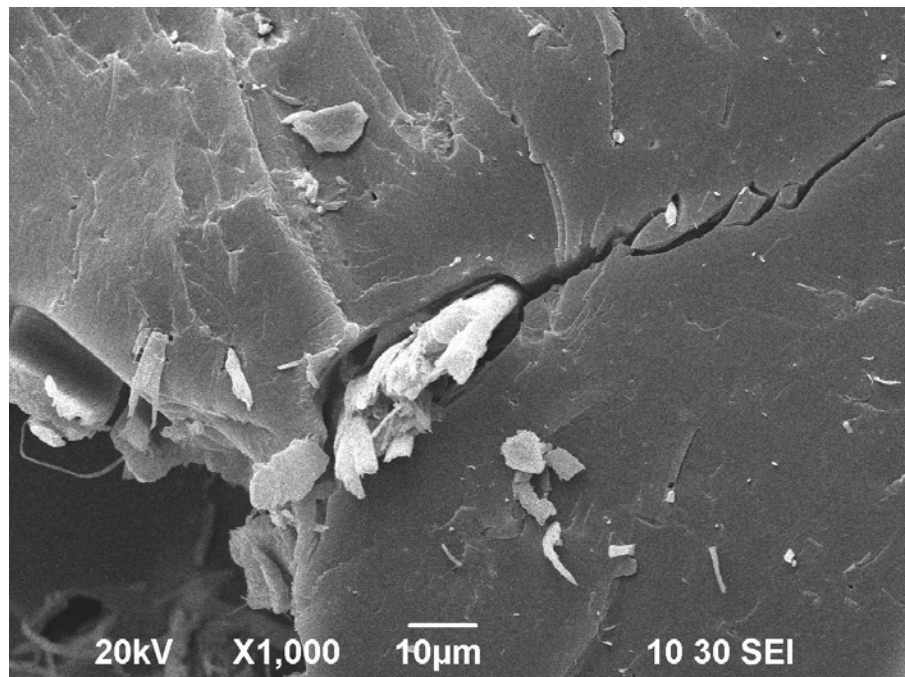
(a)
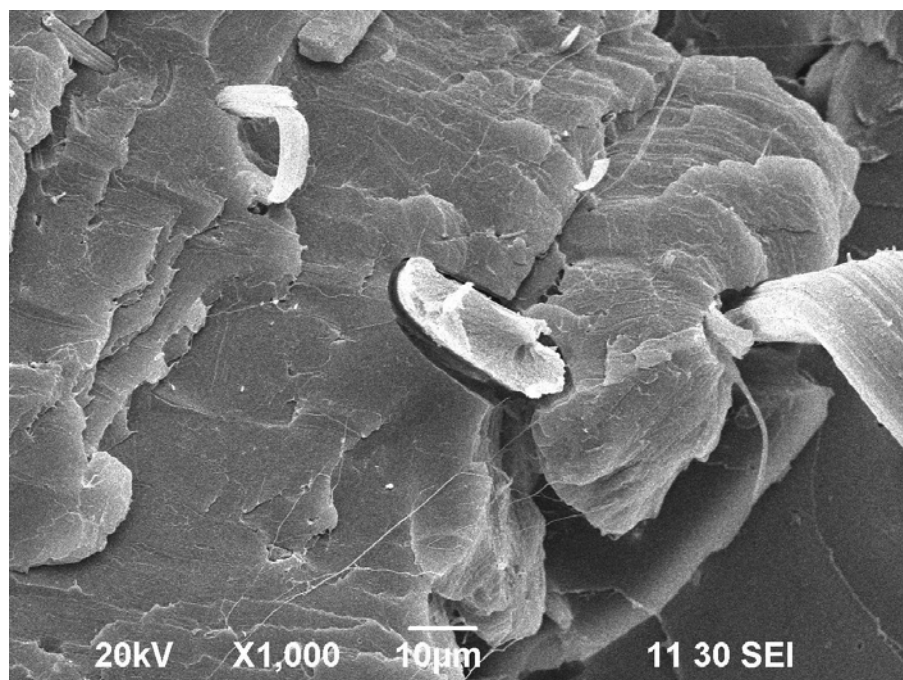
Figure 6.10. Silkworm silk fibre initiates the crack propagation.

6.4 In Vitro Degradation

In biodegradability test (in vitro), PLA and silkworm silk fibre reinforced PLA samples were placed into the enclosed tanks with Phosphate Buffered Saline (PBS). White dry powder of PBS was diluted with 1 L of deionized water with ultimately the pH level of 7.4 was achieved. Two types of samples were stored separately into the tanks with 500 ml each. The tanks were then stored in a humidified, thermo-stable and orbital-shaking incubator at 37 ^{0}C with 100rpm. pH value was examined every day in order to study the effect of acidic degradation products. PBS solution was replaced by fresh PBS solution at the end of every 2 weeks to mimic the fairly constant acidity environment in vivo. Six specific degradation time points were set at a 2-month interval, i.e. 2nd, 4th, 6th, 8th and 10th months. At each time range, eight pristine PLA and silkworm silk fibre

reinforced PLA samples each were taken out from the tanks for tensile property and flexural strength tests and for material properties analyses such as SEM. Fig. 6.11 shows the incubator used for the degradation test.

Figure 6.11. Incubator for degradation test.

There is no doublt that, for most biodegradable materials, especially artificial polymers, passive hydrolysis is the most important mode of degradation (Gijpferich 1996). Silkworm silk fibre dominates in the water uptake behaviour, which initiates the degradation of the composite. The mechanism of moisture absorption is owing to the involvement of hydrophilic natural fibre and hydrophobic matrix by water molecule diffusion in the following steps (Pickering, Properties and Performance of Natural-Fibre Composites, 2008):

(1) The diffusion of water molecules inside the micro-gaps between polymer chains,

(2) Capillary transports into the gaps and flaws at the fibre-matrix interface and

(3) The transportation through matrix micro-cracks formed during the compounding process

Based on the experimental results, the weight of the silkworm silk fibre reinforced PLA samples increased with the increase of immersion time. For these sample submerged into the solution for 6 months, it was found that the weight increases by 2.1% as shown in table 6.3. The dimensional change of the degradation samples is shown in fig. 6.12 (a) and (b). For the pristine PLA sample, there is no change in weight with time. This result may be due to the hydrophilic effect of silkworm silk fibre. In general, silkworm silk fibre has comparatively high moisture absorption which leads to swelling within the silk fibre reinforced PLA samples. Although most of the fibres were encapsulated, the equilibrium of water in the composites induces PLA of the composite absorbing water faster than pristine PLA. Therefore, the silkworm silk fibre reinforced PLA composite would absorb more water as compared with pristine PLA. This action would stop when the water content reaches to its saturation level and the degradation starts. After 10 months, it was found that the weights of the pristine PLA and the composite decreased by 0.6% and 1.2 % respectively.

Table 6.3. Weight change of the samples during the in vitro degradation test.

Duration of the degradation Test (Week)							
	0	2	4	6	8	10	12
PLA (g)	1.222	1.224	1.228	1.223	1.220	1.229	1.226
Silkworm silk fibre reinforced PLA composites (g)	1.226	1.249	1.243	1.242	1.246	1.248	1.244
Duration of the degradation Test (Week)							
	14	16	18	20	22	24	26
PLA (g)	1.231	1.232	1.236	1.232	1.232	1.231	1.222
Silkworm silk fibre reinforced PLA composites (g)	1.241	1.244	1.246	1.242	1.250	1.252	1.250
Duration of the degradation Test (Week)							
	28	30	32	34	36	38	40
PLA (g)	1.225	1.225	1.2251	1.2286	1.2286	1.2284	1.228
Silkworm silk fibre reinforced PLA composites (g)	1.235	1.24	1.2415	1.2427	1.2467	1.2465	1.231
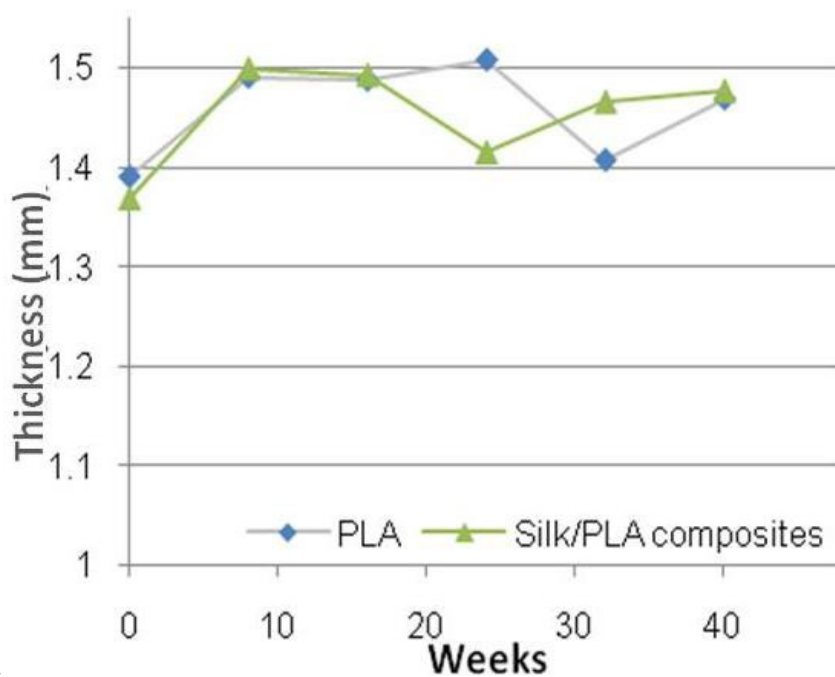
(a)
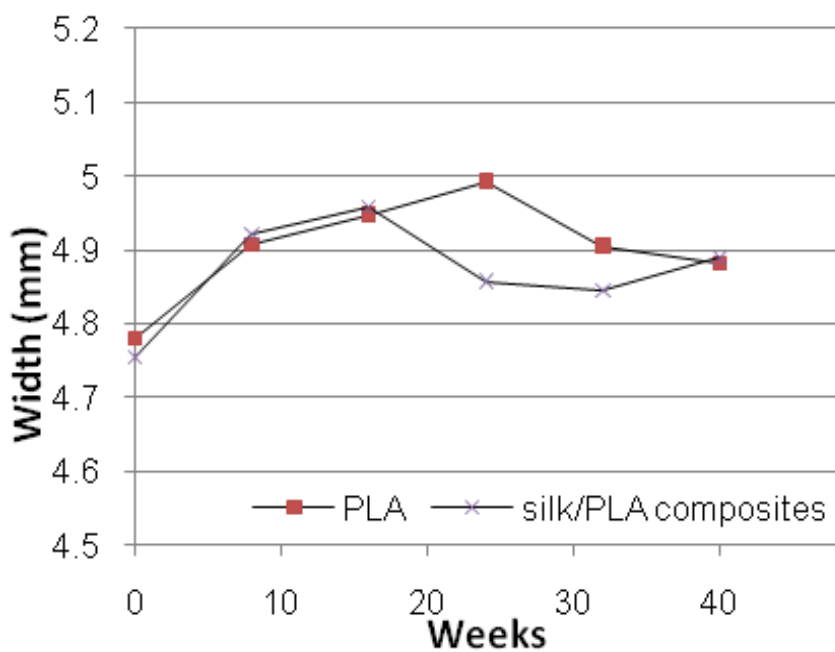
(b)

Figure 6.12. (a) & (b) Dimensional change of the degradation samples.

Besides, it has been found that the Young"s modulus, tensile strength, flexural modulus and flexural strength decrease as shown in fig. 6.13 to 6.16, of both PLA and silkworm silk fibre reinforced PLA samples after being immerged into water. Nevertheless, the properties of the silkworm silk fibre reinforced PLA samples are worse as compared with those the pristine PLA sample in general. Therefore, the mechanical properties of pristine PLA and silkworm silk fibre reinforced PLA composite were weakened because of the effects of water absorption. Water absorption in the samples would induce micromechanical damages in the resin and at the interface between the fibre and martix. It also induces the dimensional change and the internal stress development in the sample. Moreover, water molecules act as a plasticizer and penetrate into the polymer chains. These polymer chains are forced apart and become more mobile and consequently poor mechanical properties and faster degradation are resulted (Pickering, Properties and Performance of Natural-Fibre Composites, 2008; Lassila, 2002; Manfredi, 2008). Besides, Yutaka et al. have found that silkworm silk fibre is one of the proteinous materials which stimulate the production of enzymes from PLA-degrading microorganisms and consequently speed up the degradation (Tokiwa & Calabia 2006). Fig. 6.17 and 6.18 are the SEM micrographs of the fracture surface of pristine PLA and silkworm silk fibre reinforced PLA composites during degradation.
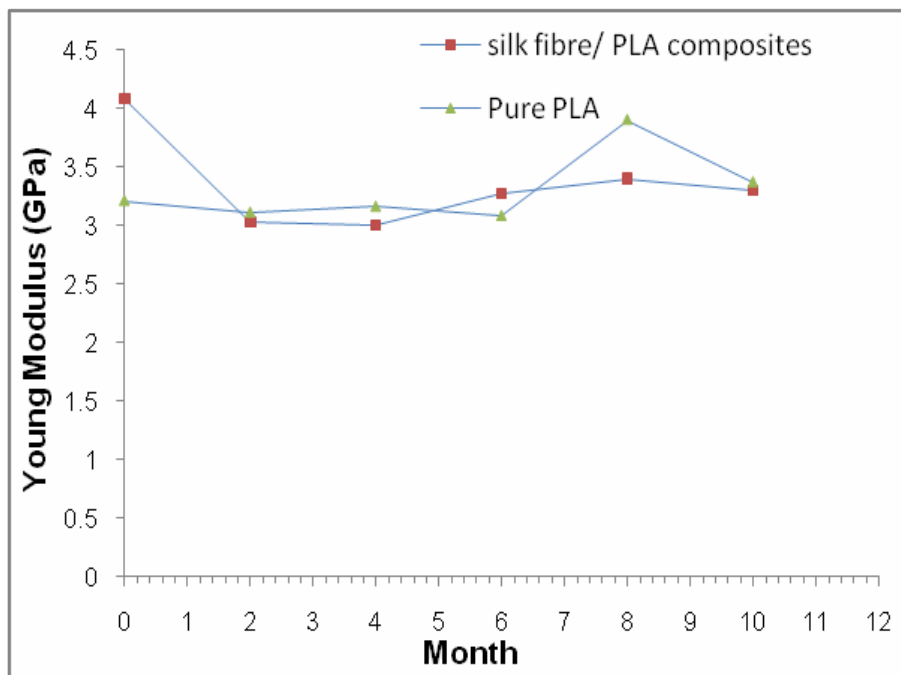
Figure 6.13. Young‟s modulus as a function of time for (a) Pristine PLA and (b) silkworm silk fibre reinforced PLA composite.
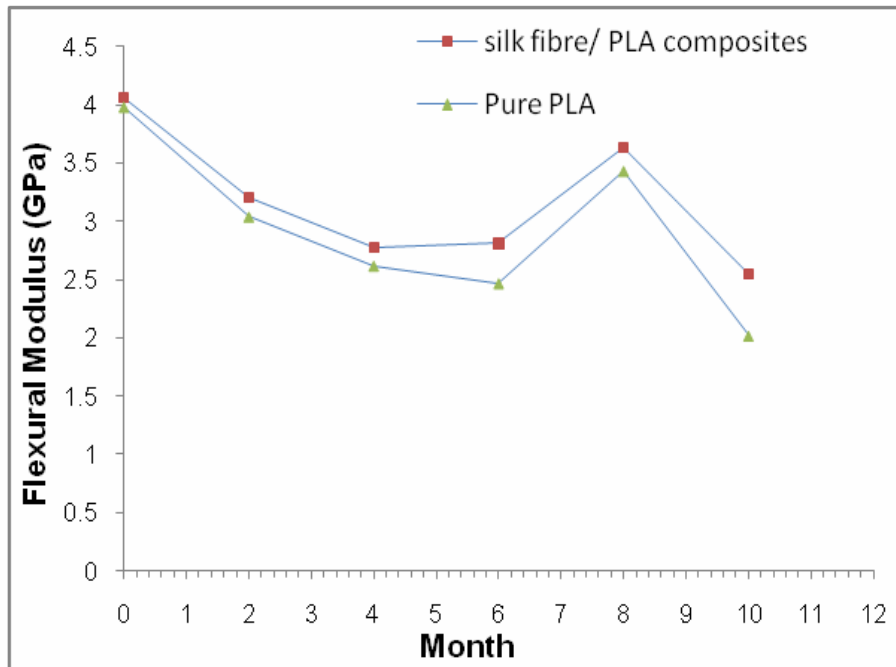
Figure 6.14. Flexural modulus as a function of time for (a) Pristine PLA and (b) silkworm silk fibre reinforced PLA composite.

167
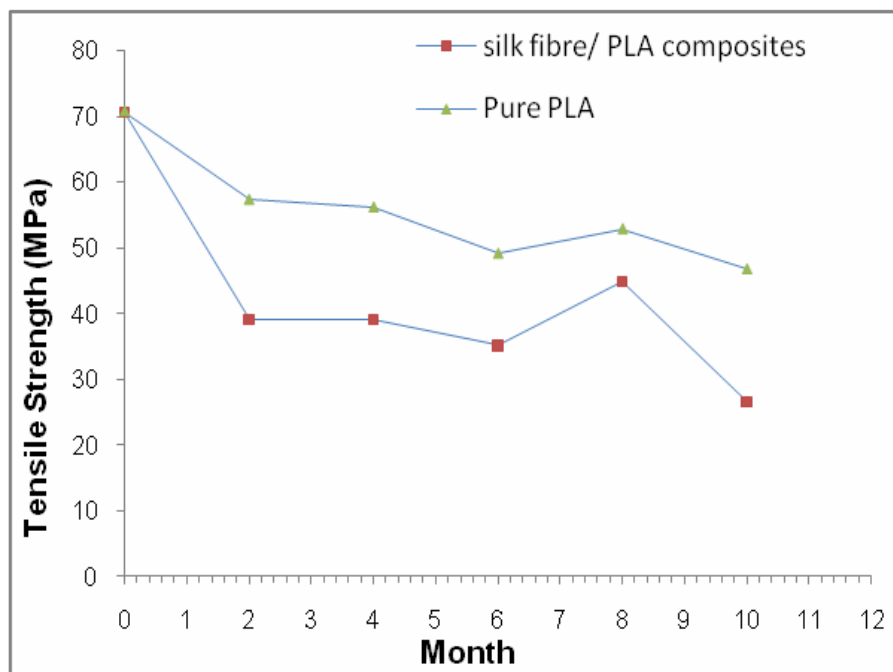
Figure 6.15. Tensile strength as a function of time for (a) Pristine PLA and (b) silkworm silk fibre reinforced PLA composite.
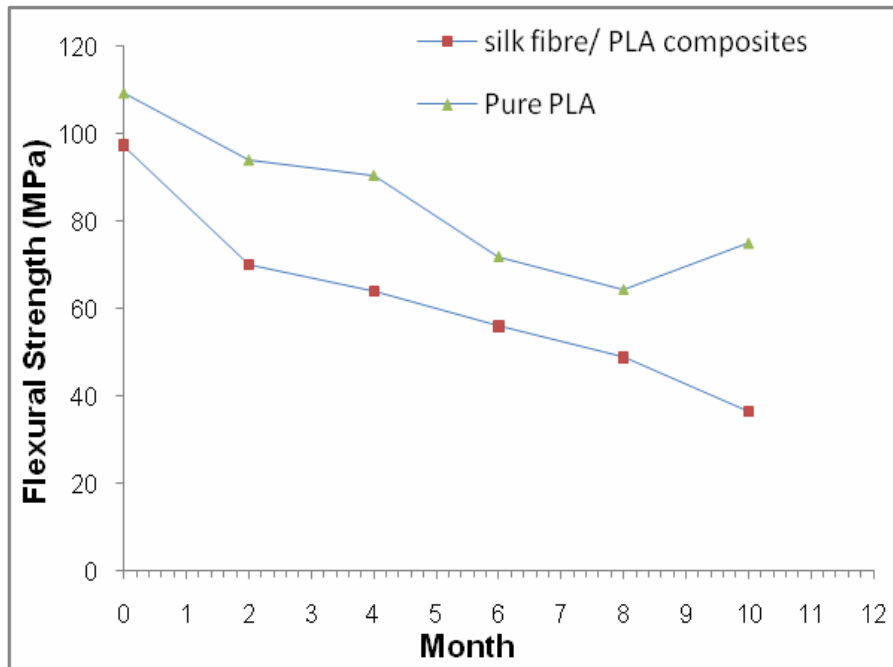
Figure 6.16. Flexural tensile strength as a function of time for (a) Pristine PLA and (b) silkworm fibre reinforced PLA composite.
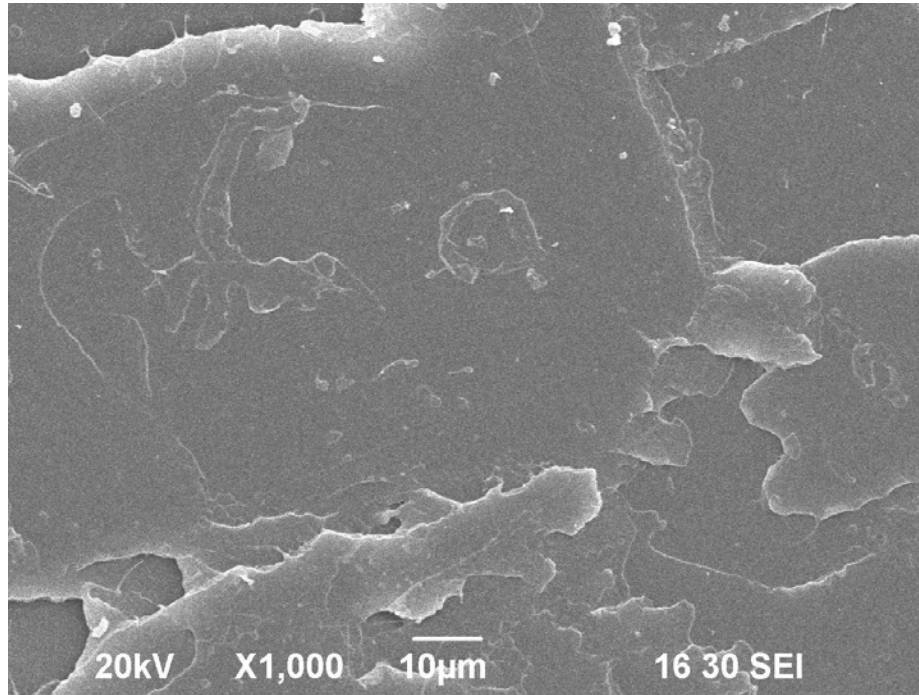
(a)
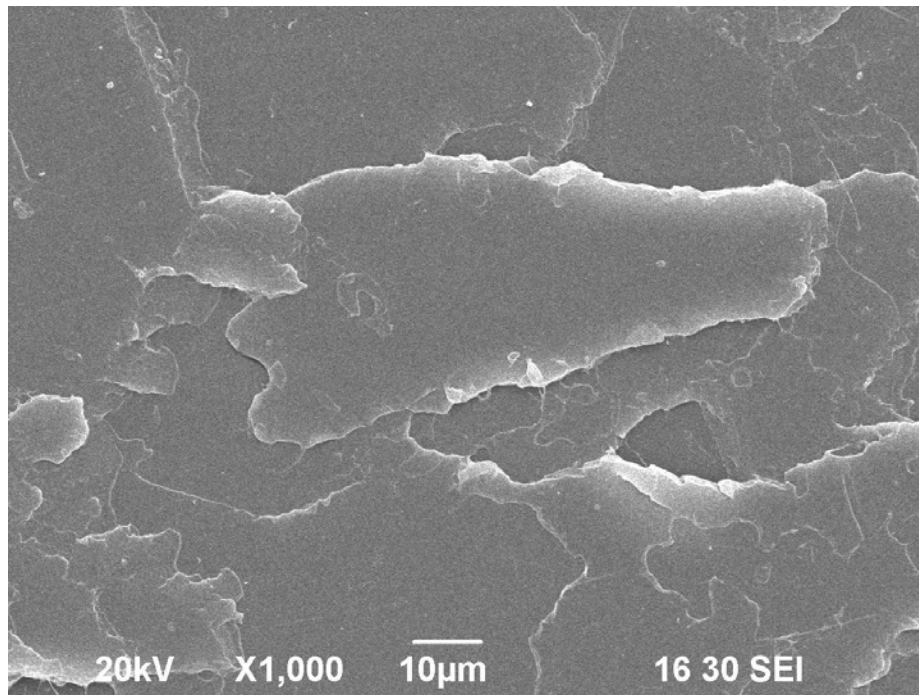
(b)
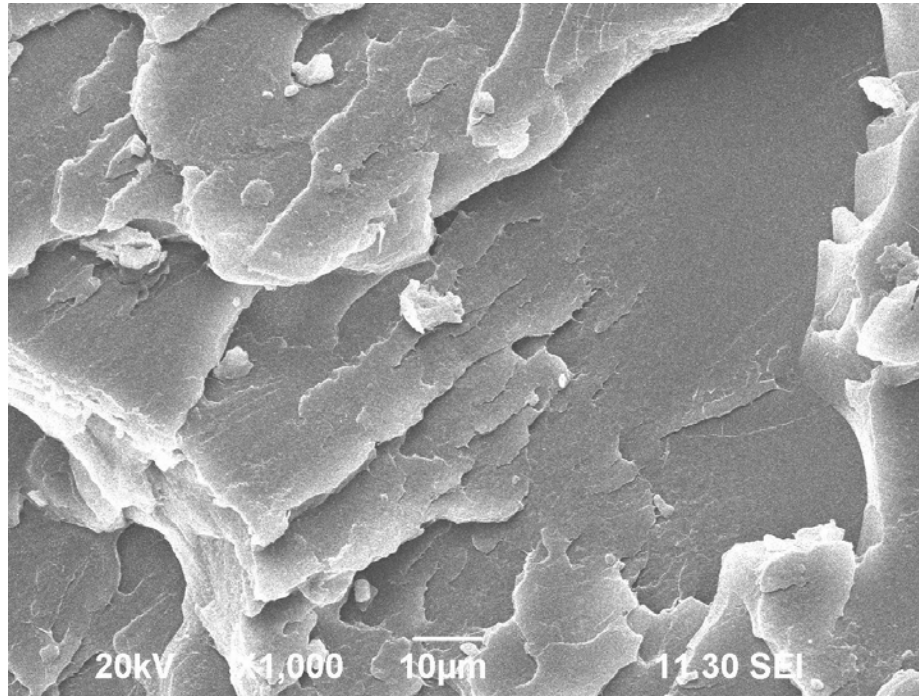
(c)
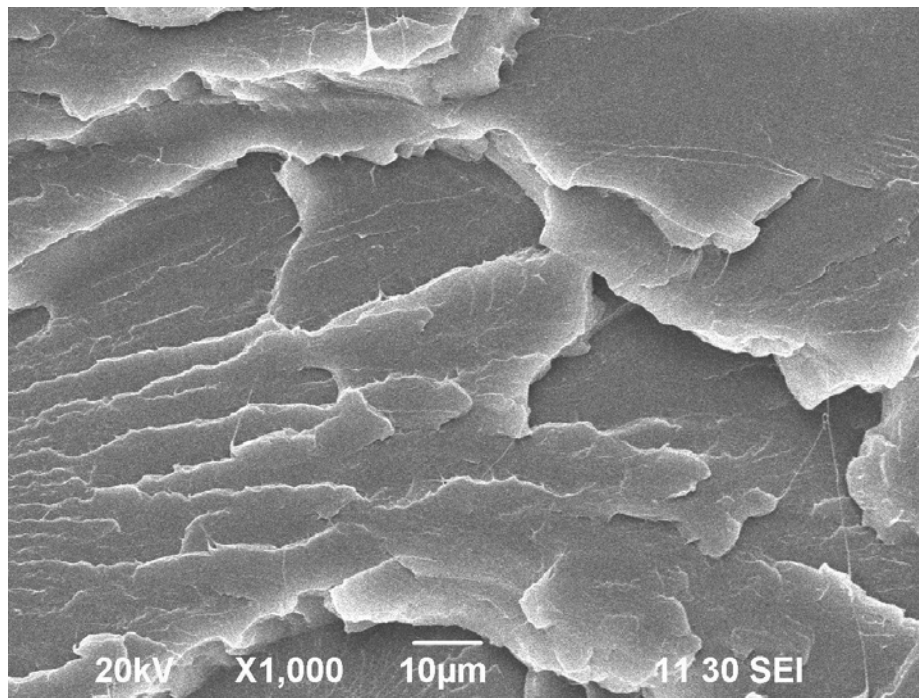
(d)
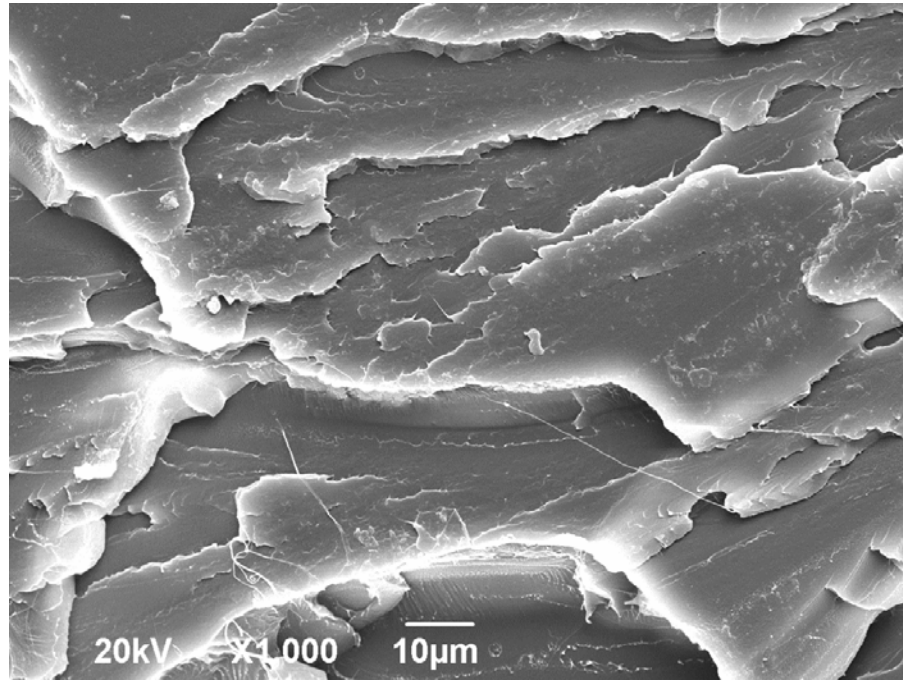
(e)
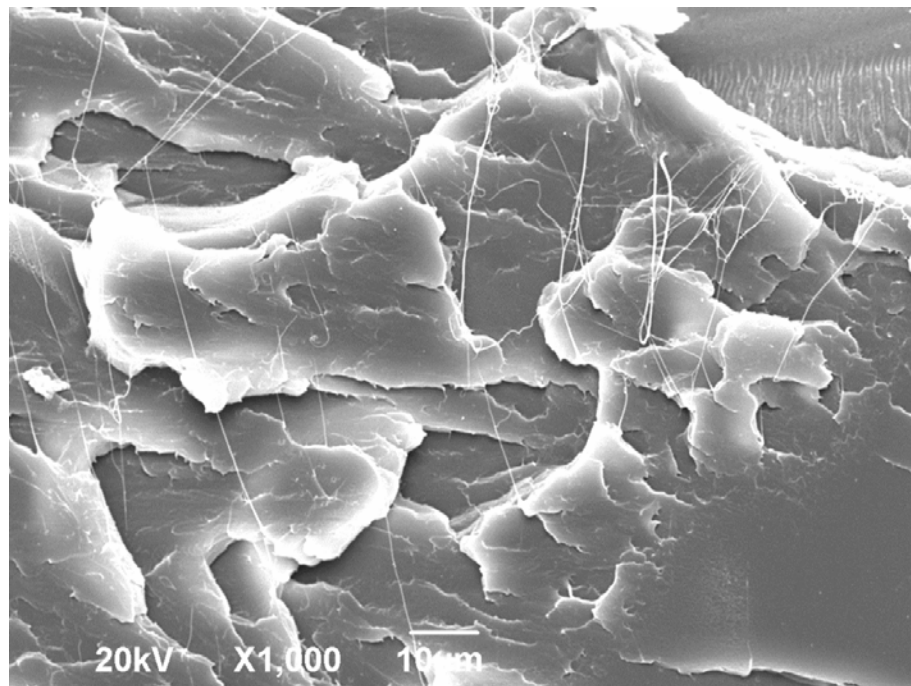
(f)

Figure 6.17. SEM micrographs of pristine PLA samples (a) before degradation and after (b) 2 months, (c) 4 months, (d) 6 months, (e) 8 months and (f) 10 months.
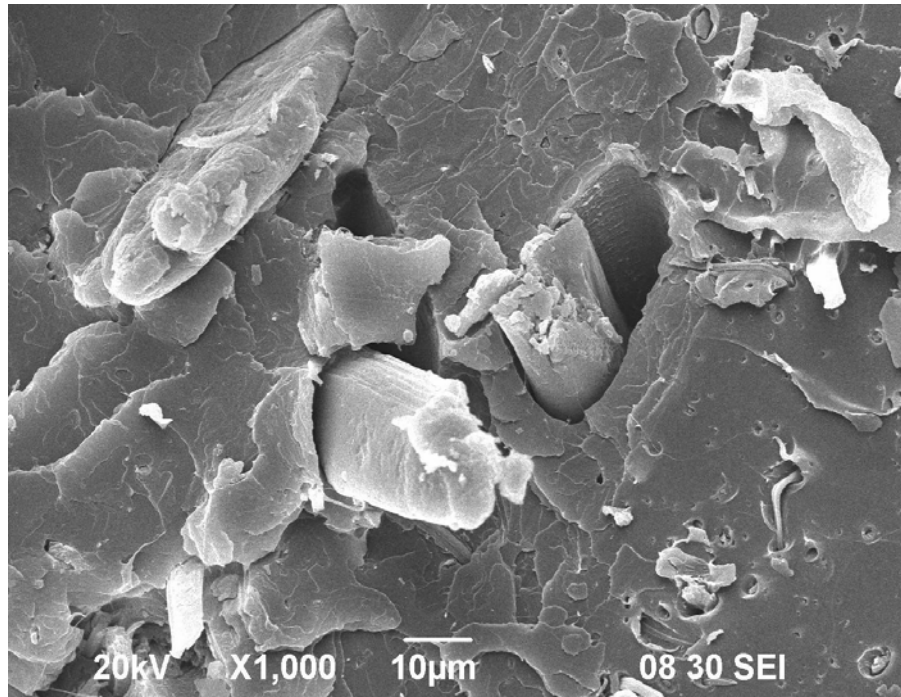
(a)
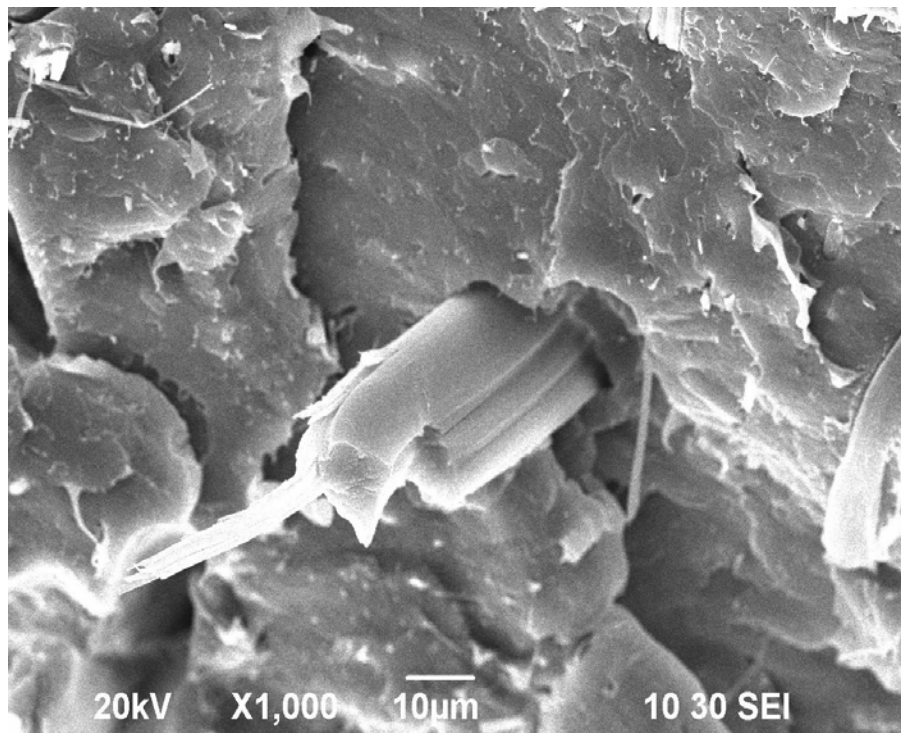
(b)
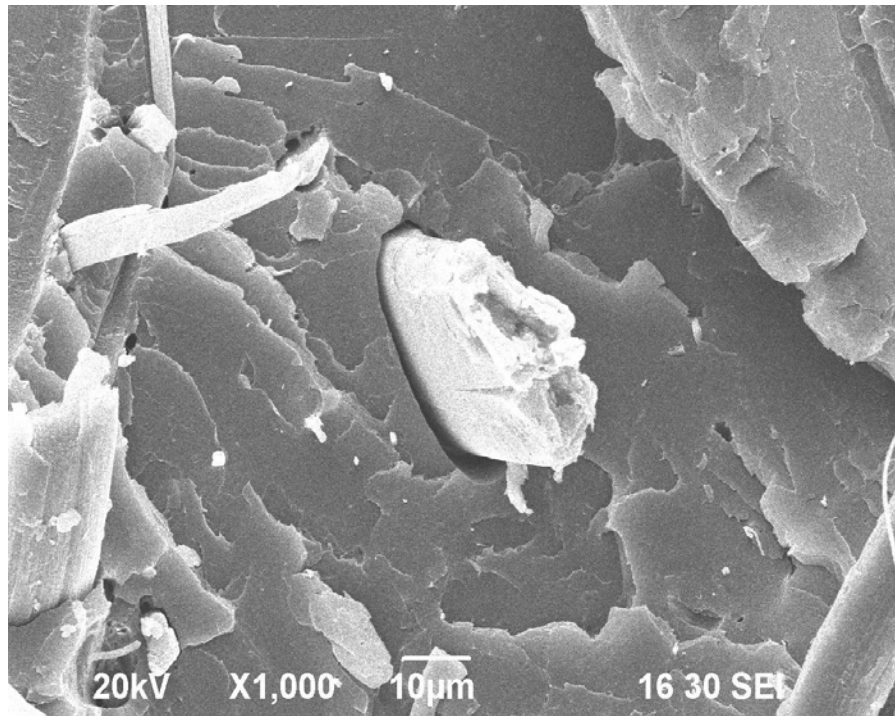
(c)
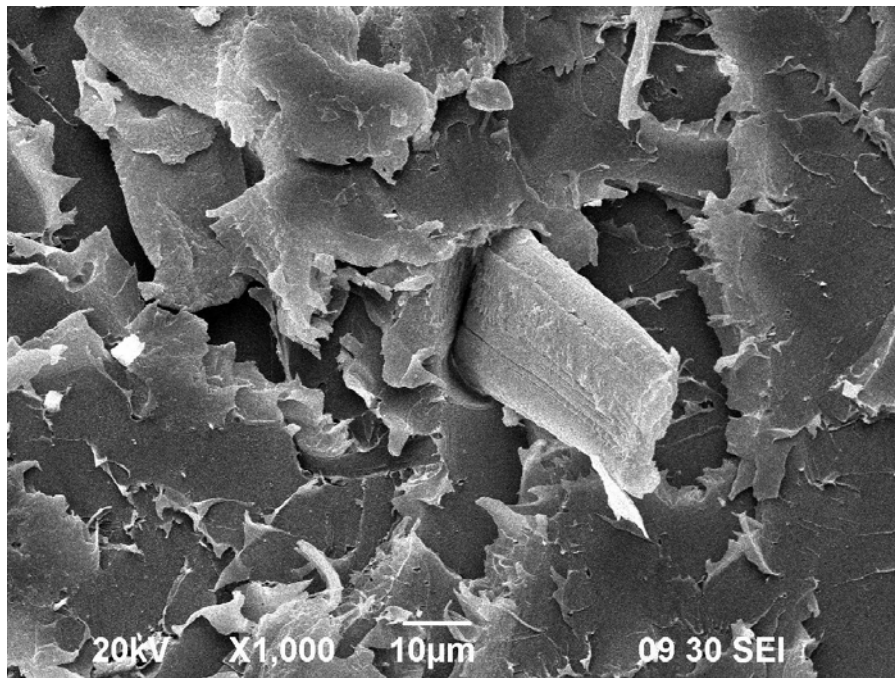
(d)
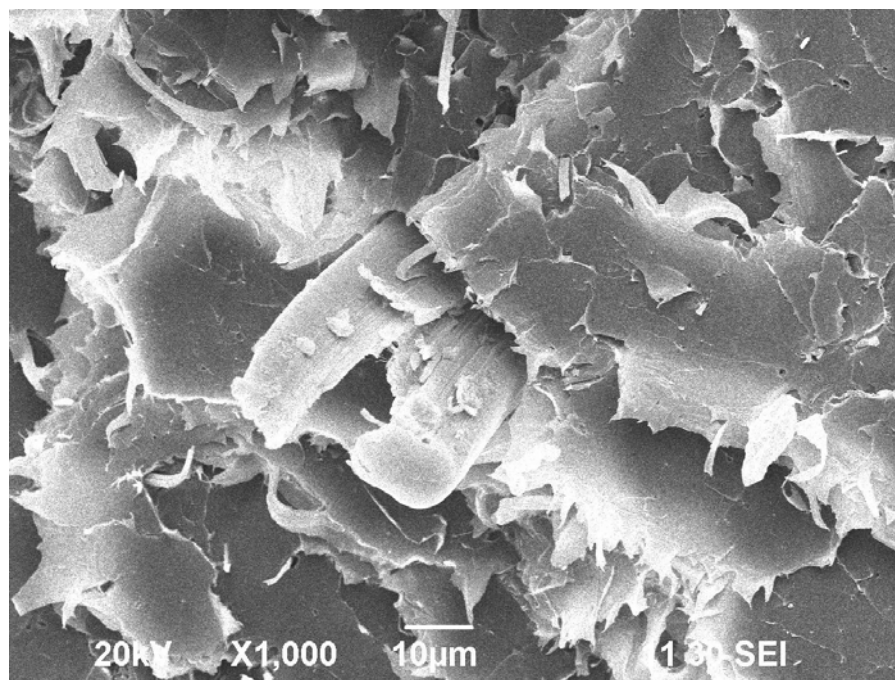
(e)
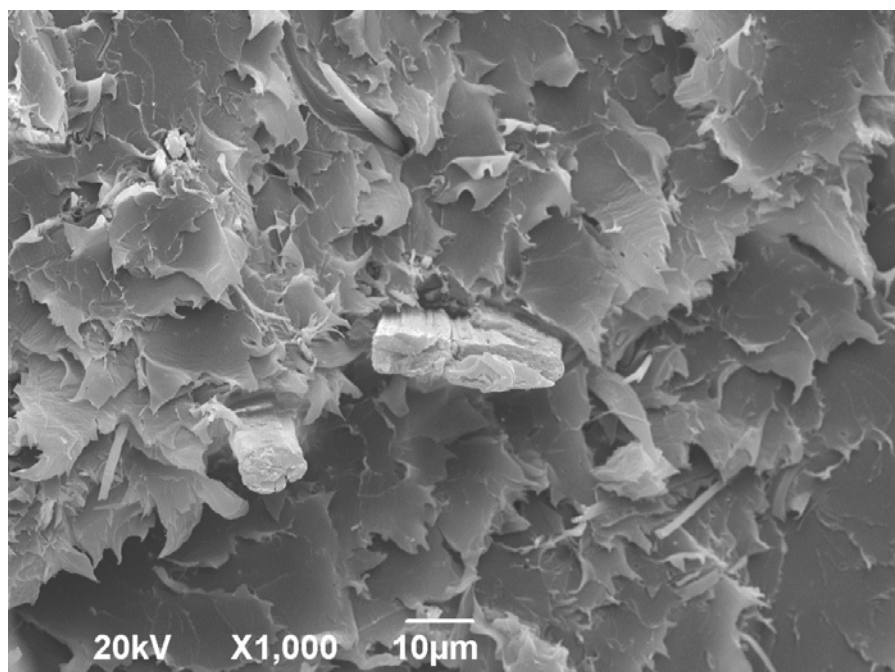
(f)

Figure 6.18. SEM micrographs of silkworm silk fibre reinforced PLA composite samples (a) before degradation and after (b) 2 months, (c) 4 months, (d) 6 months, (e) 8 months and (f) 10 months.

Fig. 6.19 shows the main type of bond within the polymer backbone that determines the rate of hydrolysis (Huda et al. 2005).
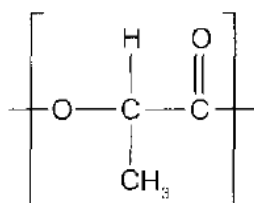
Figure 6.19. Bonding within the backbone of polyester.

All biodegradable polymers contain hydrolysable bonds. Their most important degradation mechanism is, therefore, chemical degradation via hydrolysis which is referred to as biodegradation. Hydrolysis is a bimolecular reaction in which water and the functional group possessing the labile bond are involved (Huda et al. 2005). PLA contains hydrophilic, hydrolyzable bonds (poly (a-hydroxy acids)) which processes bulk degradation. After penetration of water into the polymer matrix, degradation starts through a bulk hydrolysis of ester bonds and the molecular weight decreases (Garlotta 2001).

6.5 Dynamic Mechanical and Thermal Properties

6.5.1 Thermomechanical Analysis

Thermomechanical analysis (TMA) is a theromanalytic method for the

measurement of a change of a dimension (length or volume)or a mechanical property of the sample while it is subjected to a temperature regime. The thermal expansion of a material is the changes in length or volume due to the changes in moisture content, curing, release of stresses, phase changes and etc under heating. It is an important factor for manufacturing and functioning biodegradable and bioresorbable composite bone fixators. As TMA is used to measure variations in dimensions of a sample which is subjected to a non-oscillatory loading, it is commonly used to determine the thermal expansion nowadays (Kaeagiannidis, Stergious & Karayannidis 2008). TMA was conducted by a PerkinElmer TMA 7 instrument. The processing temperature for the TMA experiments according to the ASTM standard D 696 was controlled from 40°C to 165 $^{\circ}$C at a scan rate 10 $^{\circ}$C/min with a penetration probe 1.0mm in diameter under a uniaxial stress of 0.12 MPa. The change in length for testing specimens over a corresponding change in temperature was recorded.

Table 6.4 summarizes the results from TMA measurements. The mean coefficient of linear thermal expansion (CLTE) obtained from TMA measurement is used to reflect the dimensional changes as well as thermal stresses caused by the thermal variation [14]. The coefficient of linear thermal expansion for the desired temperature range can be calculated according to the following equation [13]:

$$\alpha = \frac{\Delta L}{L \Delta T}$$

(6.1)

where:

α =   Mean coefficient of linear thermal expansion for the reference

material at the midpoint of the ΔT range, in $°C^{-1}$,

L   =   Length of the sample at room temperature, in µm,

ΔL =   Change in length of the reference material due to heating, in µm,

ΔT =   Temperature difference over which the change in specimen length

is m measured, in °C.

Table 6.4. TMA results of the pristine PLA and the silkworm silk fibre reinforced PLA composites.

	ΔL (µm)	α (µm m^{-1} $°C^{-1}$)
Pristine PLA	46.032	227.875
Composite	32.748	164.223
Change of percentage (%)	-29	-28

As shown in the table, CLTE of the composite decreases by 28%. The results exhibit the improvement of physico-mechanical properties in the composite as compared with the pristine PLA. In general, CLTE of a fibre reinforced PLA polymer composite is lower than that of its pristine matrix system (i.e. PLA in this case) due to the low CLTE of the fibre. In the real practice, low CLTE of the composite is desirable for all engineering applications to minimize any thermo-

dimensional change of structures during manufacturing process (which may cause the generation of residual stress after curing) and in use (Lee et al. 2005). Therefore, the lower the value of CLTE measured, the better the property for a bone fixator to be achieved (Yang et al. 2005).

Krevelen and Volemetric (Yang et al. 2005) have suggested that the molar thermal expansibility of a polymer is related to the van der Waals volume of repeated units of a polymer. Moreover, Bondi (Andrzej, Adam & Dietrich 2009) has defined that the van der Waals volume as volume occupied by a molecule, which is impenetrable by the other molecules having thermal energy at ordinary temperature. As silkworm silk fibre is a macro- sized natural fibre, it cannot penetrate into such a small volume of the polymer and cause the decrement in thermal expansion of the composite. Therefore, the thermal expansion of composite is mainly affected by the interaction between the fibre and the PLA (matrix). This interaction may restrict the mobility of polymer chains which adheres on the fibre surface and thus, cause the reduction in the thermal expansion of the composite (Huang 2009). The improvement of thermo-mechanical stability and dimensional stability of biocomposites by using natural fibre has been addressed by Lee et al. (Bondi 1964). In their study, poly(butylene succinate)(PBS) was used as a base polymer reinforced by silkworm silk fibre.

6.5.2   Differential Scanning Calorimeter

DSC is a thermal analysis instrument that is used to determine the quantity of heat on the sample and the reference by a substance undergoing a physical or a

chemical change as a function of time and temperature. Perkin–Elmer DSC7 system was used for testing at ambient condition. The temperature range of the experiment was programmed to start at 0^oC and 300^oC. All the samples weighted of 5 mg were placed and sealed into an aluminium pan, and an empty aluminium pan was used as reference. The heat flow and energy changes in the aluminium pans were recorded. By observing the difference in heat flow between the samples and the reference sample, the thermal properties can be obtained which show as an endothermic peak: (Energy absorption: secondary transitions shown as a step change, melting temperature) and as an exothermic peak (Release energy: Crystallization).

Glass transition temperature (Tg) and the crystallinity of polymer have additional indirect effects on degradation rates (Huda et al. 2005). Degradation first occurs in the amorphous regions and later in the crystalline domains (Garlotta 2001). The thermal characteristics of the composites were investigated via DSC. Fig. 6.20 shows the DSC traces for both pristine PLA and silkworm silk fibre reinforced PLA compositesamples. Tg, crystallization temperature (T_c), melting temperature (T_m), crystallization enthalpy (ΔH_c) and melting enthalpy (ΔH_m) are obtained from the DSC study. The values for these transitions along with measured endotherms and exotherms are recorded in table 6.5. Moreover, the estimation of the degree of crystallinity of the samples is listed in the table. The enthalpy of melting (ΔH_{mo}) for a pristine crystal (100% crystallinity) was calculated through extrapolation to be 93.7 joules/gram (Garlotta 2001).

$$X\% = \frac{\Delta H_m}{\Delta H_{mo}}\ 100\%$$

<div align="right">(6.2)</div>

Table 6.5. Thermal characteristics of the samples measured by DSC.

Sample	$T_g/\ ^{\circ}C$	$T_c/\ ^{\circ}C$	$T_m/\ ^{\circ}C$	$\Delta H_c/J\ g^{-1}$	$\Delta H_m/J\ g^{-1}$	$X/\%$
Pristine PLA	53.7	94.86	163.44	29.46	48.0	51.2%
Silkworm silk fibre reinforced PLA composite	53.7	90.18	162.71	29.50	48.4	51.7%
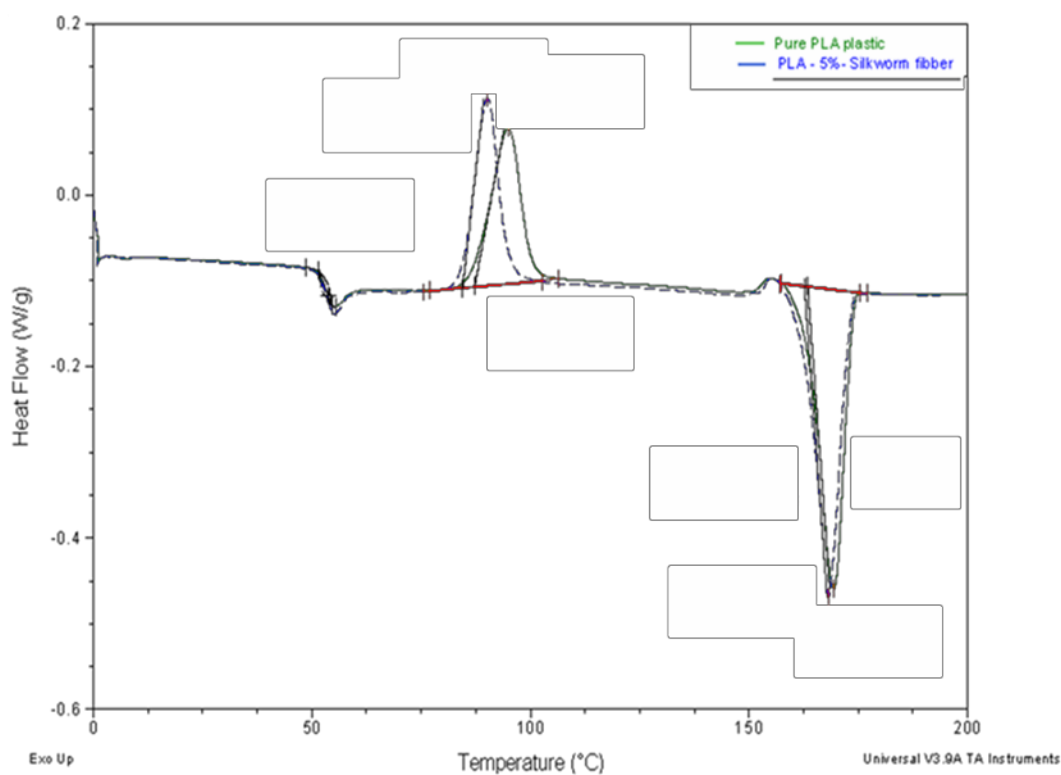
Figure 6.20. DSC curves for the pristine PLA and silkworm silk fibre reinforced PLA composite samples.

There are two main factors controlling the crystallization of polymeric composite systems. First, the additives have a nucleating effect that results in increment of crystallization temperature. Second, additives hinder the migration and diffusion of polymer molecular chains to the surface of the growing polymer crystal in the composites, resulting in a deduction for the crystallization temperature (Huda et al. 2005).

When silkworm silk fibre was added, Tg of both PLA remained unchanged, but the crystallization characteristics were influenced. Pristine PLA and silkworm silk fibre reinforced PLA composite had a crystallization temperature (Tc) of 94.86 and 90.81 ^{o}C, respectively. In this study, the crystallization temperature of pristine PLA decreased by up to 4.68 °C to the composite sample. Higher Tc values of the composite sample was measured as compared with that of the pristine PLA sample, this result indicates that the crystallization rate of the composite sample became more rapid in the non-isothermal process. When silkworm silk fibre existed, the enthalpies of crystallization and melting became larger, the width of the crystallization peaks became relatively narrow and the maximum crystallization temperatures shifted to lower temperatures, as compared with the PLA sample.

The results signify that the silkworm silk fibre hindered the migration and diffusion of PLA molecular chains to the surface of the nucleus in the composite sample. The crystallinity has additional indirect effects on degradation rates. From the result, the crystallinity reduced as silkworm silk fibre reinforced PLA. The degradation rate is therefore increased.

6.5.3   Dynamic Mechanical Analysis

As this composite is designed for bone fixators, it has to be in a functional condition at the temperature below its Tg in order to assure that the mechanical performance is adequate at all the time the composite inserted inside the human body. Creeping (dead load of fractured sections), fatigue (repeated bending) and degradation (bio-resorption) are also other key factors that may affect the performance of the composite with time. The fixators should also possess moderate stiffness and good damping properties to absorb external impact and vibration load to protect a fractured bone. Therefore, the storage modulus(E'') and loss modulus(E''') of a composite fixator should be high enough to enhance their ability to absorb and dissipate energy, respectively within the pre-determined period, i.e. during an acceptable duration when the fixator is in the process of degrading. In view of this, thermo-mechanical and dynamic mechanical analyses, and density measurement are investigated in this section.

The viscoelastic behaviour of polymer during their deformation and flowing process is mainly dependent on the temperature and time (frequency). Molecular rearrangement happens during the process can minimize the formation of localized stresses. Polymer"s molecules would store a portion of applied energy and dissipate the rest to other dissipative processes such as the formation of cracks, heat, sound and vibration motion) under a repeated loading condition. The characteristic parameter that is used to represent the viscoelasticity of polymer is "tan δ" (Faughnan & Bryan 1998). This parameter is a function of temperature and its relationship with E'' and E''' is:

$$\text{Tan}\,\delta = \frac{E''}{E'} \tag{6.3}$$

Dynamic mechanical analysis (DMA) allows for a quick and convenient measurement of material properties in which a sample is under an oscillating force and, the material"s deformation parameters including modulus and damping are measured as a function of temperature, frequency, or time, or combination thereof. The test fixtures depend on the samples, desired loading and result, used for various property characterizations. DMA provides material properties including E", E"" and relaxation processes in polymers, specially the glass transition (Tg). The storage and loss moduli are proportional to the energy stored and dissipated, respectively per cycle. The E" characterizes the elastic behavior of the material, and the E"" characterized the viscous behavior. The ratio of energy dissipated to energy stored is the tangent of the phase angle called tan delta (Tan (δ)).Moreover, weak glass transitions can be easily and precisely determined by DMA due to its approximately one decade higher sensitivity to glass transitions (Wielage et al. 2003).

DMA was processed according to the international standard D 5023-07. All samples were investigated under a flexure test by TA Instrument DMA Q800 with a multi-frequency-strain mode. Four different types of samples with the dimension of 60mm x 5mm x 1.5mm were tested, these samples were (i) pristine PLA, (ii) degraded PLA, (iii) silkworm silk fibre reinforced PLA composite and (iv) degraded silkworm silk fibre reinforced PLA composite. Pristine polymer is a

control to compare the results with remaining samples. The degraded PLA and degraded composite were prepared as specified in previous section. The actual dimensions of each sample were measured afterward. The samples were then griped horizontally by dual cantilever. The linear displacement amplitude was set to 15μm. Thermal scans were conducted from 20°C to 150°C at a ramping of 3°C/min with soak time 2 minutes for step increases.

6.5.3.1 DMA on non-degraded pristine PLA and silkworm silk fibre reinforced PLA composite

As the low storage modulus, it demonstrates the ease of deformation of a material by an applied load. Contrarily, high storage modulus is more desirable as it represents high stiffness and load bearing of the material at a specified temperature range. Fig. 6.21 shows $E^{''}$, $E^{'''}$ and $Tan(\delta)$ of the pristine PLA and the composite as a function of temperature, respectively (Idicula et al. 2005). Table 6.6 is the summary of the DMA results.
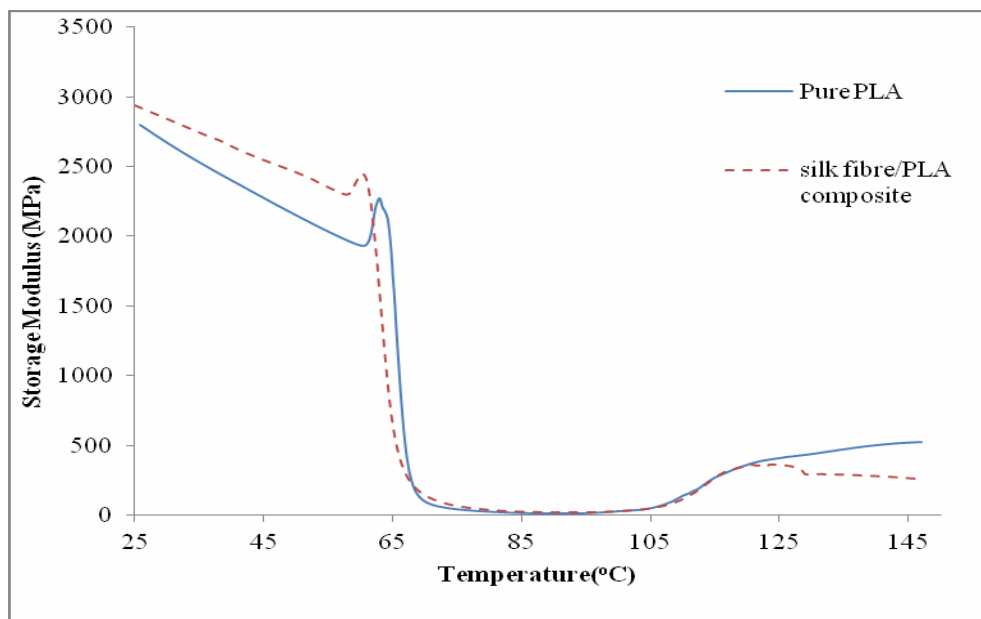
(a)
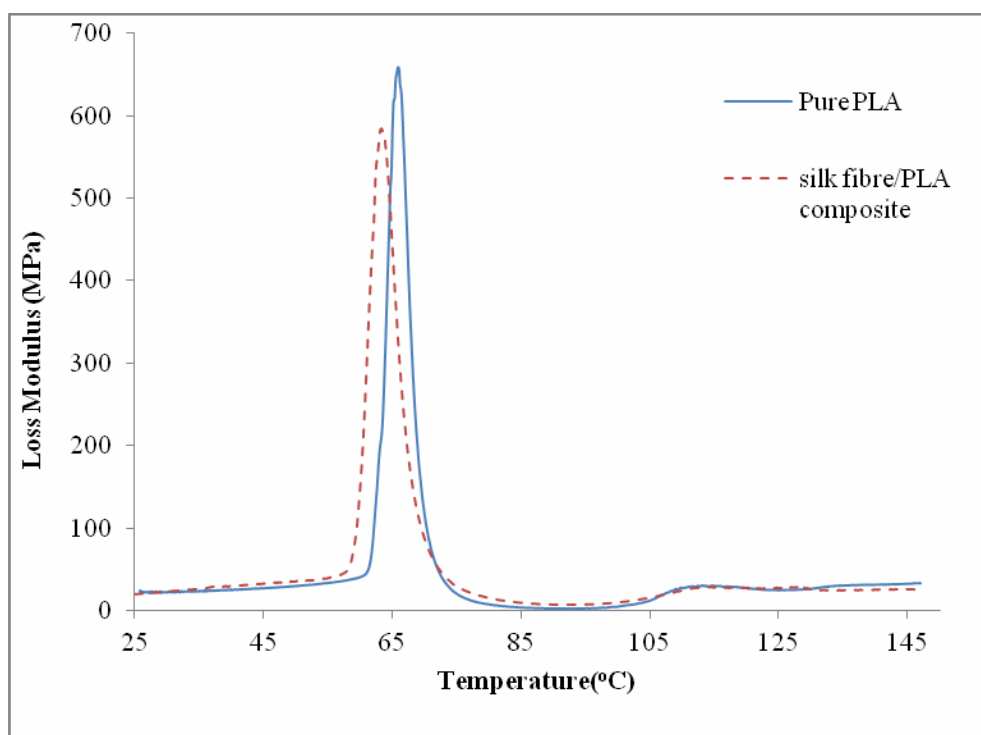
(b)
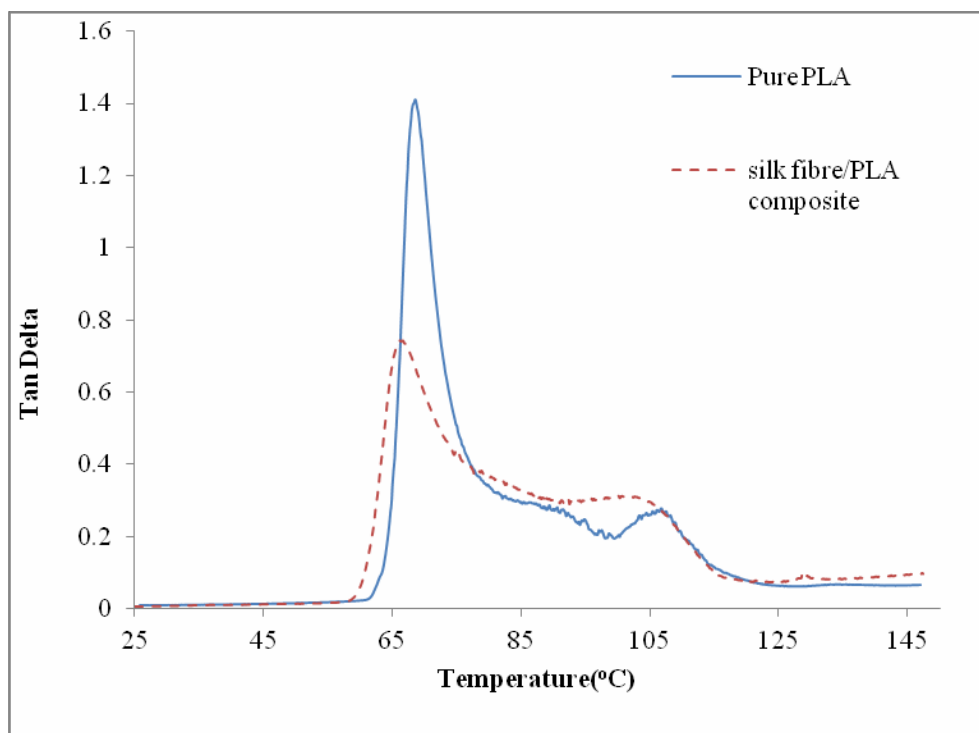
(c)

Figure 6.21. (a) Storage modulus (b) Loss modulus and (c) tan delta versus temperaure of the pristine PLA as compared with the composite.

In fig. 6.21(a), E'' of the composite is higher than that of the pristine PLA. It may be due to the existence of silkworm silk fibre which formed as physical cross linkage and allowed stress transfer between the silkworm silk fibre and the PLA. The mobility of PLA macromolecules was therefore counteracted by the silkworm silk fibres because of the difference glass transition temperatures (Tgs) between two materials. Consequently, the stiffness of the composite was increased (Averous & Boquillon 2004; Huda et al. 2005; Wielage et al. 2003). The figure shows the variation of storage modulus of the composite versus the change of temperature. At the beginning of the experiment, the macromolecules of the composite are comparatively highly immobile and exist in a close and tight

packing form and thus, resulting in high E''. As temperature increases the macromolecules become more mobile and lose their close packing arrangement. As a result, E'' of the composites decreases (Huda et al. 2005). Therefore, it is obviously observed that the E'' decreases gradually starting from an ambient temperature and then dramatically after 60 ^{o}C. The reduction in the E'' with an increase of the temperature is associated with the softening of the matrix at higher temperature.

The E'''' in viscoelastic solids measures the energy dissipated as heat representing the viscous portion. Comparing the curves of E'''' of the two different samples as shown in fig. 6.21(b), Tg is measured at a peak of the curves. The peak of the composite is slightly shifted down to a lower temperature as compared with the PLA with a narrow range at the transition region. This effect is exemplified through the broader slope of the transition region from the curves in fig. 6.21(b) and accompanied by peak widening from the loss modulus curves. The changes of the Tg between pristine PLA and the composite are dependent on the fibre length, fibre content and their interfacial bonding properties. Besides, only amorphous phase of partial crystalline PLA is involved in affecting the condition of Tg, the mobility of the PLA is counteracted by the fibres (Wielage et al. 2003).

Tan (δ) is the ratio of the E''''/E'' or, explicitly is the ratio of energy lost to energy retained in the loading cycle. High value of Tan (δ) means that once the deformation is induced, the material will not recover to its original status. The first peak at the Tan (δ) curve indicates a relaxation process while the second peak represents the Tg where molecules regain their mobility. It is found in fig. 6.21(c) that there is no substantial difference in Tan (δ) for both the composite and PLA at

37^OC, a simulated human body temperature. However, a significant decrement of the height and the sharpness of the peak are obtained as shown in the figure as the increase of content of silkworm silk fibre in PLA [23]. Such phenomena are coincident with other literatures for fibre reinforced thermoplastics [24]. Pristine PLA shows a sharp and intense peak because there is no restriction to the chain motion, where the composite hinders the chain mobility and results in the reduction of the sharpness and height of the Tan (δ) peak.

As damping in the transition region implies the imperfection of a material in its elastic phase and some of the energy is used to deform it during DMA and also directly dissipate into heat. Thus, the mechanical loss that overcomed the friction of intermolecular chains was reduced in the composite. This result indicates that the silkworm silk fibre can be used to restrict the mobility of the composite so as their E" was higher than that of the pristine PLA (Wanjun et al. 2005). The reduction in Tan (δ) also denotes an improvement in the hysteresis of the system and a reduction in the internal friction (Huda et al. 2005). Moreover, for the PLA reinforced by the silkworm silk fibre, the area under the Tan (δ) curve is smaller than that the curve measured by the pristine PLA. Since the PLA content is decreased to the same extent and only the amorphous phase of the partial crystalline polymer is involved in the glass transition (Huda, Drzal, Mohanty, & Misra, Chopped glass and recycled newspaper as reinforcement fibers in injection molded poly(lactic acid) (PLA) composites: a comparative study, 2006; Wanjun, Manjusri, Per, Lawrence, & Amar, 2005).

6.5.3.2 DMA on degraded pristine PLA and silkworm silk fibre reinforced PLA composite

Fig.6.22 and 6.23 show the dynamic mechanical properties, as a function of temperature of the pristine PLA and the composite as compared with their degraded statues, respectively. As shown in fig. 6.22 (a), the pristine PLA and degraded PLA exhibit similar initial E". As shown in table 6.7, the E" of the degraded composite is the lowest among all other samples. Comparing with degraded PLA with the pristine PLA, it can be proved that the E" of the pristine PLA decreases because of the degradation process. PLA processes the bulk erosion after absorbing the moisture. The difference to the surface erosion, bulk erosion would be taken place throughout all degraded samples. Ingress of water is normally faser than that the rate of degradation. Therefore, the weight of the samples increases at the beginning of the degradation process and their volumes were then increased subsequently.

Table 6.6. DMA Data of compression-molded composites in terms of the mean storage modulus (E"), at 25 and 37 ^{o}C, and glass transition temperature (Tg) as defined by peaks in loss modulus and tan detla.

Material	Storage Modulus		Loss Modulus		Tan detla	
	At 25°C	At 37°C	Tg (^{o}C)	At 37°C	Tg (^{o}C)	At 37°C
Pristine PLA	2.795	2.478	65.91	24.680	68.58	0.010
Composite	2.940	2.697	63.28	26.769	66.13	0.008
Degraded PLA	2.772	2.439	67.75	25.7414	70.07	0.011
Degraded composite	2.053	1.956	64.04	264.013	69.28	0.135

In table 6.6, it is found that the E″ of degraded composite is much lower than that of the degraded PLA. The decrement in the E″ is mainly caused by the water absorption of silkworm silk fibre in the composite. Silk proteins are stored in the silk gland and transported down the spinning duct in a lyotropic liquid crystalline state in silkworm silk glands. To produce this state, the protein molecules of the silkworm silk fibre must be amphiphilic, which is having a combination of hydrophobic and hydrophilic blocks or groups (Jacob et al. 2006). The hydrophilic character of natural fibre is responsible for the water absorption in the composites, and therefore increasing the amount of fibre would cause more water to be absorbed (Bini, Knight & Kaplan 2004). As the water absorbability of the silkworm silk fibre is higher than the PLA, it would accelerate the degradation process of the degraded composite. It further proves that the hydrophilic effect of the silkworm silk fibre does affect the water absorbability in its related composites.
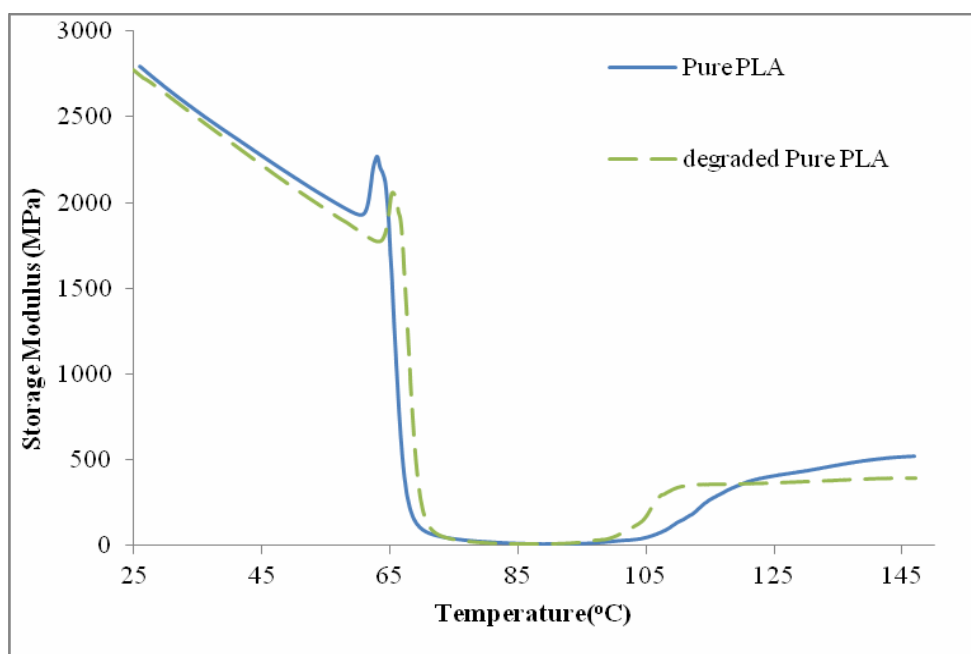
(a)
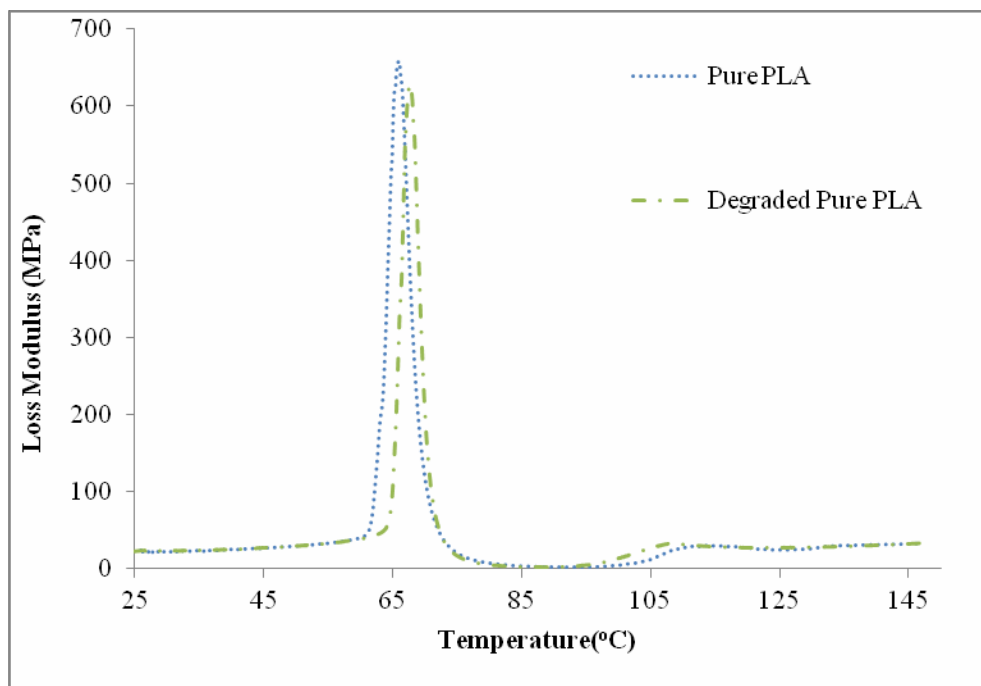
(b)
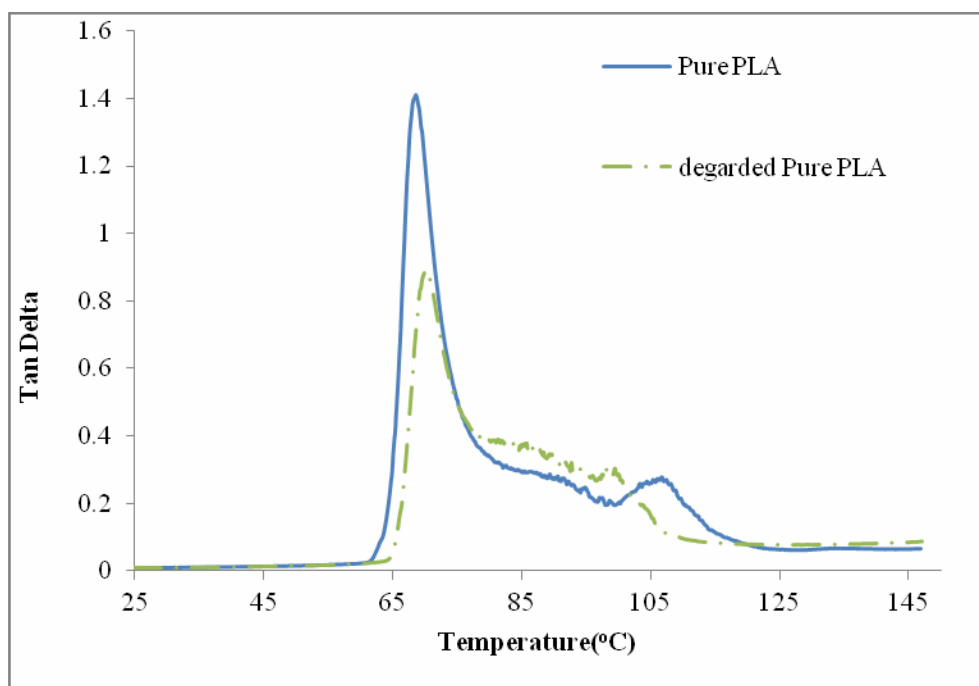
(c)

Figure 6.22. (a) Storage modulus (b) Loss modulus and (c) tan delta versus temperaure of the pristine PLA compared with the degraded PLA.
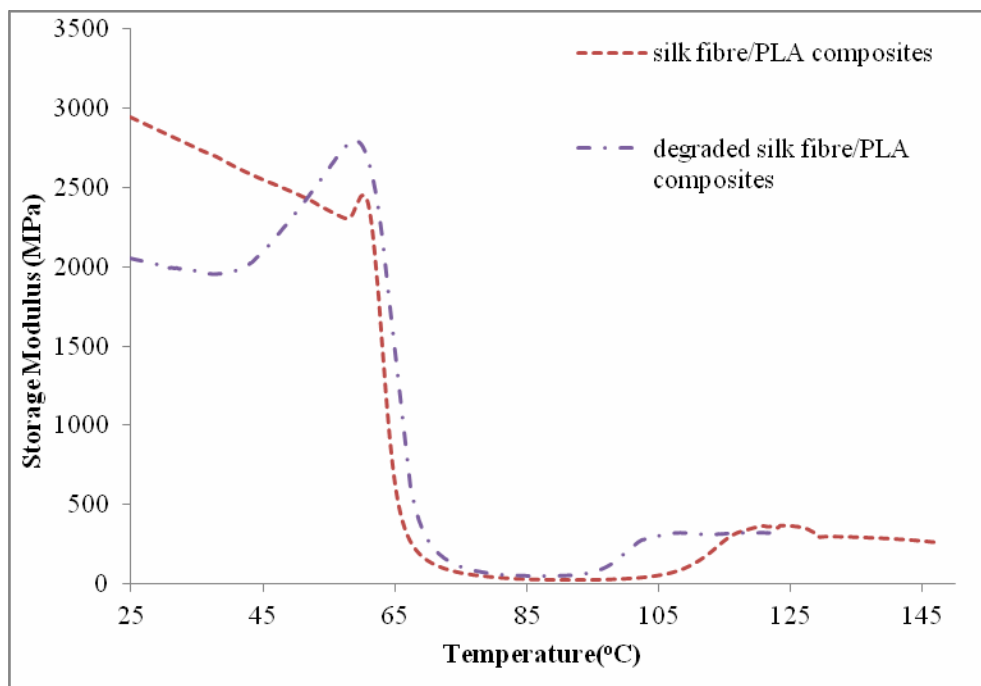
(a)
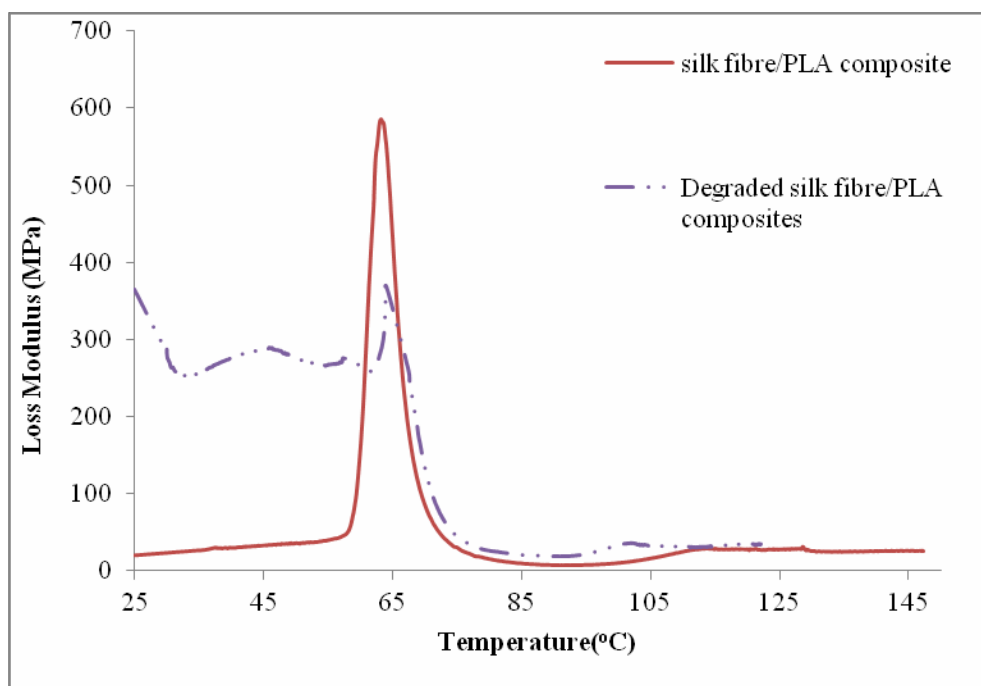
(b)
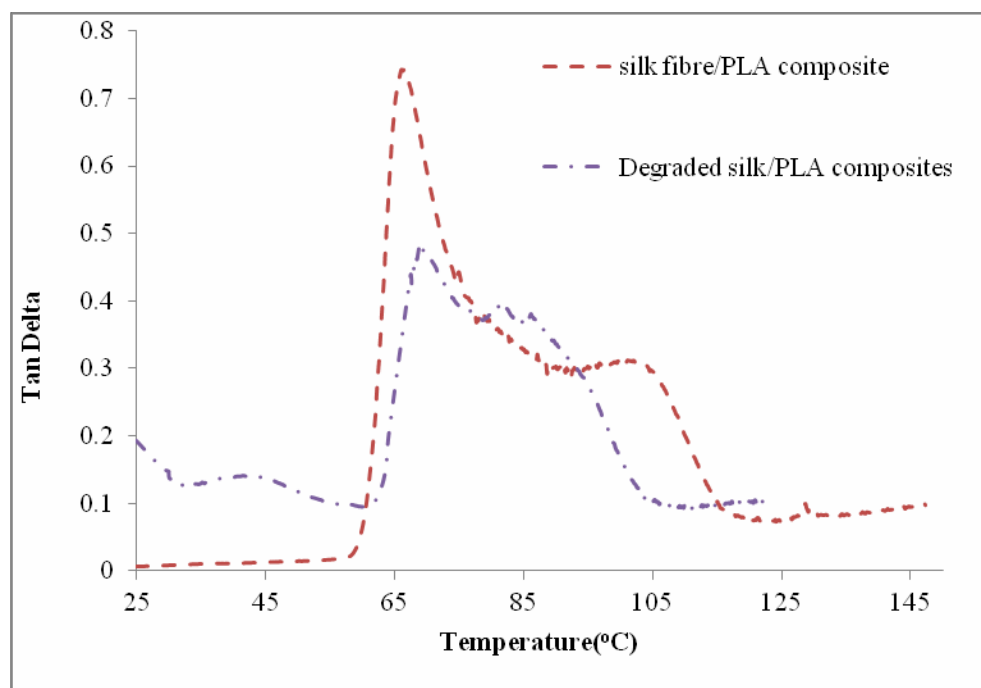
(c)

Figure 6.23. (a) Storage modulus (b) Loss modulus and (c) tan delta versus temperaure of the composite compared with the degraded composite.

Fig. 6.23(a) shows that there is a difference in a large extent of E" between the composite and the degraded composite. It is also demonstrated that within the range of 61°C and 68°C, the values of E" for all samples decrease rapidly. This implies that the contribution of fibre stiffness to the modulus of PLA is minimal at its glassy zone (Espert, Vilaplana & Karlsson 2004). Besides, fig. 6.23(a) shows a slight broadening of the loss modulus peak of degraded PLA compared with degraded silkworm silk fibre reinforced PLA composite. This could be due to the increase in energy dissipation caused by the addition of silkworm silk fibres which increase the degradation process. Tsukada et al. (Tsukada, Gotoh & Yasui 1995) have found that the shrinkage of silkworm silk fibre is about 1.3 % because of the loss of moisture during heating. As the shrinkage of the silkworm silk fibre

is different to the PLA, the deterioration of the interfacial adhesion and bond strength between the PLA and silkworm silk fibre were found which induces the dramatically drop of the initial E'' of silkworm silk fibre reinforced polymer composites. Therefore, the combined effect of the silkworm silk fibre shrinkage, and the mismatch of thermal expansions between the silkworm silk fibre and the PLA resulted in weakening the properties of the degraded composite (Huda et al. 2005).

The reduction of E'' of the degraded composite compared with the composite was due to the damage of matrix, deteriorated interfacial adhesion and poor bonding strength between the silkworm silk fibre and the matrix (Wielage et al. 2003). The deteriorated interface adhesion is susceptible to the degradation because of excessive interface reactions which would speed up the hydrolysis of the degraded composite. As a result, the interface could no longer be able to provide a full stress transfer from the matrix to the fibre effectively and thus the E'' modulus of the degraded composite decreased.

Chemical combinations between the polymer chains, Van der Waals interaction, and the hydrogen bonding in the molecular construction are responsible for the ability of the polymer to bear externally applied stresses. Moreover, the strength of the interface between fibre and matrix has the significance effect on E''. The degradation process starts with the swelling of silkworm silk fibres because of the water penetrating into the interface that develops stress at the interface and causes micro-cracking of the matrix around the swollen fibres. The cracks also accelerate the water absorption and its attack on the interface through capillarity mechanism. The residues of the degraded substances start leaching from the fibres. These

eventually lead to the ultimate debonding between the fibre and the matrix (Athijayamania et al. 2009; Chen, Miao & Ding 2009). Therefore, the voids in the composite increase and these voids also increase the surface area and thus speed up the degradation process for intra and inter-molecules bonding breakage. Therefore, the macromolecules are loose packed and not restricted. Due to the increased mobility of polymer molecules in the degraded composite with poor adhesion, E'' of degraded composite was therefore lower than that of the composite with better bonding interface. Nevertheless, the bonding between the silkworm silk fibre and PLA could be damaged easier than the internal bonding in the pristine PLA because of the opposite nature of hydrophobicity as silkworm silk fibre is amphiphilic. Besides, When samples were immersed into the PBS solution, water molecules penetrated into the PLA, the hydrolysis and plasticization of the PLA would damage the chemical bonding, in the case of experiencing a stress, greater strain may be induced, which would lead to a decrease of the E'' (Wielage et al. 2003).

Comparing the E''' and Tan (δ) of the pristine PLA with the degraded PLA, and the composite and the degraded composite, respectively as shown in fig. 6.22 (b-c) and fig. 6.23 (b-c), the Tg of degraded samples were higher than that of non-degraded samples. The glass transition can be thought as the softening point of amorphous regions of polymers. The result shown in the figures are mainly because of the water which acted as a plasticizer and the increase of the crystallinity of the degraded samples. Although the degradation process increased the crystallinity of the PLA through plasticization by water, certain regions in the PLA were hydrolyzed by bulk erosion (Cai et al. 1996; Gonzalez, Ruseckaite & Cuadrado 1999). Therefore, it can be explained that even the crystalinity of the

degraded samples increased, the modulus of the sample decreased. As the debonding of the interface caused by the distinct moisture, expanding coefficient between the fibre and matrix in the plasticization process, it would also be a factor to lower the Tan (δ) (Wielage et al. 2003). Therefore, the Tg obtained from both E'''' and Tan (δ) increased because of the increment of the mobility.

Through the degradation process, the porosity of the degraded composite and the degraded PLA increased which also increased their damping effect. Hence, a relatively less energy was used to overcome the frictional forces between molecular chains so as to decrease mechanical loss. The energy absorbing process of the degraded composite was smaller because the presence of the silkworm silk fibre in the degraded composite after the degradation proces (Faughnan & Bryan 1998).

Chapter 7

Theoretical Analysis

7.1 Introduction

As aforementioned, a silk fibre are bound together by a sericin layer, Zhao et al. has found that the diameter of a Bombyx mori silk fibre is in the range of 2–4 µm (Zhao et al. 2005). As discussed in Chapter 5, the thickness of this layer is highly affected by the degumming process and the solutions such as NaOH, water or citric acid used. However, certain amount of sericin may purposely or accidentally remain on the surface of the core fibre because of incomplete degumming (Padamwar & Pawar 2004). The intrinsic condensed structure of sericin is mainly amorphous and contains few β−structure (Tao, Li & Xie 2005). More amorphous regions of sericin bestow extensibility because the high energy absorption. Therefore, the existence of sericin layer would absorb part of energy when a composite is under loading. The strain experienced by a host biopolymer is not transferred completely to the core fibre. However, very few available theoretical analyses pertain to silk fibre reinforced biopolymer composites and most of these analyses do not take into account on the effect of sericin. Therefore, a linear, elastic and isotropic theoretical model with the consideration of sericin thickness to evaluate the differential stress between the core fibre and surrounding sericin

layer is introduced. Besides, the influence on moisture absorption in relation to the shear stress between the core fibre and the layer is also discussed as below.

7.2   Load Transfer Properties

7.2.1   Constant Load Applied Along Silkworm Silk Fibre Longitudinal Direction

The sericin layer in the composite would potentially absorb part the energy and affect the deformations of each material. Besides, the length of the core fibre, in the case of short fibre is used, is also important for the accuracy of the result because a shear stress concentration exists at the fibre ends. Fig. 7.1 depicts a three-cylinder model for analyzing the stress transfer properties of a single fibre reinforcement system. As two core fibres are stuck closely together and maintain an elliptical shape in its aspect ratio less than 2, it therefore reasonably assumes that the core fibre can be modeled as a single fibre with the radius of r_c. The longitudinal axis z represents the direction of the applied load. Transverse direction *r* represents the distance measured from the centre (*r* = 0) of the core fibre. In fig. 7.1, the subscripts c, s and h denote the core fibre, sericin coating and surrounding host polymer material, respectively. Tensile and shear moduli are given by E and G, respectively. $\tau_h(z,r)$ and $\tau_s(z,r)$ denote the shear stresses along the axial direction (i.e. fibre"s direction) at the interfaces between the polymer material and sericin layer, and between the sericin layer and the core fibre respectively. r_h, r_s, and r_c represent the outer radii of the host polymer material, sericin layer and the core fibre respectively.
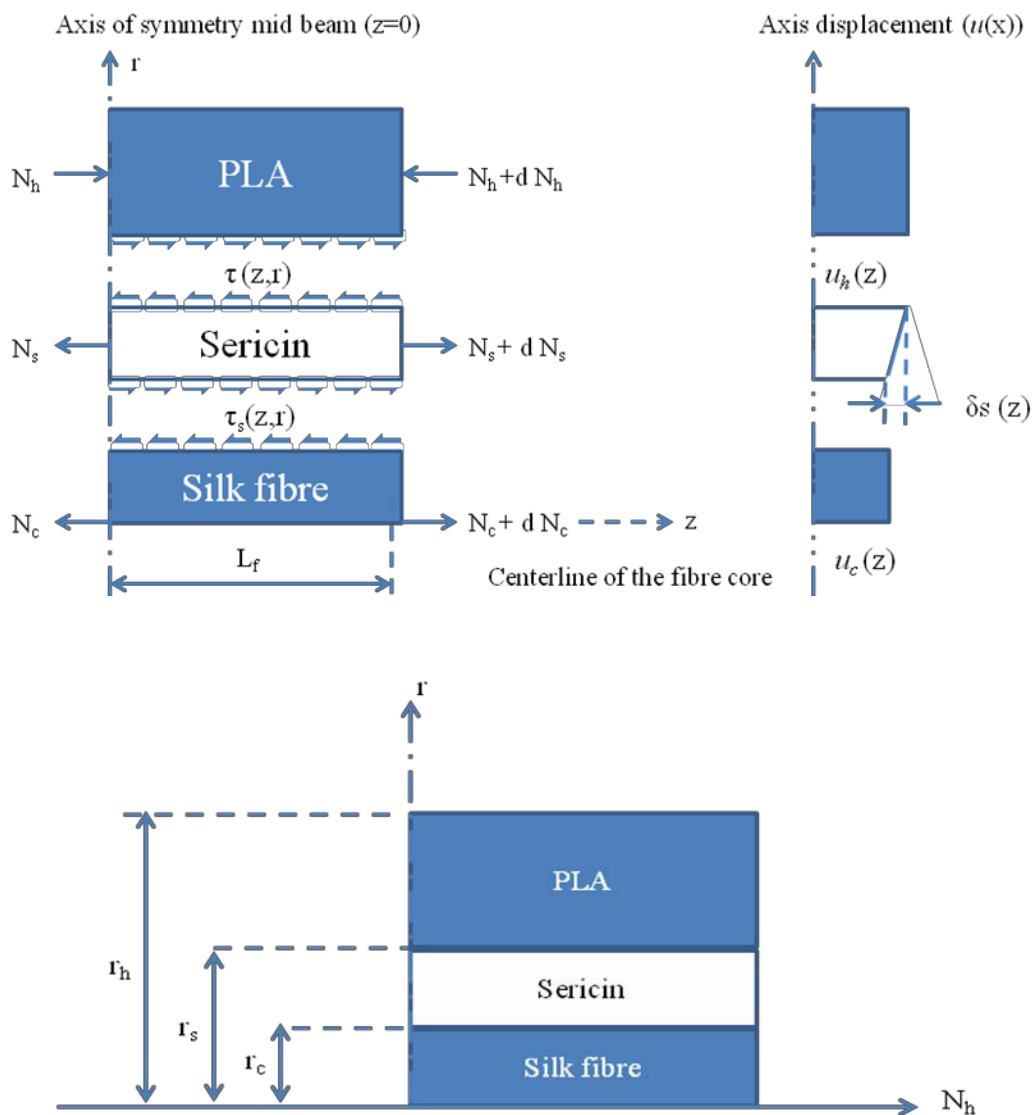
Figure 7.1. Three-cylinder model for the present study.

In the case when the composite is under an axial load, the loads are applied to the host polymer material, sericin layer and the core fibre are denoted by N_h, N_s and N_c, respectively. Because of the symmetry about both *r*- and *z*-axes, only a quarter section of the system is considered.

The following basic assumptions are made to simplify the case of current study:

1. The theory is applicable as long as all the material involved including host polymer material, sericin layer and the core fibre are linear, elastic and isotropic. This assumption is not entirely match the truth as the mentioned materials behave in a nonlinear viscoelastic manner;

2. The core fibre, sericin layer and the host polymer material are assumed to be free of voids;

3. All interfaces are perfectly bonded.

The axial displacement conditions are described by

$$u(z) = \begin{cases} u_h(r,z) = u_s(r_s,z) \\ u_s(r_c,z) = u_c(r,z) \end{cases} \tag{7.1}$$

The relative displacement (δs) of the sericin layer due to the shear deformation is given by

$$\delta_s(z) = u_h(r_s,z) - u_c(r_c,z), \tag{7.2}$$

At the mid-beam region ($z = 0$), the strains for all elements are mathematically identical, i.e.,

$$\varepsilon_h(r,0) = \varepsilon_s(r,0) = \varepsilon_c(r,0) \tag{7.3}$$

4. Thermal load is not applied in the system. The strain evaluated at the core fibre only responds to the strain induced by the load applied axially.

By considering the force equilibrium for an element of sericin layer in the loading direction as shown in fig. 7.1, the shear stress in this layer can be approximately obtained by using the following relationship:

$$\pi(r^2 - r_c^2)\sigma_s + 2\pi r_c \int_0^{L_f} \tau_c(z, r_c)dz - 2\pi r \int_0^{L_f} \tau(z, r)dz = 0 \tag{7.4}$$

Where σ_s is the axial stress in the sericin layer in the z direction, Eq.(4) can then be rewritten in the following form:

$$\frac{1}{L_f}\int_0^{L_f}(r^2 - r_c^2)\sigma_c dz + 2r_c\int_0^{L_f}\tau_c(z, r_c)dz - 2r\int_0^{L_f}\tau(z, r)dz = 0 \tag{7.5}$$

Hence, Eq.(5) is alternatively written as the following:

$$\frac{1}{L_f}(r^2 - r_c^2)\sigma_c + 2r_c\tau_c(z, r_c) - 2r\tau(z, r) = 0 \tag{7.6}$$

In general case, the length of the core fibre is greater than its diameter i.e., L >> r, so that the first term appeared in Eq.(6) becomes very small as compared to other terms in the Equation, and thus this term can be neglected in the current analysis. The relationship, in term of the shear stress in the sericin layer and the shear stress at the surface of the core fibre at any section z can be expressed by:

$$\tau(z,r) = \frac{r_c}{r}\tau_c(z,r).\ r_c \leq r \leq r_s \tag{7.7}$$

The axial displacement of the host polymer material can be obtained by considering the condition of compatibility for all elements

$$u_h(z) = \delta_s(z) + u_c(z) \tag{7.8}$$

in which the relative displacement of the sericin layer is determined by

$$\delta_s(z) = \frac{1}{G_s}\int_{r_c}^{r_s}\tau_c(z,r_c)\ dr \tag{7.9}$$

For the host polymer material and the core fibre, the axial displacements are given by

$$u_h(z) = \int_0^z \frac{\sigma_h(z)}{E_h} dz \qquad (7.10)$$

and

$$u_c(z) = \int_0^z \frac{\sigma_c(z)}{E_c} dz \qquad (7.11)$$

The tensile force of the core fibre is thus expressed as

$$N_c(z) = \pi r_c^2 \sigma_c - 2\pi r_c \int_0^z \tau_c(r_c, z) dz \qquad (7.12)$$

where σ_c is the axial stress of the core fibre at mid-beam section ($z = 0$). Substituting Eqs. (9) - (11) into Eq. (12) yields the following integral equation:

$$\int_0^z \frac{\sigma_h}{E_h} dz = \frac{1}{G_s} \int_{r_c}^{r_s} \frac{r_c}{r} \tau_c(z, r_c) dr + \int_0^z \frac{\sigma_c(z)}{E_c} dz$$

$$\int_0^z \frac{\sigma_h}{E_h} dz = \frac{1}{G_s} \int_{r_c}^{r_s} \frac{r_c}{r} \tau_c(z, r_c) dr + \int_0^z \frac{N_c(z)}{E_c \pi r_c^2} dz$$

$$\int_0^z \frac{\sigma_h}{E_h} dz = \frac{r_c}{G_s} \tau_c(z, r_c) \ln\left(\frac{r_s}{r_c}\right) + \frac{1}{E_c \pi r_c^2} \int_0^z \left[\pi r_c^2 \sigma_c - 2\pi r_s \int_0^\xi \tau_c(\xi, r_c) \right]$$

(7.13)

By differentiating Eq. (13) and combining the compatibility condition (3), the equation is simplified as

$$\frac{-2}{E_c r_c} \int_0^z \tau_c(\xi, c) \, d\xi + \left\{ \frac{r_c}{G_s} \ln\left(\frac{r_s}{r_c}\right) \right\} \frac{\partial \tau_s(z, r_s)}{\partial z} = 0 \qquad (7.14)$$

Further, differentiating Eq. (14) gives

$$\frac{\partial^2 \tau_c(z, r_c)}{\partial z^2} - \lambda^2 \tau_c(z, r_c) = 0 \qquad (7.15)$$

where

$$\lambda = \sqrt{\frac{2G_s}{E_c r_c^2 \ln (r_s/r_c)}} \qquad (7.16)$$

The solution to Eq. (20) is given by

$$\tau_c(z, r_c) = C_1 \cosh(\lambda z) + C_2 \sinh(\lambda z) \qquad (7.17)$$

Two unknowns C_1 and C_2 are determined using two boundary conditions. The first boundary condition is evaluated at z = 0. The axial load (N_c) at the core fibre is determined by the compatibility condition (Eq. (3)). The strain of the core fibre at the mid-beam region is equal to the strain of the host polymer material. The second boundary condition is evaluated at the point, where the axial load of the core fibre core is zero, i.e.,

$$N_c(0) = \sigma_h \pi r_c^2 \frac{E_c}{E_h} \text{ and } N_c(L_f) = 0 \tag{7.18}$$

in which L_f is the distance measured from the mid-beam (z = 0) to the point of zero axial load of the core fibre. Using above boundary conditions, the constraints C_1 and C_2 are obtained by

$$C_1 = \frac{\sigma_c r_c \lambda}{2\sinh(\lambda L_f)} \text{ and } C_2 = 0 \tag{7.19}$$

Combining Eqs. (7.17) and (7.19) yields the final form of shear stress distribution at the interface between the sericin layer and the fibre core

$$\tau_c(z,r_c) = \frac{\sigma_m r_c \lambda}{2\sinh(\lambda L_f)} \cosh(\lambda z) \tag{7.20}$$

Tensile force in the core fibre is determined by substituting the Eq.(7.20) into Eq.(7.12)

$$N_c(z) = \pi r_c^2 E_C \frac{\sigma_m}{E_m}\left[1 - \frac{\sinh(\lambda z)}{\sinh(\lambda L_f)}\right]$$

(7.21)

Further, distribution of stress along the core fibre is given by,

$$\sigma_c(z) = \frac{1}{\pi r_c^2}\left[\sigma_c \pi r_c^2 - 2\pi r_c\left(\frac{C_1}{\lambda}\sinh(\lambda z)\right)\right]$$

$$\sigma_c(z) = \frac{E_c \sigma_m}{E_m}\left[1 - \left(\frac{\sinh(\lambda z)}{\sinh(\lambda L_f)}\right)\right]$$

(7.22)

And the corresponding strain along the core fibre is

$$\epsilon_c(z) = \frac{\sigma_m}{E_m}\left[1 - \left(\frac{\sinh(\lambda z)}{\sinh(\lambda L_f)}\right)\right]$$

(7.23)

Therefore, the shear stress, axial stress and the axial strain of the core fibre can be obtained through Eqs. (22) to (23). The axial stress"s curves of the core fibre obtained with different bonded lengths are shown in fig. 7.2. Among three fibres with different fibre lengths, the length of the shortest fibre is smaller than the

critical length (l_c) so that the stress cannot be transferred completely.

The axial stress of the core fibre obtained through the Eq.(22) with different parameters (Young"s modulus of the core fibre and host polymer material, shear modulus and thickness of the sericin layer) along the mid-beam are plotted in fig. 7.3, 7.4, 7.5, 7.6 and 7.7 separately. In fig. 7.3, it shows that the use of lower value of Young"s modulus of core fibre, longer fibre length is needed for complete stress transfer and, the axial stress is also increased. However, it can be seen that the increment in either the Young"s modulus of the host polymer material or the shear modulus of the matrix, the length for stress transfer is reduced (fig. 7.4 and 7.5). Therefore, the critical length is reduced as the young"s modulus of the host polymer material or shear modulus increase. Fig. 7.6 shows that thicker sericin layer requires longer stress transfer length. Fig. 7.7 shows the interfacial shear stress against the length of the fibre with different sericin thicknesses. In the figure, it shows that the maximum shear stress of thinner sericin is higher than that of thicker ones. Besides, the fibre which coated by thicker sericin requires longer stress transfer length for complete stress transfer from the host polymer material to the core fibre through sericin. It is because much of energy is converted into shear deformation at the sericin.

.
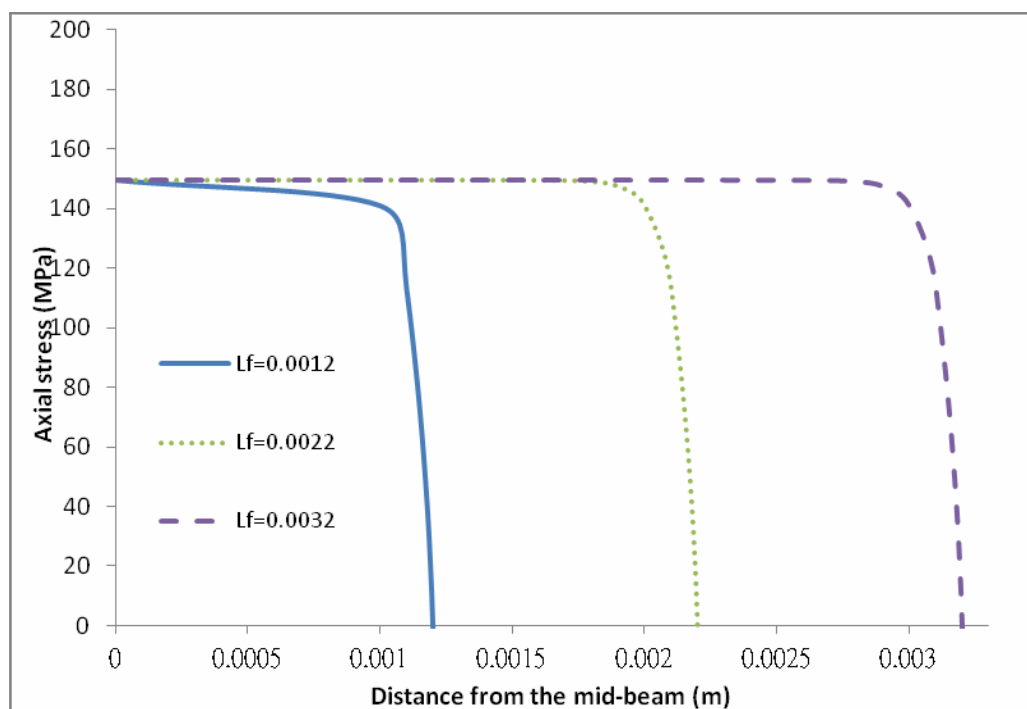
Figure 7.2. Axial stress of the core fibre against the distance measured from the mid-beam (z=0) with different embedding lengths.
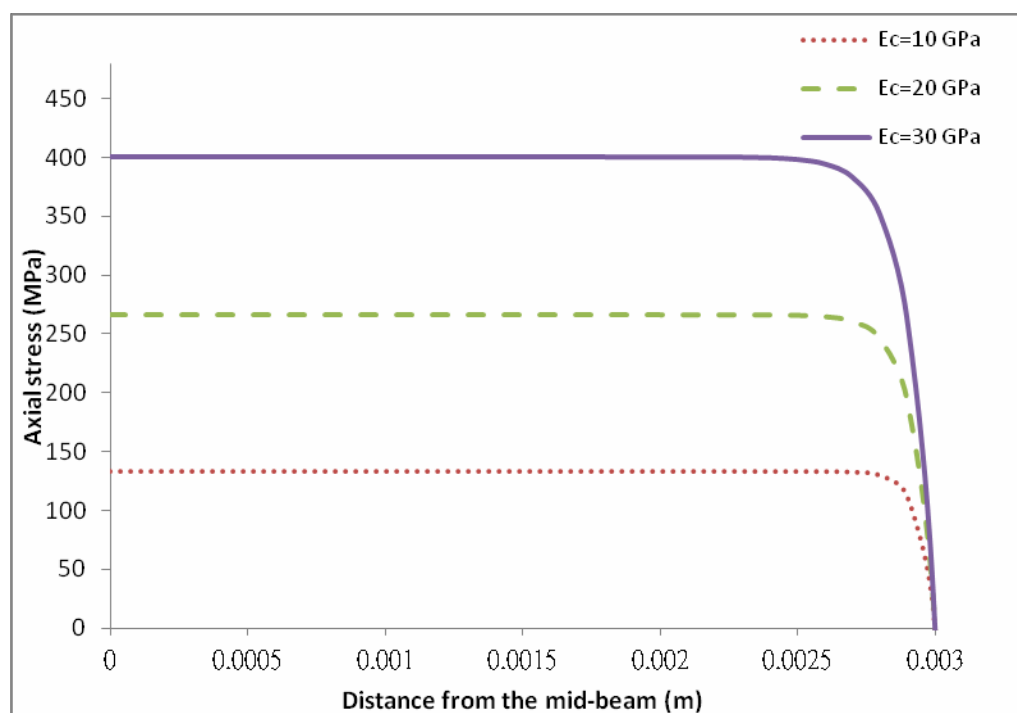
Figure 7.3. Axial stress of the core fibre against the distance measured from the mid-beam (z=0) with different Young"s modulus of the core fibre.
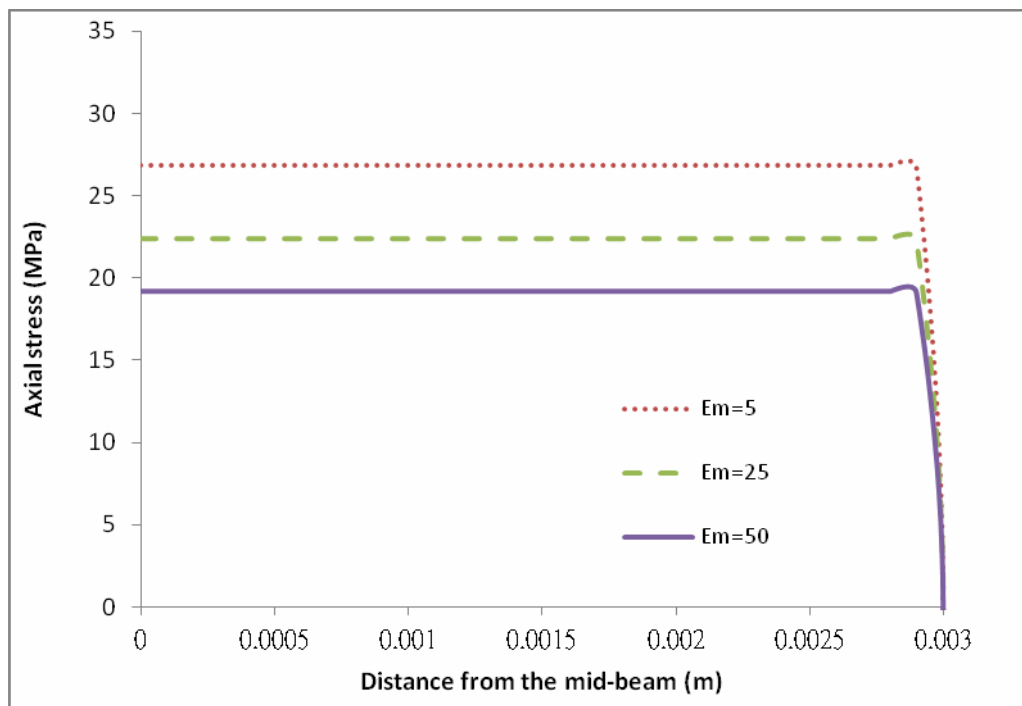
Figure 7.4. Axial stress of the core fibre against the distance measured from the mid-beam (z=0) with different Young"s modulus of the host polymer material.
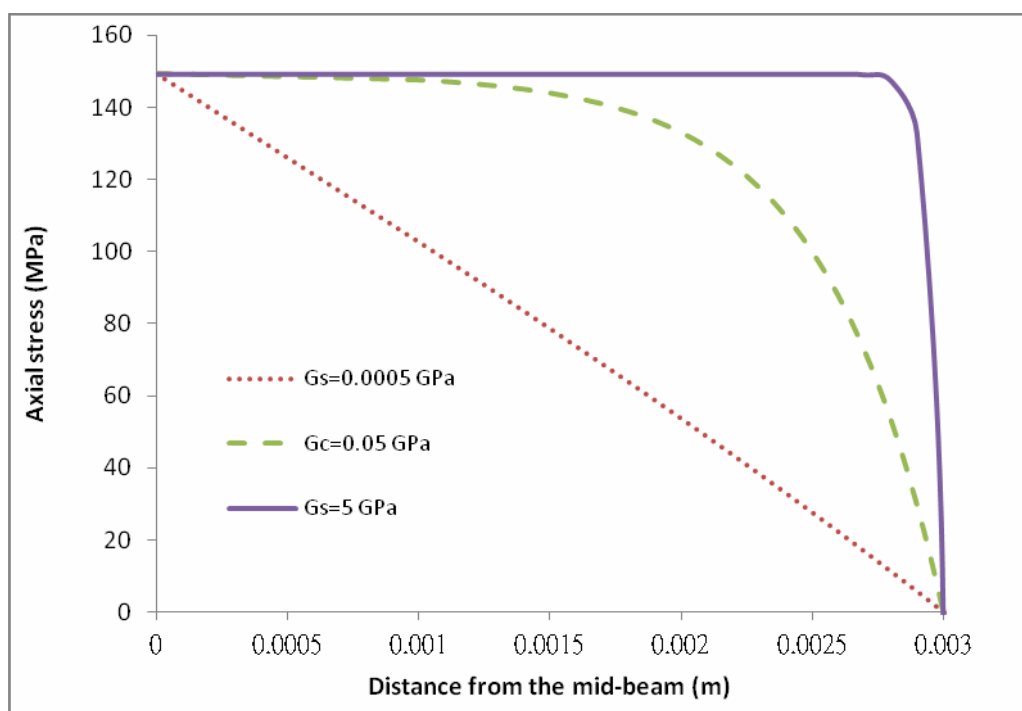
Figure 7.5. Axial stress of the core fibre against the distance measured from the mid-beam (z=0) with different shear modulus of the sericin.
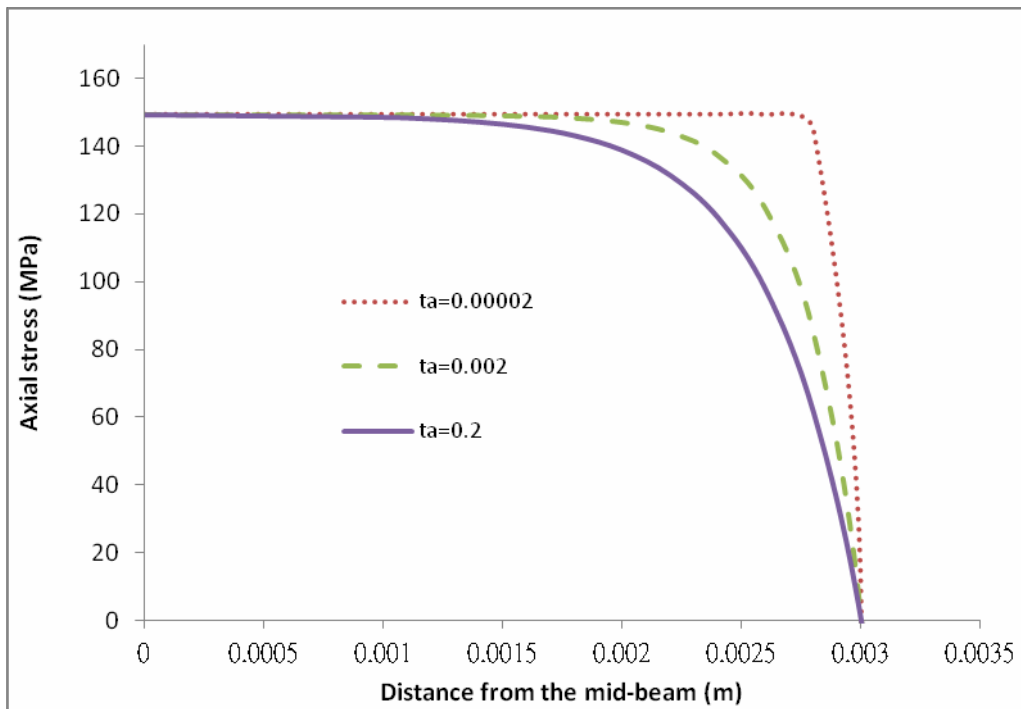
Figure. 7.6. Axial stress of the core fibre against the distance measured from the mid-beam (z=0) with different thickness of sericin.
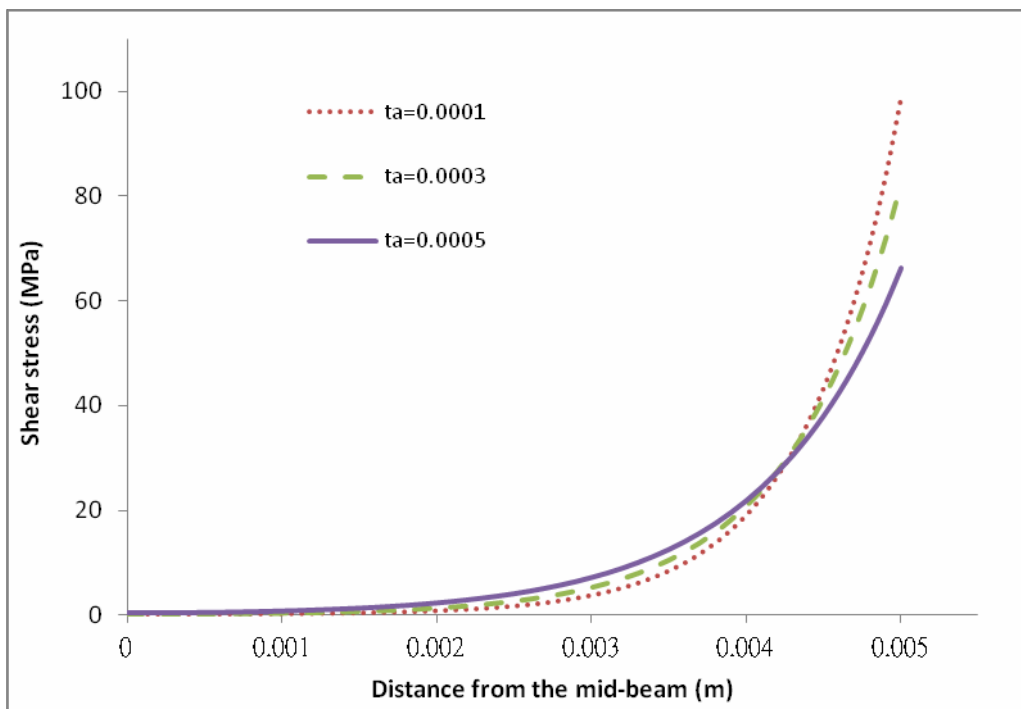
Figure. 7.7. Shear stress of the core fibre against the distance measured from the mid-beam (z=0) with different thickness of sericin.

7.2.2   Influence of Moisture Absorption on Load Transfer Properties

In general, the degradation process can be divided into 4 steps:

1. water absorption

2. reduction of mechanical properties

3. reduction of molar mass

4. weight loss

Different types of erosion for degradation are illustrated in fig. 7.8. Bulk erosion is the process in which hydrolysis takes place at the same time throughout an entire material. During the bulk erosion, the diffusion process is instantaneous which means the ingress of water is faster than that of the rate of degradation. Hence, the simultaneous decrease in molecular weight, the reduction in mechanical properties, and the loss of mass also occur throughout the material (Vieira A C 2011). The polymers which process the bulk erosion include PLA, PGA, PLGA and PCL. Another type of erosion is called "heterogeneous" or "surface erosion", in which mass loss is faster than the ingress of water into the bulk. Therefore, hydrolysis occurs in the region near the surface. As the surface is eroded and removed, the hydrolysis front moves through the material core. The examples of surface erosion"s material include poly (ortho)esters and polyanhydrides.
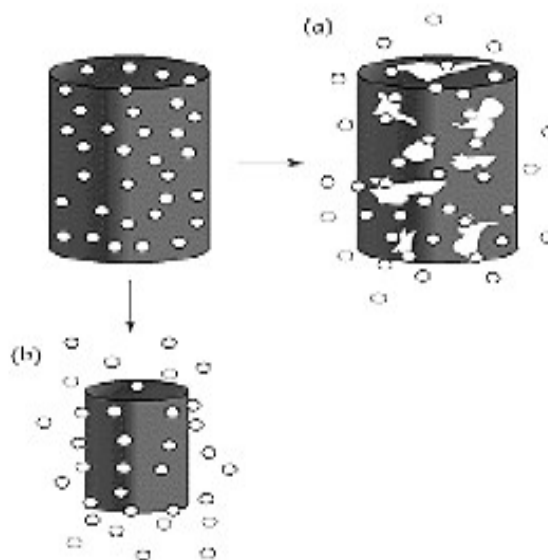
Figure 7.8. The scheme of (a) Bulk erosion and (b) surface erosion.

Surface and bulk erosions can be classified through the comparison between the characteristic time of hydrolysis and the diffusion coefficient of water. Time of hydrolysis (τ_H) is expressed as (Vieira A C 2011)

$$\tau_H = \frac{1}{kEw} = \frac{1}{u_m}$$

(7.24)

where E and w are the concentrations of ester groups and water in the material, respectively, k is the hydrolysis kinetic constant and, um is the hydrolysis rate, assuming that E and w are constants in the early stage of the reaction. Besides, if D is the diffusion coefficient of water in the polymer and L is the sample thickness, the characteristic time of diffusion (τ_D) is:

$$\tau_D = \frac{L^2}{D} \tag{7.25}$$

When $\tau_H \gg \tau_D$, water reaches the core of the material before it reacts, and the degradation starts homogenously. When $\tau_H \ll \tau_D$, water reacts totally in the superficial layer before reaching the core of the material. It can be assumed that $\tau_H \gg \tau_D$ is in the case of both PLA and silk fibre. Accordingly, it can be classified as the totally bulk erosion.

The effect of degradation on the strength of the material is significance. However, the constant slope of a linear elastic stage indicates that no significant variation in Young's modulus occurred during the degradation process (Vieira A C 2011). Therefore, the change in Young's modulus during the process of a silk fibre reinforced PLA composite shown in an experimental result is assumed as mainly dependence on the moisture content. Besides, diffusion is assumed to occur instantaneously which means the moisture content in the composites is constant throughout the whole entire.

In general, moisture absorption is depended on several parameters such as temperature, diffusion rate, applied load, materials properties, system of the composite, and type of media and time. When the composite is immersed into water, the water absorption is processed, water molecules can attach on hydrophilic materials and form hydrogen bonds. In the case of load transfer analysis, moisture absorption can alter the Young's moduli of constituents of the

composite, so as the axial stress and strain in a fibre. The Nissan"s model (Nissan 1976) represents that the elastic modulus is as a function of moisture

$$E = E_0 e^{(a-bm)} \tag{7.26}$$

Where a and b are material constants and m is the moisture content.

As the change of moisture content is depended on time, it can be measured by the change of weight of the composite. Two cases are discussed on the moisture absorption at different situations,

1. Moisture absorption affects the Young"s modulus of a host polymer material (Only the Young"s modulus of host polymer material is changed),

2. Moisture absorption affects the properties of a host polymer material and a core fibre (Young"s moduli of host polymer material and core fibre are changed based on the moisture absorption).

7.2.2.1 Effect of moisture absorption on the properties of host material

In order to specify the effect on the moisture absorption in relation to the axial stress between the sericin and the core fibre during the degradation process, certain assumptions must be addressed. The changes of the Young"s modulus either of the host polymer material or host polymer material and core fibre with

time are considered until the moisture content is saturated. Degradation can be classified into a four step process as mentioned previously. In this section, only the step 1 of degradation (moisture absorption) is concerned. Therefore, the weight change of the material is assumed dependent on the amount of moisture in the material. Besides, moisture saturation is regarded as the maximum amount of water particles that can be contained within the composite. The levels of saturation for any given type of material can be varied because of different voids content. These voids would contain water and speed up the moisture diffusion and degradation. Therefore, it is assumed that there is no predictable contrived void exists in the composite.

The process of the water absorption is under the condition that a composite is immersed into the water bath. As the atmosphere contain water which diffuse into the composite before immersing it into the water, the initial moisture content is set to be non-zero. Fig. 7.9 shows the change of Young"s modulus of the host polymer material measured from (a) the change of moisture content of host polymer material and (b) time. The results show that the Young"s modulus increases with time. This result may reflect the ability of bounded water to enhance chain mobility. The effect of the change in the Young"s modulus of host polymer material induced by the increase of moisture content on the axial stress depending on time is shown in fig. 7.10. Fig. 7.11 shows the effect on the axial stress to the Young"s modulus of host polymer material. The figures indicate that the increment in the axial stresses depends on an increase in immersion time of the composite as the Young"s modulus of host polymer material is changed.
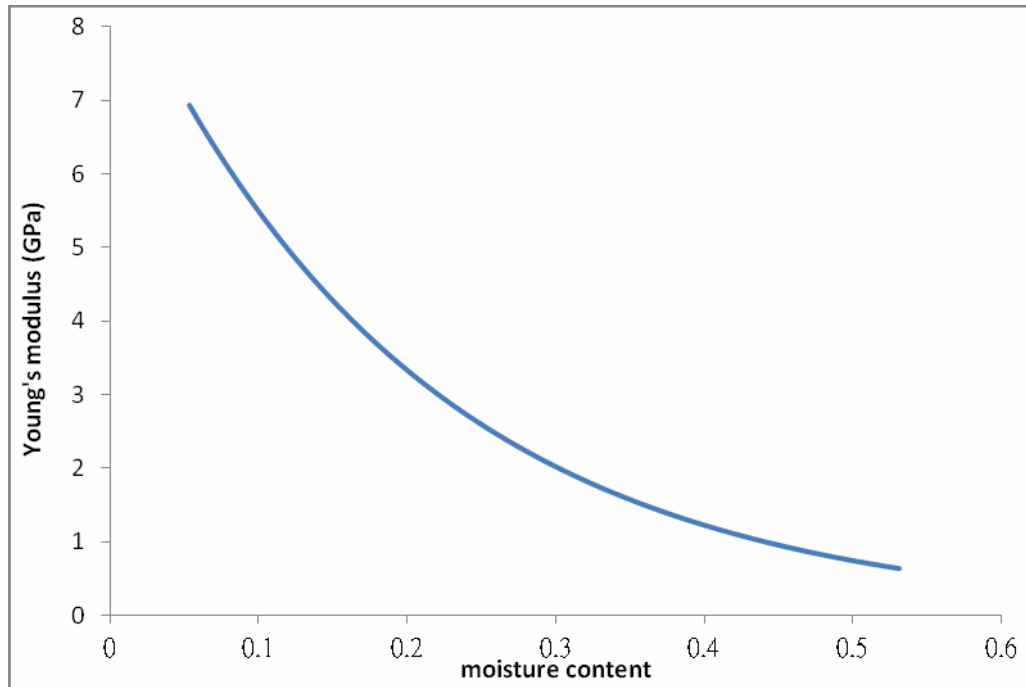
(a)
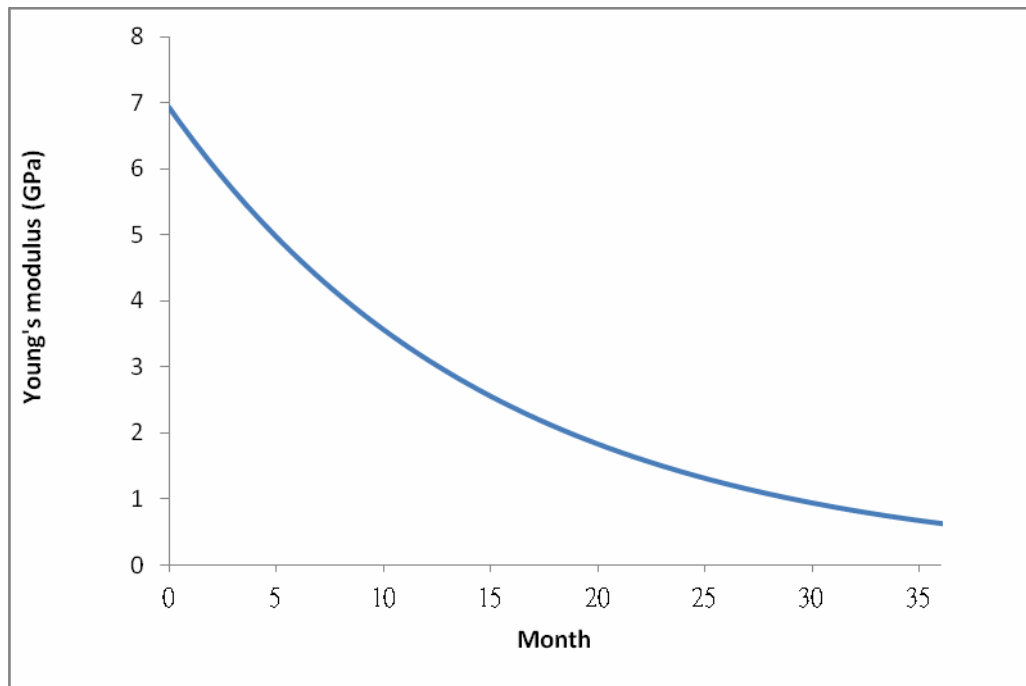
(b)

Figure 7.9. The Young"s modulus of host polymer material calculated from (a) the change of moisture content and (b) time.
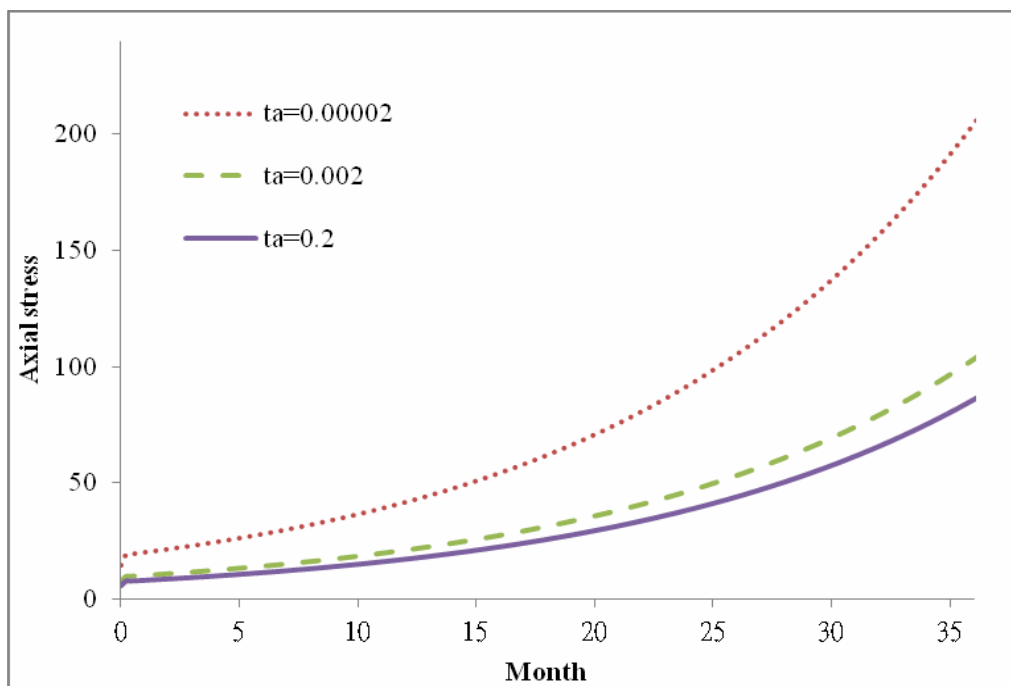
Figure 7.10. Axial stress between the sericin and the core fibre calculated from (a) the increase in moisture content based on time with different thickness of the sericin.
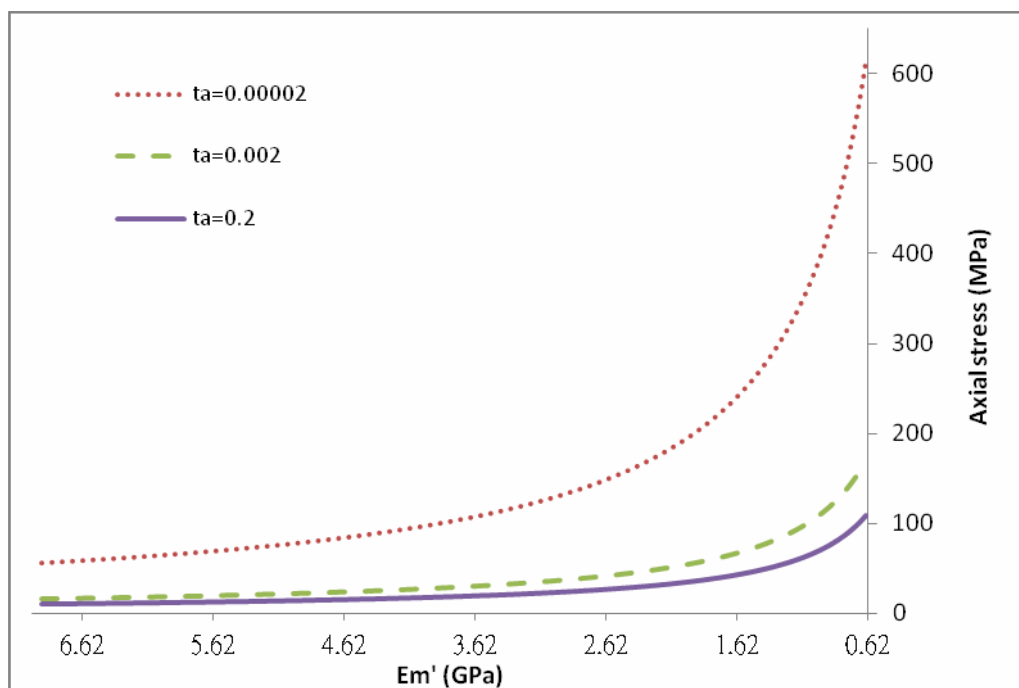
Figure 7.11. Axial stress between the sericin and the core fibre calculated from (a) the change of Young"s modulus of host polymer material based on the increase in moisture content with different thickness of the sericin.

7.2.2.2 Effect of moisture absorption on the properties of host polymer material and core fibre

In the case of both host polymer material and core fibre absorb moisture and thus change their Young"s modulus. It is assumed that their dimensional change (swelling) is not significant. Fig. 7.12 shows the Young"s modulus of host polymer material and core fibre measured from (a) the change of moisture content of host polymer material and the core fibre and (b) time. Fig. 7.13 exhibits the effect of the moisture content of host polymer material and core fibre on the axial stress depending on time. Fig. 7.13 shows the rate of increment in the axial stress with time is smaller than the result shown in fig. 7.10. In Fig. 7.13, as both of the host polymer material and core fibre absorb moisture, the effects on the axial stress by the change in Young"s moduli of both host polymer material and the core fibre are compensated.
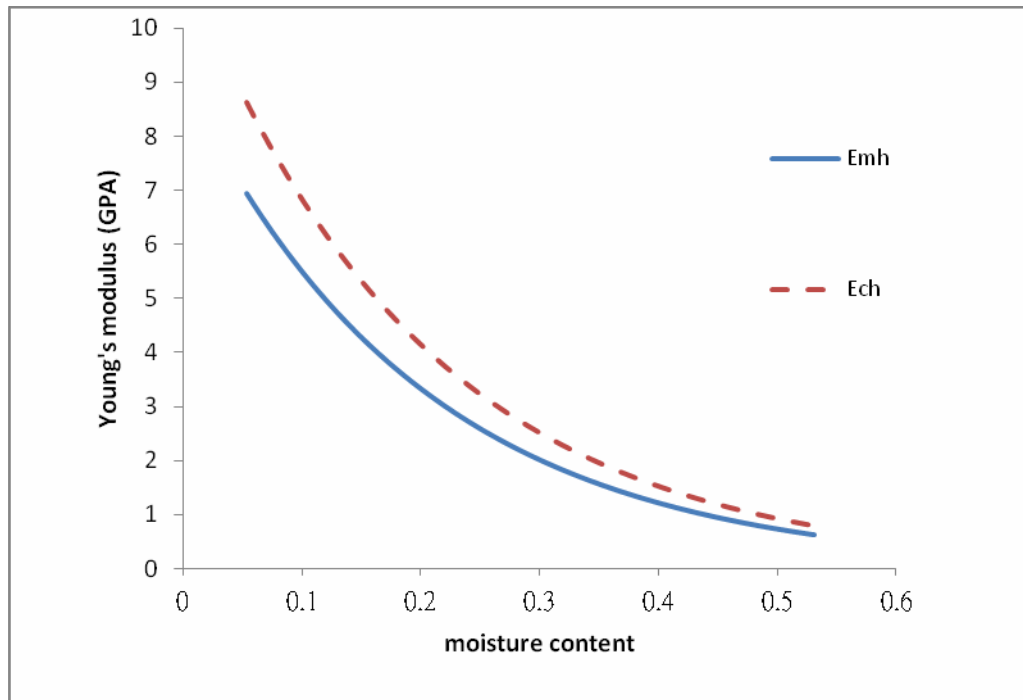
(a)
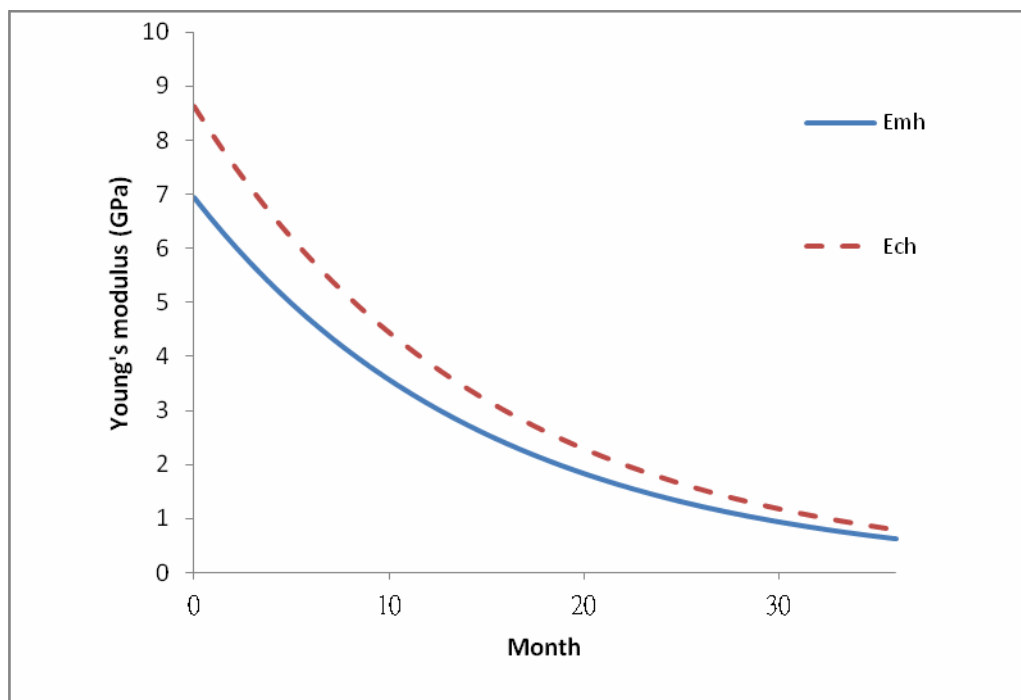
(b)

Figure 7.12. The Young"s modulus of host polymer material and core fibre measured from (a) the change of moisture content of host polymer material and (b) time.
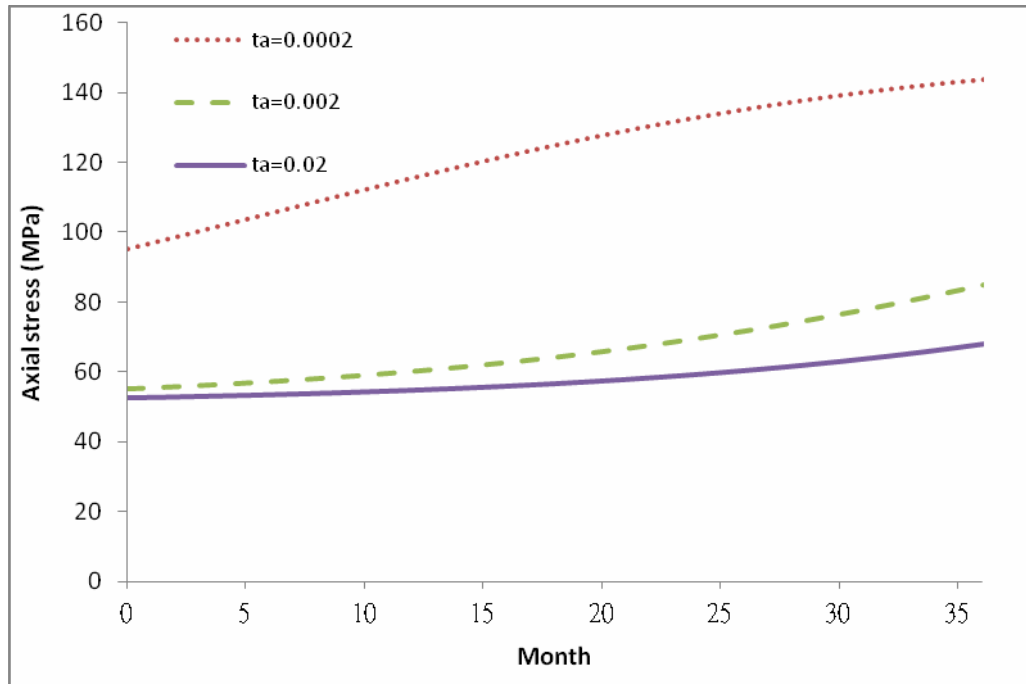
Figure 7.13. The effect of the moisture content of host polymer material and core fibre on the axial stress in the fibre depending on time.

Chapter 8

Concluding Remarks and Suggestions for Future Study

8.1 Conclusion

A comprehensive study on the development of a silkworm silk fibre reinforced PLA composite was conducted through experimental and theoretical analyses. As the use of silkworm silk fibre reinforced PLA composite is aimed at developing a suitable material for bone fixation, its modulus and biodegradation rate are the leading parameters. From the experimental results, the Young"s modulus and flexural modulus of PLA increased with the use of 5 wt% of silkworm silk fibre as reinforcement. However, the poor fibre–matrix interface is the significant factor for the strength decrement.

Hydrophilic sericin layer was found to cause poor interfacial bonding with polymer because this layer hindered the bonding between the fibre and matrix inside the composite, and thus the efficiency of stress transfer from the matrix to the fibre would decrease substantially. It results in affecting the mechanical properties of the composite.

Preprocessing of silk fibre commonly known as "degumming" is an essential

process to obtain an ideal fibre through sericin and impurity removal. Wettability, bonding and degradation at the fibre/matrix interface are the critical issues in composites manufacturing process which raise the significance of the study in the degumming process. Although degumming can improve the interfacial properties between fibre and matrix, the mechanical properties of the fibre are also attracted.

As the major amino acids groups in sericin are hydrophilic, hot water is an environmentally friendly and convenient process for Tussah silk fibre degumming. The mechanical properties including maximum tensile strength, strain and modulus and surface morphology were obtained from the experiments. Three major factors that explain the influence of degumming on the tensile properties of a silkworm silk fibre are (1) sericin removal, (2) molecular changes and (3) bonding breakage.

SEM micrographs show that the amount of impurity and the extent of damage on the surface of silk fibre after degumming are dependent on the degumming time. However, the degumming time has a little effect on the thermal properties and the secondary structure of the silkworm silk fibre.

$NaHCO_3$ solution was used for the investigation on the effect of weak alkali degumming treatment on silkworm silk fibre. The tensile and thermal properties of silkworm silk fibre degummed by different concentrations of $NaHCO_3$ solution were studeied. Experimental results revealed that the disruption of hydrogen bonds (water effect) dominated the effect of the fibre at low $NaHCO_3$ concentration. Increasing the concentration of $NaHCO_3$ resulted in increasing the pH level and thus, distorted the binding force between fibrils of the fibre. DSC analysis revealed that the fibre degummed in the solution over 5% of NaHCO3 required higher energy for melt and thermal decomposition from their crystalline

states. Nevertheless, by using NaHCO3 would minimize the risk of the damage of silkworm silk fibre as compared with commonly used strong alkali solutions for degumming.

The microbond test was processed to prove the improvement on the interfacial shear strength by degumming. Degumming processes through boiling water or NaHCO$_3$ increase the compatibillity and the friction between the silkworm silk fibre and PLA. From the experimental results, high interfacial shear strength of silkworm silk fibre reinforced PLA composite was obtained through degumming.

After immersing samples into PBS solution to simulate their exposure in a liquidised environment, like human body, their mechanical properties were altered with immersion time. The declining rate in term of the mechanical properties of composite samples was faster than that of pristine PLA. It further proves that the hydrophilic effect of the silkworm silk fibre does affect the water absorbability of its related composites. it is found that the use of silkworm silk fibre, as reinforcement can enhance the modulus of PLA as well as alter its bio-degradation rate, in which these properties are the primary parameters for the design of implants for bone fixation.

The dynamic mechanical and thermal properties of PLA, degraded PLA, silkworm silk fibre reinforced PLA composite and its degraded composite samples in relation to their biodegradation effect were studied. At the beginning, it was found that the initial storage modulus of the silkworm silk fibre reinforced PLA composite increased while its glass transition temperature decreased as compared with the PLA sample. Moreover, the coefficient of linear thermal expansions (CLTE) of the silkworm silk fibre reinforced PLA composite was reduced. This phenomenon was attributed to the fibre-matrix interaction that restricted the

mobility of polymer chains adhered to the fibre surface, and consequently reduced the Tg and CLTE. As compared with the degraded silk fibre reinforced PLA composite, it was found that the degraded composite exhibited lower initial storage modulus, loss modulus and tan delta but higher Tg than the silkworm silk fibre reinforced PLA composite. This result was mainly due to the increase of crystalinity of the composite during its degradation process.

A linear, elastic and isotropic theoretical model to evaluate the differential stress between the core fibre and the sericin with difference thickness of sericin is firstly introduced. For early degradation stage, the influence of moisture absorption on shear stress and axial stresdbetween the fibre and sericin is also discussed. Based on the theoretical analysis, we have found that the thickness of sericin layer plays a critical role in the stress transferability of the fibre reinforced polymer system.

8.2   Suggestions for Future Study

Many important aspects are suggested for the further study to enchance the widespread application of novel silkworm silk fibre reinforced PLA bone fixator in the future.

Surface coating on the bone fixator is essential for biocompatibile to the humun body which eliminates the case of foreign body response. Therefore, it is important to develop a suitable surface coating treatment on the silkworm silk fibre reinforced composite and study the effect of the surface coating in relation to its properties.

In depth investigation on the biocompatibility and bioresorable of the proposed

silkworm silk fibre reinforced PLA composite is essential. Besides, in vivo degradation experiment is also suggested. The biodegradation rate is crucial in which it have to be compromised with the cell growth rate of bone inside the human body. For the successful use of silkworm silk fibre reinforced PLA composite in bone implant applications, the mechanical properties of the composite should withstand the loads which human bone suffered daily. Nevertheless, too stiff bone implant plant would cause stress shielding of the bone and consequently, the bone may become osteoporosis. Therefore, it should require further investigation of the bone plate with desirable biodegradation rate while at the same time possess proper mechanical properties for supporting a load that an un-damaged bone should withstand.

According to the age, gender and race, the properties of the bone are different. In order to suit with different bone fracrured patients, a numerical model should be developed to estimate the properties of different silkworm silk fibre reinforced PLA composites based on various parameters including silkworm silk fibre content and orientation.

References

Abrams, LM & Castro, JM 2003, 'Predicting Molding Forces During Sheet Molding Compound(SMC) Compression Molding. I:Model Development', vol 24, no. 3, pp. 291-303.

Altman, GH, Diaz, F, Jakuba, C, Calabro, T & Horan, RL 2003, 'Silk-based biomaterials', *Biomaterials*, vol 24, pp. 401-416.

Ambrose, CG & Clanton, TO 2004, 'Bioabsorbable Implants: Review of Clinical Experience in Orthopedic Surgery', vol 32, no. 1, pp. 171-177.

Amnat, J & Tokiwa, Y 2004, 'Review Biodegradation of poly(L-lactide)', *Biotechnology Letters*, vol 26, pp. 771-777.

Andrzej, KB, Adam, J & Dietrich, S 2009, 'Mechanical properties of PLA composites with man-made cellulose and abaca fibres', *Composites: Part A*, vol 40, pp. 404-412.

Antroine, LD, Davies, P & Baley, C 2010, 'Interfacial bonding of Flax fibre/Poly(L-lactide) bio-composites', *Composites Science and Technology*, vol 70, pp. 231-239.

Arai, T, Freddi, G & Innocenti, R 2004, 'Biodegradation of Bombyx mori Silk Fibroin Fibers and Films Journal of Applied Polymer Science', *Journal of Applied Polymer Science*, vol 91, pp. 2383-2390.

Arbelaiz, A & Fernandez, B 2005, 'Mechanical properties of flax fibre/polypropylene composites. Influence of fibre/matrix modification and glass fibre hybridization', *Composites: Part A*, vol 36, p. 1637–1644.

Athijayamania, A, Thiruchitrambalamb, M, Natarajana, U & Pazhanivel, B 2009, 'Effect of moisture absorption on the mechanical properties of randomly oriented natural fibers/polyester hybrid composite', *Materials Science and Engineering A*, vol 517, pp. 344-353.

Atkins, E 2003, 'Silk's secrets', *Nature*, p. 424.

Autefage, A 2000, 'The point of view of the veterinary surgeon: bone and fracture', *Int. J. Care Injured*, vol 31, pp. 50-55.

Averous, L & Boquillon, N 2004, 'Biocomposites based on plasticized starch: thermal and mechanical behaviours', *Carbohydrate Polymers*, vol 56, pp. 111-122.

Baillie, C 2004, *Green composites: Polymer composites and the environment*, CRC Press.

Baillie, CM & Bader, MG 1994, 'Some aspects of interface adhesion of electrolytically oxidized carbon fibres in an epoxy-resin matrix', *J. Mater. Sci.*, vol 29, p. 3822.

Barone, JR & Schmidt, WF 2005, 'Polyethylene reinforced with keratin fibres obtained from chicken feathers', *Composites Science and Technology*, vol 65, pp. 173-181.

Beaumont, PW, Riewald, PG & Zweben, C 1974, 'Foreign Object Impact Damage to Composites', ASTM STP 568.

Bini, E, Knight, DP & Kaplan, DL 2004, 'Mapping Domain Structures in Silks from Insects and Spiders Related to Protein Assembly', *J. Mol. Biol.*, vol 335, pp. 27-40.

Birgitha, N 2007, 'Natural Fiber Composites Optimization of Microstructure and Processing Parameters.', Thesis.

Black, J 2006, *Biological Performance of Materials: Fundamentals of Biocompatibility*, CRC Press.

Bledzki, AK, Sperber, VE & Faruk, O 2002, 'Natural and Wood Fibre Reinforcement in Polymers', Rapra Review Reports.

Bondi, A 1964, 'van der Waals volume and radii', *Journal of Physical Chemistry*, vol 68, pp. 441-451.

Bonino, MJ 2003, 'Material Properties of Spider Silk', Thesis, University of Rochester Rochester, NY.

Bowes, JH & Kenten, RH 1950, 'The swelling of collagen in alkaline solutions', *Biochem J*, vol 46, no. 5, p. 524–529.

Bronzino, JD 1999, *Biomedical Engineering Handbook: Biomedical Engineering Fundamentals*, CRC Press.

Burns, AE & Varin, J 1998, 'Poly-L-lactic acid rod fixation results in foot surgery', *J Foot Ankle Surg*, vol 37, no. 1, pp. 37-41.

Cai, H, Dave, V, Cross, RA & McCarthy, SP 1996, 'Effects of Physical Aging, Crystallinity, and Orientation on the Enzymatic Degradation of Poly (Lactic acid)', *Cai H, Dave V, Cross RA and McCarthy SP. Effects of Physical Aging, CJournal of Polymer Science: Part B: Polymer Physics*, vol 34, pp. 2701-2708.

Chaivan, P, Pasaja, N & Boonyawan, D 2005, 'Low-temperature plasma treatment for hydrophobicity improvement of silk', *Surface & Coatings Technology*, vol 193, pp. 356-360.

Chen, H, Miao, M & Ding, X 2009, 'Influence of moisture absorption on the interfacial strength of bamboo/vinyl ester composites', *Composites: Part A*, vol 40, pp. 2013-2019.

Christensen, S & Hutchinson, B 1997, 'Fibre-matrix separation in ribbed SMC and BMC parts', *Annual Technical Conference ANTEC, Conference Processings 1997*.

Claes, L 1989, 'The Mechanical and Morphological Properties of Bone Beneath Internal Fixation Plates of Differing Rigidity', *Journal of Orthopaedic Research*, p. 717 & 177.

Comte, E & Merhi, D 2006, 'Void Formation and Transport during SMC Manufacturing: Effect of the Glass Fiber Sizing.', *Polymer composites*, vol 27, no. 3, pp. 289-298.

Cook, M 2006, *Silk is the Bomb[yx]*, < HYPERLINK "http://knitty.com/ISSUEspring06/FEATbombyx.html" http://knitty.com/ISSUEspring06/FEATbombyx.html >.

Craven, JP, Cripps, R & Viney, C 2000, 'Evaluating the silk/epoxy interface by means of the microbond test', *Composites: Part A*, vol 31, pp. 653-60.

DiGregorio, BE 2009, 'Biobased Performance Bioplastic: Mirel', *Chemistry & Biology*, vol 16, no. 1, pp. 1-2.

Dodson, B 2006, *The Weibull Analysis Handbook*, 2nd edn, Milwaukee, Wisconsin.

Dumont, P, Orge'as, L & Corre, SL 2003, 'Anisotropic viscous behavior of sheer molding compounds (SMC) during compression molding', *International Journal of Plasticity*, vol 19, pp. 625-646.

Dunaway, DL, Thiel, BL, Srinivasan, SG & Viney, C 1995, 'Characterizing the Crosssectional Geometry of Thin, Non-cylindrical, Twisted Fibers (Spider Silk)', *Journal of Materials Science*, vol 30, pp. 4161-4170.

Espert, A, Vilaplana, F & Karlsson, S 2004, 'Comparison of water absorption in natural cellulosic fibres from wood and one-year crops in polypropylene composites and its influence on their mechanical properties', *Composites: Part A*, vol 35, pp. 1267-1276.

Facca, AG 2007, 'Predicting the tensile strength of natural fibre reinforced thermoplastics', *Composites Science and Technology*, vol 67, pp. 2454-66.

Fakirov, S & Bhattacharya, D 2007, *Handbook of engineering biopolymers: homopolymers, blends and composites. Cincinnati (OH): Hanser*, Munich : Hanser ; Cincinnati, Ohio : Hanser Gardner.

Fang, K, Wang, S, Wang, C & Tian, A 2008, 'Inkjet Printing Effects of Pigment Inks on Silk Fabrics Surface-Modified with O2 Plasma', *Journal of Applied Polymer Science*, vol 107, pp. 2949-2955.

Faughnan, P & Bryan, C 1998, 'Correctlation between the dynamic mechanical properties and the fatigue behavior of filled and unfilled PRFE materials', *Journal of materials science letters*, vol 17, pp. 1743-1746.

Ferland, P & Trochu, F 1996, 'Concurrent Methods for Permeability Measurement in Resin Transfer Molding.', *Polymer Composites*, vol 17, no. 1, pp. 149-158.

Feughelman, M 1997, 'Mechanical properties and structure of alpha-keratin fibres: wool, human hair and related fibres', Univerity of New South Wales press.

Flahiff, CM, Blackwell, AS & Hollis, JM 1996, 'Analysis of a biodegradable composite for bone healing', *Journal of Biomedical Materials Research*, vol 32, pp. 419-424.

Folkesa, MJ & Russell, DAM 1980, 'Orientation effects during the flow of short-fibre reinforced thermoplastics.', *Polymer*, vol 21, no. 11, pp. 1252-1258.

Freddi, G, Allara, G & Candiani, G 1996, 'Degumming of silk fabrics with tartaric acid', *J. Soc. Dyers Colour*, vol 112, pp. 191-195.

Freddi, G, Monti, P, Nagura, M, Gotoh, Y & Tsukada, M 1997, 'Structure and Molecular Conformation of Tussah Silk Fibroin Films: Effect of Heat Treatment', *Journal of Polymer Science Part B: Polymer Physics*, vol 35, no. 5, pp. 841-847.

Freddi, G, Mossotti, R & Innocenti, R 2003, 'Degumming of silk fabric with several proteases', *Journal of Biotechnology*, vol 106, pp. 101-112.

Fua, SY, Maia, YW, Bernd, L & Yue, CY 2002, 'Synergistic effect in the fracture toughness of hybrid short glass fiber and short carbon fiber reinforced polypropylene composite', *Material science and engineering*, vol 323, no. A, pp. 326-335.

Fu, SY & Bernd, L 2009, *Science and engineering of short fibre reinforced polymer*

composites, CRC Press LLC.

Fu, CJ, Porter, D, Chen, X, Vollrath, F & Shao, Z 2011, 'Understanding the Mechanical Properties of Antheraea Pernyi Silk - From Primary Structure to Condensed Structure of the Protein', *Adv. Funct. Mater*, vol 21, pp. 729-737.

Furuzono, T, Kishida, A & Tanaka, J 2004, 'Nano-scaled hydroxyapatite/polymer composite I. Coating of sintered hydroxyapatite particles on poly(gammer-methacryloxypropyl trimethoxysilane) - grafted silk fibroin fibers through chemical bonding', *Journal of Materials Scien*, vol 15, no. 1, pp. 19-23.

Garlotta, D 2001, 'A Literature Review of Poly(Lactic Acid)', *Journal of Polymers and the Environment*, vol 9, no. 2.

Garside, P & Wyeth, G 2007, 'Crystallinity and degradation of silk: correlations between analytical signatures and physical condition on ageing', *Appl. Phys*, vol A, no. 89, pp. 871-876.

Gibson, RF 1994, *Principles of composite material mechanics*, CRC Press.

Gijpferich, A 1996, 'Mechanisms of polymer degradation and erosion', *Biomoterials*, vol 17, pp. 103-14.

Gonzaleza, AV, Cervantes-Uca, JM & Olayob, R 1999, 'Effect of fiber surface treatment on the fiber-matrix bond strength of natural fiber reinforced composites', *Composites: Part B*, vol 30, pp. 309-20.

Gonzalez, MF, Ruseckaite, RA & Cuadrado, TR 1999, 'Structural Changes of Polylactic-Acid (PLA) Microspheres under Hydrolytic Degradation', *Journal of Applied Polymer Science*, vol 71, pp. 1223-1230.

Gosline, JM, Guerette, PA, Ortlepp, CS & Savage, KN 1999, 'The mechanical design of spider silks: from fibron sequence to mechanical function', *The Journal of Experimental Biology*, vol 202, pp. 3295-3303.

Gotoh, Y, Tsukada, M & Minoura, N 1993, 'Chemical Modification of Silk Fibroin with Cyanuric Chloride-Activated Poly(ethylene glycol): Analyses of Reaction Site by 'H-NMR Spectroscopy and Conformation of the Conjugates', *Bioconlugete Chem*, vol 4, pp. 554-559.

Gulrajani, ML & Chatterjee, A 1992, 'Degumming of silk with oxalic acid', *Indian J. Fiber Text. Res.*, vol 17, pp. 39-44.

Gulrajani, ML, Sethi, S & Guptha, S 1992, 'Some studies in degumming of silk with

organic acids', *J. Soc. Dyers Colour*, vol 108, no. 2, pp. 79-86.

Hagstrand, PO & Bonjour, F 2005, 'The influence of void content on the structural flexural performance of unidirectional glass fibre reinforced polypropylene composites', *Composites Part A*, vol 36, pp. 705-714.

Hayashi, CY, Shipley, NH & Lewis, RV 1999, 'Hypotheses that correlate the sequence, structure, and mechanical properties of spider silk proteins', *International Journal of Biological Macromolecules*, vol 24, no. 2-3, pp. 24: 271-275.

Higa, M, Taniokaa, A & Kira, A 1998, 'A novel measurement method of Donnan potential at an interface between a charged membrane and mixed salt solution', *Journal of Membrane Science*, vol 140, pp. 213-220.

Hitchcock, DI 1954, 'Memberane potentials in the donnan equilibrium II', *The Journal of General Physiology*, pp. 717-727.

Hoppenfeld, S & Murthy, VL 2000, *Murthy. Treatment & Rehabilitation of Fractures*, Lippincott willians & wilkins.

Huang, G 2009, 'Dynamic mechanical analysis of the seawater treated glass/polyester composites', *Materials and Design*, vol 30, pp. 2774-2777.

Huda, MS, Drzal, LT & Misra, M 2006, 'Wood-Fiber-Reinforced Poly(lactic acid) Composites: Evaluation of the Physicomechanical and Morphological Properties.', *Journal of Applied Polymer Science*, vol 102, pp. 4856-4869.

Huda, MS, Drzal, LT, Misra, M & Mohanty, AK 2005, 'A Study on Biocomposites from Recycled Newspaper Fibre and Poly(lactic acid)', *Ind. Eng. Chem. Res*, vol 44, pp. 5593-5601.

Huda, MS, Drzal, LT, Mohanty, AK & Misra, M 2006, 'Chopped glass and recycled newspaper as reinforcement fibers in injection molded poly(lactic acid) (PLA) composites: a comparative study', *Composites Science and Technology*, vol 66, pp. 1813-1824.

Huda, MS, Mohanty, AK, Drzal, LT, Schut, E & Misra, M 2005, 'Green composites from recycled cellulose and poly(lactide acid): Physico-mechanical and morphological properties evaluation', *Journal of materials science*, vol 40, pp. 4221-4229.

Idicula, M, Malhotra, SK, Joseph, K & Thomas, S 2005, 'Dynamic mechanical analysis of randomly oriented intimately mixed short banana/sisal hydrid fibre

reinforced polyester composites', *Composites Science and Technology*, vol 65, pp. 1077-1087.

Ikada, Y & Tsuji, H 2000, 'Biodegradable polyesters for medical and ecological applications', *Macromolecular Rapid Communications*, vol 21, pp. 117-132.

Ikegawa, N 1996, 'Effect of Compression Process on Void Behavior in Structural Resin Transfer Molding', *Polymer engineering and science*, vol 36, no. 7, pp. 953-962.

Jacob, M, Francis, B, Thomas, S & Varughese, KT 2006, 'Dynamical Mechanical Analysis of Sisal/Oil Palm Hybrid Fiber-Reinforced Natural Rubber Composites', *Polymer composites*, pp. 671-680.

Jendlia, Z & Meraghni, F 2004, 'Micromechanical analysis of strain rate effect on damage evolution in sheet molding compound composites', *Composites: Part A*, vol 35, pp. 779-785.

Jiang, S 2011, 'Comparison of silk structure and fabric testing performance ordinary and puffed tussah silk', *Advanced Materials Research*, vol 211-212, pp. 904-908.

Jiang, P, Liu, H, Wang, C, Wu, L, Huang, J & Guo, C 2006, 'Tensile behavior and morphology of differently degummed silkworm (Bombyx mori) cocoon silk fibres', *Materials Letters 2006; 60: 919– 925*, vol 60, pp. 919-925.

John, GH & Thomas, RS 2009, 'Silk-inspired polymers and proteins', *Biochemical SocietyTransactions*, vol 37, pp. 677-681.

Kaeagiannidis, GP, Stergious, AC & Karayannidis, GP 2008, 'Study of crystallinity and thermomechanical analysis of annealed poly(ethylene terephthalate) films', *European polymer journal*, vol 44, pp. 1475-1486.

Kang, MK, Jung, JJ & Lee, WL 2000, 'Analysis of resin transfer moulding process with controlled multiple gates resin injection', *Composites: Part A*, vol 31, pp. 407-422.

Kang, MK, Lee, WL & Hahn, HT 2000, 'Formation of microvoids during resin-transfer molding process.', *Composites Science and Technology*, vol 60, pp. 2427-2434.

Kazayawoko, M 1999, 'Surface modification and adhesion mechanisms in woodfiber-polypropylene composites', *J Mater Sci*, vol 34, pp. 6189-99.

Kearns, V, MacIntosh, AC & Crawford, A 2008, 'Silk-based Biomaterials for Tissue Engineering.', *Topics in Tissue Engineering*, vol 4.

Keener, TJ & Stuart, RK 2004, 'Maleated coupling agents for natural fibre composites', *Composites: Part A*, vol 35, pp. 357-362.

Khan, MA & Ganster, J 2009, 'Hybrid composites of jute and man-made cellulose fibers with polypropylene by injection moulding', *Composites: Part A*, vol 40, pp. 846-848.

Khan, MR, Tsukada, M, Gotoh, Y, Morikawa, H & Freddi, G 2010, 'Physical properties and dyeability of silk fibres degummed with citric acid', *Bioresource technology 2010: 101(21); 8439-8445.*, vol 101, no. 21, pp. 8439-8445.

Ki, CS, Kim, JW, Oh, HJ, Lee, KH & Park, YH 2007, 'The effect of residual silk sericin on the structure and mechanical property of regenerated silk filament', *International Journal of Biological Macromolecules*, vol 41, no. 3, pp. 346-353.

Kim, DK, Choi, HY & Kim, N 1995, 'Experimental investigation and numerical simulation of SMC in compression molding', *Journal of Materials Processing Technology*, vol 49, pp. 333-344.

Kim, SK & Daniel, IM 2003, 'Determination of three-dimensional permeability of fiber performs by the inverse parameter estimation technique', *Composites: Part A*, vol 34, pp. 421-429.

Kim, KT & Jeong, JH 1997, 'Effect of molding parameters on compression molded sheer molding compounds parts', *Journal of Materials Processing Technology*, vol 67, no. 1, pp. 105-111.

Kim, SK, Lee, SW & Youn, JR 2002, 'Measurement of residual stresses in injection molded short fiber composites considering anisotropy and modulus variation.', *Korea-Australia Rheology Journal*, vol 14, no. 3, pp. 107-114.

Kim, UJ, Park, JY, Li, CM, Jin, HJ, Valluzzi, R & Kaplan, DL 2004, 'Structure and properties of silk hydrogels, Biomacro-molecules 5', *Biomacromolecules*, vol 5, pp. 786-792.

Kock, JW 2006, 'Physical and Mechanical properties of chicken feather materials', Thesis, Georgia Institute of Technology.

Kolybaba, M, Tabil, LG, Panigrahi, S, Crerar, WJ, Powell, T & Wang, B 2003, 'Biodegradable polymers: past, present, and future.', An ASAE Meeting Presentation.

Kurosaki, S, Otsuka, H, Kunitomo, M, Koyama, M, Pawankar, R & Matumoto, K 1999, 'Fibroin allergy: IgE mediated hypersensitivity to silk suture materials', *J Nippon Med Sch*, vol 66, no. 1, pp. 41-44.

Kweon, HY & Park, YH 2001, 'Dissolution and Characterization of Regenerated Antheraea pernyi Silk Fibroin', *Journal of Applied Polymer Science 2001; 82: 750–758.*, vol 82, pp. 750-758.

Kweon, HY, Um, IC & Park, YH 2000, 'Thermal behavior of regenerated Antheraea pernyi silk fibroin film treated with aqueous methanol', *Polymer*, vol 41, pp. 7361-7367.

Lassila, LVJ 2002, 'The influence of short-term water storage on the flexural properties of unidirectional glass fiber-reinforced', *Composites Biomaterials*, vol 23, pp. 2221-9.

Lee, YW 1999, *Silk reeling and testing manual*, Food and Agriculture Organization of the United Nations Rome.

Lee, SM, Cho, D, Park, WH & Lee, SG 2005, 'Novel silk/poly(butylene succinate) biocomposites: the effect of short fibre content on their mechanical and thermal properties', *Composites Science and Technology*, vol 65, pp. 647-657.

Lee, KS, Lee, SW, Youn, JR, Kang, TJ & Chung, K 2001, 'Confocal Microscopy Measurement of the Fiber Orientation in Short Fiber Reinforced Plastics.', *Fibers and Polymers*, vol 2, no. 1, pp. 41-50.

Lewin, M 2006, *Handbook of Fibre Chemistry (3rd Edition)*, CRC, Boca Raton, FL, USA.

Li, S & Jinjin, D 2007, 'Improvement of hydrophobic properties of silk and cotton by hexafluoropropene plasma treatment', *Applied Surface Science* , vol 253, pp. 5051-5055.

Lim, LT, Auras, R & Rubino, M 2008, 'Processing technologies for poly(lactic acid)', *Progress in Polymer Science*, vol 33, pp. 820-852.

Lin, TL & Jang, BZ 1990, 'Fracture Behavior of Hybrid Composites Containing Both Short and Continuous Fibers', *Polymer composites*, vol 17, no. 5, pp. 291-300.

Li, M, Tao, W, Kuga, S & Nishiyama, Y 2003, 'Controlling Molecular Conformation of Regenerated Wild Silk Fibroin by Aqueous Ethanol Treatment', *Polymers for Advanced Technologies*, vol 14, no. 10, pp. 694-698.

Mahmoodi, NM, Arami, M & Mazaheri, F 2010, 'Degradation of sericin (degumming) of Persian silk by ultrasound and enzymes as a cleaner and environmentally friendly process', *Journal of Cleaner Production*, vol 18, pp. 146-151.

Mallick, PK 2008, *Fiber-reinforced composites materials, manufacturing, and design*, 3rd edn, CRC Press.

Manders, PW & Bader, MG 1981, 'The strength of hybrid glass/carbon fibre composites Part 1 failure strain enhancement and failure mode', *Journal of materials science*, vol 16, pp. 2233-2245.

Manfredi, LB 2008, 'Influence of the addition of montmorillonite to the matrix of unidirectional glass fibre/epoxy composites on their mechanical and water absorption properties', *Composites: Part A*, vol 39, pp. 1726-31.

Mathur, AB & Gupta, V 2010, 'Silk fibroin-derived nanoparticles for biomedical applications, Nanomedicine 5(5)', *Nanomedicine*, vol 5, no. 5, pp. 807-820.

Matuana, LM, Balatinecz, JJ, Sodhi, RNS & Park, CB 2001, 'Surface characterization of esterified cellulosic fibers by XPS and FTIR Spectroscopy', *Wood Sci Technol*, vol 35, no. 3, pp. 191-201.

Meinel, L & Hofmann, S 2005, 'The inflammatory responses to silk films in vitro and in vivo', *Biomaterials.*, vol 26, pp. 147-155.

Michal, Z & Frantisek, S 2001, 'Unique molecular architecture of silk fibroin in the waxmoth, Galleria mellonella', *Journal of Biological Chemistry*, vol 277, no. 25, pp. 22639-22647.

Miller, B, Muri, P & Rebenfeld, L 1987, 'A microbond method for determination of the shear strength of a fibrelresin interface', *Composites science technology*, vol 28, no. 1, pp. 17-32.

Mohanty, AM & Drazal, LT 2002, 'Novel hybrid coupling agent as an adhesion promoter in natural fiber reinforced powder polypropylene composites', *J Mater Sci Lett*, vol 21, pp. 1885-8.

Mohanty, AK, Misra, M & Drzal, LT 2005, *Natural fibres, biopolymers, and biocomposites*, CRC Press taylor & Francis Group.

Mohanty, AK, Misra, M & Hinrichsen, G 2001, 'Biofibres, biodegradable polymers and biocomposites: An overview', *Macromol. Mater. Eng.*, vol 276/277, pp. 1-24.

Mondal, M & Trivedy, K 2007, 'The silk proteins, sericin and fibroin in silkworm Bombyx mori Linn - A review.', *Caspian J. Env. Sci.*, vol 5, no. 2, pp. 63-76.

Motta, A, Fambri, L & Migliaresi, C 2002, 'Regenerated Silk Fibroin Films: Thermal and Dynamic Mechanical Analysis', *Macromolecular Chemistry and Physics*, vol 203, no. 10-11, pp. 1022-1352.

NASA-Electronic 2005, *Analysis of Plastic Parts Package Delamination*, viewed 2005, < HYPERLINK nepp.nasa.gov/files/../05_016a%20Agarwal%20CSAM_FINAL_REPORT.doc >.

NatureWorks 2005, 'NatureWorksTM PLA 3051D technical data sheets'.

Osnat, H & David, PK 2007, 'Spider and mulberry silkworm silks as compatible biomaterials', *Composites: Part B*, vol 38, pp. 324-337.

Panilaitis, B & Altman, GH 2003, 'Macrophage responses to silk', *Biomaterials*, vol 35, pp. 3079-3085.

Park, BY & Kim, SC 1997;, 'Interlaminar fracture toughness of carbon fiber/ epoxy composites using short Kevlar fiber and/ or Nylon-6 powder reinforcement', *Polymer for advanced technologies*, vol 8, pp. 371-377.

Perez-Rigueiro, J, Elices, M, Llorca, J & Viney, C 2001, 'Effect of Degumming on the Tensile Properties of Silkworm (Bombyq mori) Silk Fibre', *Journal of Applied Polymer Science*, vol 84, pp. 1431-7.

Perez-Rigueiro, J, Viney, C & Elices, M 2000, 'Mechanical properties of silkworm silk in liquid media', *Polymer*, vol 41, pp. 8433-8439.

Pickering, KL 2008, *Properties and Performance of Natural-Fibre Composites*, Woodhead publishing limted.

Pierce, MC, Bertocci, GE, Vogeley, E & Moreland, MS 2004, 'Invited Review: Evaluating long bone fractures in children: a biomechanical approach with illustrative cases', *Child Abuse & Neglect*, vol 28, pp. 505-524.

Plaza, GR, Corsini, P, Rigueiro, JP, Marsano, E, Guinea, GV & Elices, M 2008, 'Effect of water on Bombyx mori regenerated silk fibers and its application in modifying their mechanical properties', *Journal of Applied Polymer Science*, vol 109, pp. 1793-1801.

Qi, F & Milford, AH 1999, 'Rheological properties of amorphous and semicrystalline polylactic acid polymers', *Industrial crops and products*, vol 10, no.

1, pp. 47-53.

Rakotomomalala, M, Wagner, S & Doring, M 2010, 'Review: Recent development in Halogen free flame retardants for expoxy resins for electrical and electrionic applications', *materials*, vol 3, pp. 4300-4327.

Ramakrishna, S, Mayer, J & Wintermantel, E 2001, 'Biomedical applications of polumer - composite materials: a review.', *Copmposites science and technology*, vol 61, pp. 1189-1224.

Ravisankar, CK 2011, 'A comparative study of Mulberry and Tasar silk', Synopsis of PH.D thesis, Visvesvaraya Technological University Belgaum.

Richard, EM 1955, 'The structure of Tussah silk fibroin, Acta Crystallogr 8', *Acta Cryst*, vol 8, p. 710.

Richardson, MOW & Zhang, ZY 2000, 'Experimental investigation and flow visualisation of the resin transfer mould filling process for non-woven hemp reinforced phenolic composites', *Composites: Part A*, vol 31, pp. 1303-1310.

Rigueiro, JP, Elices, M, Llorca, J & Viney, C 2001, 'Tensile Properties of Argiope Obtained by Forced Silking', *Journal of Applied Polymer Science*, vol 82, pp. 1928-1935.

Rigueiro, JP, Viney, C, Llorca, J & Elices, M 1998, 'Silkworm Silk as an Engineering material', *Journal of Applied Polymer Science*, vol 70, pp. 2439-2447.

Rigueiro, JP, Viney, C, Llorca, J & Elices, M 2000, 'Mechanical Properties of Single-brin Silkworm Silk', *Journal of Applied Polymer Science*, vol 75, pp. 1270-1277.

Robson, RM 1999, 'Microvoids in Bombyx mori silk. an electron microscope study', *International Journal of Biological Macromolecules*, vol 24, pp. 145-150.

Robson, RM, Lewin, M & Pearce, EM 1998, *Handbook of Fiber Chemistry*, 2nd edn, Marcel Dekker Inc, New York.

Rodriguez, E, Giacomelli, F & Varzquez, A 2004, 'Permeability - Porosity Relationship in RTM for Different Fiberglass and Natural Reinforcements.', *Journal of Composite mateials*, vol 38, no. 3, pp. 259-268.

Rokkanen, PU, Bostman, O & Hirvensalo, E 2000, 'Bioabsorbable fixation in orthopaedic surgery and traumatology', *Biomaterials*, vol 21, pp. 2607-2613.

Ruihua, HU & Lim, J-K 2007, 'Fabrication and Mechanical Properties of Completely Biodegradable Hemp Fiber Reinforced Polylactic Acid Composites',

Journal of composite materials, vol 41, no. 13, pp. 1655-1669.

Saha, N & Banerjee, AN 1996, 'Tensile behavior of unidirectional polyethylene-glass fibers/ PMMA hybrid composite laminates', *Polymer communications*, vol 37, no. 4, pp. 699-701.

Saheb, DN & Jog, JP 1999, 'Natural Fiber Polymer Composites: A Review', *Adv Polym Technol*, vol 18, no. 4, pp. 351-363.

Sahoo, S, Toh, SL & Goh, CH 2010, 'PLGA nanofiber-coated silk microfibrous scaffold for connective tissue engineering', *Journal of Biomedical Materials Research Part B: Applied Biomaterials*, vol 95B, no. 1, pp. 19-28.

Saravanan, D 2006, 'Spider silk-structure, properties and spinning', *JTATM*, vol 5, no. 1, pp. 1-20.

Sasithorn, N & Luepong, K 2010, 'Silk Degumming with Dried Latex of Carica Papaya Linn', *Rajamangala University of Technology Phra Nakhon. The First RMUTP International Conferenc*.

Schneider, A, Wang, Y, Kaplan, DL, Garlick, JA & Egles, C 2009, 'Biofunctionalized electrosupun silk mats as a topical bioactive dressing for accelerated wound healing', *Acta Biomaterialia*, vol 5, pp. 2570-2578.

Serizawa, S, Inoue, K & Iji, M 2006, 'Kenaf-Fiber-Reinforced Poly(lactic acid) Used for Electronic Products.', *Journal of Applied Polymer Science*, vol 100, pp. 618-624.

Shao, ZZ & Vollrath, F 2002, 'Suprising strength of silkworm silk', *NATURE*, p. 418.

Simpson, WS & Crawshaw, GH 2002, *Wool: Science and Technology*, Woodhead Publishing.

Singh, S & Partridge, IK 1995, 'Mixed–mode fracture in an interleaved carbon-fiber/epoxy composites', *Composites Science and Technology*, vol 55, pp. 319-327.

Sonthisombat, A & Speakman, TP 2004, 'Silk: Queen of fibres - The concise Story', Department of textile engineering, Faculty of engineering, RIT, Thailand.

Sreekumar, PA, Joseph, K & Unnikrishnan, G 2007, 'A comparative study on mechanical properties of sisal-leaf fibre-reinforced polyster composites prepared by resin transfer and compression moulding techniques.', *Composites Science and Technology*, vol 67, pp. 453-461.

Subhash, CK & Michael, JK 1996, 'Thick-section AS4-graohine/e-glass/pps hybrid composites: part 1. Tensile behaviour.', *Composites Science and Technology*, vol

56, pp. 181-192.

Tams, J & Rozema, FR 1996, 'Poly (L-lactide) bone plates and screws for internal fixation of mandibular swing osteotomies', *Int J Oral Maxillofac Surg*, vol 25, pp. 20-4.

Tanaka, T 2002, 'Thermal properties of bombyx mori and several wild silkworm', *Journal of Thermal Analysis and Calorimetry*, vol 70, pp. 825-832.

Tao, W, Li, M & Zhao, C 2007, 'Structure and properties of regenerated Antheraea pernyi silk fibroin in aqueous solution', *Int J Biol Macromol*, vol 40, no. 5, pp. 472-478.

Tencer, AF & Johnson, KD 1994, *Biomechanics in orthopedic trauma: bone fracture and fixation*, Martin dunitz.

Teoh, SH 2004, *Engineering materials for biomedical application*, World scientific Publishing Co. Pte. Ltd.

Thakur, AJ 1997, *The elements of fracture fixation*, Elsevier India.

Tokiwa, Y & Calabia, BP 2006, 'Biodegradability and biodegradation of poly(lactide)', *Appl Microbiol Biotechnol*, vol 72, p. 244–251.

Tsukada, M, Freddi, G & Massafra, MR 1998, 'Structure and Properties of Tussah Silk Fibers Graft-Copolymerized and 2-Hydroxyethyl Methacrylate', *Journal of Applied Polymer Science*, vol 67, no. 8, pp. 1393-1403.

Tsukada, M, Gotoh, Y & Yasui, H 1995, 'Comparison of chemical and physical properties of the byssus of Mytilis edulis with those of silk fibroin fibers', *J. Seric. Sci. Jpn*, vol 64, no. 5, pp. 435-445.

United Aircraft Corporation. Pratt & Whitney Aircraft Division, SEG 1975 , *Introduction to Weibull Analysis*, Pratt & Whitney Aircraft, East Hartford, Connecticut.

Usui, M & Matuhasi, T 1979, 'IgE-selective and antigenspecific unresponsiveness in mice I. Induction of the unresponsiveness by administration of ovalbumin-pullulan conjugate', *J. Immunol*, vol 122, pp. 1266-1272.

Vroman, I & Tighzert, L 2009, 'Review biodegradable polymers', *Materials*, vol 2, pp. 307-344.

Walker, L, Sohn, MS & Hu, XZ 2002, 'Improving impact resistance of carbon-fibre composites through interlaminar reinforcement', *Composites: Part A*, vol 33, pp.

893-902.

Wang, YZ 2006, 'Stem cell-based tissue engineering with silk biomaterials', *Biomaterials*, vol 27, pp. 6064-6082.

Wang, YZ 2008, 'In vivo degradation of the three-dimensional silk fibroin scaffolds', *Bio-materials*, vol 29, pp. 3415-3428.

Wanjun, L, Manjusri, M, Per, A, Lawrence, TD & Amar, KM 2005, 'Green composites from soy based plastic and pineapple leaf fiber: fabrication and properties evaluation', *Polymer*, vol 46, pp. 2710-2721.

Warrior, NA, Turner, TA, Robitaille, F & Rudd, CD 2003, 'Effect of resin proerties and processing parameters on crash energy absorbing composite structures made by RTM', *Composites: Part A*, vol 34, pp. 543-550.

White, JR 1985, 'On the layer removal analysis of residual stress Part 1 Polymer mouldings with depth-varying Young's modulus.', *Journal of materials science*, vol 20, no. 7, pp. 2377-2387.

Wielage, B, Lampke, T, Utschick, H & Soergel, F 2003, 'Processing of natural-fibre reinforced polymers and the resulting dynamic-mechanical properties', *journal of Materials Processing Technology*, vol 139, pp. 140-146.

Willians, GI & Wool, RP 2000, 'Composites from Natural Fibers and Soy Oil Resins', *Applied Composite Materials*, vol 7, pp. 421-432.

Xie, Y, Hill, C, Xiao, Z, Militz, H & Mai, C 2010, 'Silane coupling agents used for natural fiber/polymer composites: a review', *Composites Part A*, vol 41, pp. 806-819.

Yamadaa, H, Nakaob, H, Takasua, Y & Tsubouch, K 2001, 'Preparation of undegraded native molecular fibroin solution from silkworm cocoons', *Materials Science and Engineering*, vol 14, no. 1-2, pp. 41-46.

Yang, C & Bochu, W 2009, 'Biodegradation of silk biomaterials', *Int. J. Mol. Sci.*, vol 10, pp. 1514-1524.

Yang, Y & Li, S 1993, 'Silk fabric non-formaldehyde crease-resistant finishing using citric acid', *J. Text. Inst*, vol 84, no. 4, pp. 638-644.

Yang, HS, Wolcott, MP, Kim, HS & Kim, HJ 2005, 'Thermal Properties of Lignocellulosic Filler-Thermoplastic Polymer Bio-Composites', *J. Therm. Anal. Calorim*, vol 82, pp. 157-160.

Youjiang, W & Dongming, Z 1995, 'Characterization of interlaiminar fracture behaviour of woven fabric reinforced polymeric composites', *composites*, vol 26, pp. 115-124.

Yu, S & Michael, AJ 1998, 'Microstructural characterization of Bombyx mori silk fibers', *Macromolecules*, vol 31, pp. 8857-8864.

Zahn, H, Hles, JF & Nlenhaus, M 1980, 'Wool as a Biological Composite Structure', *Industrial & Engineering Chemistry Research*, vol 19, pp. 496-501.

Zhang, XM, Berghe, IV & Paul, W 2011, 'Heat and moisture promoted deterioration of raw silk estimated by amino acid analysis', *Journal of Cultural Heritage*, vol 12, no. 4, pp. 408-411.

Zhang, YP, Yang, HX, Shao, H & Hu, XC 2010, 'Antheraea pernyi silk fibre: a potential resource for artificially biospinning spider Dragline silk', *Journal of Biomedicine and Biotechnology*.

Zhihang, F & Santare, MH 2008, 'Interlaminar shear strength of glass fiber reinforced epoxy composites enhanced with multi-walled carbon nanotubes,', *Composites: part A*, vol 39, pp. 540-554.

Zulkifli, R, Azhari, CH, Ghazali, MJ & Ismail, AR 2009, 'Interlaminar Fracture Toughness of Multi-Layer Woven Silk/Epoxy Composites Treated with Coupling Agent', *European Journal of Scientific Research*, vol 27, no. 3, pp. 454-462.

Appendix I

(Mechanical modeling of the stiffness of the fibre)

The following models are applied to silkworm silk fibre reinforcement:

1. Rule of mixtures (ROM) [53];

2. Shear-lag analysis[51];

3. Two-dimension random orientation developed by Tsai and Pagano [52] and

4. Halpin–Tsai equation [53]

Mechanical modeling of the stiffness of the fibre, using a micromechanical composite model requires more than 12% crystallinity [54]. 50– 63% crystallinity in wild-type silkworm cocoons which is discussed in P.22 in this report [42]. Researchers used 50% volume fraction of crystals, and still needed a surface layer of intermediate mechanical properties around the crystals in order to model the stiffness and strength of the fibre. This indicates that the "oriented amorphous" material must have the mechanical properties that are much better than that of a regular amorphous material [54]. Therefore, the volume fraction of silk fibre are assumed as 60% according to the information of silkworm silk which contains β-sheet micro-crystals from Gillespie et al. [55]. Table 7 shows the parameters and values which are used in the current theoretical study.

Table 7. Parameters and values for Micromechanical model

Parameters	Values
V_F	60%
S	3.5
v_m	0.35
E_m	3.9 GPa
E_f	5.79 GPa
l_f	5 mm
d_f	86.9 µm

1. Rule of mixtures (ROM)

$$E = E_f V_f + E_m V_m$$

2. Shear-lag model:

$$E_c = V_f E_f \left(1 - \frac{tanh(\eta s)}{\eta s}\right) + (1 - V_F) E_m$$

Where $tanh(ns) = \dfrac{sinh(ns)}{cosh(ns)} = \dfrac{\frac{e^{ns} - e^{ns}}{2}}{\frac{e^{ns} + e^{ns}}{2}}$

$$\eta = \sqrt{\frac{2E_m}{E_f(1+v_m)ln(1/V_F)}}$$

3. Two-dimension random orientation developed by Tsai and Pagano

$$E_r = \frac{3}{8}E_{11} + \frac{5}{8}E_{22}$$

Where

$$E_{11} = \frac{1+2(lf/df)\eta_L V_F}{1-\eta_L V_F}E_m$$

$$E_{22} = \frac{1+2\eta_T V_f}{1-\eta_T V_f}E_m$$

$$\eta_T = \frac{Ef/Em-1}{Ef/Em+2}$$

$$\eta_L = \frac{Ef/Em-1}{Ef/Em+2(lf/df)}$$

4. Halpin–Tsai equation

$$E = E_m\frac{1+\xi\eta V_F}{1-\eta V_F}$$

3

$$\text{where } \eta = \frac{(Ef/Em)-1}{(Ef/Em)+\xi} \text{ and } \xi = 2\left(\frac{l_f}{d_f}\right)$$

Table 8 shows the result of modulus calculated by various micromechanical models. From the sum of errors squared criterion. Shear-lag analysis equation was found to be more suitable for the prediction of the modulus of silk fibre reinforced PLA biocomposite.

Table 8. Comparing the performance of the various micromechanical models by using the sum of errors squared criterion

Micromechanical model	Result by calculation	Total error (sum of squared deviations)
Rule of mixtures (ROM)	5.034	0.574
Shear-lag analysis	4.53	0.100
Two-dimension random orientation (by Tsai and Pagano)	4.9903	0.530
Halpin–Tsai equati	5.0322	0.5722

Appendix II

(Copies of the selected publicated papers)

Interfacial bonding and degumming effects on silk fibre/polymer biocomposites

Mei-po Ho[1], Hao Wang[1], Kin-tak Lau[1, 2*] Joong-hee Lee[3] and David Hui[4]

[1] Centre of Excellence in Engineered Fibre Composites, Faculty of Engineering and Surveying, University of Southern Queensland, Toowoomba, Queensland Australia
[2] Department of Mechanical Engineering, The Hong Kong Polytechnic University, Kowloon, Hong Kong, SAR, China
[3] Department of BIN Fusion Technology, Chonbuk National University, Jeonju, Korea
[4] Department of Mechanical Engineering, University of New Orleans, New Orleans, LA 70148, USA.
[*] Corresponding author: Kin-tak.Lau@usq.edu.au; mmktlau@polyu.edu.hk

Abstract

Silk fibre has been popularly used for bio-medical engineering and surgically-operational applications for centuries because of its biocompatible and bioresorbable properties. Using silk fibre as reinforcement for bio-polymers could enhance the stiffness of scaffoldings and bone implants. However, raw silk fibre consists of silk fibroin that is bound together by a hydrophilic glued-liked protein layer called "sericin". Degumming is a surface modification process for sericin removal which allows a wide control of the silk fibre's properties, making the silk fibre possible to be properly used for the development and production of novel bio-composites with specific mechanical and biodegradable properties. Some critical issues such as wettability, bonding efficiency and biodegradability at the fibre/matrix interface are of interesting topics in the study of the degumming process. Therefore, it is a need to detailedly study the effect on different degumming processes to the properties of the silk fibre for real-life applications.

Effect of degumming time on silkworm silk fibre for biodegradable polymer composites

Mei-po Ho [a], Hao Wang [a], Kin-tak Lau [a,b,*]

[a] Centre of Excellence in Engineered Fibre Composites, Faculty of Engineering and Surveying, University of Southern Queensland, Toowoomba, Queensland, Australia
[b] Department of Mechanical Engineering, The Hong Kong Polytechnic University, Kowloon, Hong Kong Special Administrative Region

article info

abstract

Recently, many studies have been conducted on exploitation of natural materials for modern product development and bioengineering applications. Apart from plant-based materials (such as sisal, hemp, jute, bamboo and palm fibre), animal-based fibre is a kind of sustainable natural materials for making novel composites. Silkworm silk fibre extracted from cocoon has been well recognized as a promising material for bio-medical engineering applications because of its superior mechanical and bioresorbable properties. However, when producing silk fibre reinforced biodegradable/bioresorbable polymer composites, hydrophilic sericin has been found to cause poor interfacial bonding with most polymers and thus, it results in affecting the resultant properties of the composites. Besides, sericin layers on fibroin surface may also cause an adverse effect towards biocompatibility and hypersensitivity to silk for implant applications. Therefore, a proper pre-treatment should be done for sericin removal. Degumming is a surface modification process which allows a wide control of the silk fibre's properties, making the silk fibre possible to be used for the development and production of novel bio-composites with unique/specific mechanical and biodegradable properties. In this paper, a cleaner and environmentally friendly surface modification technique for tussah silk in polymer based composites is proposed. The effectiveness of different degumming parameters including degumming time and temperature on tussah silk is discussed through the analyses of their mechanical and morphological properties. Based on results obtained, it was found that the mechanical properties of tussah silk are affected by the degumming time due to the change of the fibre structure and fibroin alignment.

Crown Copyright © 2011 Published by Elsevier B.V. All rights reserved.

1. Introduction

Silk fibre has been well recognized as one kind of animal-based natural materials for bio-medical engineering applications because of its superior mechanical and bioresorbable properties. It is a naturally sustainable material and can be extracted and decomposed easily by the nature. By mixing this fibre with recyclable, biodegradable or bioresorbable polymer(s) can produce novel composites. In fact, silk fibres as sutures for human wound dressing have been used for centuries [1]. Recently, regenerated silk solutions have been used to form a variety of biomaterials, such as gels, sponges and films, for medical applications [2]. Moreover, silk has been exploited as a scaffold biomaterial for cell culture and tissue engineering in vitro and in vivo [3]. When producing silk fibre reinforced polymer composites, hydrophilic sericin layer has been found to cause poor interfacial bonding with polymer because this layer hinders the bonding between the fibre and matrix inside the composites, and thus the efficiency of stress transfer from the matrix to the fibre would decrease substantially. It results in affecting the mechanical properties of the composites [4].

Tussah silk, is a type of silk fibre from the species of wild silkworm called Antheraea pernyi (A. pernyi). Cocoon is built at the end of the larval stage of a silkworm and can be casing spun a fine soft thread called silk. The primarily function of the cocoon is pupa protection during metamorphosis until the formation of adult moth. A tussah silk is produced from glands in a silkworm and each of glands comprises posterior and middle regions and an outlet for silk spinning. A fibrous silk core produced by the posterior region is a kind of silk protein, known as a "silk fibroin" which is stored in the glands as an aqueous solution. The fibroin is a structured protein and filament core protein of fibres. Another kind of protein in the silk fibre is named sericin. This non-uniform sticky coating is provided from the middle region of the gland and encased the fibroins to bind the fibroins together with presumably protective functions to the fibrous silk core [5,6]. Sericin protect the fibroin vary from microbial degradation, animal digestion, and other damages. These

* Corresponding author at: Centre of Excellence in Engineered Fibre Composites, Faculty of Engineering and Surveying, University of Southern Queensland, Toowoomba, Queensland, Australia. Tel.: +61 4631 1336; fax: +61 4631 1336.
E-mail addresses: Kin-tak.Lau@usq.edu.au, mmktlau@polyu.edu.hk (K.-t. Lau).

protections include: (1) oxidation resistant, (2) antibacterial, (3) UV resistant and against light damage [7].

Sericin is insoluble in cold water. However, it is hydrolyzed by the breakages of long protein molecules to smaller fractions, which are easily to be dispersed or dissolved into hot water [8]. Although the sericin layer accounts for less than 8% of the total material of the silk [9], a long and continuous fibre can only be reeled from the cocoon after the adhesive sericin coating has been soften or eliminated. Therefore, sericin layer has been removed as waste material from core fibroin during raw silk production such as reeling mill and the other stages of silk processing. Preprocessing of silk commonly known as "degumming" is an essential process to obtain an ideal fibre because of its compositions. Silk degumming process is scouring the sericin and some impurities from silk fibre. The principle of degumming process using water or other degumming agents such as soap, alkali, synthetic detergents, or organic acids is hydrolysing the sericin, breaking the peptide linkage of amino acid into small molecules and dissolving the sericin into the water finally. However, degumming may weaken at least one type of non-covalent interactions of core fibroin, such as hydrogen bond and Van der Waal's force [10]. This factor associated with degumming could affect the tensile properties of silkworm silk because of the change of the microstructure of core fibroins.

Silks are belonged to a group of high molecular weight organic polymers with several low molecular components (sericin). The tussah silk is classified as group three structure (which is characterized by 10.6 Å intersheet packing that is consistent with high alanine content) as partial sequence of H-fibroin is not disclose regular polyalanine repeat. The H-fibroin of tussah silk fibre is made up of 80 tandemly arranged repeats where there are alternative appearances of the poly (1-alanine) region and the Gly-rich region [5,11,12]. The repetitive organization and the presence of high content of short side chain amino acids are preserved in the tussah silk polymer system. The amino acid composition of tussah silk fibroin is characterized by an abundance of alanine (Ala), glycine (Gly), and serine (Ser) and significant amounts of asparagine (Asp) and arginine (Arg). In particular, glycine in tussah silk is 26 residue % and alanine is 44.2 residue % (Table 1) [13]. Basically, alanine is hydrophobic and glycine is amphiphilic which induces the hydrophobic fibroins. On the other hand, most of amino acids in sericin protein have strongly polar side groups, such as hydroxyl, carboxyl, and amino groups [14]. Serine and threonine are the carbohydrates can be covalently linked to its —OH group while aspartic acid and glutamic acid contain free carboxyl group makes it acidic and hydrophilic. The residues serine (Ser), threonine (Thr), aspartic acid (Asp) and glutamic acid (Glu) in sericin are consequently causing the hydrophilic property of sericin [15]. Therefore when the tussah silk fibres are boiled in the hot water, sericin will be dissolved

Table 1
Composition of fibroins of the tussah silk [13].

Amino-acid residue	Tussah silk (residue %)
Glycine	26.6
Alanine	44.2
Serine	11.8
Tyrosine	4.9
Aspartic acid	4.7
Arginine	2.6
Valine	0.6
Glutamic acid	0.8
Tryptophan	1.1
Phenylalanine	0.5
Isoleucine	0.4
Leucine	0.4
Histidine	0.8
Proline	0.3
Threonine	0.1
Lysine	0.1
Cystine	–
Mean residue weight	83.5

but fibroin will not. The hydrophobicity of chain segments inside tussah silk fibroin macromolecular is quite different from that of common type of a domestic Bombyx mori fibroin. Tussah silk is regular stretches of 12 or more consecutive alanine residues interrupted by glycine-rich regions (Fig. 1). It is easily to form hydrophobic interactions between the chain segments and promote the formation of β-sheet structure as the hydrophobicity of poly-alanine blocks inside tussah silk fibroin is stronger than B. mori silk fibroin as B. mori silk fibroin is made up of Gly-X (X equal to Ala or Ser) repeats inside [17].

The structure of tussah silk fibroin is a semicrystalline polymer of natural fibrous protein mainly consisting of the two important phases: (1) highly β-sheet crystals contribute strength and rigidity and (2) non-crystalline form consisting of microvoids and amorphous structures contribute elasticity. The main secondary crystal structure of tussah silk was found to be predominantly antiparallel β-sheet similar to spider major ampullate silks but also with certain amount of a-helix which is distributed throughout the silk fibre [9]. The β-sheets of tussah silk fibre form the basis for the tensile strength and toughness of the material, and it stacks by hydrophobic interactions, and interact bilaterally with alanine side chains which are formed through hydrogen bonds between adjacent peptide chains [16].

It has not been well understood that how the boiling water affects the performance and the morphology of tussah silk fibre during the degumming process. In this paper, the mechanical properties and structures of the degummed tussah silk fibres under

Bombyx mori fibroin

GAGAGSGAGAGSGAGAGSGAGAGSGAGAGSGAGAGYGAGVGVGYGAGYGAGAGAGYGA
GAGSGAASGAGAGSGAGAGSGAGAGSGAGAGSGAGAGSGAGAGSGAGAGSGAGAGSGAG
AGSGAGAGSGAGVGSGAGAGSGAGAGVGYGAGAGVGYGAGAGSGAASGAGAGSGAGAGS
GAGAGSGAGAGSGAGAGSGAGAGSGAGAGSGAGAGSG

Antherara pernyi fibroin

AAAAAAAAAAAAAGSGAGGSGGYGGYGGYGSDSAAAAAAAAAAAAAAGSSAGGAGGG
YGWGDGGYGSDSAAAAAAAAAAAAA

Fig. 1. Typical amino acid sequence of repetitive core of Bombyx mori fibroin and A. pernyi fibroin. The highlighted are definite β-sheet forming segments. The accession number for Bombyx mori fibroin is P05790 which tussah silk fibroin is O76786 [9].

different treated conditions as compared with undegummed fibre are investigated by using Instron material testing system, optical microscope, and scanning electron microscope (SEM).

2. Material preparation and experiments

Tussah silk fibre was supplied by Ocean Verve Ltd., Hong Kong. The shape of ordinary tussah silk fibre is in a flat triangular form. The fibre is fine, high ductile and strong. The ability of light reflection itself makes whole silk fibre shiny. Silk fibres were separated carefully from a bundle of fibres. Special care was taken to avoid stretching the fibre plastically during the whole experiment process. Extracted silk fibres were cut into 200 mm and placed in a 100 mL breaker for the preparation of degumming treatments, and sufficient distilled boiling water was added to completely immerse the fibres into the water. The beakers with the fibres were heated in a hot water bath for 10 min, 30 min, 45 min and 60 min, respectively. Afterward the hot water treated fibres were washed with cold distilled water and dried immediately at 80 °C for 4 h. Raw silk fibre was referred to as an untreated sample dried by 80 °C for 4 h similar to other hot water treated fibres. As the water disrupts hydrogen bonds of the fibre which would promote the substitution of protein–protein hydrogen bonds by water–protein hydrogen bonds and thus reduce the mechanical properties of the silk fibre [18], undesirable change of the fibre diameter would occur to hinder the effect of degumming. Therefore, drying up the fibres before the experiments was crucial and all the tests were performed immediately after the fibres had been removed from an oven. Each sample was mounted on cardboard frames by tapes and removed any slack without stretching the specimen. Fig. 2 shows the experimental setup for the tensile test for this study. The cardboard frame was cut with scissors through the discontinuous line as shown in the figure before starting the experiment. The diameter of centre hole was 100 mm. All samples must be well aligned to the loading direction to avoid any mis-measurement of the strength of fibres.
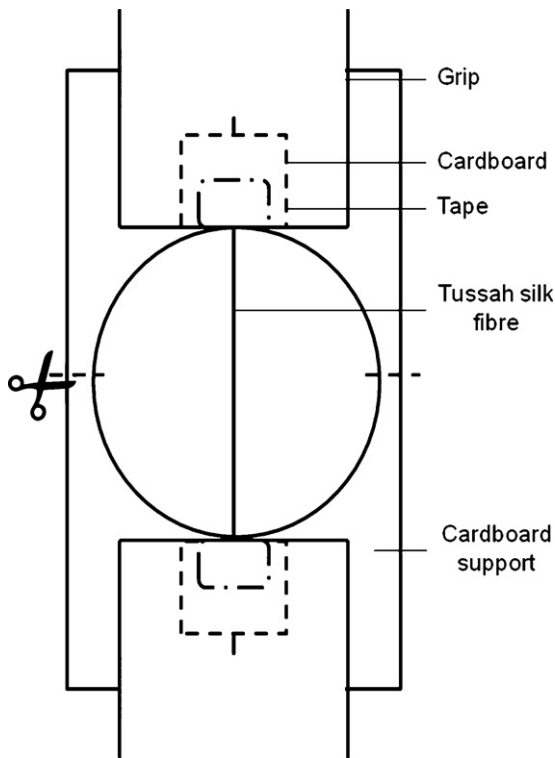
Fig. 2. Experiment setup for the tensile property test for silk fibres.
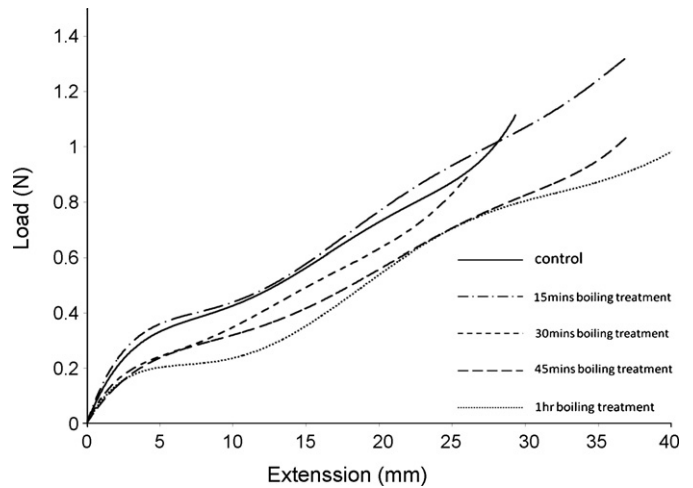
Fig. 3. Load–displacement curves of control and degummed tussah silk fibres.
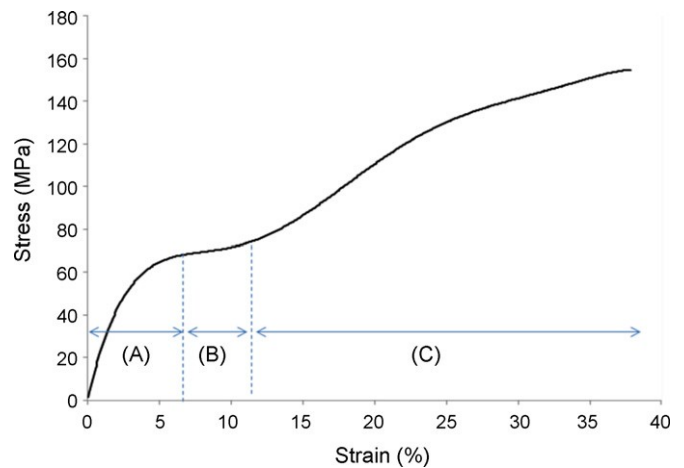
Fig. 4. Stress–strain curves of ordinary tussah silk fibre as (A) initial linear elastic region, (B) a yield region, and (C) a hardening region.

All measurements were carried out on the MTS Alliance RT/10 materials testing machine at a crosshead speed of 60 mm/min and under standard environmental conditions (20 °C, 60% relative humidity). The samples were tested according to ASTM D 3822. The diameter of silk fibre samples was characterized by using optical microscope (Olympus SZ-PT). Some samples were further coated by gold for scanning electron microscope (JEOL Model JSM-6490) imaging.

3. Results and discussion

The representative tensile load–displacement curves of tussah silk fibres are given in Fig. 3. The tensile test was processed with the gauge length of 100 mm. Tussah silk fibres which were degummed for 15 min in the hot water show a better load carrying capacity as compared with other samples. Table 2 summarizes the results

Table 2
Load and elongation at break of the tussah silk fibres pre-treated at different temperatures.

	Degummed time (min)				
	0	15	30	45	60
Load (N)	0.35	0.38	0.24	0.23	0.18
Elongation (mm)	5.6	5.9	4.9	4.7	3.8

Fig. 5. Stress–strain curves of tussah silk fibres degummed at different time periods.

Fig. 6. Weibull distributions for the strength of the tussah silk fibres.
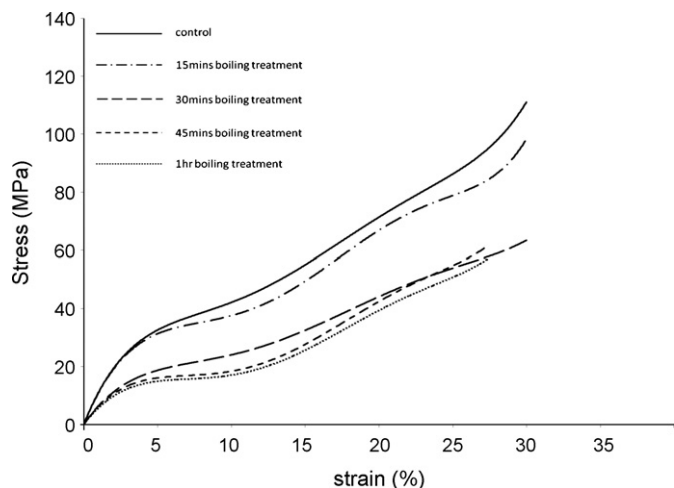
obtained from tensile test including average F_p (load) and ε_p (elongation) at the elastic limit point of all samples (extracted the results from 10 samples at each type of heat-treated fibres). Jiang et al. have suggested that the degumming process has two principal quantitative effects on the load-displacement plot including initial slope and the elastic limit (i.e. yield point) [10]. For the sample degummed for 15 min, the initial slope is steeper as compared with the result of the control samples. However, for the samples degummed over 15 min, their initial slope and the elastic limit (i.e., yield point) are lower than that of the controls. Based on the results of all curves, it is clear to see that for the fibres degummed over 1 h caused the substantial decrease of their elastic region (by 50% as compared with the sample degummed for 15 min) because of the damages of the fibroins.

After obtaining the load–displacement results, nominal strains of the samples were calculated. Nominal stress was also obtained by dividing the applied load to the cross sectional area of each fibre as the diameter was measured directly under the microscopy. The graphical representation of the relation between stress and strain was obtained as stress–strain curve thereafter. Similar to spider dragline silk, the tussah silk fibre exhibits three regions with turn in its stress–strain curve. These regions include an initial linear elastic region (A), a yield region (B), and a hardening region (C) which are clearly shown in Fig. 4. Fig. 5 shows the stress–strain curves of all samples. This type of sigmoidal "rubber like" shape of the stress–strain curves obtained from the experiment which is well matched with the result obtained from Zhang et al. [11].

Table 3 is the summary of the mechanical property parameters of the samples including elastic modulus E (initial modulus), slope of yield region, slope of hardening region, the strain at the proportional limit, the tensile strength and the strain at breaking. The relationship between the mechanical properties of the samples and the degumming time are listed in Tables 2 and 3. Based on the influences on the degumming time, samples which heat-treated for 15 min are the best among the degummed samples in term of
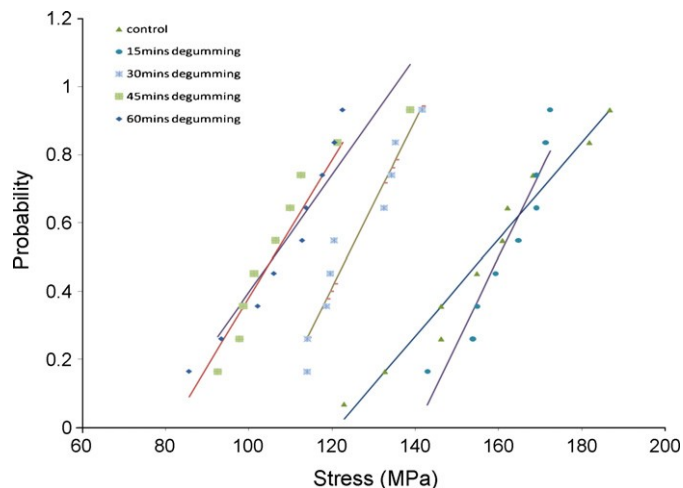
the tensile strength. Moreover, from the tables, it is shown that fibres degummed for 15 min are more compliant and have better tensile strength, initial modulus, slope of yield region and strain at breaking than that of other degummed samples. On the other hand, for the samples being degummed over 15 min, their initial tensile modulus, slope of yield region, slope of hardening region, strain at the proportional limit, tensile strength and strain breaking and yield points for degummed samples start to decrease gradually and drop dramatically when the degumming process is taken over 30 min. According to the results shown, it can be concluded that by increasing the time for degumming until heat-treated 15 min, maximum tensile properties reach but start to decline when the samples degummed over 15 min.

Certain factors whereby explain the influence of degumming on the tensile properties of single silkworm silk fibre including (1) sericin removal, (2) molecular changes and (3) bonding breakage. Focusing on the amino acids residues, the amino acid sequence of polypeptides plays a very important role in the solubility and crystallization of silk fibroins [21]. Glycine and alanine predominate in silk fibroin. In particular, the glycine in tussah silk is 26 residue % and alanine is 44.2 residue % [13]. Therefore, tussah silk fibroin is predominantly hydrophobic as alanine is hydrophobic and the glycine is amphiphilic. On the contrary, residues serine, threonine, aspartic acid and glutamic acid are the main components of sericin. Serine and threonine are carbohydrate that can be covalently linked to its hydroxyl ($-$OH) group. While aspartic acid and glutamic acid contain free carboxyl group making it acidic and hydrophilic. Sericin is therefore hydrophilic and comprised of more random structures [15,21]. Removal of sericin layers on the fibre surface would contribute significantly to the change of cross sectional area and subsequently the tensile properties of the fibres. The level of degumming is mainly depended on the treatment time. At the beginning of degumming, the water starts to dissolve the sericin on the fibre surface and cause the decrement in the diameter of the fibre. The strength of the fibre being degummed for 15 min

Table 3
Summary of the tensile stress, strain, and modulus of the samples.

	Initial modulus (GPa)	Slope of yield region	Slope of hardening region	Strain at the proportional limit	Tensile strength (MPa)	Strain at breaking
Control	102.86	5.714	32	5.3	156.293	28.05
Degumming after 15 min	112	20	30	4.5	159.837	34.127
Degumming after 30 min	55	5.714	6.67	4	124.081	28.838
Degumming after 45 min	51.43	5	6.67	3.7	106.982	27.489
Degumming after 60 min	45.71	0.333	6.67	3	104.922	22.625
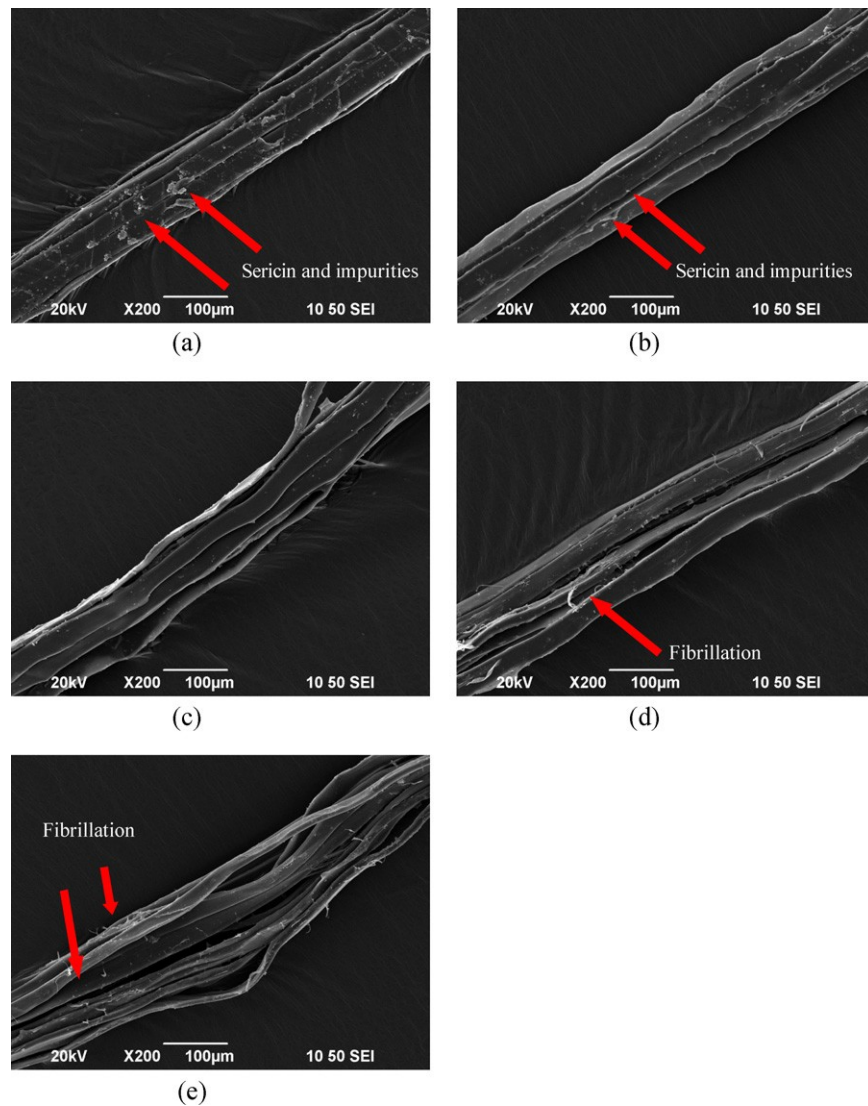
Fig. 7. Surface of tussah silk fibres degummed for (a) 0 min (control sample), (b) 15 min, (c) 30 min, (d) 45 min, (e) 60 min.

increases because of the decrease of the cross sectional area. As load-bearing capacity of sericin is very small compared to that of fibroin, removal of the sericin represents not only the decrement in the cross sectional area, but also the increment in the effective cross sectional area. Another effect on sericin removal for the reasons of the increase strength of the degummed tussah silk fibre for 15 min is their filaments are twisted in nature. After degumming, the filaments of fibre, due to the missing of binding agent (i.e. sericin) would potentially align towards the loading direction. Thus, the friction in-between the filaments were reduced and the load bearing capacity increases because of the alignment of the fibre to the loading direction. In such case, the fibre can take a large portion of tensile load instead of friction. Nevertheless, this scenario is totally reverted when the degumming time increases. As the sericin which acts as the glue to bind up all fibroin filaments together, degumming would cause the removal of sericin and thus the fibres are in a loose pack form. The scattering of the fibre would increase its diameter. It can be seen that fibres heat-treated after 15 min had less strength as compared with the control sample because of fibre scattering.

Molecular change is one of the consequences of degumming which infers the tensile properties of control and degummed silk fibres. In the secondary structure, the repetitive primary sequence in hydrophobic residues of silk fibroin composing of short side chain amino acids dominate the anti-parallel (3-sheet structure. These structures permit tight packing of stacked sheets of hydrogen bonded anti-parallel chains of the protein [23]. In a silk fibre, strong crystalline regions which provide tensile strength are interspersed by, the soft and more flexible amorphous peptide chains which are responsible for the elasticity of silk and also help with the distribution of stress [20,24]. Under tensile loading, the amorphous chains are extended, and the crystalline networks are rotated during the stretching and shrinking to produce a strongly preferred molecular orientation which is parallel to the fibre axis. Moreover, once the fibre extended physically, partly amorphous chains in the fibroin would be crystallized as a rigid and highly oriented network [28]. Therefore, amorphous structure also contributes the strength because of the crystallized amorphous region. On the other hand, heavy chain and light chain fibroin inside a silk fibroin with a single linkage called disulfide bridge convey the fibre with its remarkable mechanical behaviour [25]. The heavy chain of SF comprised crystalline and amorphous regions but is mainly composed of beta-sheets [23]. However, excessive heating period would affect the fibroin heavy chain [10]. Besides, the water molecules damage and scissor the chain which is occurring in the amorphous component preferentially [25] but, crystallites can also be deteriorated in an
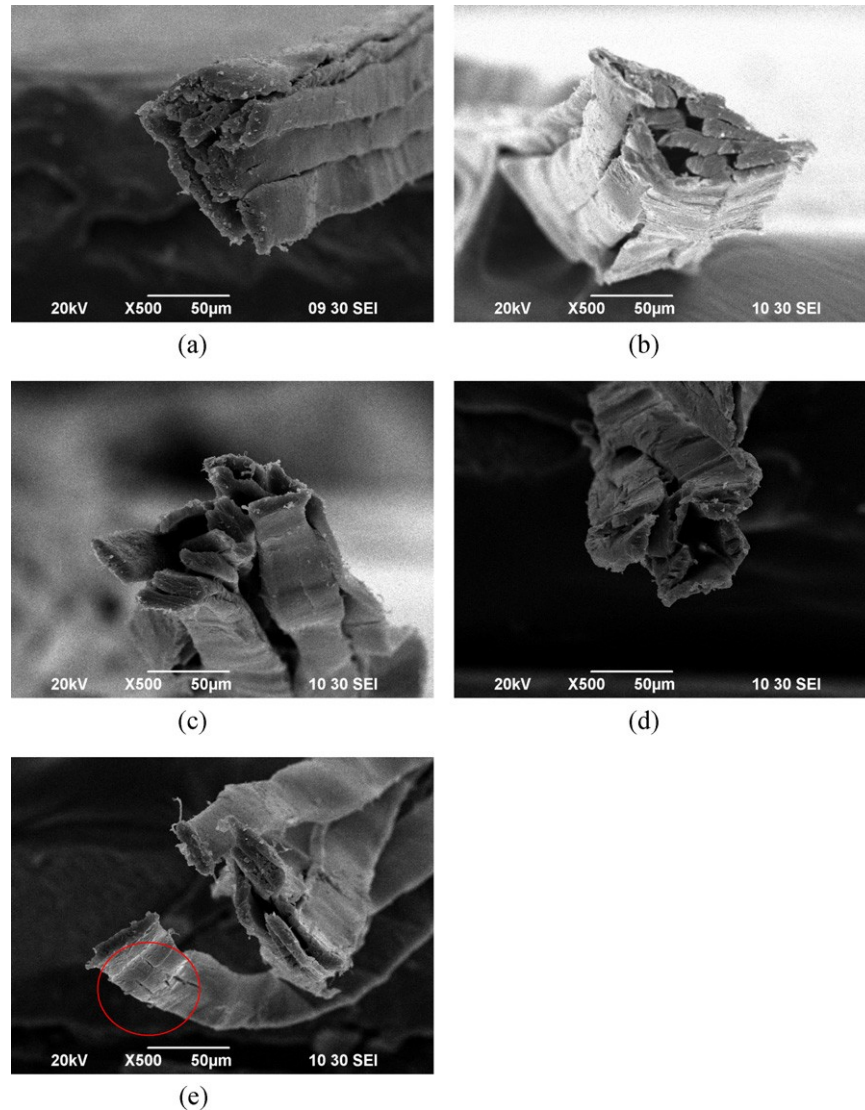
Fig. 8. SEM images of tussah silk fibres degummed for (a) 0 min (control sample), (b) 15 min, (c) 30 min, (d) 45 min and (e) 60 min.

extreme case [26,27]. The degumming effect will damage the amorphous structure as the first place after the removal of sericin. It can be seen that the strains of the fibres drop dramatically after being heated over 45 min. Hence, the low tensile strength of degummed

Fig. 9. Micrometer-sized calcium oxalate crystals on the surface of tussah silk fibre.

silk may probably reflects the damage of both amorphous and crystalline structures.

There are specific interactions among the blocks and, between the chain-ends and larger hydrophilic blocks. The β-sheet structure of tussah silk fibre is depicted as the formation of poly-ala structure with the placement of successive alanine residues on alternate sides of a backbone. Each chain can then be interlocked with an adjacent chain via hydrophobic interactions [29]. Thus, the strength of interactions between the β-sheet structures of these proteins predicts the tensile strength of the silk [29]. Besides, the dimension of the chain axis and hydrogen bond are similar for all types of silks, while difference is in the inter-sheet spacing. As most natural fibres owe their strength from hydrogen bond, hydrogen bond plays an important role in the secondary, tertiary, and quaternary structures of proteins. However, degumming weaken at least one type of non-covalent interaction. This interpretation is consistent with the fact that water act as a plasticizer. Water penetrates the amorphous regions and interrupting the inter- and intra-molecular hydrogen bonds so that the displacements of protein chain segments and stress relaxation are increased and thus easier to respond any driving force for microstructural change consequently [19,30]. Heating the fibre up to 100 °C only provides a thermal energy equivalent to 3.1 kJ/mol, which is below the range of typical hydrogen
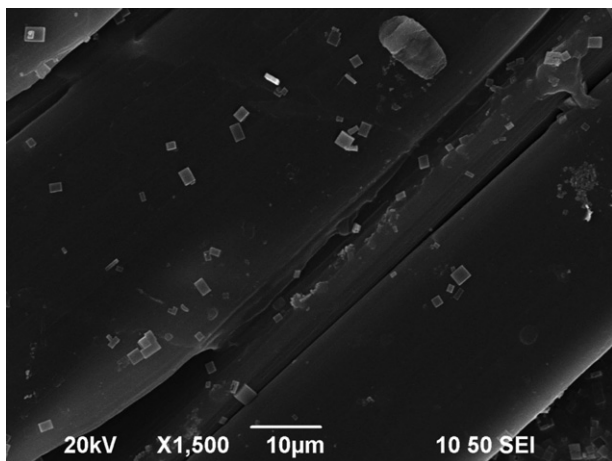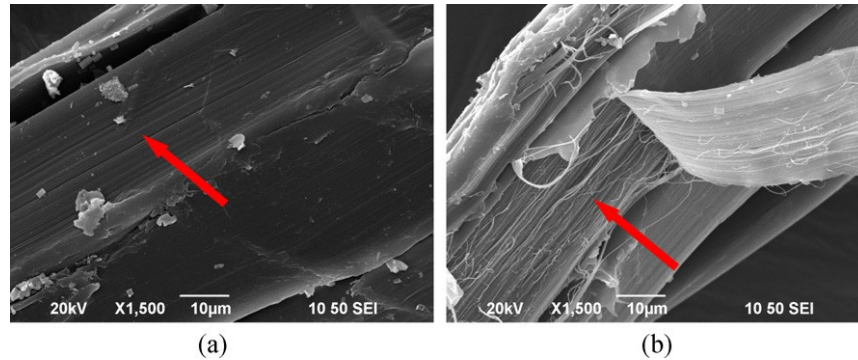
Fig. 10. (a) and (b) Defects of the degummed tussah silk fibre indicated by arrows.

bonding energy. Therefore, this way is unlikely to disrupt the pattern of hydrogen bond of silk fibre significantly in the dry condition [19] but is likely to affect the structure of the silk fibre by immersion it into the water during the heating duration. During degumming, the effects of water with heat disrupt the hydrogen bond and disorder the structures. Hydrogen bond becomes weak and loses its strength when heated. The existing peptide bonds, salt linkages and hydrogen bonds of the silk fibre tend to break down once the temperature exceeds 100 °C. As the crystalline units cross-link the protein chains in the fibre via hydrogen bond, disrupting the hydrogen bond would decline the load bearing of the fibre [8]. Fibroin has a high degree of crystalline due to stacked (3-sheets. In a stretched fibre, the external force propagates along the fibre axis by straightening the disordered protein chains (amorphous region) and subjecting the crystalline regions to a tensile loading along the (3-strand axis. Accordingly, as the crystalline units cross-link the protein chains in the fibre via hydrogen bond, disrupt the hydrogen bond would decline the load bearing of the fibre [8].

Weibull distributions for the strength of the tussah silk fibres are shown in Fig. 6. The data is scattered for both the undegummed and degummed tussah silk fibres. The reason for scattering the tussah silk tensile data is intrinsic to the most of the natural fibres. Moreover, difficult and imperfect measurements of the fibre diameter and the roughness of the fibre surface would also reduce the reproducibility of the strength of the silk fibre. Among all the samples, the data for degummed 30 min is more dispersed. It may because the impurity non-uniform sericin on the surface is removed unequally and, boiling water starts to attack the fibroin at the same time. Therefore, after degummed 30 min the portion of the sericin removal is not equal to all fibres and thus induces the stress data dispersive.

The temperature of the water used for degumming must be high enough as it is used to degrade and remove the sericin layer from the fibres. The fibroin would be damaged as all the sericin from the silk fibre as the protective surface coating is removed. Therefore, increasing the time of degumming will increase the damage of the fibroin. As the boiling water disrupts the hydrogen bond of the fibre, it would promote the substitution of protein–protein hydrogen bond by water–protein hydrogen bond. The decrement in tensile strength of degummed silk probably reflects this damage. Another reason is contributed from the sericin removal. Hydrophilic sericin envelops fibroin. Notwithstanding sericin is insoluble in cold water, it is easily hydrolyzed in hot water, whereby the breaking down the long protein molecules into the smaller fractions which are easily dissolved in hot water [8]. The removal of sericin is found from the SEM micrographs.

The surface morphology of heat-treated silk fibres according to different degumming time intervals was investigated by SEM. The SEM micrographs are illustrated in Figs. 7(a)–(e) and 8(a)–(e). Fig. 7(a), the ordinary tussah silk fibre is not circular in cross section

but is in flat triangle shape. A tussah silk is bonded and comprised many fibroin strands. Each fibroin strand itself is a bundle of several fibrils and the periphery of the silk fibroin strands coagulate many sericin particles irregularly [22]. In addition, the tussah silk fibre obtained directly from the spinneret of silkworm is free from calcium oxalate crystals at micrometer size but these crystals are usually observed on the undegummed cocoon silks. These micrometer-sized calcium oxalate crystals are the type of an excretion by the silkworm and it can be shown in Fig. 9 which is same as the finding from Fu et al. [9].

For the control samples which were not treated with hot distilled water as shown in Figs. 7(a) and 8(a), the surface characteristic of the tussah silk fibre is fairly rough. This rough surface was clearly evident to large amount of sericin coating. The sericin appears as some partially non-uniform coating on the surface of the fibroins and various granules and impurity deposits are visible in the vacant spaces in-between the fibroins. Different surface morphologies and fibre damages of the raw silk fibres and degummed silks in various conditions are observed according to the SEM micrographs. The micrographs of samples degummed for 15 min show good degumming result and no sign of destruction or damage on the silk fibres surfaces (Figs. 7b and 8). The fibres surfaces are greatly smooth, which show that only very shallow longitudinal striations attributable to the fibrillar structure for the truly degummed silk fibres.

After 30 min boiled samples is free from non-uniform coating, any granules and impurity. In some parts of the fibroin, sericin layers are dissolved and fibroins are split away from the main fibre axis leaving the clean fibroin fibre surface to appear. In micrographs of Figs. 7(c)–(e) and 8(c)–(e) are shown the surfaces of degummed silk fibres after 30 min, it is found that the sericin are almost completely removed on the fibroin surfaces but some damages were observed on the fibroins surfaces. The cases get even worse as much more damages were observed for 60 min heat-treated. The higher magnification of SEM examination of the tussah silk fibres showed that the individual silk fibroin strands are split off (Fig. 10(a)). Fibrillation of some fibroin threads also occurs (Fig. 10(b)). Moreover, based on Fig. 7(a)–(e), it is found that the fibre diameters increase gradually when extended the degumming time. It is mainly because the binder (sericin) is dissolved and removed so that the fibroins disperse.

4. Conclusion

Preprocessing of silk commonly known as degumming is an essential process to obtain an ideal fibre because of its fibre structure. Silk degumming process scours the sericin and some impurities from silk fibres. Through the measurement of the mechanical properties and surface morphology of the samples,

the results show that using boiling water for degumming of tussah silk fibre for 15 min obtain the maximum tensile strength, stain and modulus. As the major amino acids groups in sericin are hydrophilic, hot water degumming treatment dissolves the sericin into the water during the degumming process. Three major factors that explain the influence of degumming on the tensile properties of a silkworm silk fibre are:

(1) Sericin removal,
(2) Molecular changes and
(3) Bonding breakage.

From the SEM analysis, the micrographs show that all the impurities are removed and no damage on the surfaces can be found after degumming. As degummed silk fibre is used as reinforcement for biodegradable polymer composites, a further study on developing theoretical or numerical models to predict the mechanical and biodegradable properties of the composites with different fibre arrangements and volume fractions is required.

Acknowledgment

References

[1] Y.Z. Wang, In vivo degradation of three-dimensional silk fibroin scaffolds, Biomaterials 29 (2008) 3415–3428.
[2] C. Vepari, D.L. Kaplan, Silk as a biomaterial, Prog. Polym. Sci. 32 (2007) 991–1007.
[3] Y.Z. Wang, Stem cell-based tissue engineering with silk biomaterials, Biomaterials 27 (2006) 6064–6082.
[4] M.P. Ho, K.T. Lau, H. Wang, Characteristics of a silk fibre reinforced biodegradable plastic. Composite structures, Composites: Part B 42 (2011) 117–122.
[5] Z. Michal, S. František, Unique molecular architecture of silk fibroin in the waxmoth, Galleria mellonella, J. Biol. Chem. 277 (25) (2001) 22639–22647.
[6] E. Atkins, Silk's secrets, Nature (2003) 424.
[7] H. Osnat, P.K. David, Spider and mulberry silkworm silks as compatible biomaterials, Composites: Part B 38 (2007) 324–337.
[8] M. Mondal, K. Trivedy, The silk proteins, sericin and fibroin in silkworm, Bombyx mori, Linn—a review, Caspian J. Environ. Sci. 5 (2) (2007) 63–76.
[9] C.J. Fu, D. Porter, Understanding the mechanical properties of Antheraea Pernyi Silk—from primary structure to condensed structure of the protein, Adv. Funct. Mater. 21 (2011) 729–737.
[10] J. Ping, L. Huifen, Tensile behavior and morphology of differently degummed silkworm (Bombyx mori) cocoon silk fibres, Mater. Lett. 60 (2006) 919–925.
[11] Y.P. Zhang, H.X. Yang, H. Shao, X.C. Hu, Antheraea pernyi silk fibre: a potential resource for artificially biospinning spider Dragline silk, J. Biomed. Biotechnol. (2010).
[12] C. Yang, W. Bochu, Biodegradation of silk biomaterials, Int. J. Mol. Sci. 10 (2009) 1514–1524.
[13] E.M. Richard, The structure of Tussah silk fibroin, Acta Crystallogr 8 (1955) 710.
[14] S. Yu, A.J. Michael, Microstructural characterization of Bombyx mori silk fibers, Macromolecules 31 (1998) 8857–8864.
[15] Z. Xiaomei, Heat and moisture promoted deterioration of raw silk estimated by amino acid analysis, J. Cult. Heritage. 12 (2011) 408–411.
[16] S. František, Construction of silk fiber core in Lepidoptera, Biomacromolecules 5 (2004) 666–674.
[17] W. Tao, M. Li, C. Zhao, Structure and properties of regenerated Antheraea pernyi silk fibroin in aqueous solution, Int. J. Biol. Macromol. 40 (5) (2007) 472–478.
[18] J. Perez-Rigueiro, C. Viney, Mechanical properties of silkworm silk in liquid media, Polymer 41 (2000) 8433–8439.
[19] J. Perez-Rigueiro, Effect of degumming on the tensile properties of silkworm (Bombyx mori) silk fibre, J. Appl. Polym. Sci. 84 (2001) 1431–1437.
[20] B. Elisabetta, P.K. David, Mapping domain structures in silks from insects and spiders related to protein assembly, J. Mol. Biol. 335 (2004) 27–40.
[21] T. Tanaka, Thermal properties of Bombyx mori and several wild silkworm, J. Thermal Anal. Calorim. 70 (2002) 825–832.
[22] C. Ran, Comparison of silk structure and fabric testing performance ordinary and puffed tussah silk, Adv. Mater. Res. 211–212 (2011) 904–908.
[23] K. Ung-Jin, P. Jaehyung, Structure and properties of silk hydrogels, Biomacromolecules 5 (2004) 786–792.
[24] B.M. Anshu, G. Vishal, Silk fibroin-derived nanoparticles for biomedical applications, Nanomedicine 5 (5) (2010) 807–820.
[25] R.P. Gustavo, Paola Corsini, Effect of water on Bombyx mori regenerated silk fibers and its application in modifying their mechanical properties, J. Appl. Polym. Sci. 109 (2008) 1793–1801.
[26] P. Garside, P. Wyeth, Crystallinity and degradation of silk: correlations between analytical signatures and physical condition on ageing, Appl. Phys. A 89 (2007) 871–876.
[27] V. Charu, L.K. David, Silk as a biomaterial, Prog. Polym. Sci. 32 (8–9) (2007) 991–1007.
[28] J.M. Gosline, P.A. Guerette, The mechanical design of spider silks: from fibron sequence to mechanical function, J. Exp. Biol. 202 (1999) 3295–3303.
[29] Y.H. Cheryl, H. Nichola, Hypotheses that correlate the sequence, structure, and mechanical properties of spider silk proteins, Int. J. Biol. Macromol. 24 (1999) 271–275.
[30] S. Sambit, PLGA nanofiber-coated silk microfibrous scaffold for connective tissue engineering, J. Biomed. Mater. Res. B: Appl. Biomater. 95B (1) (2010) 19–28.

Short Communication

Design of an impact resistant glass fibre/epoxy composites using short silk fibres

Mei-po Ho, Kin-tak Lau [⇑]

Centre of Excellence in Engineered Fibre Composites, Faculty of Engineering and Surveying, University of Southern Queensland, Toowoomba, Queensland 4350, Australia

abstract

The prevailing utilisation of light and strong structural materials has led to an increasing demand to engineering industries on developing different types of advanced composites. Thus, the development of simple and low cost woven glass fibre composites with an improvement on their tensile and impact properties is suggested. In this paper, the hybridization of a glass fibre reinforced composite is achieved by using low cost short silk fibres as a medium to enhance its cross-ply strength. The comparison on the tensile and impact properties of the composite reinforced by the short silk fibre (with the content from 0.3 to 0.6 wt%) with a pristine glass fibre composite sample was conducted. Fracture surfaces were analysed by using scanning electron microscopy (SEM). Experimental results indicated that the maximum Young's modulus and ductility index (DI) of a silk reinforced composite increased by 50% and 75%, respectively as compared with the pristine one. Furthermore, the visual examination on drop-weight test samples proved that the impact resistance of the silk reinforced composite was better than that of the pristine sample as well. According to the results obtained, it was found that the addition of 0.4 wt% short silk fibre into glass fibre composite was shown to be the advisable reinforcement content to achieve better tensile and impact strengths.

© 2011 Elsevier Ltd. All rights reserved.

1. Introduction

Fibre-reinforced polymer composites have been widely used in different engineering applications for many decades. The main advantages of using these composites instead of traditional materials like steel and concrete include their light in weight properties, high strength to weight ratio and good resistance in fracture (along their fibre direction(s)). As the composites are made by strong fibres (carbon, glass or aramid) and soft matrix (epoxy, polyester, vinyl-ester and others), it can produce their properties are very strong in tension, and also good in energy absorption. Woven fabric is the most common type of reinforcement form to make glass fibre reinforced polymer composites due to its simplicity in composites' lay-up process and strength estimation by using simple classical lamination theory. However, there are some drawbacks which hinder the attraction of using this glass fibre composite such as (1) weak in the out-of-plane direction as compared with their in-plane direction [1] and (2) high energy consumption in the manufacturing process. Compared with other isotropic materials, the mechanical properties of laminate composites are behaved anisotropically. Residual stresses may also be easily induced during the manufacturing process due to differential thermal coefficients of expansion between fibre and matrix.

Since the fabrics have to be laid up one-by-one with being isolated by a layer of matrix (described ideally), the out-of-plane properties are totally controlled by the properties of matrix and its bonding efficiency with glass fibres. To improve the out-of-plane properties of the composites with minimising the cost involvement, low cost short silk fibres would be a good material to be used, like z-pins as inter-laminar reinforcement.

Crucially, the advantage of a well designed hybrid composite is the combination of the properties of their respective constituents and even the addition of qualities that neither their constituent possesses. Therefore, the short fibre inter-laminar reinforcement technique, as a method which is simpler, cheaper and unnecessary of imposing an extra complicated process in existing manufacturing process is proposed. Hybrid composite is classified as sandwich type, intra-ply type and inter-ply type. Fig. 1 illustrates the schematic explanation of the classification of the fibre hybrid composites. Sandwich-type hybrid composites normally consist of two or more different types of layers to form light weight structures. Typically, this type of structures is used to sustain bending loads (the core is made by a light material such as foam while the skins are made by high strength fibre composite materials) [2,3]. Intra-ply is defined as the layer of fabric weaved by different types of fibres [4,5], its purpose is to design a composite with the strengths are different in both longitudinal and lateral directions. Common practice is to weave carbon fibres in 0° direction (main loading direction) and glass fibres are in 90° direction to form a fabric. Inter-ply fibre hybrid composite is often called ''inter-laminar

⇑ Corresponding author. Tel.: +852 2766 7730.
E-mail address: Kin-tak.Lau@usq.edu.au (K.-t. Lau).
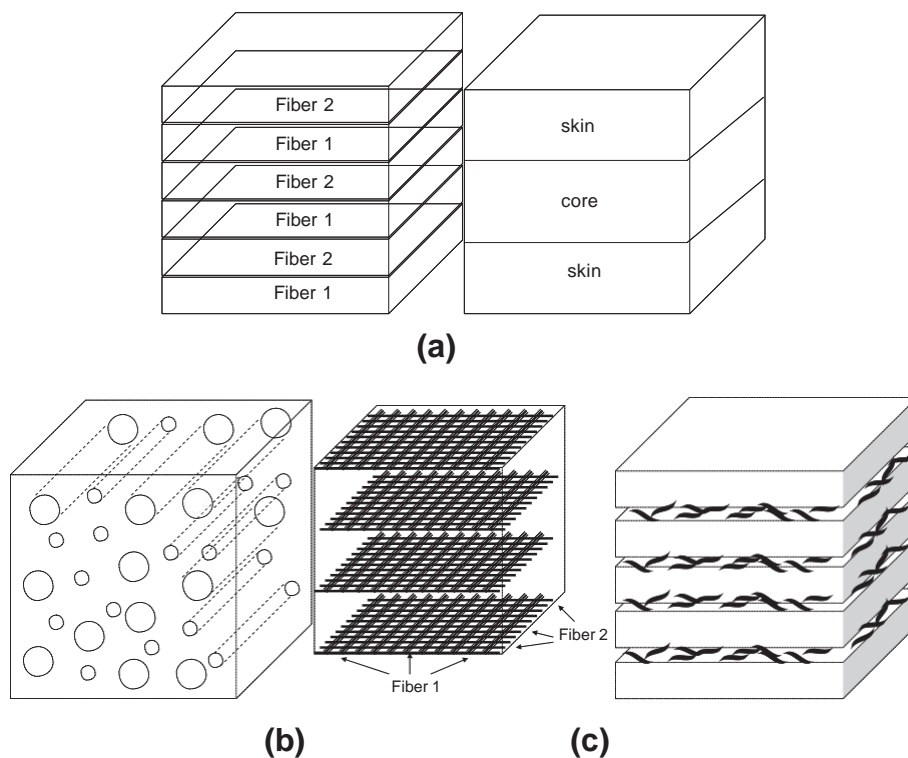
Fig. 1. (a) Sandwich type, (b) intra-ply type and (c) inter-ply type.

Table 1
Comparison of natural fibre reinforcement materials with E-glass.

Properties	E-glass	Flax	Jute	Hemp	Sisal	Silk fibre	Coir
Density (g/cm^3)	2.57	1.4	1.46	1.48	1.33	1.23–1.34	1.25
Tensile strength (MPa)	3450	800–1500	400–800	550–900	600–700	157	230
Tensile modulus (GPa)	72	60–80	10–30	70	38	103	6
Moisture absorption (wt%)	None	7	12	8	11	7.41	10

reinforcement composite''. This type of hybrid composite is clarified as only one type of fibre made up of individual piles, but specific type of material is dispersed in between the plies to improve their out-of-plane properties.

In general, the failure mechanisms of short fibre reinforced polymers are in semi-elastic failure, fibre pullout or short fibre breakage which effect in increasing the energy absorption capability. By using the similar principle into long fibre reinforced polymer composites, it could enhance the fracture toughness of the composites as the short fibre can be used to reinforce the strength between different plies and also absorb energy during foreign object impact [6]. As aforementioned, for fabric reinforced composites, the mechanical properties are mainly governed by the properties of matrix, it therefore by appropriately adding short fibres can improve the bonding strength between the plies and thus, the out-of-plane properties of the composites [7].

Although many research have been conducted by using carbon, glass or kevlar fibres as short fibre reinforcements for laminate composites, their raw materials cost and pre-processing time are concerns to most composite manufacturers, particularly in the consideration of producing composites with good out-of-plane and impact properties.

Natural fibres included plant-based, such as hemp, sisal and bamboo, and animal-based such as spider silk and silkworm silk, have been frequently used as reinforcements for many polymer-based materials [8]. It has been proved that the mechanical properties of natural fibre reinforced polymer composites are much better than pristine polymer materials (Table 1). Therefore, they are potential candidates for serving the purpose of reinforcing laminate composites. Moreover, compare with other type of artificial inter-laminar short fibre, natural fibre such as silk fibre which is natural available.

Many researchers attempted to use short fibre to reinforce composites made by woven fabrics in order to increase their fracture energy [9–11]. However, few of them focused on the tensile and impact properties of these composites reinforced by short natural fibres to form a hybrid composite. Among the numerous natural fibres, silk fibre is a natural protein fibre which is biodegradable and highly crystalline with a well-aligned structure. Moreover, silk fibre has a high extensibility among natural fibres. The objective of this study is to develop a hybrid composite that is low cost, light weighted with improved tensile modulus and inter-laminar properties, and possesses adequate strength and elongation at break for different engineering applications. In the work, woven glass fibre and chopped silk fibre were used to fabricate the hybrid composite. The mechanical properties of the hybrid composite compared with a pristine woven glass fibre/epoxy sample were studied. The optimised fraction of the short silk fibre and fabrication method of the composite in order to achieve the maximal strength is also discussed.

Table 2
Density of the short silk fibre and the thickness of samples.

Percentage of silk fibre reinforced	0	0 0.6%	0.5%	0.4%	0.3%
Density of short silk fibre (g/m²)	0	28.571	22.857	17.143	11.429
Thickness (mm)	1.565	1.711	1.706	1.771	1.768

Table 3
Tensile properties of type 1 samples.

Specimen type (%SF)	E (MPa)	UTS (MPa)	Strain (mm/mm)
GFR	10858.31	327.10	0.855
GF with 0.6	12500.00	346.77	0.796
GF with 0.5	15189.71	378.37	0.780
GF with 0.4	16374.27	304.77	0.731
GF with 0.3	12500.00	268.40	0.713

2. Experiment set up

Plain weave glass fabrics (style AF218) were supplied from COLAN AUSTRALIA. Epoxy resin AA0341 A and Hardener AA0341 B supplied by CHEMATCO LTD were used (mixture ratio = 4:1) to form matrix for the composite. Tussah silk fibre supplied by Ocean Verve Ltd. was used as inter-laminar reinforcements. Degumming is a key process to remove the surface coating layer, named ''sericin'' by the mean of thermo-chemical treatment of the cocoon. Although this surface modification can affect the mechanical properties of silk significantly, it is normally done to enhance interfacial adhesion between fibre and matrix for polymer-based composite systems. The silk fibres were cut gently into 6 mm to prevent the fibres were stressed plastically during fabrication process. Composite samples were made by simple hand lay-up process followed by vacuum bagging. Short silk fibres were distributed evenly on the surface of each layer after resin had applied. A total of seven plies of glass fabrics were used to make the hybrid composite. Table 2 shows the density (g/m²) of silk fibre and the thickness of samples with different weight percentages of silk fibre.

3. Tensile property test

All samples were cut to the dimension of 200 mm × 25 mm for making testing coupons. To avoid any stress concentration induced at both ends of the coupons during testing, four 25 mm × 25 mm plastic taps were glued by epoxy adhesive on both end sections of the coupons. An extensometer with a gauge length of 50 mm was attached to the centre of specimen to measure the strain response. The tensile property test was conducted by using MTS Alliance RT/50 with the cross-head speed as 1 mm/min. The test procedure was followed according to the ASTM D3039.

All testing results are presented in Table 3. The Young's modulus of the hybrid composites is defined as the slope of the stress–strain curve in their initial linear-elastic region. It is observed in Fig. 2 that the tensile strengths are found to increase with the increase of the content of short silk fibre. However, for the samples with less than 0.5 wt% of silk fibre, their strength is lower than that of a pristine (glass fibre/epoxy) sample. The highest tensile strength was reached for the sample with 0.5 wt% of silk fibre, over 16% increase of strength as compared with the pristine sample. In terms of the Young's modulus of the samples, Fig. 3 shows that the Young's modulus increases dramatically when silk fibres were added into the glass fibre composite. With the use of 0.3 wt%, 0.4 wt%, 0.5 wt% and 0.6 wt% of the silk fibres, the increase of the Young's moduli are 15%, 51%, 40% and 15% respectively. In this figure, it is obvious that the Young's modulus decreases when
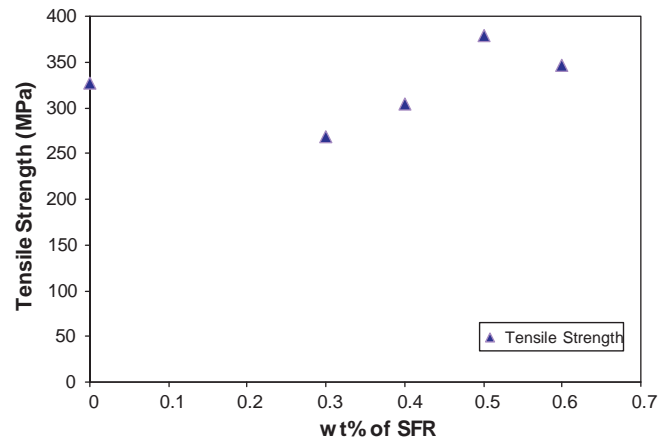
Fig. 2. Tensile stress (MPa) versus content of short silk fibre (SSF) for type 1 sample.
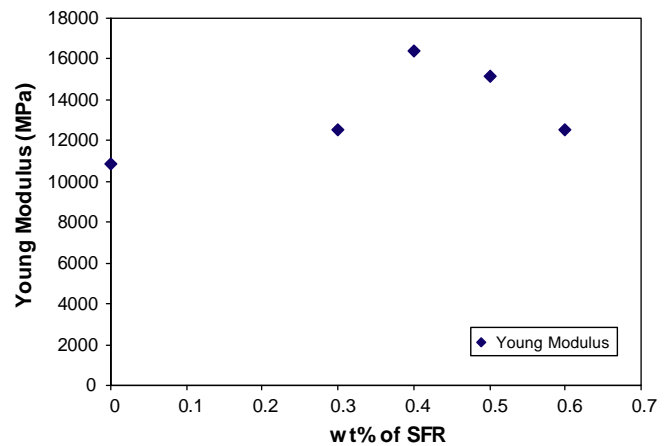
Fig. 3. Young modulus (MPa) versus content of short silk fibre (SSF) for type 1 sample.
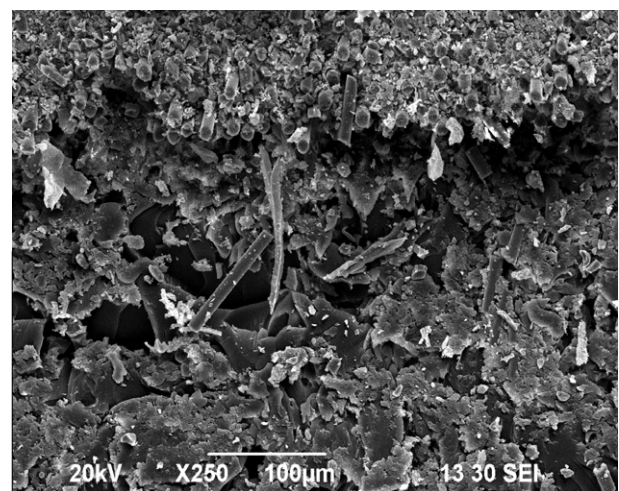
Fig. 4. SEM micrograph shows that short silk fibres link two ply of glass fabric.

the amount of silk fibres increase beyond 0.4 wt%. Fig. 4 shows the fracture surface of the sample with 0.4 wt% of silk fibres and it also indicates that the silk fibres could be effectively used to link up two plies together. Glass fibre breakage is obviously seen at the top (tow) of the figure and silk fibres penetrated through the top and bottom plies.
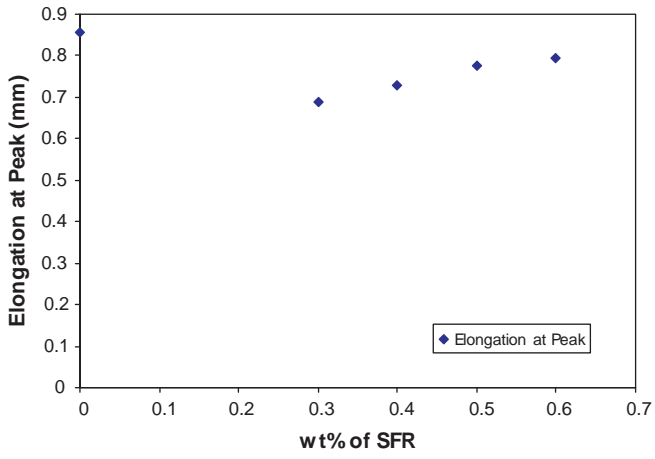
Fig. 5. Elongation (mm) versus content of short silk fibre (SSF) for type 1 sample.
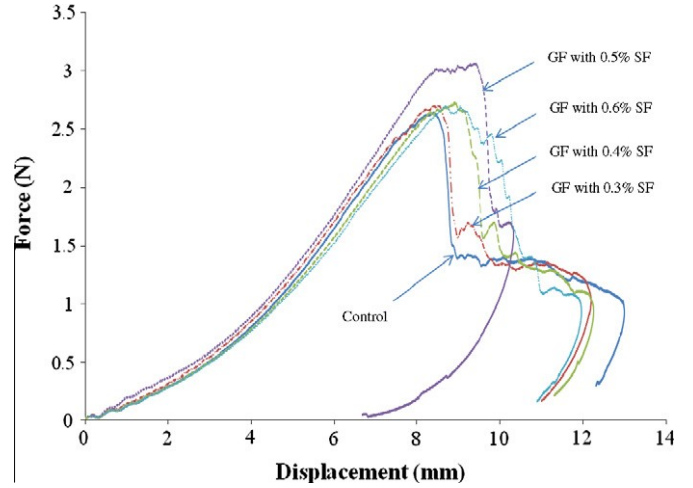
Fig. 6. Froce–displacement curves for impact test samples.
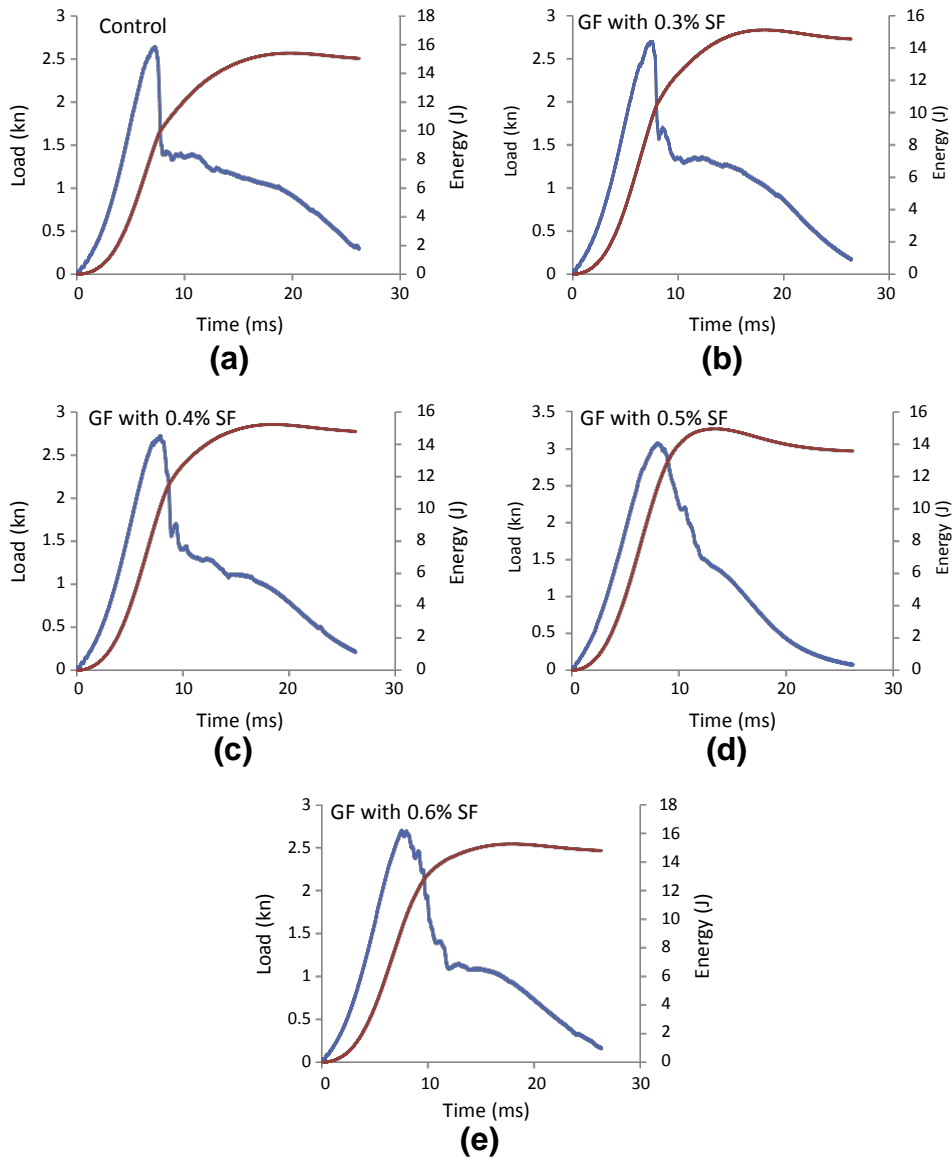
Fig. 7. Load and energy history curves of impact test for composites containing short silk fibre (a) control sample (0% short fibre), (b) glass fibre with 0.3% short silk fibre, (c) glass fibre with 0.4% short silk fibre, (d) glass fibre with 0.5% short silk fibre and (e) glass fibre with 0.6% short silk fibre.

Table 4
Impact data for control glass fabric and short silk fibre reinforced glass fabric composites.

Sample	P_{max} (kN)	E_m (J)	E_p (J)	V_i (m/s)	E_a (J)	E_i (J)	DI
GFR (control)	2.633	9.194	3.641	1.235	14.713	15.224	0.324
GF with 0.3% SF	2.683	9.405	5.335	1.233	14.724	15.243	0.568
GF with 0.4% SF	2.729	10.116	5.511	1.240	14.805	15.498	0.543
GF with 0.5% SF	2.895	10.752	5.695	1.233	14.854	15.283	0.493
GF with 0.6% SF	2.727	9.950	4.658	1.239	14.357	15.316	0.474

P_{max} is the peak load, E_m is the crack initiation energy, E_p is the propagation energy, V_i is the impact velocity, E_a is the absorbed energy, E_t is the total impact energy and DI is the ductility index, T is the total time of the impact test.
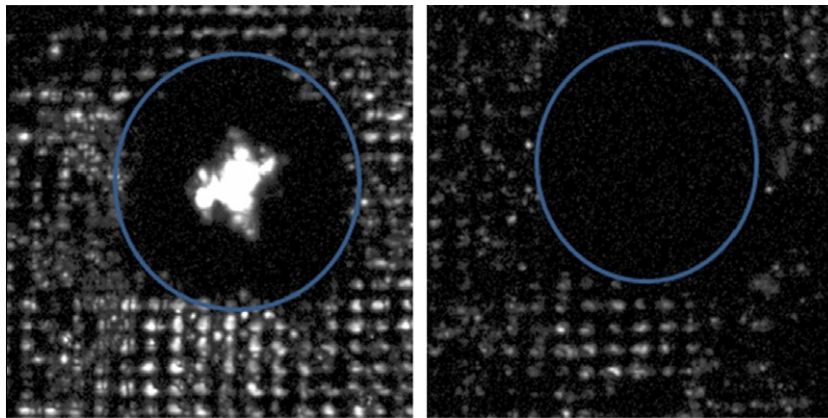
Fig. 8. C-scan of (a) pristine sample, (b) 5 wt% short silk fibre reinforced glass fabric composite.

Based on the results shown, it can be seen that increasing the amount of silk fibres to a certain percentage may cause the reduction of the amount of matrix filling the gap between plies which eventually caused the poor mechanical properties of the samples. Fig. 5 shows the adverse effect on the elongation at break of the coupons with different wt% of silk fibres. Therefore, their failure mechanism may be governed by three key factors, they are (i) bonding strength between the matrix and glass fibre; (ii) bonding strength between the matrix and silk fibre and (iii) bridging strength between glass fabrics by the silk fibres.

Principally, a composite sample with high tensile strength reflects that the stress transfer properties between the fibre and matrix were improved. It is because the silk fibres can act as the stress transfer media between the woven glass fibre and the matrix, and perhaps, from one ply to another. Some silk fibres, during the layup process may cross through the fabrics to form a network joining two fabrics together. Besides, more tortuous paths of crack growth for increasing fracture surface area of the composites containing short silk fibre is another reason of higher tensile strength. Such short fibre bridging effect implies that the unbroken in-plane randomly oriented short silk fibres link to the opposite fracture surface at the bridged zone. Therefore, more energy is needed to produce the crack propagation. However, a problem is raised in fibre reinforced polymer composites is the formation of resin rich regions inside the composites. It may not only lead to the low fracture toughness of the composites but also to other undesirable effects toward the mechanical properties.

As mentioned, short silk fibres were used to form the hybrid composite in this project and their aim is to overcome poor inter-laminar strength across plies [12]. During the layup process, vacuum bagging technique was used to remove excessive air inside the composite. Vacuum bagging technique also allows proper pressure applied onto the top of the composite in order to form a uniform thickness.

As shown in Figs. 2 and 3, the Young's modulus and tensile strength decrease for the silk fibre content exceeds 0.6 wt%. It

indicates that the silk fibres acted as small composite on its own with an inner structure prone to be broken by stress transferred by the matrix at the maximum strength. Thus, they at that time formed flaws which in turn acted as a crack initiator [13].

3.1. Impact test

The impact test was conducted by using INSTRON DDYNATUP 9250HV. All samples were cut to the final dimension of 100 mm × 100 mm for testing. The drop height was set at 0.8 m from the top surface of specimens. The mass of striker was 15.98 kg. The testing results including force–time curve, force-displacement, fracture energy and propagation energy were obtained by the testing machine automatically. Fig. 6 shows the relationship between force and displacement of the testing samples during the impact process. Fig. 7 shows load and energy curves of impact test for composites based on time. The results of the impact test are summarised in Table 4. It shows that increasing the amount of silk fibres in the composite results in increasing the maximum load, the crack initiation energy (E_m), the propagation energy (E_p), absorb energy (E_a) proportionally. Ductility index (DI) has proposed by Beaumont et al. which is the ratio of the propagation energy to the initiation energy for a sample under impact [14]. According to Table 3, most of the hybrid composites show higher DI value than the control pristine sample does. However, the DI value is not proportional to the total fracture energy which is same the finding from Lin and Jang [7].

Therefore, it is proved that the short fibres could play an important role in absorbing impact energy through their elastic-deformation and bridging plies together. However, when the content of silk fibres increased beyond 0.5 wt%, it is found that the maximum propagation energy decreases significantly. This may be due to the difficulty in wetting up the silk fibres and glass fibres as the viscosity increased during the manufacturing process, and thus, induced more voids inside the composite.

However, it was found that DI increases by 75% for the composite with silk fibre content of 0.3 wt%. This result shows that the crack
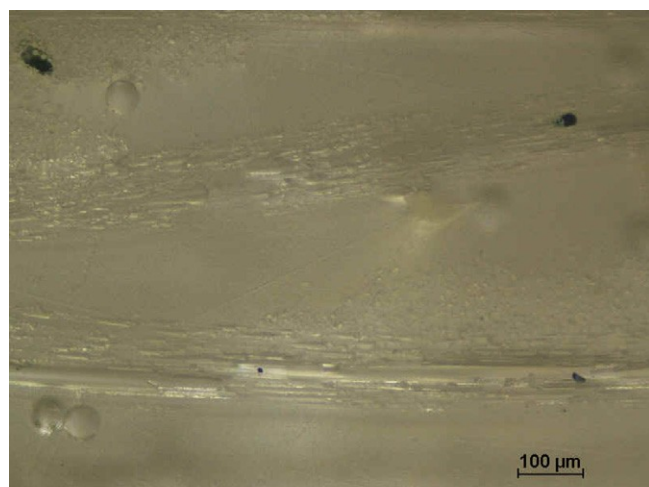
(a)
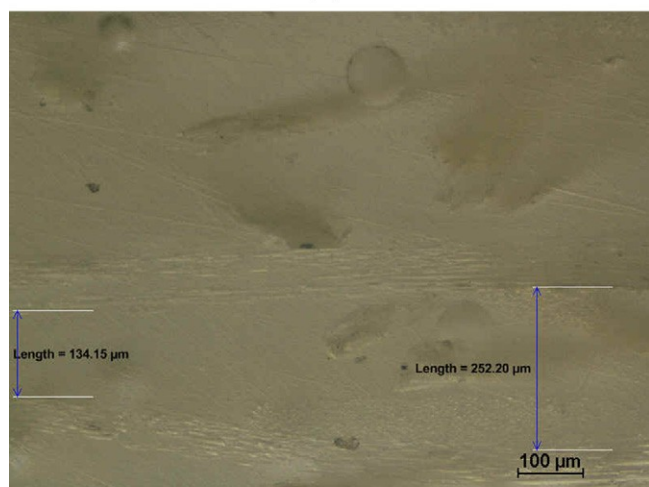
(b)

Fig. 9. (a) and (b) Showing the short silk fibres are placed in between two ply of glass fabric and attached to the woven glass fabric taken by optical microscope.

propagation behaviour of the hybrid composite can absorb more impact energy as compared with the pristine sample, i.e. the greater amount of incident energy to be dissipated into the hybrid composite [7]. Fig. 8 shows the C-scan images of pristine sample and a testing sample with 5 wt% of silk fibres after impact. It is obvious that penetration damage occurred in the sample without being reinforced by silk fibres while the hybrid composite had no penetration damage and only slight delamination appeared. Fig. 9a and b were taken by an optical microscope which show the short silk fibres

are fitted in between the plies of glass fabrics which allow a good stress transfer and act as cross-ply reinforcements.

4. Conclusion

A hybrid composite for combination of two types of fibres results in reduction of the effects of their less desirable properties and consequently balances of their pro and con properties in their inherently constitutional composite materials. Short silk fibres were introduced into the woven fibre reinforced polymer composites to form a new hybrid composite which possesses better Young's modulus and impact resistance properties. The mechanical properties enhancement of the hybrid composite was due to the silk fibre acted as a media for stress transfer from one ply to another. Based on the results shown, it indicated that the maximum Young's modulus and ductility index (DI) of the hybrid composite increased by 50% and 75%, respectively as compared with the pristine one. Furthermore, the visual examination on drop-weight test samples proved that the impact resistance of the silk reinforced composite was better than that of the pristine sample as well. According to the results obtained, it was found that the addition of 0.4 wt% short silk fibre into glass fibre composite was shown to be the advisable reinforcement content to achieve better tensile and impact strengths.

References

[1] Gibson Ronald F. Principles of composite material mechanics. McGraw-Hill; 1994.
[2] Saha N, Banerjee AN. Tensile behavior of unidirectional polyethylene-glass fibers/PMMA hybrid composite laminates. Polym Commun 1996;37(4):699–701.
[3] Subhash CK, Michael JK. Thick-section AS4-graohine/e-glass/pps hybrid composites: part 1. Tensile behaviour. Compos Sci Technol 1996;56:181–92.
[4] Shao-Yun F, Yiu-Wing M. Synergistic effect in the fracture toughness of hybrid short glass fiber and short carbon fiber reinforced polypropylene composite. Mater Sci Eng 2002;323(A):326–35.
[5] Manders PW, Bader MG. The strength of hybrid glass/carbon fibre composites part 1 failure strain enhancement and failure mode. J Mater Sci 1981;16:2233–45.
[6] Laurence W, Min-Seok S. Improving impact resistance of carbon-fibre composites through interlaminar reinforcement. Compos Part A 2002;33: 893–902.
[7] Lin TL, Jang BZ. Fracture behavior of hybrid composites containing both short and continuous fibers. Polym Compos 1990;17(5).
[8] Arbelaiz A, Fernandez B. Mechanical properties of flax fibre/polypropylene composites. Influence of fibre/matrix modification and glass fibre hybridization. Compos Part A 2005;36:1637–44.
[9] Singh S, Partridge IK. Mixed-mode fracture in an interleaved carbon-fiber/epoxy composites. Compos Sci Technol 1995;55:319–27.
[10] Zhihang F, Santare MH. Interlaminar shear strength of glass fiber reinforced epoxy composites enhanced with multi-walled carbon nanotubes. Compos Part A 2008;39:540–54.
[11] Park BY, Kim SC. Interlaminar fracture toughness of carbon fiber/epoxy composites using short Kevlar fiber and/or Nylon-6 powder reinforcement. Polym Adv Technol 1997;8:371–7.
[12] Youjiang W, Dongming Z. Characterization of interlaminar fracture behaviour of woven fabric reinforced polymeric composites. Composites 1995;26:115–24.
[13] Khan Mubarak A, Ganster Johannes. Hybrid composites of jute and man-made cellulose fibers with polypropylene by injection moulding. Compos Part A 2009;40:846–51.
[14] Beaumont PWR, Riewald PG, Zweben C. Foreign object impact damage to composites. ASTM STP 1974;568:134.

Recent research trend in natural-fibre composites

Since the mid 50's, interest in research and engineering has been shifting from traditional monolithic materials to fibre-reinforced polymer-based materials due to their unique advantages of high strength-to-weight ratio, non-corrosive properties and high fracture toughness for aerospace and military applications.

By

Alan K.T. Lau and Mabel M. P. Ho
Centre of Excellence in Engineered Fibre
Composites
University of Southern Queensland

These composite materials, which consist of high-strength fibres such as carbon, glass or aramid and a low-strength polymeric matrix, have dominated the aerospace, leisure, automotive, construction and sporting industries. In some industries particularly concerned with time and transportation costs, fibre-reinforced polymer composites do provide a great benefit due to their weight reduction potential, which increases the product volume that can be transported and reduces fuel consumption and thus carbon footprints. Unfortunately, in terms of environmental-friendliness, these fibres have serious drawbacks for the development of certain domestic products (like furniture, partitions and other secondary structural components) since they are non-renewable, non-recyclable and non-biodegradable, involve high energy consumption in the manufacturing process and pose health risks when inhaled.

Advantages

Although glass-fibre-reinforced composites have been widely used for many years to provide solutions to many structural problems due to their low cost and moderate strength, the use of these materials, in turn, leads to serious environmental problems that most Western countries are now concerned with. Recently, due to a strong emphasis on environmental awareness worldwide, much attention has been placed on the development of recyclable and environmentally-sustainable composite materials. In many countries, environmental legislation and consumer demand are increasing the pressure on manufacturers of materials and end-products to consider the environmental impact of their products at all stages of their life cycle, including recycling and ultimate disposal. In the United States, this encourages manufacturers to produce materials and products according to the "4Rs" principle, namely (i) Reduce the amount and toxicity of trash to be discarded (sourced reduction); (ii) Reuse containers and products; (iii) Repair what is broken (iv) Recycle as much as possible, which includes buying products with recycled content. Once these processes are played out, the materials are finally entitled to be disposed of in a landfill.

Based on the above-mentioned arguments, natural fibres (both plant- and animal-based) are being selected as a new class of reinforcements when developing composites for domestic and bio-medical engineering products. Table 1 shows the mechanical properties of different types of natural fibre and the resulting composites. Many studies have shown that hemp, sisal, jute, palm and bamboo fibres are excellent reinforcements to be combined with thermoplastic matrices to produce "green composites". Due to the renewability of these fibres, their extensive use would not induce any substantial harmful effect to the environment, particularly in terms of climate change. However, the growth cycle of the plants and geographical concerns may be an issue in the decision-making process for the type of fibre to be used. In China, Japan and Malaysia, for example, bamboo farms have to work out a sustainable plan on the use of bamboo and, in case of excessive growth, the farm owners may be fined by the government. In general, the growth cycle of bamboo is 6-8 months and its CO_2 absorption rate and O_2 production rate are almost 3 times that of other plants, so the supply of fibres in these regions is not an issue. Figures 1 and 2 show the families of natural fibres that can be potentially used for polymer-based composites.

Table 1: Material and mechanical properties of E-glass and other plant-based fibres								
Properties \ fibres	E-glass	Hemp	Jute	Ramie	Coir	Sisal	Flax	Cotton
Density (g/m^3)	2.55	1.48	1.46	1.5	1.25	1.33	1.4	1.51
Tensile strength (MPa)	2400	550-900	400-800	500	220	600-700	800-1500	400
Tensile modulus (GPa)	73	70	9770	44	6	38	60-80	12
Elongation at break (%)	3	1.6	1.8	2	15-25	39142	1.2-1.6	39357
Moisture absorption (%)	---	8	12	41608	10	11	7	44408

The structure, composition and filament arrangement in a single fibre are very complex. The filament wiring pattern and surface morphology are different even if the fibre types are the same. Since plant-based fibres are naturally available and their pre-processing cost is relatively lower than with other fibres for moderate-strength products, they are ideal materials for making domestic products, building and construction components (secondary structural members), and interior parts for automotive and aircraft engineering applications.

Fig. 1: Different types of plant-based natural fibres

Critical problems

Although much work has been carried out along these lines, there are still many critical problems that may affect the use of plant-based fibres in composite materials including the consistency of their quality and geometry, processing temperatures, water absorbability, hydrophilic and hydrophobic properties, interfacial bonding properties between the fibre and matrix (with and without surface treatment), and wettability under different manufacturing conditions.

Apart from plant-based fibres, animal fibres are another type of natural fibre that have been adopted recently for bio-medical engineering applications. Cocoon silk, spider silk, chicken feather fibre and human hair have also been used as reinforcement in bio-degradable/bio-resorbable polymers to form fully-biodegradable polymer composites. These fibres can be used as inlay made by protein-type materials and can be absorbed by the human body without inducing any adverse effects. Recent works focused on the combination of cocoon silk and chicken feather fibre with poly-lactic acid (PLA) to form a composite to be embedded in the human body for bone fixation.

Moreover, these fibres can also be used as cross-ply reinforcement to enhance the delamination resistance properties of typical plain-weave-fibre composites. The use of hair, indeed, is an ideal option as the source is abundant and it can be combined with polyester and polypropylene to form moderate-strength plastic materials.

However, from a psychological point of view, some users may refuse to use products based on materials extracted from the human body, therefore the idea was dropped by the industry (mainly in Asian countries). Chicken feather fibre may be a good alternative as a reinforcement fibre when developing new composites. Down feathers have demonstrated better mechanical strength than flight feathers when combined with epoxy and PLA, due to the hollow structure of the tip of the feather (Figure 3).

Fig. 2: Families of natural fibres for composites development

Research & development
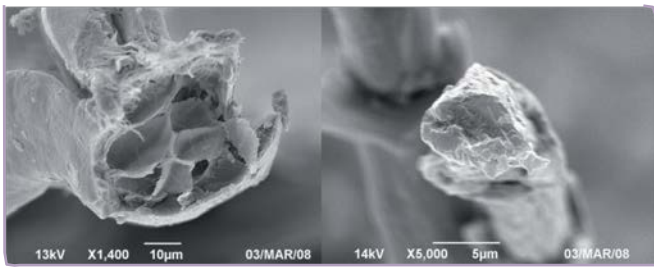
Fig. 3: Flight feather fibre (left), down feather fibre (right) from a chicken

Fig. 4: Cocoon shells treated at different temperatures

Table 2 shows the mechanical properties of different types of animal fibres used as reinforcement for polymer-based materials. The difficulties in adopting animal-based fibres for polymer-based composites are pretty much the same as in the case of plant-based fibres. However, the origin of the fibre sources and the sterilizing process are critical since the resulting composites will be used as implants or bone fixators. The processing temperature for injection moulding has to be accurately controlled. Typically, the degradation temperature of animal fibre such as silk is around 190°C, while it ranges from 180°C to 200°C for PLA. Surface treatments are commonly used to enhance the bonding strength between the fibre and matrix. In general, the Young's modulus of silk fibre/PLA composites, as compared with virgin PLA samples, increases while the tensile strength decreases. Degumming is normally needed to remove the surface protein layer of animal fibres. This layer may retard the bonding strength and thus, the strength of the composites. Since the cost/kg of animal fibre is relatively high as compared with plant-based fibres, they are normally used in bio-medical engineering applications instead of domestic product development.

Potential

The potential use of natural-fibre composites is thoughtfully examined in scientific literature and many discussions and initiatives have been ongoing in different countries. The mechanical properties of most plant-fibre-reinforced composites increase when increasing the amount of fibre in the polymer matrix. However, the ultimate strength decreases, as reported by different papers.

The use of plant- and animal-based fibres in product design and engineering has attracted much attention in bioengineering industries, and comprehensive research has been carried out in this field over the past few years. However, many issues such as their interfacial bonding and stress transfer properties have not yet been solved. To widen the application of these fibres in solving environmental problems, more studies are needed in the future.

The Centre of Excellence in Engineered Fibre Composites (CEEFC, Australia) has identified "green composites" as one of its focuses. Its work includes projects using natural-fibre composites (both plant- and animal-based) and geopolymers. Several projects are currently conducted in co-operation with the industry in the areas of building and construction structures, artificial reef design and development, hemp- and bamboo-fibre-reinforced polymers and bio-degradable and bio-resorbable bone fixators. The ultimate goal is to find other polymer reinforcement alternatives in order to develop new high-strength, low-cost and environmentally-friendly materials for different engineering and product applications. ■

More information
www.xxx

Table 2. Properties of animal-based fibres			
Animal fibre	Tensile strength (MPa)	Elongation at break (%)	Young's modulus (MPa)
Spider silk	875-972	17-18	40117
Cocoon silk	610-690	40999	15-17
Wool	120-174	25-35	2.3-3.4
Human hair:			
- Elderly	---	---	3.43
- Young	---	---	4.46

Critical factors on manufacturing processes of natural fibre composites

Mei-po Ho [a], Hao Wang [a], Joong-Hee Lee [b], Chun-kit Ho [c], Kin-tak Lau [a,d,⇑], Jinsong Leng [e], David Hui [f]

[a] Centre of Excellence in Engineered Fibre Composites, Faculty of Engineering and Surveying, University of Southern Queensland, Toowoomba, Queensland, Australia
[b] Department of BIN Fusion Technology, Chonbuk National University, Jeonju, Republic of Korea
[c] Department of Physics, The University of Science and Technology, Hong Kong, SAR, China
[d] Department of Mechanical Engineering, The Hong Kong Polytechnic University, Kowloon, Hong Kong, SAR, China
[e] Smart Materials and Structures Laboratory, Harbin Institute of Technology, China
[f] Department of Mechanical Engineering, University of New Orleans, New Orleans, LA 70148, USA

abstract

Elevated environmental awareness of the general public in reducing carbon footprints and the use non-naturally decomposed solid wastes has resulted in an increasing use of natural materials, biodegradable and recyclable polymers and their composites for a wide range of engineering applications. The properties of natural fibre reinforced polymer composites are generally governed by the pre-treated process of fibre and the manufacturing process of the composites. These properties can be tailored for various types of applications by properly selecting suitable fibres, matrices, additives and production methods. Besides, due to the complexity of fibre structures, different mechanical performances of the composites are obtained even with the use of the same fibre types with different matrices. Some critical issues like poor wettability, poor bonding and degradation at the fibre/matrix interface (a hydrophilic and hydrophobic effect) and damage of the fibre during the manufacturing process are the main causes of the reduction of the composites' strength. In this paper, different manufacturing processes and their suitability for natural fibre composites, based on the materials, mechanical and thermal properties of the fibres and matrices are discussed in detail.

Crown Copyright © 2011 Published by Elsevier Ltd. All rights reserved.

1. Introduction

Petroleum is a fossil fuel which is estimated to last for only another 50–60 years at the current rate of consumption [1]. Elevated environmental consciousness in the general public and preservation of non-renewable petroleum-based materials especially for petroleum-based plastics have resulted in an extensive use of natural fibre reinforced polymer composites for commercial and medical applications. Excessive use of petroleum-based plastics causes to a serious depletion of landfill capacities. Besides, the severe government's plastic waste control legislations and the growing interest among the customers in sustainable and environmentally friendly products drive the retailers and manufacturers trending towards their investment on the development of sustainable materials with acceptable cost, to alleviate an impact from global warming (including the reduction of carbon footprints). Therefore, the public awareness of increased un-decomposable solid wastes and their impact to the environment has awakened a new interest in the area of developing fully biodegradable polymers (also called

''biocomposites'') with controllable mechanical properties and biodegradation rate.

Recently, biodegradable materials have continued attracting much attention worldwide. Within the period of 2005 and 2009, the global market on the demand of biodegradable polymers was double in size. Among all countries in the World in 2009, Europe had the largest growth in the range of 5–10% on the use of biodegradable polymers as compared with 2008. The total consumption of biodegradable polymers is forecasted to grow at an average annual rate of nearly 13% from 2009 to 2014 in North America, Europe and Asia, which are accounted as the major global markets for materials' consumption [2]. However, high price and limited properties of the fully degradable polymer hinder the diversity of the usage. Therefore, in order to tackle on these problems and retard the exhaustion of natural resources, different projects along the line of developing biodegradable composites have emerged recently and it is general believed that these are one of most key materials in all industries in coming centuries. In aircraft and automotive engineering industries, some new projects have been created on the use of natural fibre (hemp, flax) reinforced biodegradable and fire-proof polymer composites. Natural fibre biodegradable polymer composites are generally defined as a type of materials which are generally composed of natural fibre and biodegradable polymer, as a matrix. The properties of these composites can be tailored for

⇑ Corresponding author at: Centre of Excellence in Engineered Fibre Composites, Faculty of Engineering and Surveying, University of Southern Queensland, Toowoomba, Queensland, Australia.
E-mail addresses: mmktlau@polyu.edu.hk, Kin-tak.Lau@usq.edu.au (K.-t. Lau).

various types of applications by a proper selection of fibres, matrix, additives and manufacturing process. The pre-treatment process of fibre plays a key role it controls the overall interfacial bonding properties and thus, successful stress transfer of resultant composites.

Normally, natural fibre polymer composites are fabricated by using traditional manufacturing techniques which are designed for conventional fibre reinforced polymer composites and thermoplastics. These techniques include resin transfer moulding (RTM), vacuum infusion, compression moulding, direct extrusion, compounding and injection moulding. Nevertheless, such techniques have been well developed and accumulated experience has proofed their successability for producing composites with controllable quality. However, their suitability for natural fibre reinforced polymer composites is still unsure due to the materials, geometrical, mechanical, thermal and structural properties of the natural fibres and biodegradable polymers are somehow, different with synthetic fibres and petroleum-based plastics, respectively. For example, chemical treatments on the fibre surface are normally required to compensate its incompatible bonding effect at the interface between the hydrophilic fibre and hydrophobic matrix. Other technical problems such as the uniformity of fibre distributed inside the composites, thermal degradations and weathering effect of fibre and matrix, water absorption of both fibre and matrix, wettability of resin impregnated into spaces between fibrils and breakage of fibres during mechanical stirring/mixing stages during the manufacturing processes also limit the use of natural fibres and biodegradable polymers for new composite development. Recently, seeking for technologies for developing fireproof natural fibre reinforced polymer composites is also one of key topics worldwide to apply them for aircraft interior components. Therefore, the resultant properties of composites in relation to the selections of right materials, pre-processing methods and manufacturing process are inextricably intertwined. In this article, different types of natural fibres and biodegradable polymers, their specific pre-processing techniques and fabrication methods are introduced and discussed in detail.

2. Materials selections

2.1. Natural fibres

Natural fibre is a type of renewable sources and a new generation of reinforcements and supplements for polymer based materials. Briefly grouping different categories of natural fibres, they can be divided based on their origin, derivations of plant, animal and mineral types which are detailedly shown in Fig. 1, [3–6]. These sustainable and eco-efficient fibres have been applied as substitutions for glass fibre and other synthetic polymer fibres for diverse engineering applications. Their remarkable advantages compared with those conventional inorganic manmade fillers enhance their commercial and research potentials. Natural fibres normally are abundantly-renewable resource so that their cost is relatively low as compared with other synthetic fibres. With the consideration of environmental consciousness, natural fibres are biodegradable so as they can alleviate the problem of massive solid wastes produced and relief the pressure of landfills if they are used for replacing other non-degradable materials for product development. Besides, according to their inherent properties, natural fibres are flexible for processing due to their less susceptible to machine tool damage and health hazards during the manufacturing and etc. Moreover, natural fibres possess many advantageous characteristics such as desirable fibre aspect ratio, low density and relatively high tensile and flexural moduli [7]. Table 1 summarizes the mechanical properties of natural and man-made fibres.

2.2. Plant-based fibres

By grinding the bark, the cell walls of most plant-based fibres can be viewed in Fig. 2a. The schematic representation of the cell wall of a natural plant is shown in Fig. 2b and this structure is often called as ''macrofibril''. The cell wall consists of a hollow tube, which has four different layers: one primary cell wall and three secondary cell walls and a lumen. The lumen is an open channel in the centre of the macrofibril. Each layer is composed of cellulose embedded in a matrix of hemicellulose and lignin [4]. The microfibril is composed of crystalline and amorphous regions alternately, as is shown in Fig. 2c [4].

The age of the plant, climate conditions and fibre processing techniques would greatly influence the structure of fibres as well as their chemical composition. The primary constituents of plant-based fibres (lignocelluloses) are cellulose, hemicelluloses and lignin. Cellulose contains alcoholic hydroxyl groups so that it is hydrophilic in nature [4]. The moisture content of plant-based fibre could reach to 8–12.6% [8]. Cellulose is a highly crystalline structure which contains as much as 80% of crystalline regions. The microcrystalline structure of cellulose includes crystalline regions (higher packing density) of high order, which are extensively distributed throughout the fibre, and lower order amorphous regions (lower packing density) [4]. Hemicellulose is made up of highly branched polysaccharides including glucose, mannose, galactose, xylose, a group of polysaccharides (excluding pectin) attached to the cellulose after the removal of pectin. Hemicellulose contains different types of sugar units. It is also a highly branched polymer (contrasting with the linear cellulose) and has a degree of polymerisation 10–1000 times lower than that of cellulose [4]. Lignin is amorphous, highly complex, mainly aromatic, polymers of phenyl-propane units [2]. Lignin stiffens the cell walls and acts as a protective barrier for the cellulose. The function of Lignin is a structural support material in plants. During synthesis of plant cell walls, polysaccharides such as cellulose and hemicellulose are laid down first, and lignin fills the spaces between the polysaccharide fibres and cementing them together. This lignification process causes a stiffening of cell walls, and the carbohydrate is protected from chemical and physical damage [8].

The basic chemical structure of cellulose in all plant-based fibres is similar but they have different degrees of polymerisation whereas the cell geometry of each type of celluloses varies with the fibres. These factors contribute to the diverse properties of the green fibre (Fig. 3).

2.3. Animal-based fibre

An animal fibre generally is comprised of proteins such as collagen and keratin. It can be divided into animal hair and silk. Animal hair fibre is defined as the fibre which is taken from animals and hairy mammals. Examples of animal hair are sheep's wool, cashmere, alpaca hair, horse hair. Sheep's Wool is mainly composed of a-keratins, a protein which mainly forms the horny layer of the epidermis and of epidermal appendages such as hair. Wool is a multi-component fibre which consists of about 170 different protein molecules and these protein molecules constitute the morphological components of wool [9]. The diameter of wool fibre is in the range of 20–40 μm and the cross-section is elliptical [10]. The wool fibre is typically divided into three morphological components including cuticle, cortex and cell membrane. The microfibrils in the cortex represent approximately 50–60% by mass of the cortex material, the bonding between the microfibrils and their embedding matrix within the cortex and the presence of the organised helics within the microfibrils dominate the mechanical and water absorption properties of wool fibres [11]. Another type of animal hair is avian fibres, which are feathers and feather fibre. Chicken
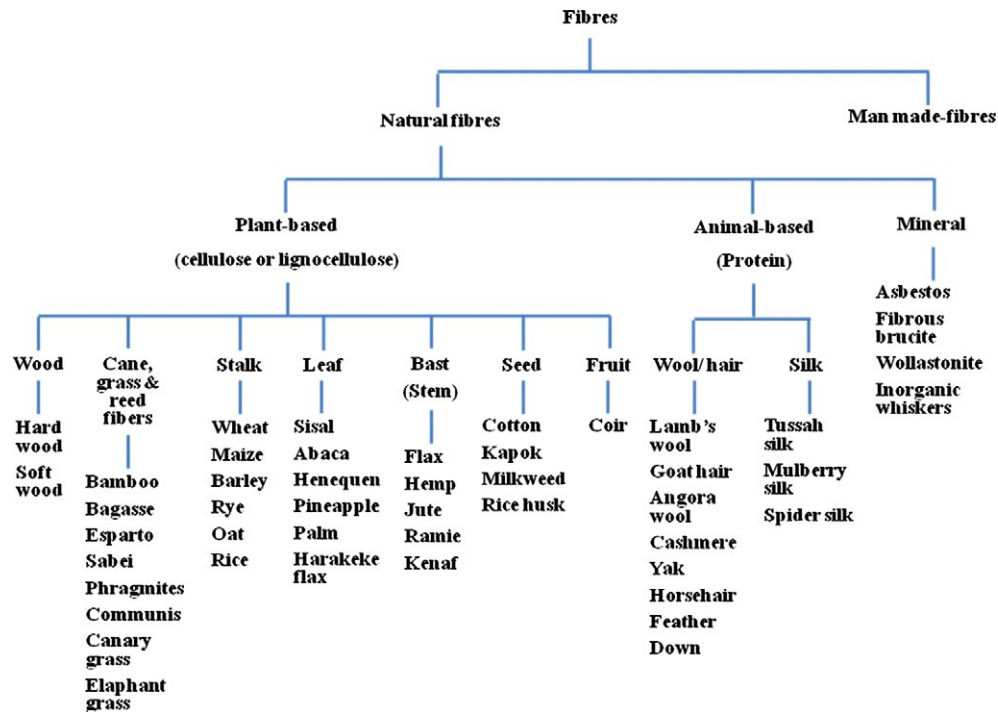
Fig. 1. The classification of different natural fibres.

Table 1
Mechanical properties of natural and man-made fibres.

Fibre	Density (g/cm^3)	Elongation (%)	Tensile strength (MPa)	Young's modulus	Refs.
Natural fibre					
Cotton	1.5–1.6	7.0–8.0	287–597	5.5–12.6	[8]
Jute	1.3	1.5–1.8	393–773	26.5	[8]
Flax	1.5	2.7–3.2	345–1035	27.6	[8]
Hemp		1.6	690		[8]
Ramie		3.6–3.8	400–938	61.4–128	[8]
Sisal	1.5	2.0–2.5	511–635	9.4–22.0	[8]
Coir	1.2	30.0	175	4.0–6.02	[8]
Viscose (cord)		11.4	593	11.0	[8]
Soft wood kraft	1.5		1000	40.0	[8]
Kenaf		1.5	930	53	[10]
Nettle		1.7	650	38	[10]
Abaca			430–760		[10]
Oil palm	0.7–1.55	3.2	248	25	[10]
Pineapple		2.4	170–1627	60–82	[9]
Banna		3	529–914	27–32	[9]
Wool		25–35	120–174	2.3–3.4	[9]
Spider silk		17–18	875–972	11–13	[9]
B. mori silk	1.33	19.55	208.45	6.10	[11]
Twisted B. mori silk		20.57	156.27	3.82	[11]
Tussah silk	1.32	33.48	248.77	5.79	[11]
Man-made fibre					
E-glass	2.5	2.5	2000–3500	70.0	[8]
Aramid	1.4	3.3–3.7	3000–3150	63.0–67.0	[8]
Carbon	1.4	1.4–1.8	4000	230.0–240.0	[8]

feathers are approximately 91% protein (keratin), 1% lipids, and 8% water. Their fibre diameters were found to be in the range of 5–50 1m [12]. Experimental results have showed that the tensile strength varies indirectly with the moisture content. The tensile strength of feather rachis conditioned at 100% relative humidity was 106 MPa. The tensile strength of feather rachis conditioned at 0% relative humidity was 221 MPa [12]. The Young's modulus increased remarkably along the length of the rachis, with the highest values at the feather tip. X-ray diffraction measurements showed more keratin molecule orientation further out along the rachis.

Moreover, the fibre located closer to the bird is smaller in diameter and has lower physical properties compared with the fibre which is far from the rachis [13]. It is obvious that flight feather fibre exists in a hollow form while down fibre is in solid. In terms of the purpose of fibre-reinforcement, the use of down fibre appears much better than that the use of flight fibre [14].

Silk fibre is a type of fibre collected from dried saliva of bugs or insects during the preparation of cocoons. Silks are generally defined as protein polymers that are spun into fibres by some Lepidoptera larvae such as silkworms, spiders, scorpions, mites
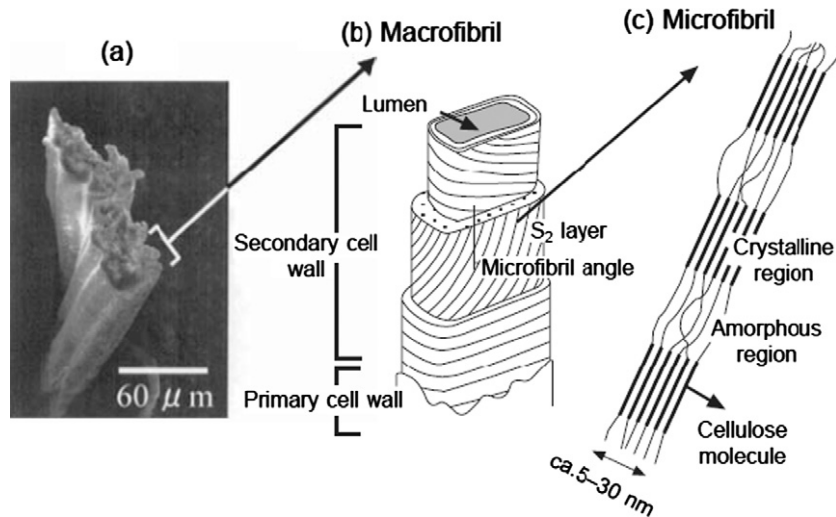
Fig. 2. (a) Scanning electron micrograh of a kenaf bark fibre, and schematic representations of, (b) macrofibril and (c) microfibril of natural plant [4].
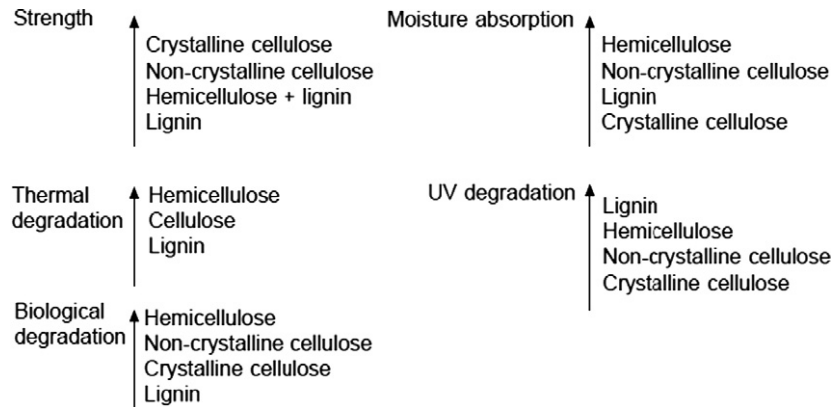
Fig. 3. Properties of cellulose fibres and their dependence on chemical constituents [4].

and flies [15]. Spiders have six or seven sets of glands including major and minor ampullate, flagelliform, aggregate, cylindrical, aciniform and piriform for production of fibres with different amino acid composition. These silks serve as: (1) orb-web Frame, (2) prey capture, (3) wrapping, (4) joint and attachment, (5) reproduction, (6) vibrational sensor and (7) dispersion [16]. The mechanical properties of the dragline silk are highly influenced by the composition of amino acids, insect size, diet conditions, body temperature and drawing speed. [16] Some spider silks exhibit over 200% elongation. Compare with kevlar fibre, the tensile strength of spider silk is a factor of four less than kevlar fibre (3.4–4.1 GPa), but the energy used to break the silk is about three times greater $(1 \times 10^5 \, \text{J kg}^{-1})$ [17]. However, the predatory nature of spider silk causes it difficult to handle so that the production of spider silk fibre is relatively low compared to silkworm silk fibre [15].

Arthropods including spider and silkworm have evolved to produce a variety of task-specific silk-protein-based fibre. However, Silkworm silk fibre is different to the spider silk fibre as only one type of silk generate by individual silkworm but individual spider can generate 6–7 types of silk for different purposes. Moreover, the dragline produced by spider silk cannot yet be produced in sufficient quantity to support any industrial process. Moreover, the glue-like proteins are generally absent in the spider silk. Therefore, silkworm silk is found to be a higher potential material used for industry and medical application.

The silkworm cocoon is built at the end of the larval stage and protects the pupa during metamorphosis to an adult moth. It contains silk protein, known as silk fibroin which is stored in the glands of insects and spiders as an aqueous solution. It is understood that the water is acting as a plasticizing agent, keeping the protein malleable [18]. Silk protein is usually produced within specialised glands after biosynthesis in epithelial cells, followed by secretion into the lumen of these glands and prepared to spin out as filament [15]. During the spinning, the concentration of silk in the solution is gradually increased, formation of shear and elongational stresses acting on the fibroin solution in the gland. Elongational flow orients the fibroin chains, and the fibroin (liquid) is converted into partly crystalline, insoluble fibrous filaments (solid) [27]. The bulk of the polymer chains in the crystalline regions are oriented parallel to the fibre axis [18]. Simpson et al. [19] have found that the speed of spinning controls the mechanical properties of fibre.

Silkworm silk, the core filament is an inhomogeneously distributed polymer blend of mainly two proteins that is coated with glycoproteins and lipids [20]. The silkworm cocoon silk fibre is composed of two cores of fibroin because their gland is a paired organ which surround by a cementing layer of sericin in a structure known as bave shown in Fig. 4 [21]. The core fibres are encased in a sericin coat, a family of glue-like proteins that hold two fibroin fibres together to form the composite fibres of the cocoon case [22]. This glue-like proteins is called sericin which is amorphous in nature and acts as binder to ensure the structural integrity of the cocoon [23]. The fibroin fibre itself is a bundle of several fibrils with a diameter of 1 1m. A fibril contains 15 nm wide microfibrils.
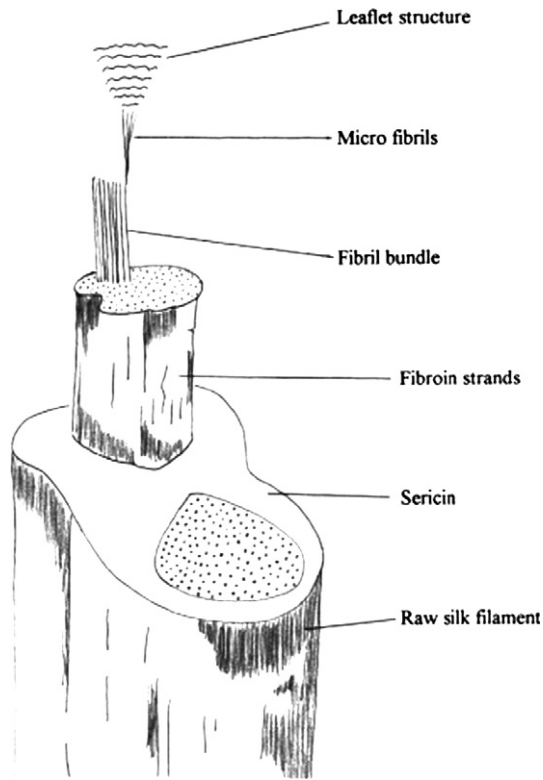
Fig. 4. Structure of silkworm silk fibre [21].

Microfibrils are packed together to form the fibril bundle and several fibril bundles produce a single strand [23,24].

The convenience of reeling long (300–1200) continuous fibre from the cocoon has certainly contributed to its success as a textile fibre. However, a long and continuous fibre can only be reeled from the cocoon after the adhesive sericin coating is removed. Sericin removal requires thermo-chemical treatment of the cocoon in a process conventionally known as degumming [21]. However, degumming would weaken at least one type of non-covalent interaction of core fibroin, such as hydrogen bonds and Van der Waal's bonds. The two important factors associated with degumming could affect the tensile properties of silkworm silk because of the change in the microstructure of two core fibroins [22].

Compared with the commercially Mulberry silkworm silk (Bombyx mori), Tussah silk is a textured silk with the brownish toned. It is mainly due to tannin from the variety of trees fed by the caterpillars. Most silkworm cocoon and spider dragline silk fibres contain assembled anti-parallel b-pleated sheet crystalline structures. Silks are considered semi-crystalline materials with 30–50% crystallinity in spider silks, 62–65% in cocoon silk fibroin from the silkworm B. mori, and 50–63% in wild-type silkworm cocoons [27]. Fig. 5 shows the cross section, longitudinal view and perspective of silk filaments.

2.4. Biodegradable polymers

Conventional polymers such as polyethylene (PE) and polypropylene (PP) are used for many years and have been developed to be an absolutely necessary part of our life in almost every area nowadays. With time and the rapid development of science and technology, the mechanical property, stability and durability of conventional polymers have been improved continuously. However, these long lasting polymers seem inappropriate in application of the product which has short product life cycle, such as plastic plates and fork for party. These polymers persist for hundred years in a landfill after disposal. Therefore, advantages as disadvantage, high durable property of these polymers increase the environmental burden. Moreover, these polymers are often disposed and stained with food residue; increase the complexity of the plastic recycling. The cost of recycling of plastic is thus so high and so that there is no choose to land filling or incineration of plastic. As the public starts focusing on the huge environmental accumulation of these long lasting polymers and pollution problem caused during and after the life cycle of the polymers (such as manufacturing and disposal process), and fitting the modern society, the study on naturally-degradable polymers with short life cycle is needed.

Biodegradable polymers were first introduced in 1980s [25] which are designed to degrade upon disposal by the action of microorganisms. In general, polymers are solid, non-metallic compounds with high molecular weight. They are comprised of repeated marcomolecules, and have varying characteristics. Material usage and final mode of biodegradation are dependent on the composition and processing method employed [26]. These polymers means capable of undergoing decomposition into carbon dioxide, methane water, inorganic compounds or biomass in which the predominant mechanisms is the enzymatic action of micro-organisms that can be measured by standard tests, over a specific period of time, reflecting available disposal conditions.
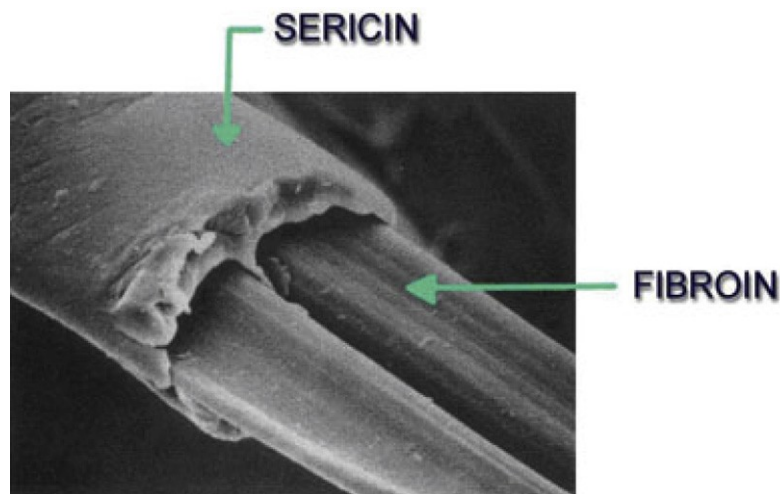
Fig. 5. Cross section, longitudinal view and perspective of silk filaments.

These polymers can be also classified on the basis of the origin, that is, naturally occurring or synthetic in Fig. 6 [27]. Natural polymers are available in large quantities from renewable sources, while synthetic polymers are produced from non-renewable petroleum-based resources. Nowadays, degradable polymers used in various forms including films, moulded articles, sheet, etc. The potential applications of biodegradable applications include: (1) film such as plastic shopping bags and bin bags, (2) cling wrap, (3) flushable sanitary products, (4) sheet and non-woven packaging, (5) bottles and container, (6) loose fill foam and (7) medical application. Among these biodegradable polymers, aliphatic polyesters

constitute the most attractive family have been extensively studied. Table 2 summarizes the properties of aliphatic polyesters. Polyesters play a predominant role as biodegradable plastics due to their potentially hydrolysable ester bonds.

Poly (lactic acid) (PLA) belongs to the family of aliphatic polyesters derived from a-hydroxy acids. PLA is a compostable polymer derived from renewable sources which is mainly from starch and sugar. Since PLA is compostable and derived from sustainable sources, it has been viewed as a promising material to reduce societal solid waste disposal problems [28]. A high-molecular PLA cannot be directly synthesised from the molecule of lactic acid, mainly
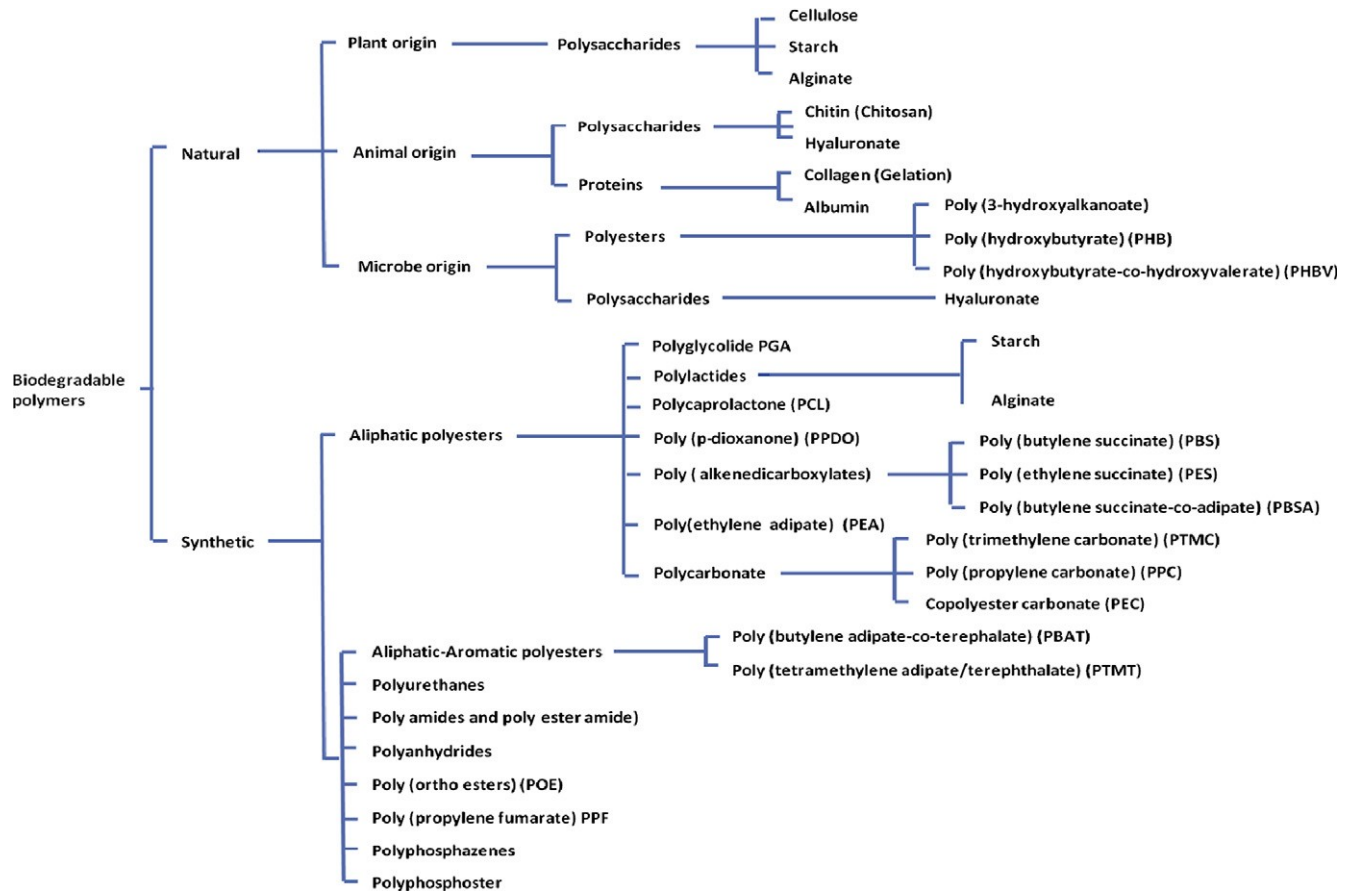
Fig. 6. Natural and synthetic biodegradable polymers [27].

Table 2
The properties of aliphatic polyesters.

Examples	Crystallinity	Glass transition temp.	Melting point	Modulus	Loss strength (month)	Loss mass (month)	Processing temp.	Refs.
Poly (butylene succinate) (PBS)		−45 to −10	90–120	0.4–0.6			160–200	[32,38]
Poly(ethylene succinate) (PES)		−45 to −10	90–120				160–200	
Polyglycolide (PGA)	45–55%	35–40	200	12.5 Gpa	1–2	6–12		[38]
Polycaprolactone (PCL)	67	-60	55–60	0.19		24–36		[38–40]
Polylactides								
Poly L-lactide (PLLA)	rv37	60–65	170–180	4.8	rv6	12–24		[38,39]
Poly D-lactide (PDLA)								
Poly DL-lactide (PDLLA)		55–60		1.9	1–2	12–16		[38]
Polydioxanone PDS, PPDO	High	<20	2.1	1.5	1–2	6–12		[38,35,42]
Poly hydroxyalkanoates PHA								
Poly(3-hydroxybutyrate) (PHB)	80	5	173–180	0.9–4				[40,41]
PHV								
PHH								
Poly(trimethylene carbonate) PTMC						3–4		[38]

because of the generation of water during the condensation process (leading to the degradation of the PLA formed and formation of only low-molecular oligomer). In general, three different ways can be followed to solve this problem:

(1) Addition of chain-coupling agents during the condensation process.
(2) Dimerization the oligomer into cyclic lactide (see above), distillation of solution to take out the water condensed and then production of the PLA by ring-opening polymerisation.
(3) Azeotropical dehydration during the condensation process, removing the water during the process by change of pressure.

PLA belongs to the family of the polyester and is generally linear (without strong entanglement, branching between the chains). The structure of the molecule influences its mechanical and thermal properties (for PLA 3051D: T_g is 55–65 oC, T_c 150–165 oC and tensile strength rv48 MPa [29]), which are quite similar to other polyesters (such as PET). The thermal properties are however a bit lower, due to the absence of the benzoic cycle (chain more free to move). Its chemical properties and water resistance are weakened by the presence of the carbonyl group (C@O), which allows hydrolysis degradation. Like most of the polymers, the different macromolecules (chains) are bonded together by hydrogen bonds (Van de Waals forces). Most important mechanical and thermal properties (crystallinity rate, T_g and Tm) are then influenced by the concentration and disposition of different enantiomers (L- and/or D-lactic acid). Indeed, the chains made of a unique basic element can align each other easier in a configuration favoring inter chain bonds. Thus the lowest T_g is found in racemic mixing of L- and D-enantiomers while the highest properties are obtained by stereo complex PDLA and PLLA blends (respectively using the D- and L-enantiomers) and reach a maximum with a ratio of 50:50. Like most polymers, PLA is hydrophobic. It can only absorb 1% water content and undergo hydrolytic degradation, making it biodegradable and environmentally friendly. PLA normally undergoes three main degradation processes: (i) chemical hydrolysis, (ii) enzymatic degradation and/or (iii) microbial degradation [30]. During chemical hydrolysis, the water molecule attacks the double bounding C@O of the PLA, like shown below:

The enzymatic degradation occurs mainly in the amorphous region of the polymer and seems to attack preferentially the ester bonds of L-lactic acid (cleaving the polymer). The PLA-degrading and the silk fibroin-degrading enzymes belong roughly to the same groups and it seems that the L-lactic acid unit of PLA is recognised as similar to the L-alanine unit of silk fibroin. The same conclusion can be made for the microbial degradation, where the bacteria's ability to degrade the PLA and silk are linkable. One can moreover note that the bacteria able to degrade PLA are more scarce than the ones able to degrade most of others polyesters [15].

In order for PLA to be processed on large-scale production lines in applications such as injection moulding, blow moulding, thermoforming, and extrusion, the polymer must possess adequate thermal stability to prevent degradation and maintain molecular weight and properties. PLA undergoes thermal degradation at temperatures above 200 oC (392.8 oF) by hydrolysis, lactide reformation, oxidative main chain scission, and inter- or intra-molecular transesterification reactions. PLA homopolymers have a glass transition and melt temperature at about 55 oC and 175 oC, respectively. They require processing temperatures over 180 oC. At this temperature, unzipping and chain scission reactions leading to loss of molecular weight, as well as thermal degradations, are known to occur. Consequently, PLA homopolymers have a very narrow processing window. The rheological properties of PLA, especially the

shear viscosity, have important effects on thermal processes, such as injection moulding, extrusion, film blowing, sheet forming, fibre spinning, and thermoforming. Poly-Lactide melts are shear thinning, similar to polystyrene. Its working temperature is dependent on the melt viscosity, which is, in turn, dependent on the weight-average molecular weight of PLA, the amount of plasticizer, the shear rate, the type of melt processing, and the amount of work put into the polymer. Under the same processing conditions, semi-crystalline PLA had a higher shear viscosity than amorphous PLA. As the temperature increased, the shear viscosity decreased for both types of PLA. The PLA melt was characterised as a pseudo plastic, non-Newtonian fluid [31].

3. Processing of raw materials

3.1. Selection criteria

Suitable manufacturing processes must be utilised to transform the materials to the final shape without causing any defect of products. For the selection a suitable process to fabricate biodegradable polymer-related composites, design and manufacturing engineers would mainly focus on numbers of criteria including desired properties, size and shape of resultant composites, processing characteristics of raw materials, the production speed and the manufacturing cost. The size of the composites is a dominating factor for the preliminary assessment on a suitable type of manufacturing processes to be used. For small to medium sized components, injection and compression mouldings are preferred due to their simplicity and fast processing cycle. However, for large structures, they are typically manufactured by open moulding and autoclave processes. Similar to other plastic products, the complexity of shape of a product also influences the type of manufacturing processes to be used. For example, filament winding is the most suitable method for manufacturing composites pressure vessels and cylinders. Recent development has also used carbon fibre wrapped on the surface of forged Aluminium cylinders to form ultra-high pressure tanks.

Pultrusion is mainly used for producing long and uniform cross-section parts. In some extent, optic fibre can be integrated into the pultrusion process to produce self-structural-health monitored composite structures. The shape of the parts being made is highly dependent on the shape of the die. Somehow, several stages of heat control are needed to cure the composite parts. Depending on the performance of composites products, suitable raw materials (thermosets/thermoplastics, high/low viscosity, processing temperature) should be chosen with an appropriate composite fabrication technology.

However, in certain extent, the criteria of selecting the right manufacturing processes for natural fibre composites are different with that to be used for traditional polymers. The properties of natural fibre composites are highly dependent on the length, orientation, diameter and content of fibre. The surface condition of the fibre also plays a key role as it would affect the bonding interface between the fibre and surrounding matrix. Removal of a surface coating of fibre (like silk and coir fibres) or pretreatment of fibre (like hemp) by using chemical process may be needed to ensure a good bonding is resulted. Theoretically, high tensile strength could be achieved by increasing the amount of fibre used. However, it may not be done by using injection moulding process as the expansion of fibre in wet condition could cause a sucking effect. Therefore, compression moulding may be used for a simple form of composites products.

Natural fibres extracted from wool and cocoon silks are comprised of numerous of micro-fibrils. It has been reported that these fibres after degumming, only two triangular fibrils (brins) would be remained, and these fibrils are formed by several thousands of
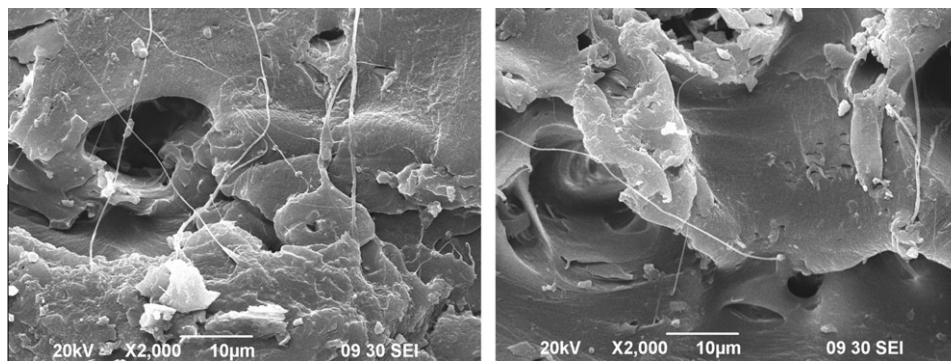
Fig. 7. Scanning electron micrographs showing the micro fibrils of the silk inside the composites.

micro-fibrils as shown in Fig. 7. A noteworthy weakness in the natural fibre reinforced thermoplastic composites is the poor interfacial bonding between the fibre and matrix. The interfacial adhesion between them plays an important role in determining the performance of the composites. This is mainly due to their dissimilar hydrophobicity as the surface of fibre is hydrophilic while organic plastics are generally hydrophobic, they are incompatible and prevent efficient fibre–matrix bonding. The incorporation of hydrophilic fibres in polymers leads to heterogeneous systems whose properties are inferior due to poor adhesion between the fibres and the matrix [32–34]. Therefore, these debonded fibres dilute the matrix content and act as flaws which reduce the effective cross sectional area and, finally poor mechanical strength is resulted. Moreover, the formation of fibres agglomeration, due to the inter-fibre hydrogen bonding which prevents thorough dispersion of fibres during the manufacturing process and thus weakens the strength and affects the appearance of the composites [32,35].

Thus the treatment of natural fibres for adhesion improvement is a critical step in the development of the composites. Different treatments such as pre-impregnation, surface modifications, chemical reactions and plasma have been studied for interfacial shear strength improvement in order to develop composites with better mechanical properties [32,33,36–38]. Natural fibre always cannot be wetted completely by following the general manufacturing processes as they are not designed for wetting fibre with tight-packing fibrils. The viscosity of polymers is normally too high for impregnation. Better fibre pre-impregnation allows a better fibre wetting and thus enhances the mechanical interlocking between fibre and matrix [36].

The surface modifications of fibres by using compatibilizer or coupling agent for effective stress transfer across the interface were explored. The compatibilizer is a kind of polymeric interfacial agent or polymers with functional groups that graft onto the chain of polymers. Besides, coupling agent is a chemical substance which is able to react chemically on the both natural fibre and the polymer matrix during processing to form or promote a stronger bond at the interface as bridges in order to improve the mechanical properties of resultant composites. The nature of bond formed between a specific coupling agent and fibres depends strongly on the characteristics of the fibre surface to which the coupling agent is adhered [32]. The coupling agents are tetrafunctional organometallic compounds which are commonly known as silane, zirconate, or titanate coupling agents [33]. Rozli Zulkifli et al. [38] have found that the silk/epoxy composite with fibre surfaces which treated by silane-based coupling agent shown an improvement of the adhesion. Keener and Stuart [34] used polyethylene couplers and the results indicated that the tensile strength and impact property of the coupled composites were improved as compared with non-coupled blend composites. Kazayawoko et al. [35] used Maleated

polypropylene (MAPP) as a coupling agent and the effectiveness of MAPP has been attributed to its ability to wet and disperse the wood fibre efficiently.

Chemical treatments such as dewaxing, delignification, acetylation, and chemical grafting are used to modify the surface properties of the fibres and enhance the performance of composites [33]. Alkaline processing is one of the most common chemical treatments in the industry which are not only used for increasing the surface roughness of the natural fibre that results in a better mechanical interlocking, but also for the increments of the amount of cellulose exposed on the plant fibre surface, thus increasing the number of possible reaction sites. Valadez-Gonzaleza et al. [36] have explored the fibre–matrix interphase physicochemical interactions of the natural fibre reinforced plastic. They have found that the fibre surface area was increased by the means of alkaline treatment.

Plasma treatment is an environmentally-friendly new technology which can alter the surface properties of the materials without interfering their bulk properties. Chaivan et al. [36] have studied the utilisation of SF6 plasma treatment for improvement in hydrophobic property of silk fibre. A reproducible and significant increase in the hydrophobic property compared with the untreated sample was obtained.

4. Moulding processes

4.1. Injection moulding

Injection moulding of composites is a process that forces a measured amount of mixture which contains molten polymer and fibre into mould cavities. Many studies have been conducted on the potential of using natural fibres as reinforcement for renewable polymers to make a composite through injection moulding [40–45]. The original thermoplastic polymer used by this process was designed for plastic pellets. For fibre reinforced composites, the pellets with chopped fibres are fed individually through a funnel-shaped feed hopper into a heated compression barrel with a rotating screw (''screws'' for twin-screw extruder). The purpose of heating the barrel is to transform the solid pellets into viscous liquid which can be drove through the sprue nozzle and finally forced into the matched-metal closed mould cavities. The mould is tightly clamped against injection pressure where the polymer solidifies, freezing the orientation and distribution of fibres. The composite is then removed from the closed mould after it is sufficiently cooled to be ejected to form a part of desired shape. As the mixture is required to move toward to the sprue nozzle, polymer is pressurised because of the screw mechanism. The function of the screw is to (1) generate heat by viscous shearing to melt the

polymer, some heat that is used for melting pellets evolved from the friction in between pellets, barrel and screw [45], (2) apply the shear force to mix the polymer and fibre and (3) act as a piston to force the mixture of fibres and molten polymer through sprue nozzle into a matched-metal closed mould. It has been reported that as the temperature increases, the shear viscosity of biodegradable polymers would decrease which makes the flow easier. Besides, as the shear rate increases, the viscosity of the polymer melts would also be decreased significantly. This change of viscosity is caused mainly by the breaking of PLA molecule chains due to the strong shear forces and temperature [46].

Fibre that is used in the injection moulding is usually chopped into short fibre according to the critical fibre length criterion in which the stress should be fully transferred from the matrix to the fibre and the fibre can be loaded to its full capacity assuming a good interfacial bonding is resulted. However, the traditional injection moulding process limits the fibre length that solidifies in the final part since the high shear rates in the barrel and the passage of fibres through narrow gates and openings in the mould which cause significant fibre attrition. Therefore, the fibre length in practice is normally shorter than the predicted fibre length because of the fibre attrition. This fibre attrition causes the fibre length below the critical length as expected, the fibres shorter than the critical length would not be able to carry their maximum load effectively. In an extreme case, the fibre rather acts as a defect in the material not only because of its length effect, but also on the poor bonding properties. Nevertheless, if the fibre length is beyond the pre-determined critical length, it will carry an increasing fraction of the applied load and may fracture prior to the failure of the matrix. Therefore, it is necessary to carefully determine the critical length of the fibre before injection moulding is performed. On the other hand, increasing fibre content would theoretically improve the stiffness and the strength of resultant composites. However, in practice, the traditional injection modelling process would limit the amount of fibres to be injected because of the fibre cluttering, narrow gate and sprue and, viscosity of the fibre/polymer mixture. Another main issue is the volume expansion of the fibre after mixing with the liquid form of matrix.

Residual stress and fibre orientation with respect to the depth are also the critical issues which affect the modulus distribution of the injection moulded composites. Residual stress is an internal stress which occurs as a result of the rapidly cooling of molten polymer in the absence of external forces. In general, the residual stress distribution shows tensile stresses at the surface and core regions and compressive stress at the intermediate region, which is well-known as the characteristic residual stress distribution in injection-moulded parts [47]. Numerous of researches have therefore studied the residual stress distribution of composites made by the injection moulding process [46–49]. (1) High pressure gradient, (2) non-uniform temperature profile caused by inhomogeneous cooling of the polymer melt, (3) orientation of polymer chains and (4) the difference in thermal expansion coefficient between matrix and fibres are the common phenomena which residual stresses may be introduced in injection moulded polymers or composites during filling, packing, and cooling stages.

When the flow is ceased, the molecule orientation starts to relax while solidification process subsequently occurs before this process is completed. It would impede the relaxation of the molecular orientation which is then frozen in, the residual stress is therefore formed inside the part. Residual stress in a pure thermoplastic polymer and its fibre composites cause an earlier fracture of the composites which affect the quality of products seriously. Stress distribution along the flow path is influenced by the pressure history of the molten mixture at the beginning of the injection moulding process to the end of filling up the mould cavity. The various features of the stress profiles are explained by the influence of

the pressure decay rate in the injection-moulding process [49]. These residual stresses also result in warpage and shrinkage of the final products and may induce reduction of mechanical properties. Therefore, the dimensional accuracy and properties of the final products are highly related to the residual stress distribution in the moulded part [47]. For natural fibres, as their moisture absorption characteristics, impurities and voids formation inside injection moulded composites may be resulted as high temperature is used during the process and cause water molecules trapped inside micro-fibrils to be gasified.

Fibre orientation in an injection moulded short fibre composite is experienced variation with respect to the thickness direction as well as the in-plane direction. It induces the mechanical properties of the composite such as modulus and tensile strength may vary in the thickness direction according to the corresponding orientation status. For the range of fibre concentrations encountered commercially, fibres do not appear to have any direct effect on the matrix orientation. As the fibre concentration increases, however, the matrix orientation becomes dominated by the orientation of the fibres [50]. During the injection moulding process for composites, a complex molten polymer flow field is generated and fibres are therefore oriented. The orientation of fibres will be fixed until the matrix is solidified. Convergent flow results in high fibre alignment along the flow direction, whereas diverging flow causes the fibres to align at 90o to the major flow direction. Shear flow produces a decrease in alignment parallel to the flow direction and the effect is pronounced at low flow rates. In generally, the fibres align in the direction of shearing and also in the direction of stretching. The shear flow near the mould walls aligns the fibres in the direction of the injection flow and this layer is called the skin. Below the skin layer, the molten mixture continues to experience shear and fibres orient along the shear lines. Finally, the core layer is formed as the fibres are swayed by the bulk deformation of the flow in the mould which usually has an elongated component, causing the material to stretch in and out of the paper direction aligning the fibres. This skin core structure shown in Fig. 8 is a common microstructural observation [48,51]. However, the skin core structure is less significant in the small sample with low fibre volume fraction. To assess the alignment of fibres during the manufacturing process in a small sample, small and thin dumbbell shaped composite samples were made by injection moulding. A microscopy was used accordingly to observe the fibre orientation through the image analysis technique. According to Fig. 9, most of the fibres are well aligned along the sample's axis (i.e. the loading direction), only a small amount of obliqued fibres.

There are numerous issues that should be concern during the injection moulding process to obtain the optimal properties of the resulting natural fibre composites and avoid development of residual stress which cause warpage, stress cracking, and long-term deformation. Process, material and geometric parameters should be optimised to minimise these problems happen. Process parameters include the melt temperature, injection and screw speeds, injection pressure and the mould temperature that can be controlled on the injection units. Increasing mould temperature results in a decreasing overall stress level, while the compressive stress region is shifted onto the surface [49]. According to recent research investigations, for biocomposites, the machine temperature of biodegradable polymer, such as Poly-lactic-acid (PLA) composites was made by using injection moulding process should be restricted in the range of 150–210 oC depending on the type of PLAs and their crystallinity from diverse manufacturers.

Molten polymer rheology, and fibre type and content are the material parameters which affect the manufacturing process and the properties of resultant composites. Under the same processing conditions, semicrystalline PLA had a higher shear viscosity than that of amorphous PLA [46]. The geometric parameters also play
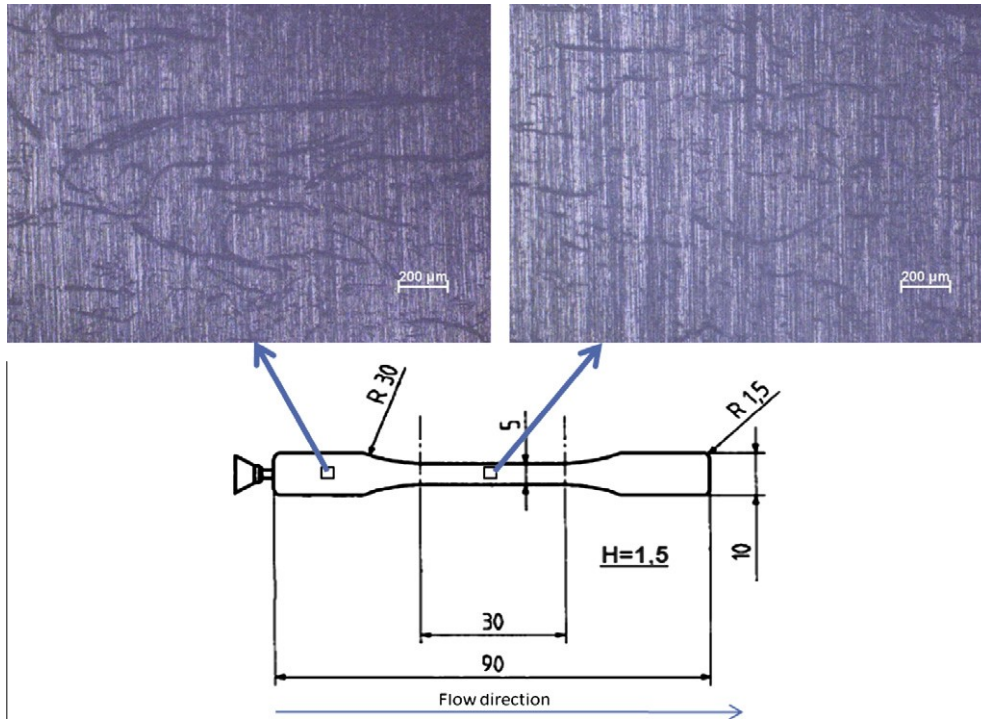
Fig. 8. Micro graphs of cut-off view (along the longitudinal direction of the sample) of the silk fibre/PLA composite with 5 vol.% silk fibre: (a) wide section and (b) narrow section.
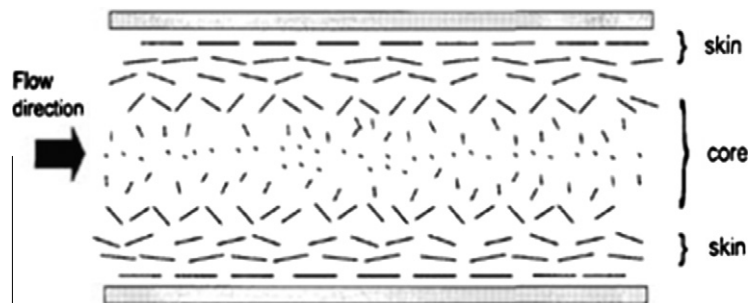
Fig. 9. Influence of flow on fibre orientation: Skin-fibres are mostly aligned along the flow direction; Core-fibres are mostly aligned perpendicular to the flow direction.

a key role on the residual stress elimination. The mould cavity shape and size, the locations of injection gates and the vents that allow the air to escape are the examples of geometric parameter which not only affect the residual stress, but also the air trapping and stress concentration.

4.2. Compression moulding

Many studies have been conducted on the feasibility of using natural fibres as reinforcement mixed with renewable polymers to form a new class of biocomposites through compression moulding process [40–44]. This process is a combination of hot-press and autoclave processes. For autoclave process, thermoplastic prepregs are laid up on a mould in a desired sequence. An entire laminate is then bagged under vacuum and placed inside an autoclave. The laminate is then heated up following a preset heat-pressure cycle and a resultant composite is formed after curing [52]. However, for the hot-press processing, a close mould may or may not be necessary [53]. With the use of close-moulds, the precut and weighed amount of fibres (in the forms of chopped, mat or stitched) are stacked together and placed inside a pre-heated mould cavity.

For natural fibre, the fracture of some fibres may occur before resin films are molten if excessive pressure is applied. Sheet moulding compounds (SMCs) and bulk moulding compounds (BMCs) are traditional initial charges for compression moulding process. The charges usually cover 30–70% of the female mould cavity surface [52]. The mould is closed and then pressurised before temperature is applied. The compounds are molten to form the shape of the cavity. Afterward, the mould is opened and the part is ejected. As the fibre can be gently placed inside the mould and no shear stress and vigorous motion are applied, the damage of the fibre can be kept as minimal. In this case, long fibre can be used to produce a biocomposites with higher volume fracture. For the natural fibre composites, short fibres or fibre mats could be pre-mixed with the compounds for compression moulding, it would act as reinforcement to reduce the shrinkage of final products.

4.3. Hot pressing

As mentioned in the previous section, hot press is favourable for simple flat samples as only two hot plates are needed to compress all fibre and matrix together and then heat was applied

subsequently. However, the viscosity of the matrix during the pressing and heating processes is a concern as it is not easy to be controlled, in particular for think samples. The viscosity of the molten matrix should be low enough to impregnate into the space between fibres and high enough to avoid spurting out. As natural fibres are made by many small filaments, it also takes time for wetting them. Therefore, the controls of viscosity, pressure, holding time, temperature in relation to the types of fibres and matrix, thickness and size of samples are critical to produce quality composites. Several minor defects such as residual stresses, voids, warpage, fibre breakage, sink marks and scorching would cause the reduction of the mechanical properties of the composites. Therefore, process, material and geometric parameters should be optimised to minimise possible defects appear. One more critical issue is, for biodegradable polymers, their processing temperature is normally below 200 oC to avoid the degradation of the polymers. If the products are thick, the heat is required to be transferred from the surfaces of the products toward the core. Carefully studying the temperature gradient is essential to avoid overheating on the surface or sub-temperature in the core to melt the polymers.

Based on the past experience, it was found that the tensile properties of natural fibre composites decrease when the set mould temperature and flow velocity decrease. Most of natural fibres are normally distributed randomly at the beginning and finally aligned toward the matrix flow direction for flat plate moulding [54,55]. The required temperature and pressure for the moulding process may be varied depending upon the thermal and rheological properties of the matrix. Flow of the material is required to expel air entrapped in the mould as well as in the charge. Void morphology in the sample has a negative effect on the flexural modulus and strength, but a clear positive effect on the beam stiffness [56]. During the moulding process, a complex heat transfer and a viscous flow phenomenon take place in the cavity [57]. For a good moulded part, a rapid mould-closing speed is desirable since it avoids the possibility of premature gelation and produces most uniform flow patterns regardless of the charge thickness [52].

Material parameters, for example, increasing the filler content also acts as a heat sink within inside the material as it would decrease the total amount of heat liberated [52]. The initial charge shape, size and its placement location in the mould are crucial parameters as they influence the final properties of a product. The amount of flow in compression moulding is small but critical to the properties and the quality of final parts because the flow controls the orientation of short fibres which is the main factor to determine the physical and mechanical properties of a resultant composite. To help control the moulding process smoothly and effectively, an optimised fibre which possesses high-surface energy, a low expansion, and low swelling should be used so as to lead to a better wetting and impregnation [58].

A slight excess of material is usually placed inside the mould to ensure it is completely filled. It is possible to have varying degrees of flow of fibres and/or of melt in compression moulding, the fibres are initially randomly oriented. However, as the mixture becomes fluid in the mould it deforms and the deformation changes the orientation of the fibres. Orientation distributions can be extremely complicated. Some locations the fibre can retain at randomly oriented, whereas others may have high degree of alignment toward the flow direction. Increasing the fibre content also leads to enhance the anisotropy of final moulding products [59]. A low-viscosity paste may flow too rapidly and cause air entrapment [58]. Different temperatures inside moulded parts would generate different degrees of residual stresses, particular at think sections. Thus, the temperature distribution and rate of cooling are important in determining how these stresses relax during cooling status [54].

The geometry of the moulding part is important which affects the flowing behaviour and fibre orientation. Fibre content inside the rib and around the sharp turning sections is normally much lower than that of other flat sections. It was also found that the larger the rib thickness, the easier the flow (with the fibres) into the ribs. However, a small lead-in radius would reduce the flow or increase the flow resistance into the ribs [60]. High pressure loss at the entrance of the rib is due to viscous friction. This pressure loss will result in fibre–matrix separation in these areas which in turn would weaken the structural integrity of resultant parts and lead to increased sink-mark depth. For the curing process concerned, the material at the centre of the rib sub-structure cures relatively slower than other flat-plate sections. The fibres are dense near to the top surface and around the rib corners, whilst a resin-rich area appeared just below the top surface at the centre [57].) High pressures are required for moulding parts that contain deep ribs and bosses [52]. Thick structures are not easily produced by this technique because of heat conduction. The charge surface temperature quickly attains to the mould temperature and remains relatively uniform compared with the centreline temperature. The centreline temperature increases slowly until the curing reaction is initiated at the mid-thickness of the part. For thin parts, the temperature rise is nearly uniform across the thickness and the maximum temperature in the material seldom exceeds the mould temperature. When the SMCs are placed at the room temperature on the hot mould, the surface of the SMCs soften and make them forming a resin-rich lubricating layer. Thus, for the purposes of modelling, the flow field can be divided into two regions: the core, which occupies most of the flow domain: and a thin lubricating layer. This is shown schematically in Fig. 10 [61]. For a thin part, the extensional deformation becomes more uniform and approaches the same flow pattern observed at fast mould-closing speeds [52]. For a thick part, high moulding temperatures should be avoided. Since the surface temperature first attains to the resin gel temperature, curing begins first at the surface and progresses inward. Curing occurs more rapidly at higher mould temperature but the peak exotherm temperature also increases [100]. Residual curing stresses in the moulded part are reduced as the thermal gradient remains nearly constant across the thickness through preheating [52].

4.4. Resin transfer moulding (RTM)

Liquid composite moulding processes encompass resin transfer moulding (RTM), vacuum assisted resin transfer moulding (VARTM), structural reaction injection moulding (S-RIM), co-injection resin transfer moulding (CIRTM) and other subsets where the basic approach is to separately inject the liquid resin into a bed of stationary preforms. The RTM process has become a popular composite manufacturing process due to its capability for high volume
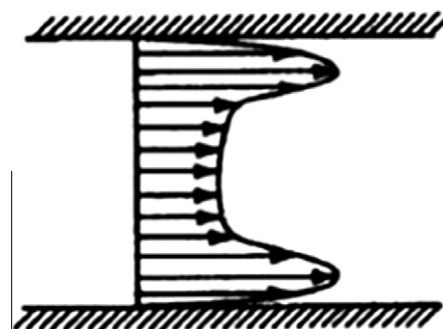

Fig. 10. Transverse velocity profile for ''Preferential flow'' [61].

Table 3
Common applications of natural fibre reinforced composites.

Potential application	Examples
Automotive	Door panels, seat backs, headliners, dash boards, car door, Transport pallets, trunk liners, Decking, rear parcel shelves, spare tyre covers, other interior trim, spare-wheel pan, trim bin
Aircraft	Interior panelling
Construction	Railing, bridge, siding profiles
Household products and furniture	Table, chair, fencing elements, Door panels, interior panelling, Window frames, door-frame profiles, food tray, partition
Electrical and electronics	Mobile cases, laptops cases
Sports and leisure items	Sports and leisure items: Tennis Racket, bicycle, Frames, Snowboards

production and cost effectiveness. Many studies have been made on the potential of natural fibres as reinforcement with renewable polymers as matrix through RTM [62–67]. In the RTM process, dry fibre perform (impregnating) or porous fibrous preform is placed into the mould cavity. Two matching mould halves are clamped tightly to avoid leakage of resin during injection process. Then, using dispensing equipment, a pressurised molten plastic is injected into the heated mould using single or multiple inlet ports in the mould depending on the complexity of the shape of a final product until the mould is filled with resin. After cooling, the part is then removed from the mould [62]. Post-curing normally is needed to ensure the resin is fully cured (chemically reacted between the resin and its catalyst).

In the RTM process, the resin injection pressure, temperature of the mould, permeability of the fibre mat, preform architecture and permeability, resin viscosity, gate location and configuration, vent control and preform placement techniques are the major processing variables. In general, higher injection pressure and mould temperature would shorten the manufacturing cycle time due to the viscosity of resin is low. However, an excessive injection pressure may cause deformation of the mould and wash-out of the fibre preform. An excessively high mould temperature may induce pre-mature resin gelation and cause short shot. All of the process variables are interrelated and have effects on the mechanical properties of final products. These processing variables have significant effects on different aspects, such as fibre wetting out and impregnation, injection gate design, ''dry patch'' and void formation [68].

For natural fibre composites, small clearances may exist between the fibre preform and mould edges because of loose edge fibre bundles, poor fitting size, or deformation of the fibre preform in the RTM process. The clearance results in a preferential resin flow path during the mould filling stage. This edge flow can disrupt the uniformity of the flow pattern and cause incomplete wetting of the preform. This phenomenon intensifies with the decrease of preform permeability. At an early stage of the injection process, the velocity differences are very high and then gradually reduce. This is due to the gradual increase in flow resistance which leads to smaller differences in velocity. Edge flow is introduced due to the clearance between the preform and the mould edge. The presence of edge flow leads to the interruption of flow uniformity and the resin near the edge has a tendency to flow much faster than in the main area due to lower resistance. Edge flow is less sensitive to injection pressure variations but fibre concentrations have a dramatic influence. The deployment of preforms larger than the mould eliminates the problem. ''Quasi-one-dimensional steady'' flow is preferred in order to achieve successful mould filling with complete impregnation and proper ventilation [69].

For fast resin flow without increasing injection pressure, resin can be injected using multiple injection gates. However, with improper injection schemes, the resin front becomes complicated

and numerous air bubbles may form where the flow fronts merge [68]. Because of the high flow resistance and slow flow and impregnation, the resin has a tendency to flow along the channel of least resistance under injection pressure and therefore the effect is intensified. Consequently both the values of mould filling distance differences between the centre and edge and the arrival time of edge flow at the bottom are substantially increased. The edge flow has an adverse effect on the mould filling process which leads to the formation of dry spots and spillage [70]. Due to aforementioned problems, it would induce a difficulty to assure full wetting inside the preform because of the inconsistence of the geometry of natural fibre and inhomogeneous fibre architecture. Such inhomogeneity leads to non-uniform permeability of the fibre preform, which in turn causes the resin velocity to vary from point to point at a micro scale. The capillary pressure, which also prevails at this length scale, exacerbates the spatial variation of the resin velocity. The resulting microscopic perturbations in the resin flow front allow voids to form [71].

While the average velocity field of the resin may appear smooth, the local velocity can vary considerably from point to point at the micro scale. The reason is that the fibre preform has a non-uniform microstructure, and hence its local permeability and the local capillary pressure may differ between inside and outside fibre tows [71]. It has been shown that there is a marked increase in voidage in the areas where flows meet and this is correlated to a deterioration of mechanical properties. The void content within a composite material produced by RTM will depend on the void content of the resin prior to injection and the extent of void formation and growth during mould filling and cure. In general, vacuuming of the mould and injection pot are required prior to the injection process starts.

5. Potential applications

5.1. Ecological applications

Recent increase of the prices of petroleum-based products, strict governmental regulations and taxation systems on carbon footprints and well-educated young generation on the acceptance of adopting green products have driven the growth of developing materials with the use of natural resource to another peak. It therefore creates a new business model for all engineering enterprises to re-invent their capital including human resource to adopt this new change. The application of natural fibre reinforced polymer composites and natural-based resins for replacing existing synthetic polymer or glass fibre reinforced materials is huge. Automotive and aircraft industries have been actively developing different kinds of natural fibres, mainly on hemp, flax and sisal and bioresins systems for their interior components. High specific properties with lower prices of natural fibre composites are making it attractive for various applications. According to Lucintel, a leading global management consulting and market research firm, the global natural fibre composites market reached to US $2.1 billion in 2010. This market is expected to grow with a CAGR (compound annual growth rate) of 10% over the next 5 years (2011–2016) [72]. Nowadays, new construction materials using natural fibre are well suited for anisotropic and specially tailored lightweight structural components parts such as interior panels inside cars, partitions (or called ''dividers'') inside airplanes and coats and other secondary structures with low temperature servicing condition. Table 3 summarizes the potential applications of natural fibre composites in automotive, electrical and electronics, sports and leisure items, construction, aircraft and household products & furniture industries [73–75]. Besides, as natural fibre is formed by several thousands of fibrils together which is an idea structure for energy absorption including sound wave energy, so it is good for best

using its inherent advantage for developing noise barriers and impact resistance structures. Moreover, eco-friendly measures taken by the electronic industry is another major growth driver for these composites in electrical and electronics applications. Recently, a major research focus on natural fibre composites, mainly on the plane-based fibre is on their fire resistance properties. Many reports have addressed that by using natural fibres as supplement and/or reinforcement of thermoplastics, the amount of Carbon Monoxide provided during fire is less than that of their host materials.

5.2. Bio-medical applications

For biomedical applications, protein based natural fibre such as silkworm silk, feather and spider silk fibres are suggested rather than other type of plant based natural fibre. Silk fibres as sutures for human wound dressing have been used for centuries [76]. Recently, regenerated silk solutions have been used to form a variety of biomaterials, such as gels, sponges and films, for medical applications [77]. Moreover, silk has been exploited as a scaffold biomaterial for cell culture and tissue engineering in vitro and in vivo [78]. Bioengineering is usually defined as a basic research-oriented activity closely related to biotechnology and genetic engineering which are used for the modification of animal or plant cells, or parts of cells, to restore their function or repair their damage regions, or to develop new microorganisms for beneficial ends [1]. Concerning the implementation of technology in bio-engineering, biomaterials are mainly used in the applications of directing, supplementing, or replacing the functions of living tissues in the human body [72].

Natural fibre composites, mainly on the animal-based fibres are being used for bone repairs and implant development recently as a replacement for traditional metallic materials such as stainless steel and titanium. Although stainless steel and titanium provide sufficient strength and rigidity to align the bone and control motion while healing of bone fracture, they are too stiff as compared with the properties of nature bone [Alan Paper]. By using the animal based fibre as reinforcement for biodegradable polymer for tail-making a new class of biocomposites can enhance the strength of recovered bones and also minimise the risk of the second surgery for removing any metallic implants inside the body. In general, several critical issues are guided on choosing the appropriate natural fibre composites for biomedical and bioengineering applications, these include: (1) biodegradability, (2) bioresorbability, (3) biocompatibility, (4) sterilizability (5) functionability (6) manufacturability, and (7) mechanical and thermal properties [79–81]. Although many works have been conducted along the similar line on applying animal fibres into new class of bio-grade polymer composites, the path is still a long way to go for viva and in vivo examinations.

6. Conclusion

The development of natural fibre reinforced polymer composites has been a hot topic recently due to the increasing environmental awareness on reducing the use of fossil fuel and its related products. Natural fibre can be classified for plant-based and animal-based. The selection criteria are highly dependent on their type, application and cost. However, there is still uncertain on which type of manufacturing processes that are suitable for producing these composites as their materials and mechanical characteristics are different as compared with traditional carbon and glass fibre composites in general. Some processes, their original design were not targeted for natural fibres, while their technologies have been well developed for fast and reliable composite production. This paper addresses a comprehensive review on different types of composites manufacturing process and their effects to the natural fibre and its composites.

References

[1] Bronzino JD. Biomedical engineering handbook: biomedical engineering fundamentals. CRC Press; 1999.
[2] Global Biomaterial Market (2009–2014). Markets and Markets; 2009.
[3] Bledzki AK, Sperber VE, Faruk O. Natural and wood fibre reinforcement in polymers. Rapra Rev Reports 2002;13(8):2.
[4] Baillie C. Green composites: polymer composites and the environment. CRC Press; 2004.
[5] Mohanty AK, Misra M, Drzal LT. Natural fibres, biopolymers, and biocomposites. Francis Group: CRC Press Taylor; 2005.
[6] Pickering KL. Properties and performance of natural-fibre composites. Woodhead Publishing Limited; 2008.
[7] Xie Y, Hill CAS, Xiao Z, Militz H, Mai C. Silane coupling agents used for natural fiber/polymer composites: a review. Composites Part A 2010;41:806–19.
[8] Mohanty AK, Misra M, Hinrichsen G. Biofibres. Biodegradable polymers and biocomposites: an overview. Macromol Mater Eng 2001;276–277:1–24.
[9] Zahn H, Hles JF, Nlenhaus M. Wool as a biological composite structure. Ind Eng Chem Res 1980;19:496–501.
[10] Simpson WS, Crawshaw GH. Wool: science and technology. Cambridge: England Woodhead Publishing; 2002.
[11] Feughelman M. Mechanical properties and structure of alpha-keratin fibres: wool, human hair and related fibres. University of New South Wales Press; 1997.
[12] Kock JW. Physical and Mechanical properties of chicken feather materials. Thesis. Georgia Institute of Technology; 2006.
[13] Barone JR, Schmidt WF. Polyethylene reinforced with keratin fibres obtained from chicken feathers. Compos Sci Technol 2005;65:173–81.
[14] Cheng S, Lau KT, Liu T, Zhao YQ, Lam PM, Yin YS. Mechanical and thermal properties of chicken feather fiber/PLA green composites. Composites: Part B 2009;40:650–4.
[15] Altman GH, Diaz F, Jakuba C, Calabro T, Horan RL. Silk-based biomaterials. Biomaterials 2003;24:401–16.
[16] Saravanan D. Spider silk- structure, properties and spinning. J Text Apparel, Technol Manage 2006;5(1):1–20.
[17] Bonino MJ. Material Properties of Spider Silk. Thesis. NY: University of Rochester Rochester; 2003.
[18] Atkins E. Silk's secrets. Nature 2003;424.
[19] Shao ZZ, Vollrath F. Surprising strength of silkworm silk. Nature 2002:418.
[20] Hardy1 John G, Scheibel1 Thomas R. Silk-inspired polymers and proteins. Biochem Soc Trans 2009;37:677–81.
[21] Perez-Rigueiro J, Elices M, Llorca J. Effect of Degumming on the Tensile Properties of Silkworm (Bombyx mori) Silk Fibre. J Appl Polym Sci 2002;84: 1431–7.
[22] Jiang P, Liu H, Wang C. Tensile behavior and morphology of differently degummed silkworm (Bombyx mori) cocoon silk fibres. Mater Lett 2006;60:919–25.
[23] Fakirov S, Bhattacharya D. Handbook of engineering biopolymers: homopolymers, blends and composites. Cincinnati (OH): Hanser; 2007.
[24] Lewin, Menachem. Handbook of fibre chemistry, 3rd ed. Boca Raton (FL), USA: CRC Press; 2006.
[25] Vroman I, Tighzert L. Review biodegradable polymers. Materials 2009;2: 307–44.
[26] Kolybaba M, Tabil LG, Panigrahi S, Crerar WJ, Powell T, Wang B. Biodegradable polymers: past, present, and future. An ASAE Meeting Presentation 2003; RRV03-0007.
[27] Ikada Y, Tsuji H. Biodegradable polyesters for medical and ecological applications. Macromol Rapid Commun 2000;21:117–32.
[28] Lim LT, Auras R, Rubino M. Processing technologies for poly(lactic acid). Prog Polym Sci 2008;33:820–52.
[29] NatureWorks™ PLA 3051D technical data sheets, NatureWorks LCC.
[30] Amnat J, Tokiwa Y. Review biodegradation of poly(L-lactide). Biotechnol Lett 2004;26:771–7.
[31] Antoine LD, Davies P, Baley C. Interfacial bonding of flax fibre/Poly(L-lactide) bio-composites. Compos Sci Technol 2010;70:231–9.
[32] Matuana LM, Balatinecz JJ. Surface characterization of esterified cellulosic fibers by XPS and FTIR Spectroscopy. Wood Sci Technol 2001;35:191–201.
[33] Saheb DN, Jog JP. Natural fiber polymer composites: a review. Adv Polym Technol 1999;18(4):351–63.
[34] Keener TJ, Stuart RK. Maleated coupling agents for natural fibre composites. Composites: Part A 2004;35:357–62.
[35] Kazayawoko M. Surface modification and adhesion mechanisms in woodfiber-polypropylene composites. J Mater Sci 1999;34:6189–99.

[36] Gonzaleza AV, Cervantes-Uca JM, Olayob R. Effect of fiber surface treatment on the fiber–matrix bond strength of natural fiber reinforced composites. Composites: Part B 1999;30:309–20.

[37] Mohanty AM, Drazal LT. Novel hybrid coupling agent as an adhesion promoter in natural fiber reinforced powder polypropylene composites. J Mater Sci Lett 2002;21:1885–8.

[38] Zulkifli R, Azhari CH, Ghazali MJ, Ismail AR. Interlaminar fracture toughness of multi-layer woven silk/epoxy composites treated with coupling agent. Eur J Sci Res 2009;27:454.

[39] Chaivan P, Pasaja N, Boonyawan D. Low-temperature plasma treatment for hydrophobicity improvement of silk. Surf Coat Technol 2005;193:356–60.

[40] Serizawa S, Inoue K, Iji M. Kenaf-fiber-reinforced poly(lactic acid) used for electronic products. J Appl Polym Sci 2006;100:618–24.

[41] Huda MS, Huda MS. Green composites from recycled cellulose and poly (lactic acid): physico-mechanical and morphological properties evaluation. J Mater Sci 2005;40:4221–9.

[42] Huda MS, Drzal LT, Misra M. Wood-fiber-reinforced poly(lactic acid) composites: evaluation of the physicomechanical and morphological properties. J Appl Polym Sci 2006;102:4856–69.

[43] Huda MS, Lawrence TD. A study on biocomposites from recycled newspaper fiber and poly(lactic acid). Ind Eng Chem Res 2005;44:5593–601.

[44] Huda MS, Drzal LT, Mohanty AK, Misra M. Chopped glass and recycled newspaper as reinforcement fibers in injection molded poly(lactic acid) (PLA) composites: a comparative study. Compos Sci Technol 2006;66:1813–24.

[45] Birgitha N. Natural fiber composites optimization of microstructure and processing parameters. Thesis; 2007.

[46] Qi Fang, Hanna Milford A. Rheological properties of amorphous and semicrystalline polylactic acid polymers. Ind Crops Prod 1999;10(1):47–53.

[47] Kim SK, Lee SW, Youn JR. Measurement of residual stresses in injection molded short fiber composites considering anisotropy and modulus variation. Korea-Aust Rheol J 2002;14(3):107–14.

[48] Lee KS, Lee SW, Youn JR, Kang TJ, Chung K. Confocal microscopy measurement of the fiber orientation in short fiber reinforced plastics. Fibers Polym 2001;2(1):41–50.

[49] White JR. On the layer removal analysis of residual stress Part 1. Polymer mouldings with depth-varying Young's modulus. J Mater Sci 1985;20(7):2377–87.

[50] Folkesa MJ, Russell DAM. Orientation effects during the flow of short-fibre reinforced thermoplastics. Polymer 1980;21(11):1252–8.

[51] Chen J, Sellers K. Nanotechnology and the environment overview of manufacturing processes. CRC Press; 2009.

[52] Mallick PK. Fiber-reinforced composites materials, manufacturing, and design. 3rd ed. CRC Press; 2008.

[53] Ruihua HU, LIM JK. Fabrication and mechanical properties of completely biodegradable hemp fiber reinforced polylactic acid composites. J Compos Mater 2007;41 (13).

[54] Kim KT, Jeong JH. Effect of molding parameters on compression molded sheet molding compounds parts. J Mater Process Technol 1997;67(1):105–11.

[55] Jendlia Z, Meraghni F. Micromechanical analysis of strain rate effect on damage evolution in sheet molding compound composites. Composites: Part A 2004;35:779–85.

[56] Hagstrand PO, Bonjour F. The influence of void content on the structural flexural performance of unidirectional glass fibre reinforced polypropylene composites. Composites Part A 2005;36:705–14.

[57] Kim DK, Choi HY, Kim N. Experimental investigation and numerical simulation of SMC in compression molding. J Mater Process Technol 1995;49:333–44.

[58] Comte E, Merhi D. Void formation and transport during SMC manufacturing: effect of the glass fiber sizing. Polym Compos 2006;27(3):289–98.

[59] Dumont P, Orgéas L, Corre SL. Anisotropic viscous behavior of sheet molding compounds (SMC) during compression molding. Int J Plast 2003;19:625–46.

[60] Christensen SK, Hutchinson B. Fibre-matrix separation in ribbed SMC and BMC parts. In: Annual Technical Conference ANTEC, Conference Proceedings 1997;1:782–5.

[61] Abrams LM, Castro JM. Predicting molding forces during sheet molding compound (SMC) compression molding. I: model development. Polym Compos 2003;24(3):291–303.

[62] Sreekumar PA, Joseph K, Unnikrishnan G. A comparative study on mechanical properties of sisal-leaf fibre-reinforced polyester composites prepared by resin transfer and compression moulding techniques. Compos Sci Technol 2007;67:453–61.

[63] Willians GI, Wool RP. Composites from natural fibers and soy oil resins. Appl Compos Mater 2000;7:421–32.

[64] Ferland P, Trochu F. Concurrent methods for permeability measurement in resin transfer molding. Polym Compos 1996;17(1):149–58.

[65] Kim SK, Daniel IM. Determination of three-dimensional permeability of fiber performs by the inverse parameter estimation technique. Composites: Part A 2003;34:421–9.

[66] Ikegawa N. Effect of Compression Process on Void Behavior in Structural Resin Transfer Molding. Polym Eng Sci 1996;36(7):953–62.

[67] Warrior NA, Turner TA, Robitaille F, Rudd CD. Effect of resin properties and processing parameters on crash energy absorbing composite structures made by RTM. Composites: Part A 2003;34:543–50.

[68] Kang MK, Jung JJ, Lee WI. Analysis of resin transfer moulding process with controlled multiple gates resin injection. Composites: Part A 2000;31:407–22.

[69] Richardson MOW, Zhang ZY. Experimental investigation and flow visualisation of the resin transfer mould filling process for non-woven hemp reinforced phenolic composites. Composites: Part A 2000;31:1303–10.

[70] Rodriguez E, Giacomelli F, Vazquez A. Permeability–porosity relationship in RTM for different fiberglass and natural reinforcements. J Compos Mater 2004;38(3):259–68.

[71] Kang MK, Lee WL, Hahn HT. Formation of microvoids during resin-transfer molding process. Compos Sci Technol 2000;60:2427–34.

[72] Black J. Biological performance of materials: fundamentals of biocompatibility. CRC Press; 2006.

[73] Flahiff CM, Blackwell AS, Hollis JM. Analysis of a biodegradable composite for bone healing. J Biomed Mater Res 1996;32:419–24.

[74] Claes L. The mechanical and morphological properties of bone beneath internal fixation plates of differing rigidity. J Orthop Res 1989;7(2):170–7.

[75] Burns AE, Varin J. Poly-L-lactic acid rod fixation results in foot surgery. J Foot Ankle Surg 1998;37(1):37–41.

[76] Wang YZ. In vivo degradation of three-dimensional silk fibroin scaffolds. Biomaterials 2008;29:3415–28.

[77] Vepari C, Kaplan DL. Silk as a biomaterial. Prog Polym Sci 2007;32(8-9):991–1007.

[78] Wang YZ. Stem cell-based tissue engineering with silk biomaterials. Biomaterials 2006;27:6064–82.

[79] Teoh SH. Engineering materials for biomedical application. World scientific; 2004.

[80] DiGregorio BE. Biobased performance bioplastic: mirel. Chem Biol 2009;16(1):1–2.

[81] Ambrose CG, Clanton TO. Bioabsorbable implants: review of clinical experience in orthopedic surgery. Ann Biomed Eng 2004;32(1):171–7.

Characteristics of a silk fibre reinforced biodegradable plastic

Mei-po Ho [a], Kin-tak Lau [a,b,⇑], Hao Wang [b], Debes Bhattacharyya [c]

[a] Department of Mechanical Engineering, The Hong Kong Polytechnic University, Kowloon, Hong Kong SAR, China
[b] Centre of Excellence in Engineered Fibre Composites, Faculty of Engineering and Surveying, University of Southern Queensland, Toowoomba, Queensland, Australia
[c] Centre for Advanced Composite Materials, Department of Mechanical Engineering, The University of Auckland, Private Bag 92019, Auckland, New Zealand

abstract

Silk fibre is one kind of well recognized animal fibres for bio-medical engineering and surgical operation applications because of its biocompatible and bio-resorbable properties. Recently, the use of silk fibre as reinforcement for some bio-polymers to enhance the stiffnesses of scaffolds and bone fixators has been a hot research topic. However, their mechanical and biodegradable properties have not yet been fully understood by many researchers, scientists and bio-medical engineers although these properties would govern the usefulness of resultant products. In this paper, a study on the mechanical properties and bio-degradability of silk fibre reinforced Poly (lactic-acid) (PLA) composites is conducted. It has been found that the Young's modulus and flexural modulus of the composites increased with the use of silk fibre reinforcement while their tensile and flexural strengths decreased. This phenomenon is attributed to the disruption of inter- and intra-molecular bonding on the silk fibre with PLA during the mixing process, and consequent reduction of the silk fibre strength. Moreover, bio-degradability tests showed that the hydrophilic properties of the silk may alter the biodegradation properties of the composites compared to that of a pristine PLA sample.

© 2010 Published by Elsevier Ltd.

1. Introduction

Petroleum is a fossil fuel that can only be last for another 50–60 years at the current rate of consumption [2]. Preservation of non-renewable petroleum-based materials especial for petroleum-based plastics is a critical topic because of the increasing environmental consciousness in the society. Excessive use of petroleum-based plastics inducing a huge amount of solid waste disposals would cause a serious depletion of landfill capacities. Besides, the severe government's plastic waste control legislation and the growing interest among the customers in sustainable and environmentally friendly products drive the retailers and manufacturers to trend towards developing more sustainable materials for alleviating the impact of global warming. Therefore, the awareness of soared waste problems and their impact on the environment has awakened a new interest in the area of materials science. To tackle on this problem, different types of fully biodegradable composites are being developed recently, as substitutions for non-biodegradable petroleum-based plastics, and even metallic components.

Recently, biodegradable materials have continued attracting popular attention worldwide. Within the period of 2005 and 2009, the global market for the demand of biodegradable polymers was doubled in size. In 2009, among all countries in the world, Europe had the largest growth in the market of biodegradable polymers in the range of 5–10% as compared with 2008 [1] and this growth has kept continuing. The forecast on the total consumption of biodegradable polymers is to grow at an average annual rate of nearly 13% from 2009 to 2014 in North America, Europe and Asia, which are accounted as the major global markets for materials consumption.

Biodegradable composites are generally believed as one of the key materials in coming centuries. They are generally composed of biodegradable fibre (such as nature fibre and synthesized bio-polymer based fibre) and biodegradable polymer matrix, and manufactured by various processes, their properties can be tailor-made to satisfy various product requirements for specific applications. One of the major applications of biodegradable composites is to produce artificial joints and tissues for human body use.

Bio-engineering is usually defined as a basic research-oriented activity closely related to biotechnology and genetic engineering which are used for the modification of animal or plant cells, or parts of cells, to (i) restore their function, (ii) repair their damage regions and (iii) develop new microorganisms for beneficial ends [2]. Concerning the implementation of technology in bio-engineering and bio-materials are mainly used in the applications of directing, supplementing, or replacing the functions of living tissues in the human body [3].

⇑ Corresponding author at: Department of Mechanical Engineering, The Hong Kong Polytechnic University, Kowloon, Hong Kong SAR, China. Tel.: +852 2766 7730; fax: +852 2365 4703.
E-mail addresses: mmktlau@polyu.edu.hk, Kin-tak.Lau@usq.edu.au (K.-t. Lau).

The term of ''Bio-composite'' is a new and advanced bio-material, which is found in use for bone repair and implant application recently as a replacement for traditional metallic materials such as stainless steel and titanium. Although stainless steel and titanium provide sufficient strength and rigidity to align the bone and control motion while healing of bone fracture, they are too stiff as compared with the properties of a natural bone. The Young's modulus of steel typically falls into the range of 150–200 GPa while the bone is only 6–20 GPa. Therefore, metallic implant plates carry the majority of load which leads to that stress-shielded bone delay bridging. Moreover, the incompletely healed bone is susceptible to refracture after removal of the metallic implant plate. This weaken bone also suffers serious bone loss (osteoporosis) including intracortical porosity, cortical thinning and correspondingly greater loss of mechanical properties [4,5].

Besides, the need of the second surgery for removing a metallic fixator, corrosion of the fixator inside the human body and bone atrophy associated with rigid metallic fixation devices increase the probably of bone infection [6]. Moreover, the postoperative radiotherapy as well as X-ray for diagnostic imaging on healing bone is interfered by metallic implant plates. It is because the presence of metallic plates changes the local dose distribution and these changes result from backscattering effects which cause overdosage in front of and underdosage behind the plates [7].

To overcome the disadvantages of using traditional metallic bone fixator, silkworm silk fibre reinforced polymer composites, based on their inherent mechanical, biocompatible and bioresorable properties have been found as a desirable versatile bio-material for bone plate fixation. Silk fibres as sutures for human wound dressing have been used for centuries [8]. Recently, regenerated silk solutions have been used to form a variety of bio-materials, such as gels, sponges and films, for medical applications [9]. Moreover, silk has been exploited as a scaffold bio-material for cell culture and tissue engineering in vitro and in vivo [10]. However, this topic is in need of further study and clarification as no comprehensive study, particularly on the correlationship between thermal,

mechanical and degradation properties of the silkworm silk fibre reinforced composites have been conducted to date.

2. Experiment details

The biodegradable polymer-PLA as a matrix under investigation in the current study is a neat grade commercialized by Cargill-Dow under the brand name NatureWorks® PLA Polymer. Silk fibre with the average fibre diameter of 100 μm was supplied by Ocean Verve Ltd., Hong Kong. The inherent body structure of silkworm is composed of two cores of fibroin which exists in a paired of organ. The fibroin fibre itself is a bundle of several fibrils with a diameter of 1 μm and one fibril contains 15 nm wide micro-fibrils [11,12]. As a silk fibre is comprised of many small bundles of filaments, there is no doubt that the wetability of its resultant composites is the key to ensure good bonding/complete chemical bonding between all fibres and matrix is achieved.

Besides, a sericin layer also plays a critical role as it may isolate the physical contact or direct chemical bonding between the fibre and matrix. This layer is mainly made by protein as a coating and adhesive of the silkworm silk fibre. In this study, the coating was pre-removed by the supplier and the fibre received as in a form of reeling. As mentioned in a previous literature [13], this layer would affect the bonding between the fibre and polymer-based matrix, and thus worsen the mechanical properties of silk fibre composites.

For the tensile and flexural strength tests, all samples were made by using Hakke MiniLab twin-screw micro-extruder. Before mixing the fibre with PLA, degummed fibre were chopped into 5 mm in length in order to avoid coiling with the screws and stretching the fibres plastically either co- or counter rotating during injection process. These fibres were pre-placed inside an oven for drying to minimise excessive water/moisture content into them before the process. The optimal fibre content, in terms of mouldability inside the PLA environment was 5 wt.% based on our preliminary study. A uniform temperature of 180 ℃ was maintained at all zones inside

Table 1
Experimental results extracted from the tensile property and flexural strength tests.

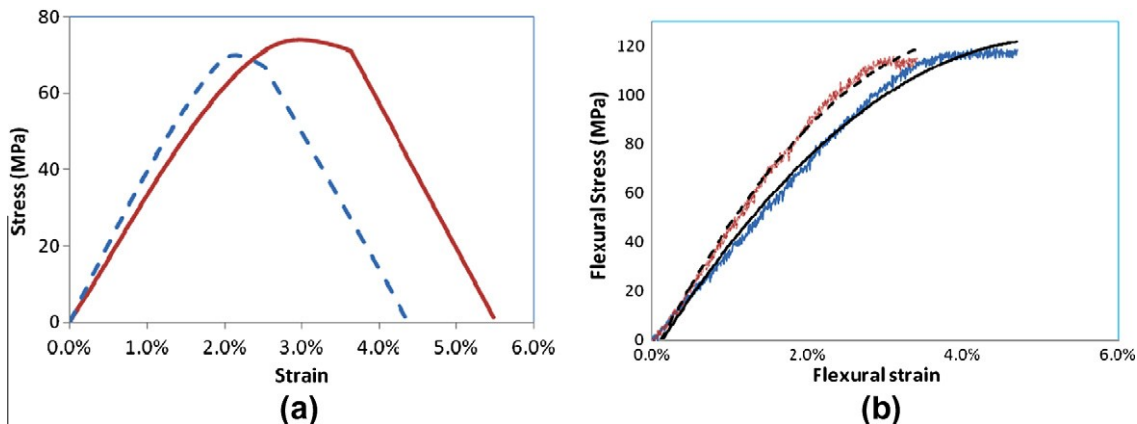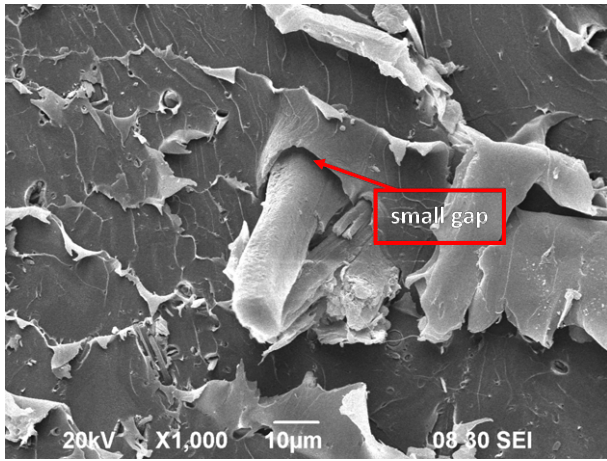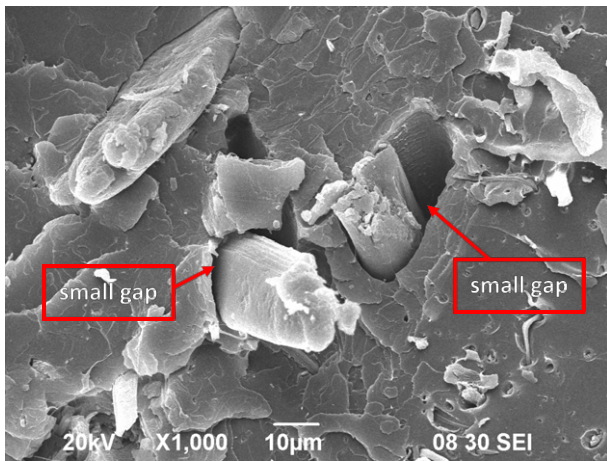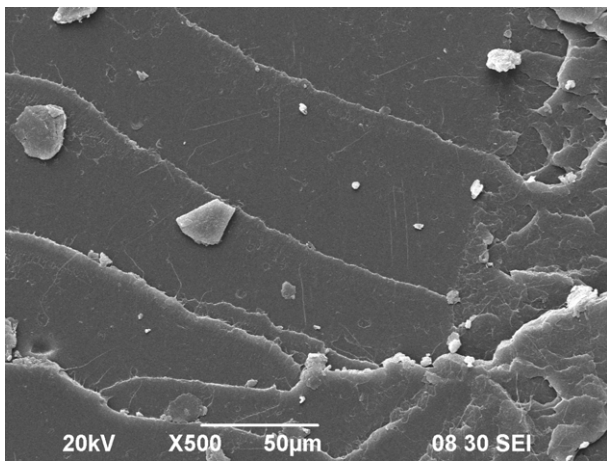|	Young's modulus (GPa)	Tensile strength (MPa)	Strain at break (%)	Flexural modulus (GPa)	Flexural strength (MPa)	Maximum strain (flexural) (%)
PLA	3.21 ± 0.08	70.73 ± 2.4	5.5 ± 1.7	3.98 ± 0.23	109.4 ± 14.5	4.1 ± 0.75
5 wt.% Silk fibre/PLA	4.08 ± 0.05	70.6 ± 1.1	3.8 ± 0.5	4.06 ± 0.20	97.41 ± 21.8	2.9 ± 0.99
Percentage increase	27%	−0.18%	−31%	2%	−11%	−29%

Fig. 1. (a) Tensile stress–strain curves of (i) pure PLA – solid line and (ii) silk/PLA composite – dashed line.

further injection moulding. The mixture was then transferred to a Thermo Hakke small scale injection moulding machine. The injection cylinder and the mould were pre-heated to desirable temperatures of 200 oC and 45 oC, respectively, silk fibre/PLA samples were made in a dumbbell shape according to ASTM D3039 and in regular plates with the size of 90 mm x 10 mm for the tensile property and flexural strength tests, respectively.

Afterwards, the samples were mounted onto a MTS testing machine [Alliance RT/50] with tailor-made supporting fixtures for conducting the test; the crosshead speed of the tensile property and flexural strength tests were 1.5 mm/min and 0.946 mm/min, respectively. An extensometer was used to measure any small change in linear dimension during the tensile test. Table 1 shows the tensile and flexural properties obtained from the tests for PLA and silk fibre/PLA samples.

In terms of bio-degradability test (in vitro), PLA and silk fibre/PLA samples were placed into separated tanks contained Phosphate Buffered Saline (PBS) solution. White dry powder of PBS was diluted with 1L of deionised water with ultimately the pH level of 7.4 being achieved. Two types of samples were stored into the tanks with 500 ml of solution each. The tanks were then stored in a humidified, thermostable and orbital-shaking incubator at 37 oC with 100 rpm. In order to investigate the changes in mechanical properties of the samples, the samples were characterized by weight change, tensile test, bending test and morphology study at different stages during the biodegradation process.

3. Results and discussion

According to the results shown, the Young's modulus and flexural modulus of the silk fibre/PLA samples increase by 27% and 2%, respectively as compared with a pristine PLA sample (Table 1). It can be seen that the chopped silk fibres can play a role of effectively enhancing the tensile modulus of PLA. However, the enhancement in flexural modulus is small. Fig. 1a and b shows the stress–strain curves obtained from the experiments. In these figures, they show that the tensile and flexural strengths as well as ductility of the silk fibre/PLA samples as compared with the pristine PLA.

The major factors affecting the mechanical performance of short fibre reinforced composites include fibre–matrix interface, fibre length, fibre content and fibre orientation. In our pervious study, 5 mm is the most optimal silk fibre length for injection moulding which can prevent the fibre from being coiled with the screws or stressed plastically. Fibre content is another factor in influencing the tensile strength but it is limited by the restriction of the injection moulding and the sample size. At low fibre content (5%) of silk fibre/PLA composite sample, the matrix is not restrained by enough fibres and highly localized strain occurs in the matrix, causing the bond between matrix and fibre to break. Therefore, the debonded fibres dilute the matrix content and act as flaws which reduce the effective cross sectional area and, finally poor mechanical strength is resulted.

Fibres, due to their surface contour can provide mechanical interlocking, if they align along the loading direction, to the surrounding matrix to allow good stress transfer when the composite is under tensile loading. To assess the alignment of fibres during the manufacturing process, small and thin dumbbell shaped composite samples were made by injection moulding [14]. A microscopy was used accordingly to observe the fibre orientation through the image analysis technique. According to Fig. 3, most of the fibres are well aligned along the sample's axis (i.e. the loading direction), only a small amount of obliqued fibres.

Notwithstanding fibre length, fibre content and fibre orientation affect the properties of the composites, interfacial bonding

Fig. 2. Scanning electron micrographs showing the fractured surfaces of (a) and (b) silk/PLA composites with the fibre pull out compare with (c) pure PLA.

the machine so as to ensure that PLA was in a processing temperature condition, and also this temperature is below the degradation temperature of the fibre. The screwing speed and the mixing duration were set as 100 rpm and 10 min, respectively. The first run of the extrusion was discarded and the strands of an extrusion mixture were then directly collected by a pre-heated injection cylinder for

between silk fibre and PLA plays a decisive role on expressing the phenomenon on the increment in the modulus but decrement in the strength. In order to illustrate the relation between the mechanical properties and fibre–matrix interfacial bonding of the composite, the sequences of the loading of fibre and surrounding matrix of the composite with the interfacial bonding are discussed.

During the tensile loading process, matrix supposedly takes load a bit earlier than that of the fibre at the very beginning stage. Continuously increasing the load may cause fibres and matrix to share the load and fibres take higher load subsequently through the stress transfer by surface friction of the fibres. Modulus is determined at low strain levels where the fibre–matrix interfaces under very low shear force. Therefore, as the modulus is a property of material at low strain and is not very sensitive to the fibre–matrix interface, thus the modulus of composites is higher than that of a pure PLA. At the certain level of load applied at that time the strain increases into the non-elastic region, debonding between the fibre and matrix happens as the shear force with the normal force at the bonding region may overcome the surface frictional force. The strength of composites is a direct indicator of the strength of interfacial bonds since the applied stress is more efficiently transferred through the interface [14,15]. The interfacial debonding limits the stress transfer through the interface and thereby, as all fibres are debonded, areas with the fibres exist like a cavity without any reinforcement which cause the ultimate strength decreases consequently.

Therefore, poor bonding between the fibre and the matrix would dominate over other factors of strength reduction. Sericin and the hydrophilic characteristic of the silk fibre as the reasons for poor bonding are discussed as follows. A small gap is observed between the fibre and the matrix on the fracture surface of the composite (Fig. 2). Silk fibre used for this project was collected as in an ''as-it-Is'' form, which was degummed by boiling water from the supplier. This degumming procedure removes the more soluble components of sericin, but does not clean all the sericin as both sericin and fibroin core are protein. Thus partial sericin would remain on the surface. [16]. Sericin hinders the bonding between the fibre and matrix, and the efficiency of stress transferred between resin and fibre decreased from the weak interfacial regions thus. Moreover, the fibre used in this project was not undergone any chemical treatment with compatilizer, modifier and/or other bonding agents due to our target application is for the development of bone implants (no excessive chemical treatment of natural materials is allowed), it is therefore expected that a weak bonding between them was still the case here.

Natural silkworm silk fibre contains hydroxyl groups which is called hydrophilic. In this composite system, one (fibre) is in hydrophilic while another is hydrophobic (matrix) properties, their interface cannot be assumed to be securely (chemically) bonded together due to the inherently poor compatibility and thus induce poor bonding and limit the load transfer through the interface. Therefore, the tensile strength of the composites would not be improved by the addition of silk fibre. However, mechanical interlocking still existed due to the roughness of the fibre and this kind of weak bonding dominates the reasons for diminished strength and strain The roughness of the fibre is basically formed
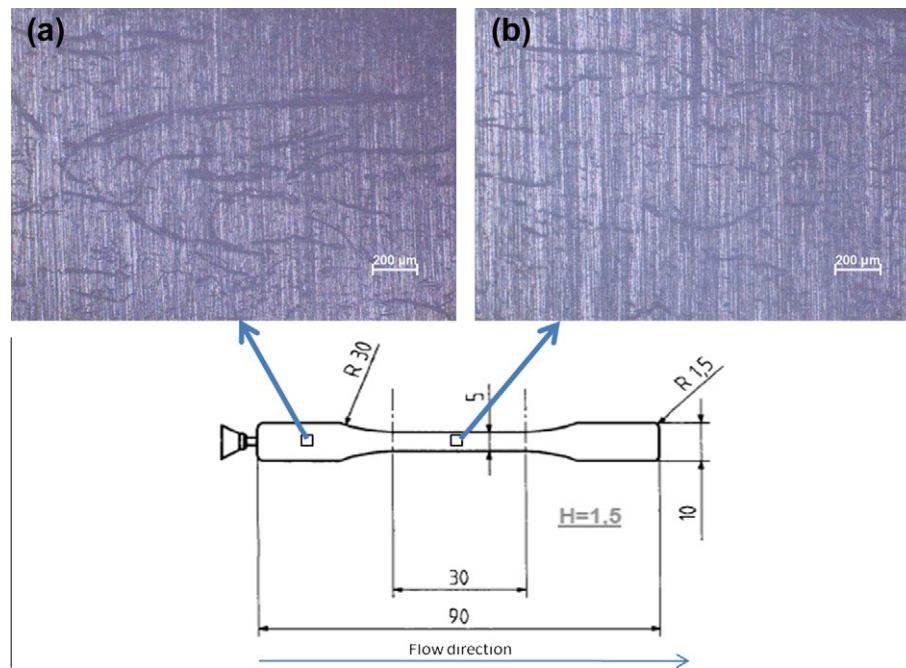
Fig. 3. Micrographs of cut-off view (along the longitudinal direction of the sample) of the silk fibre/PLA composite with 5 vol.% silk fibre: (a) wide section and (b) narrow section.

Table 2
The weight of pure PLA samples and silk/PLA biocomposites during biodegradation test.

	Duration of the degradation test (week)								
	0 Before test	2	4	6	8	10	12	14	16
PLA (g)	1.22	1.22	1.23	1.22	1.22	1.23	1.22	1.23	1.23
5 wt.% Silk fibre/PLA (g)	1.22	1.25	1.24	1.24	1.25	1.25	1.24	1.24	1.25

Fig. 4. Young modulus as a function of time for: (a) pure PLA and (b) silk fibre/PLA composite.

Fig. 6. Tensile strength as a function of time for: (a) pure PLA and (b) silk fibre/PLA composite.

Fig. 5. Flexural modulus as a function of time for: (a) pure PLA and (b) silk fibre/PLA composite.

Fig. 7. Flexural tensile strength as a function of time for: (a) pure PLA and (b) silk fibre/PLA composite.

during the spinning process of cocoon, two fibroin fibres which contain numerous silk filaments with different diameters bundled together to form the fibre.
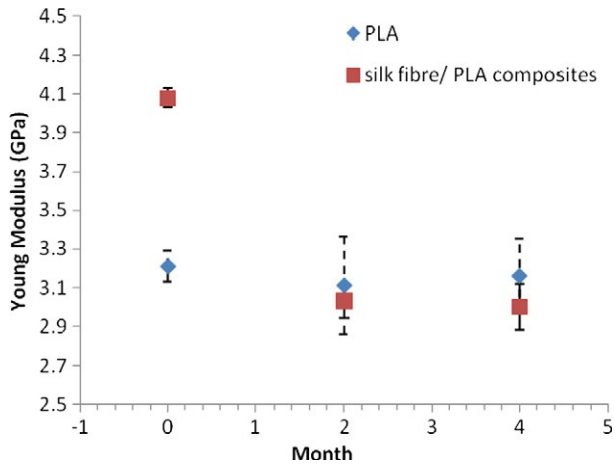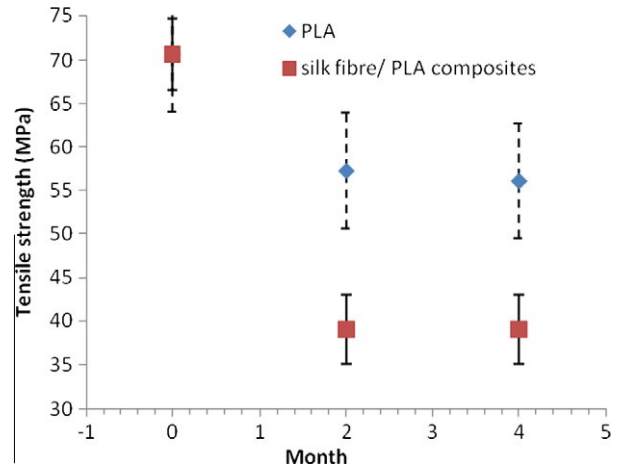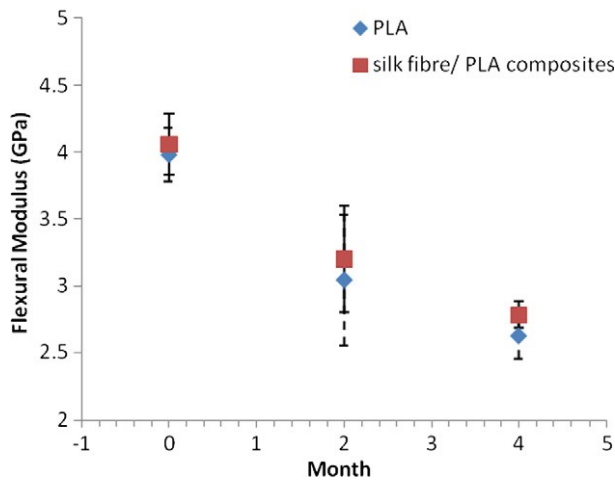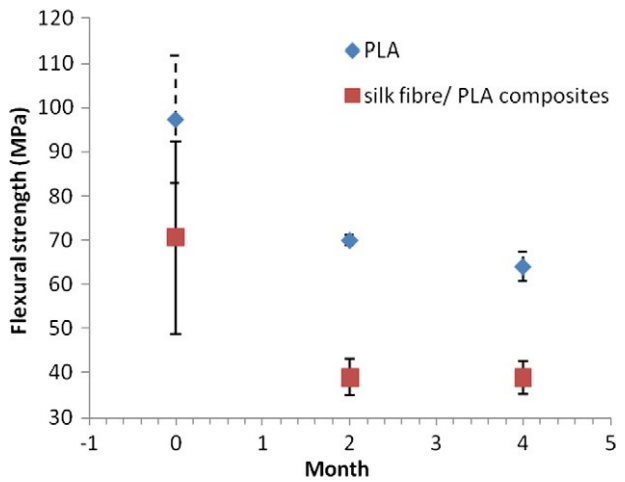
Clearly, for most biodegradable materials, especially artificial polymers, passive hydrolysis is the most important mode of degradation [17]. Silk fibre dominates in the water uptake behaviour, which initiates the degradation of the composite. The mechanism of moisture absorption is owing to the involvement of hydrophilic natural fibre and hydrophobic matrix by water molecule diffusion in the following steps [18]:

(1) The diffusion of water molecules inside the micro-gaps between polymer chains.
(2) Capillary transports into the gaps and flaws at the fibre–matrix interface.
(3) The transportation through matrix micro-cracks formed during the compounding process.

Based on the experimental results, the weight of the silk fibre/PLA sample increased with the increase of immersion time. For the silk fibre/PLA sample submerged into the solution for 4 months, it was found that the weight increases by 2.4% as shown in Table 2. For the pristine PLA sample, there is no change in weight with time at all. This result may be due to the hydrophilic effect of

silk fibre. In general, silk fibre has comparatively high moisture absorption which leads to swelling within the silk fibre/PLA sample. Although most of the fibres are encapsulated, the equilibrium of water in the composites induces PLA of the composite absorbing water faster than pure PLA. Therefore, the silk fibre/PLA composite would absorb water more quickly for water penetration into interfacial bonding until silk fibres get saturated.

Besides, it has been found that the Young's modulus, tensile strength, flexural modulus and flexural strength decrease as shown in Figs. 4–7, of both PLA and silk fibre/PLA samples after being immerged into water. Nevertheless, the properties of the silk fibre/PLA samples are worse as compared to those the neat PLA sample in general. Therefore, the mechanical properties of pure PLA and silk fibre/PLA composite were weakened because of the effects of water absorption. Water absorption of the samples has been associated with micromechanical damage in the resin and at the fibre–matrix interface as well as reduction of dimensional stability, development of internal stresses. Moreover, water molecules act as a plasticizer and penetrate into the polymer chains. These polymer chains are forced apart and become more mobile and consequently poor mechanical properties and faster degradation are resulted [18–20]. Besides, Tokiwa et al. have found that silk fibroin is one of the proteinous materials which stimulate the production of enzymes from PLA-degrading microorganisms and consequently
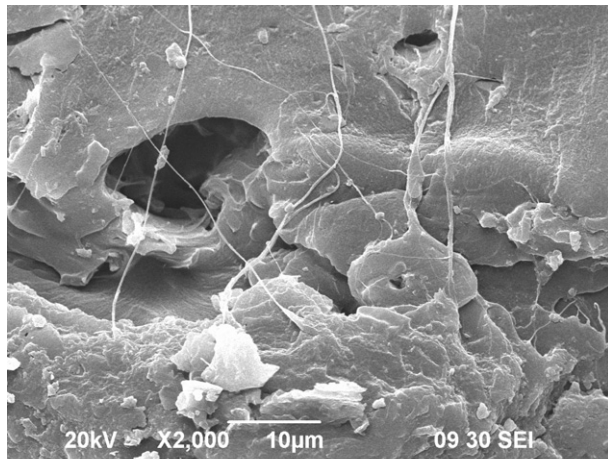
(a)
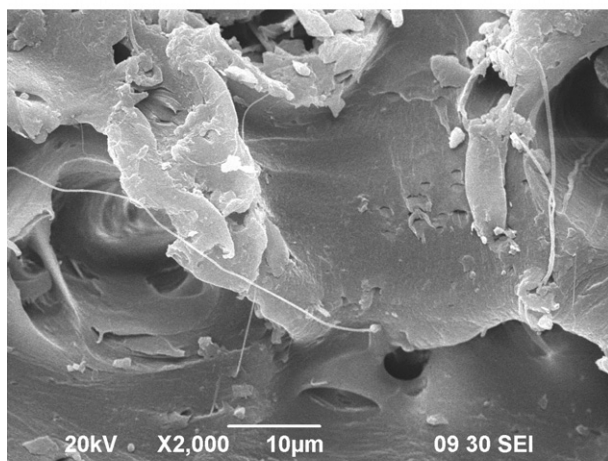
(b)

Fig. 8. (a) and (b) Scanning electron micrographs showing the micro-fibrils of the silk inside the composites.

immersion time. The declining rate of mechanical properties of the samples was demonstrated faster than that of pure PLA. It further proves that the hydrophilic effect of the silk fibre does affect the water absorbability in its related composites.

In the current study, it is found that the use of silk fibre, as reinforcement can enhance the modulus of PLA as well as alter its rate of bio-degradability, in which these properties are the primary parameters for the design of implants for bone fixation. The bio-degradation rate is crucial in which it have to be compromised with the cell growth rate of bone inside the human body. Besides, for the successful use of silk fibre/PLA composites in bone implant applications, the mechanical properties of the composite should withstand the loads which human bone suffered daily. Nevertheless, too stiff bone implant plant causes stress shielding of the bone and consequently the bone may become osteoporosis. Therefore, it should require further investigation of the bone plate with desirable biodegradation rate while at the same time possess proper mechanical properties (high modulus rv20 GPa, close to natural bone properties) with moderate strength) for supporting a load that an un-damaged bone should withstand.

speed up the degradation [21]. Silk fibre comprises numerous of micro-fibrils. After the degumming of silk fibre, they can be divided into two triangular of fibrils (brins) and furthermore, a fibril can be separated into individual micro-fibrils shown in Fig. 8 by the screws during injection moulding. These micro-fibrils may connect together from one end to another end, so the moisture can be easily penetrate into the silk fibre/PLA composites.

4. Conclusion

As the use of silk fibre reinforced PLA composites is aimed at developing a suitable material for bone fixation, their moduli and biodegradation rate are the leading parameters for the design of implant plates. Before the degradation test, the Young's modulus and flexural modulus of PLA increased over 27% and 2% respectively, with the use of 5 wt.% of silk fibre as reinforcement. The reduction of strength is mainly because of the poor interfacial bonding. However, the limited fibre content in injection moulding process and the poor fibre–matrix interface are the significant factors for strength decrement. After immersing samples into PBS solution to simulate their exposure in a liquidised environment, like human body, their mechanical properties were altered with

References

[1] Global Biomaterial Market (2009–2014). Markets and Markets; 2009.
[2] Bronzino JD. Biomedical engineering handbook: biomedical engineering fundamentals. CRC Press; 1999.
[3] Black J. Biological performance of materials: fundamentals of biocompatibility. CRC Press 2006.
[4] Flahiff CM, Blackwell AS, Hollis JM. Analysis of a biodegradable composite for bone healing. J Biomed Mater Res 1996;32:419–24.
[5] Claes L. The mechanical and morphological properties of bone beneath internal fixation plates of differing rigidity. J Orthopaed Res 1989;7(2):170–7.
[6] Burns AE, Varin J. Poly-L-lactic acid rod fixation results in foot surgery. J Foot Ankle Surg 1998;37(1):37–41.
[7] Tams J, Rozema FR. Poly (L-lactide) bone plates and screws for internal fixation of mandibular swing osteotomies. Int J Oral Maxillofac Surg 1996;25:20–4.
[8] Wang YZ. In vivo degradation of three-dimensional silk fibroin scaffolds. Biomaterials 2008;29:3415–28.
[9] Vepari C, Kaplan DL. Silk as a biomaterial. Prog Polym Sci 2007;32:991–1007.
[10] Wang YZ. Stem cell-based tissue engineering with silk biomaterials. Biomaterials 2006;27:6064–82.
[11] Fakirov S, Bhattacharya D. Handbook of engineering biopolymers: homopolymers, blends and composites. Cincinnati Ohio: Hanser; 2007 [chapter 16].
[12] Lee YW. Silk reeling and testing manual. Food & Agriculture Org; 1999. [chapter 2].
[13] Cheung HY, Ho MP, Lau KT. Natural fibre reinforced composites for bioengineering and environmental engineering applications. Compos Part B: Eng 2009;40:655–63.
[14] Fu SY, Bernd Lauke. Science and engineering of short fibre reinforced polymer composites. CRC Press LLC; 2009.
[15] Facca Angelo G. Predicting the tensile strength of natural fibre reinforced thermoplastics. Compos Sci Technol 2007;67:2454–66.
[16] Craven JP, Cripps R, Viney C. Evaluating the silk/epoxy interface by means of the microbond test. Composites: Part A 2000;31:653–60.
[17] Gijpferich A. Mechanisms of polymer degradation and erosion. Biomaterials 1996;17:103–14.
[18] Pickering K. Properties and performance of natural-fibre composites. CRC Press; 2008 [part 3].
[19] Lassila LVJ. The influence of short-term water storage on the flexural properties of unidirectional glass fiber-reinforced. Compos Biomater 2002;23:2221–9.
[20] Manfredi LB. Influence of the addition of montmorillonite to the matrix of unidirectional glass fibre/epoxy composites on their mechanical and water absorption properties. Composites: Part A 2008;39:1726–31.
[21] Tokiwa Y, Calabia BP. Biodegradability and biodegradation of poly(lactide). Appl Microbiol Biotechnol 2006;72:244–51.

Natural fibre-reinforced composites for bioengineering and environmental engineering applications

Hoi-yan Cheung [a,*], Mei-po Ho [a], Kin-tak Lau [a,b,*], Francisco Cardona [b], David Hui [c]

[a] Department of Mechanical Engineering, The Hong Kong Polytechnic University, Kowloon, Hong Kong, SAR, China
[b] Centre for Excellence in Engineered Fibre Composites, Faculty of Engineering & Surveying, University of Southern Queensland, Toowoomba, Qld 4350, Australia
[c] Department of Mechanical Engineering, University of New Orleans, New Orleans, LA 70148, USA

abstract

Recently, the mankind has realized that unless environment is protected, he himself will be threatened by the over consumption of natural resource as well as substantial reduction of fresh air produced in the world. Conservation of forests and optimal utilization of agricultural and other renewable resources like solar and wind energies, and recently, tidal energy have become important topics worldwide. In such concern, the use of renewable resources such as plant and animal based fibre-reinforce polymeric composites, has been becoming an important design criterion for designing and manufacturing components for all industrial products. Research on biodegradable polymeric composites, can contribute for green and safe environment to some extent. In the biomedical and bioengineered field, the use of natural fibre mixed with biodegradable and bioresorbable polymers can produce joints and bone fixtures to alleviate pain for patients. In this paper, a comprehensive review on different kinds of natural fibre composites will be given. Their potential in future development of different kinds of engineering and domestic products will also be discussed in detail.

© 2009 Elsevier Ltd. All rights reserved.

1. Introduction

1.1. Environmental concern

Since the past few decades, research and engineering interest has been shifting from traditional monolithic materials to fibre-reinforced polymer-based materials due to their unique advantages of high strength to weight ratio, non-corrosive property and high fracture toughness. These composite materials consisted of high strength fibres such as carbon, glass and aramid, and low strength polymeric matrix, now have dominated the aerospace, leisure, automotive, construction and sporting industries. Unfortunately, these fibres have serious drawbacks such as (i) non-renewable, (ii) non-recyclable, (iii) high energy consumption in the manufacturing process, (iv) health risk when inhaled and (v) non-biodegradable. Biodegradation is the chemical breakdown of materials by the action of living organisms which leads to changes in physical properties. It is a concept of vast scope, ringing form decomposition of environmental wastes involving micro-organisms to host-induced of biomaterials.

Although glass fibre-reinforced composites have been widely used due to its advantages of low cost and moderate strength,

for many years to provide solutions to many structural problems, the use of these materials, in turn would induce a serious environmental problem that most Western countries are now concerning. Recently, due to a strong emphasis on environmental awareness worldwide, it has brought much attention in the development of recyclable and environmentally sustainable composite materials. Environmental legislation as well as consumer demand in many countries is increasing the pressure on manufacturers of materials and end-products to consider the environmental impact of their products at all stages of their life cycle, including recycling and ultimate disposal [31]. In the United State, it encourages manufacturers to produce materials and products by practicing the 4Rs, which are (i) Reduce the amount and toxicity of trash to be discard (sourced reduction); (ii) Reuse containers and products; (iii) Repair what is broken (iv) Recycle as much as possible, which includes buying products with recycled content. After these processes are gone, the materials finally are entitled to be disposed to the landfill.

1.2. Bio-engineering concern

Bioengineering refers to the application of concepts and methods of the physical science and mathematics in an engineering approach towards solving problems in repair and reconstructions of lost, damaged or deceased (or ''non-functional'') tissues. Any material that is used for this purpose can be regarded as a biomaterial.

* Corresponding authors.
  E-mail addresses: karen.chy@gmail.com (H.-Y. Cheung), alan.ktlau@usq.edu.au, mmktlau@polyu.edu.hk (K.-t. Lau).

According to Williams [1], a biomaterial is a material used in implants or medical devices, intended to interact with biological systems. Those common types of medical devices include the substitute heart valves and artificial hearts, artificial hip and knee joints, dental implants, internal and external fracture fixators and skin repair templates, and etc. One of the major features of biocomposite materials is that they can be tailor made to meet different applications' requirements. The most common types of conventional composites are usually composed of epoxy, unsaturated polyester resin, polyurethanes (PU) or phenolic reinforced by glass, carbon or aramid fibres. These composite structures lead to the problem of conventional removal after the end of life time, as the components are closely interconnected, relatively stable and thus difficult to separate and recycle.

In bone repair, stainless steel and titanium have been used as bone plates for many years due to their unique biocompatible properties. However, the use of these materials for bone repair requires several times of subsequent surgical operations to remove the plates and other fasteners, which may cause unnecessary pain or inconvenience to the patients. Uneven growth of bone cells underneath and surrounding the plates may cause porosis. Refracture of the bones may also occur after the plate removal due to the differential stiffness between the bone and the plates. Table 1 shows the mechanical properties of different types of biomaterials used for the implant application. The comparison of the bone and cartilage properties, with other materials is also given. Therefore, less stiff materials should be used for making plates for bone fixation. Poly(lactic acid) (PLA) has been well recognized as a good material with both biodegradable and bioresorbable properties that can be inserted into the human body without inducing any harmful effect. However, since a degradable implant does not have to be removed surgically once it is no longer needed, degradable polymers are of value in short-term applications that require only the temporary presence of a device. The most concern relating to the use of degradable implants is the toxicity of the implant's degradation products. Besides, the low strength of the degradable polymers also limits the range of their applications.

2. Natural fibre

Within the past few years, there has been a dramatic increase in the use of natural fibres such as leaves from flax, jute, hemp, pineapple and sisal for making a new type of environmentally–friendly composites. Recent advances in natural fibre development, genetic engineering, and composites science offer significant opportunities for improved materials from renewable resources with enhanced support for global sustainability. Table 2 shows the mechanical properties of different types of potential natural fibres for composite applications. A material that can be used for medical application must possess a lot of specific characteristics, which are different with that for the general domestic-used plastic products. The most

Table 2
Mechanical properties of different types of potential natural fibres for composite applications.

	Tensile strength (MPa)	Elongation at break (%)	Young modulus (GPa)
Natural fibres			
Flax	300–1500	1.3–10	24–80
Jute	200–800	1.16–8	10–55
Sisal	80–840	2–25	9–38
Kenaf	295–1191	3.5	2.86
Pineapple	170–1627	2.4	60–82
Banana	529–914	3	27–32
Coir	106–175	14.21–49	4–6
Oil palm (empty fruit)	130–248	9.7–14	3.58
Oil palm (fruit)	80	17	
Ramie	348–938	1.2–8	44–128
Hemp	310–900	1.6–6	30–70
Wool	120–174	25–35	2.3–3.4
Spider silk	875–972	17–18	11–13
Cotton	264–800	3–8	5–12.6
Human tissues			
Hard tissue (tooth, bone, human compact bone, longitudinal direction)	130–160	1–3	17–20
Skin	7.6	78	
Tendon	53–150	9.4–12	1.5
Elastic cartilage	3	30	
Heart valves	0.45–2.6	10–15.3	
Aorta	0.07–1.1	77–81	

fundamental requirements are related to biocompatibility, without having any adverse effect to the host tissues. Therefore, those traditional composite structures with non-biocompatible matrix or reinforcement are substituted by bio-engineered composites. Table 3 summarizes several important factors that are needed to be considered in selecting a material for the biomedical applications.

In the environmental concern, the use of these fibre mixed with biodegradable polymers, like PLA and poly(glycolide) (PGA) can produce biodegradable composites (somehow, they are called ''Green composites'' or ''Environmentally–friendly plastics''). These composites should possess moderate strength and/or thermal stability while they must be recyclable after being used. However, the currently problems of using pure biodegradable polymers are their low strength and low service temperature, such as their glass transition temperature (T_g). In general, T_g of these polymers is around 40–60 oC, which is much below other synthetic polymers. In Tables 4 and 5, the characteristics of synthetic polymers, bioresorbable and biocompatible polymers are shown. Fig. 1 also shows the chemical structures of widely investigated biocompatible and biodegradable polymers. Polyethylene (PE) is normally in its high-density (HDPE) form in biomedical application because low-density material cannot withstand sterilization temperatures. Polypropylene (PP) is an isotactic crystalline polymer with high rigidity, good chemical resistance and moderate strength, which has a higher fracture toughness than HDPE. Polytetrafluoro-ethylene (PTFE) is a very high melting ($T_m = 312$ oC) and high crystallinity polymer. PLA and PGA and their co-polymers are used in resorbable surgical sutures. The degradation products are endogenous compounds and such are non-toxic. For the tables, it is obvious that those synthetic polymers for being used in biomedical devices have better thermal properties than that of bioresorbable polymers. However, the mechanical properties of all these polymers are relatively low as compared with traditional metallic materials for implants and other fixation applications.

Bio-composites consist of biodegradable polymer as matrix and usually bio-fibres as reinforcing elements which are generally low cost, low density, high toughness, acceptable specific strength properties, good thermal properties, ease of separation, enhanced

Table 1
Mechanical properties of typical implant materials and tissues.

	Elastic modulus (GPa)	Yield strength (MPa)	Tensile Strength (MPa)	Elongation to failure (%)
Al_2O_3	350	–	1000–10,000	0
CoCr Alloy	225	525	735	10
Stainless steel	210	240	600	55
316	120	830	900	18
Ti–6Al–4V	15–30	30–70	70–150	0–8
Bone (Cortical)	3.0	–	35–50	0.5
PMMA	0.6–1.8	–	23–40	200–400
HDPE Cartilage	Strong viscoelastic	–	7–1	20

Table 3
Key factors for the selection of materials for biomedical applications [2].

Factors	Description		
	Chemical/biological characteristics	Physical characteristics	Mechanical/structural characteristics
1st Level material properties	• Chemical composition (bulk and surface)	• Density	• Elastic modulus • Shear modulus • Poisson's ratio • Yield strength • Compressive strength
2nd Level material properties	• Adhesion	• Surface topology • Texture • Roughness	• Hardness • Flexural modulus • Flexural strength
Specific functional requirements (based on applications)	• Biofunctionality • Bioinert • Bioactive • Biostability • Biodegradation behavior	• Form and geometry • Coefficient of thermal expansion • Electrical conductivity • Color, aesthetics • Refractive index • Opacity or translucency	• Stiffness or rigidity • Fracture toughness • Fatigue strength • Creep resistance • Friction and wear resistance • Adhesion strength • Impact strength • Proof stress • Abrasion resistance
Processing & Fabrication	• Reproducibility, quality, sterilizability, packaging, secondary processability		
Characteristics of host: tissue, organ, species, age, sex, race, health condition, activity, systemic response Medical/surgical procedure, period of application/usage			
Cost			

Table 4
Characteristics of different kinds of polymers.

Type	Thermal properties	Construction/useful form
Synthetic polymers		
Polyethylene (PE) Polypropylene	T_m = 203–208 oC	Heath care products, light weight orthopaedic casts, ligament prostheses
(PP) Poly(tetrafluoro-ethylene)	T_m = 223–233 oC	Surgical drapes, and gowns
(PTFE) Nylon 6	T_m = 313–315 oC	Vascular fabrics, heart valve sewing rings, orthopaedic ligaments
Poly(ethylene terephthalate (PET))	T_g = 45 oC, T_m = 220 oC	Sutures
	T_g = 65–105 oC, T_m = 265 oC	Sutures
Bio-absorbable synthetic polymers		
Poly(glycolide) (PGA)	T_g = 40–45 oC, T_m = 225 oC	Absorbable sutures and meshes
Poly(p-dioxanone) (PDS)	T_g = 10 oC, T_m = 205 oC	Sutures, intramedullary pins
Poly(lactic-acid) (PLA)	T_g = 60 oC and T_m = 166 oC	Bone fixture

energy recovery and biodegradability. Bio-fibres are chosen as reinforcements since they can reduce the chance of tool wear when processing, dermal and respiratory irritation. Conversely, these fibres are usually small in cross-sections and cannot be directly used in engineering applications; they are embedded in matrix materials to form biocomposites. The matrix serves as binder to bind the fibres together and transfer loads to the fibres. In order to develop and promote these natural fibres and their composites, it is necessary to understand their physico-mechanical properties.

3. Plant-based fibres

As aforementioned, with the increasing global energy crisis and ecology risk, plant-based fibre-reinforced polymer composites have attracted much interest owing to their potential of serving as alternatives for artificial fibre composites, like glass and carbon. Although the strength of such fibres (more than one type) are general lower than that of the traditional advanced composites, in certain extent, the strength of plant-based fibre-reinforced composites is sufficient enough for domestic or household plastic products. Many attempts have been done in the past few years on using jute, bamboo, sisal, coir, hemp, flax, pineapple leaves, etc., for reinforcing different kinds of thermoplastic and thermoset polymers to form green composites.

Wambua et al. [3] conducted a series of experiments to comprehensively study the strength enhancement of different plant-based fibre polymeric composites. They have reported that the successful production of good quality of plant-based composites is highly re-

Table 5
Mechanical properties of biomedical polymers.

Polymer	Water absorption (%)	Bulk modulus (GPa)	Tensile strength (MPa)	Elongation at break (%)	T_g (oC)	T_m (oC)
Polyethylene (PE)	0.001–0.02	0.8–2.2	30–40	130–500	71–76	203–208
Polypropylene (PP)	0.01–0.035	1.6–2.5	21–40	50–800	117–132	222–233
Polyurethane (PU)	0.1–0.9	1.5–2	28–40	600–720	93–121	233–272
Polytetrafluoro-ethylene (PTFE)	0.01–0.05	1–2	15–40	250–550	145–146	312–315
Polyvinyl-chloride	0.04–0.75	3.4	10–75	10–400	121–183	217
Polyamides	0.25–3.5	2.4–3.3	44–90	40–250	145–185	256–282
Polycarbonate (PC)	0.15–0.7	2.8–4.6	56–75	8–130	214	258–273
Bombyx mori silk	0.2–1	0.015–0.017	610–690	4–16	–	–
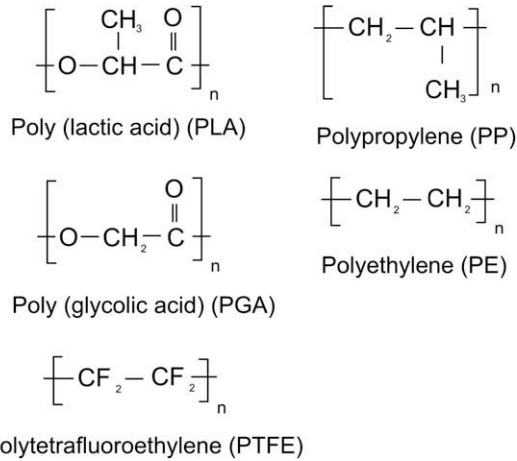
Fig. 1. Chemical structures of widely investigated biocompatible and bio-degradable polymers.

Fig. 2. Hollow section of a sisal fibre [5].

Fig. 3. Raw Cocoon silks (a) and side view of the silk fibre (b).

lied on their bonding properties between the fibre and matrix. This also governs their biodegradability in real life applications. It was found that a hemp fibre composite with 30% fibre volume fraction (V_f), demonstrated 73% better tensile strength than that of kenaf, sisal and jute fibre composites. The use of coir fibre showed the lowest strength (only 20% of that of the hemp fibre composite). According to the information shown in Table 6, the attribution to strength increment may be due to the strength of fibres, as well as their interfacial bonding properties. It was found that the use of hemp, jute and flax fibres bore better strength as compared with jute, ramie and cotton fibres. Coir fibre possesses the lowest tensile strength as compared with others. Rahman et al. [4] have indicated that the tensile strength decreased while the Young modulus, flexural strength and charpy impact strength increased with increasing the content of jute fibre for jute/polypropylene (PP) composites. Silva et al. [5] have shown that hollow structure inside the sisal fibre was found (Figs. 2 and 3) that would ultimately weaken the strength of its composites, as the net cross-sectional area decreases, and thus stress taken by the fibre is then increased. Selection of right portion with higher density of the fibre is needed to maximize the load bearing capability of the fibre is achieved.

A notable remark for making high strength biodegradable composites found in the table is the water absorbability of different types of plane-based fibre. Cotton and ramie demonstrate high possibility in absorbing moisture during composite manufacturing process, while hemp and flax are relatively less. This would seriously affect the integrity and complete chemical reaction due to excessive water molecules exist of a resultant composite. Such moisture penetration into composite materials occurs by three different conditions, they would diffuse inside the micro-gaps between (i) the polymer chains; (ii) the interface between the fibre and matrix and (iii) existing cracks. The control of manufacturing environment, such as low humidity or under vacuum, is essential to minimize any moisture molecules trapped inside the composite. Drying process is normally required to remove excessive moisture. As compared with the modulus of the hemp, flax and E-glass, they
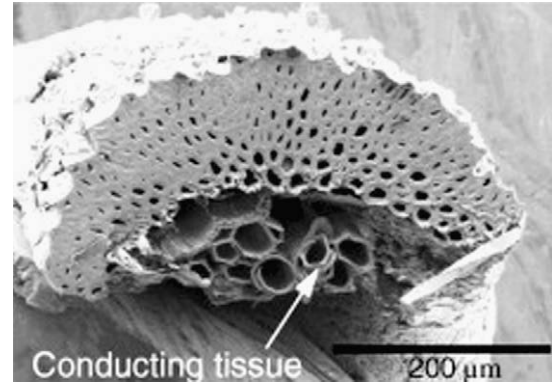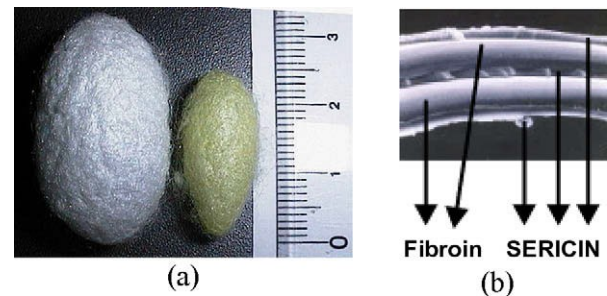
are almost the same but the weight of the plant-based fibres is much lower than the E-glass.

Wood fibre, due to its low density, high specific strength and Young modulus, non-abrasive to processing equipment, low cost and importantly biodegradable, has also attracted much attention in the last decade [6]. However, the main disadvantage of wood fibre is its hydrophilic nature as compared with carbon and glass fibres. Besides, the use of bamboo, a million tonne of wastes from this material produced every year, for producing polymer-based composites have been found in the past few years. The microstructure of bamboo is different from wood, for example, the different content of lignin and different polarity of materials. Wang et al. [7] studied the use of bamboo particles to reinforce Polyvinylchloride (PVC) to form a new type of composites. However, the results, in terms of their mechanical properties were not consistent with their moisture contents and mesh granule size.

4. Animal-based fibres

4.1. Silk-based fibre

Apart from the plant-based fibres, animal-based fibres become other alternatives for producing biodegradable, biomedical and bio-resorbable composite materials for bioengineering and orthopaedic applications. The content of these fibres are mainly made

Table 6
Material and mechanical properties of E-glass and other plant-based fibres.

Properties/fibres	E-glass	Hemp	Jute	Ramie	Coir	Sisal	Flax	Cotton
Density (g=m^3)	2.55	1.48	1.46	1.5	1.25	1.33	1.4	1.51
Tensile strength (MPa)	2400	550–900	400–800	500	220	600–700	800–1500	400
Tensile modulus (GPa)	73	70	10–30	44	6	38	60–80	12
Elongation at break (%)	3	1.6	1.8	2	15–25	2–3	1.2–1.6	3–10
Moisture absorption (%)	–	8	12	12–17	10	11	7	8–25

by proteins, like wool, spider and silkworm silk. The enhanced environmental stability of silk fibres in comparison to globular proteins is due to the extensive hydrogen bonding, the hydrophobic nature of much of the protein, and the significant crystallinity.

Silk proteins – known as silk fibroins are stored in the glands of insects and spiders as an aqueous solution. During the spinning process, silkworm accelerates and decelerates its head in arcs to each change of direction, and the concentration of silk in the solution is gradually increased and finally, elongation stress is applied to produce a partly crystalline, insoluble fibrous thread in which the bulk of the polymer chains in the crystalline regions are oriented parallel to the fibre axis. Faster spinning speed leads to stronger but more brittle fibres where slower speed leads to weaker and more extensible fibres. At even greater speed, silk toughness decreased, mainly due to the loss of extensibility [8].

Cocoons are natural polymeric composite shells made of a single continuous silk strand with length in the range of 1000–1500 m and conglutinated by sericin [9]. This protein layer resists oxidation, is antibacterial, ultra-violet (UV) resistant, and absorbs and releases moisture easily. Since this protein layer can be cross-linked, copolymerized, and blended with other macromolecular materials, especially artificial polymers, to produce materials with improved properties. In average, the cocoon production is about 1 million tonnes worldwide, and this is equivalent to 400,000 tonnes of dry cocoon (see Fig. 2). In the tissue engineering area, silks have been identified as a kind of biomaterials, used for healing process for bone, tendons or ligament repairs. Slowly degrading biomaterials which can maintain tissue integrity following implantation, while continually transferring the load-bearing burden to the developing biological functional tissue are desired. In such phenomena, the gradual transfer of the load-bearing burden to the developing and/or remodelling tissue should support the restoration and maintenance of tissue function over the life of the patient.

Silk fibre spun out from silkworm cocoons are consisted of fibroin in the inner layer and sericin in the outer layer, all are protein based. From outside to inside layers of cocoon, the volume fractions of sericin decreases while the relative content of fibroin increases. Also, it is known that silk fibroin consists of both hydrophilic and hydrophobic regions which is a block-like polymeric system. These fibres have a highly non-uniform cross-sectional geometry with respect to both shape and absolute dimensions. By changing the reeling conditions, silkworm silk can be stronger, stiffer and more extensible, approaching to the properties of spider dragline silk [10]. Each raw silk thread has a lengthwise striation, consisting of two separate but irregularly entwined fibroin filaments embedded in sericin. Silk sericin is a minor protein that envelops silk fibroin fibre and glues them together to form cocoon shape. Fibroin and sericin in silk account for about 75 and 25 wt%, respectively. Silk fibre is biodegradable and highly crystalline with a well-aligned structure.

Composition, structure and material properties of silk fibre produced by spiders, silkworms, scorpions, mites and flies may differ widely depending on the specific source and the uncontrollable reeling conditions of those insects. Spinning under controlled conditions will have more uniform cross-sectional area of silk fibre, reproducible molecular alignment and fewer micro-structural flaws. The size and weight of cocoons decrease with an increase in temperature and cocoons can bear efficiently both external static forces and dynamic impact loadings [10]. Normal compact cocoon exhibits a high ability of elastic deformation with an elastic strain limit higher than 20% in both longitudinal and transverse directions. Anisotropic properties mainly due to the non-uniform distribution and orientations of silk segments and the inner layer of cocoon has low porosity (higher silk density) and smaller average diameter of silk, therefore, there is an increase in elastic modulus and strength

from outside to inside layers. That is, the thinner the silk, the higher the elastic modulus and tensile strength and the maximum values at the innermost layer. On the other hand, temperature above the glass transition temperature, the cocoon and its layers become softer and softer and behave similar to a rubber-like material. Silk fibre have higher tensile strength than glass fibre or synthetic organic fibre, good elasticity, and excellent resilience [11]. They resist failure in compression, stable at physiological temperatures and sericin coating is water-soluble proteinaceous glue.

Fibroin is a semi-crystalline polymer of natural fibrous protein mainly consists of two phases [12]: namely b–sheet crystals and non-crystalline including micro-voids and amorphous structure, by which the structure of sericin coating is amorphous acting as an adhesive binder to maintain the fibroin core and the overall structural integrity of the cocoon. Degumming is a key process during which sericin is removed by thermo-chemical treatment of the cocoon. Although this surface modification can affect the tensile behavior and the mechanical properties of silk significantly, it is normally done to enhance interfacial adhesion between fibre and matrix.

In addition, according to Altman [13], silks are insoluble in most solvents, including water, dilute acid and alkali. Reactivity of silk fibre with chemical agents is positively correlated to the largeness of internal and external surface areas [14]. When fabricating silk-based composites, the amount of resin gained by fibre is strongly related to the degree of swelling of the non-crystalline regions, that is, the amorphous regions and the micro-voids inside the fibre.

4.2. Chicken feather fibre

Chicken feather fibre (CFF) has attracted much attention to different product design and engineering industries recently, so as the use of CFF as reinforcements for polymer-based biodegradable materials has emerged gradually. The advantages of using this natural fibre over traditional reinforcing fibres in biocomposites are low cost, low density, acceptable specific strength, recycability, bio-degradability etc. CFF, because of its renewable and recyclable characteristics, have been appreciated as a new class of reinforcements for polymer-based biocomposites. However, the full understanding of their mechanical properties, surface morphologies, environmental influences due to moisture and chemical attacks, bonding characteristics between silk fibroin and surrounding matrix and manufacturing process is essential.

According to the survey conducted recently, a chicken processing plant produces about 4000 pounds of chicken feathers every hour. In most western countries, these feathers are used as (i) feather fibre feed; (ii) air filter elements that replaces traditional wood pulps (retarding the trees cut down rate) and (iii) lightweight feather composites. Chicken feathers are approximately 91% protein (keratin), 1% lipids, and 8% water. The amino acid sequence of a chicken feather is very similar to that of other feathers and also has a great deal in common with reptilian keratins from claws [15]. The sequence is largely composed of cystine, glycine, proline, and serine, and contains almost no histidine, lysine, or methionine. In fact, a CFF is made up of two parts, the fibres and the quills (see Fig. 4). The fibre is thin filamentous materials that merge from the middle core material called quills. In simple terms, the quill is hard, central axis off which soft, interlocking fibres branch. Smaller feathers have a greater proportion of fibre, which has a higher aspect ratio than the quill. The presence of quill among fibres results in a more granular, lightweight, and bulky material. A typical quill has dimensions on the order of centimeters (length) by millimeters (diameter). Fibre diameters were found to be in the range of 5–50 lm. The density of CFF is lighter than other synthetic and natural reinforcements, thus, CFF inclusion in a composite could potentially lower composite density, whereas the den-
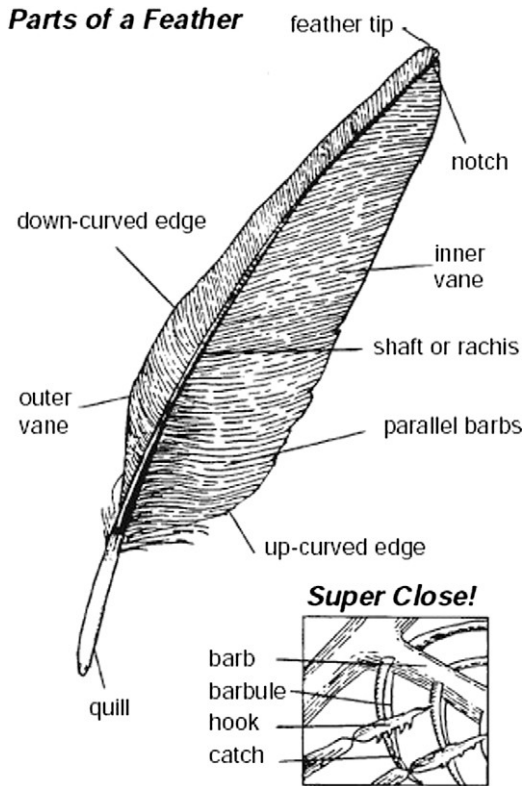
Parts of a Feather

Fig. 4. A typical chicken feather fibre.

235 oC while an outer quills is 225 oC. High T_g represents that a tighter keratin structure is formed to which water is more strongly bonded. Fibres and inner quills do not begin to lose water below 100 oC. The moisture evolution temperature of the CFF and quill occurs in the range of 100–110 oC [16]. This suggests that it may be possible to have a fully dry fibres and inner quills at 110 oC.

The length and diameter (sometime in the form of bundles) of CFF would highly affect their properties and impregnatability of resin into a resultant composite. Therefore, the control of resin temperature (thus, its viscosity), while at the same time to manage the sonication (ultrasonic vibration) time to facilitate the resin penetration rate into the fibres are essential. Short or longer fibres would highly affect the stress transferability as well as shear strength of the composites. The fibres, themselves also would be a barrier to the movement of polymer chains inside the composites and it may result in increasing their strength and thermal properties, but reduce their fracture toughness. These properties will be studied in detail, in this project. Fig. 6 shows the SEM image of the down chicken feather fibre and its strength compared with other type of feathers. It was found that the development of chicken feather fibre biocomposites have been increasing in recent years, and the outcome are expected to be able to alleviate the global waste problem.

5. Applications

5.1. Wound sutures

Silk fibre has been used in biomedical applications particularly as sutures by which the silk fibroin fibre is usually coated with waxes or silicone to enhance material properties and reduce fraying. But in fact, there are lots of confusing questions about the usage of this kind of fibre as there is the absence of detailed characterization of the fibre used including the extent of extraction of the sericin coating, the chemical nature of wax-like coatings sometimes used, and many related processing factors. For example, the sericin glue-like proteins are the major causes of adverse problems with biocompatibility and hypersensitivity to silk. The variability of source materials has raised the potential concerns with this class of fibrous protein. Yet, silk's knot strength, handling characteristics and ability to lay low to the tissue surface make it popular suture in cardiovascular applications where bland tissue reactions are desirable for the coherence of the sutured structures [17].

5.2. Scaffolds tissue engineering

A three-dimensional scaffold permits the in vitro cultivation of cell–polymer constructs that can be readily manipulated, shaped, and fixed to the defect site [18]. The matrix acts as the translator

sity of a typical composite with synthetic reinforcing increases as fibre content increases. Hence, light weight composite materials can be produced by inclusion of CFF to plastics which even reduces the transportation cost. The barbs at the upper portion of the feather are firm, compact, and closely knit, while those at the lower portion are downy, i.e. soft, loose, and fluffy. The down feather provides insulation, and the flight feather provides an airfoil, protects the body from moisture, the skin from injury, and colors and shapes for displays. Fig. 5 shows the cross-sectional views of the flight and down feather fibres. It is obvious that flight feather fibre exited in a hollow form while down fibre is in solid. In terms of the purpose of fibre-reinforcement, the use of down fibre appears much better than that the use of flight fibre.

The moisture content of CFF is an important factor that can highly influence their weight and mechanical properties. The moisture content of processed CFFs can vary depending upon processing and environmental conditions. The glass transition temperature (T_gÞ of the feather fibres and inner quills is approximately
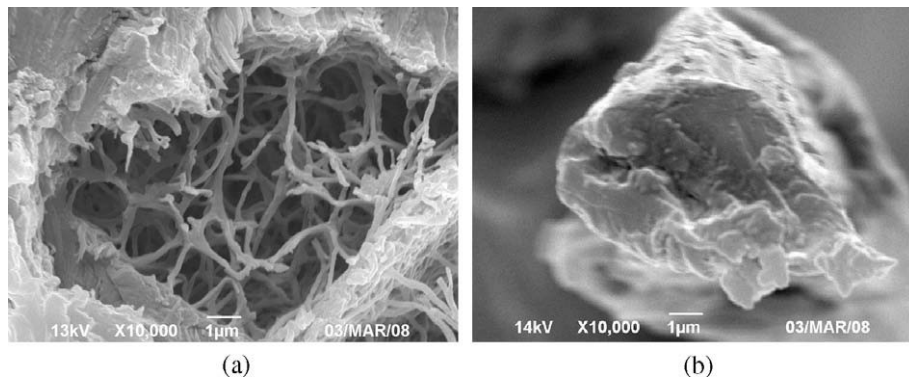

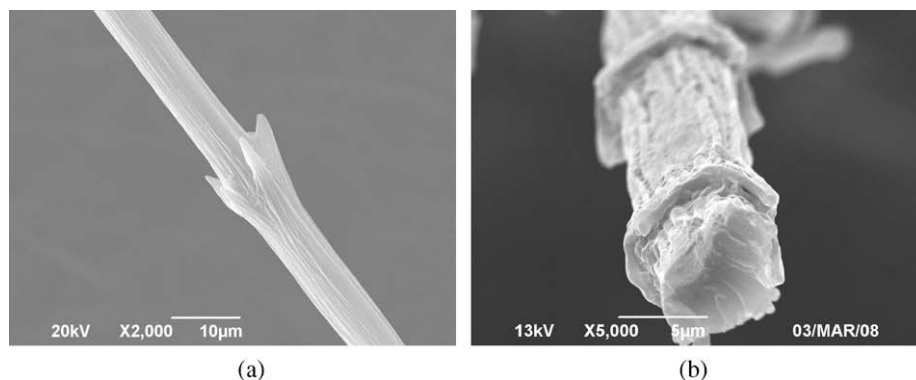Fig. 5. Flight chicken feather fibre (a) and down chicken feather fibre (b).

Fig. 6. SEM images of the chicken feather fibre.

between the local environment (either in vitro or in vivo) and the developing tissue, aiding in the development of biologically viable functional tissue. However, during the 1960s to the early 1980s, the use of virgin silk negatively impacted the general acceptance of this biomaterial from the surgical practitioner perspective, for examples, the reaction of silk to the host tissue and the inflammatory potential of silk. Recently, silk matrices are being rediscovered and reconsidered as potentially useful biomaterials for a range of applications in clinical repairs and as scaffolds for tissue engineering.

Silk, as a protein, is susceptible to proteolytic degradation in vivo and over longer period of time in vivo will slowly be absorbed. Degradation rate of implants mainly depend on health and physiological status of patient, mechanical environment of the implantation site, and types and dimensions of the silk fibres. Slow rate of degradation of silk in vitro and in vivo makes it useful in biodegradable scaffolds for slow tissue ingrowths since the biodegradable scaffolds must be able to retain at the implantation site, including maintains their mechanical properties and supports the growth of cells, until the regenerated tissue is capable to fulfill the desired functions. The degradation rate should be matched with the rate of neo-tissue formation so as to compromise the load-bearing capabilities of the tissue.

Additionally, scaffold structures including size and connective of pores determine the transport of nutrients, metabolites and regulatory molecules to and from cells. The matrix must support cell attachment, spreading, growth and differentiation. Meinel et al. [19] concentrated on cartilage tissue engineering with the use of silk protein scaffold and the authors identified and reported that silk scaffolds are particularly suitable for tissue engineering of cartilage starting from human mesenchymal stem cells (hMSC), which are derived from bone marrow, mainly due to their high porosity, slow degradation, and structural integrity.

Recent research with silk has focused on the development of a wire rope matrix for the development of autologous tissue engineered anterior cruciate ligaments (ACL) using a patient's own adult stem cells [20]. Silk fibroin offers versatility in matrix scaffold design for a number of tissue engineering needs in which mechanical performance and biological interactions are major factors for success, including bone, ligaments, tendons, blood vessels and cartilage. Silk fibroin can also be processed into foams, films, fibres and meshes.

5.3. Silk-based biocomposites

Annamaria et al. [21] discovered in the studies that environmentally–friendly biodegradable polymers can be produced by blending silk sericin with other resins. Nomura et al. [22] identified that polyurethane foams incorporating sericin are said to have

excellent moisture-absorbing and –desorbing properties. Hatakeyama [23] also reported for producing sericin-containing polyurethane with excellent mechanical and thermal properties. Sericin blends well with water-soluble polymers, especially with polyvinyl alcohol (PVA). Ishikawa et al. [24] investigated the fine structure and the physical properties of blended films made of sericin and PVA. Moreover, a recent patent reported on a PVA/sericin cross-linked hydrogel membrane produced by using dimethyl urea as the cross-linking agent had a high strength, high moisture content and durability for usage as a functional film [25].

Silk fibroin film has good dissolved oxygen permeability in wet state but it is too brittle to be used on its own when in dry state; whereas for chitosan, it is a biocompatible and biodegradable material which can be easily shaped into films and fibres. Park et al. and Kweon et al. [26,27] introduced an idea of silk fibroin/chitosan blends as potential biomedical composites as the crystallinity and mechanical properties of silk fibroin are greatly enhanced with increasing chitosan content.

Another type of bio-composites is the silk fibroin/alginate blend sponges. For biotechnological and biomedical fields, silk fibroin's reproducibility, environmental and biological compatibility, and non-toxicity benefit in many different clinical applications. As the collective properties, especially mechanical properties of silk fibroin sponges in dry state are too weak to handle as wound dressing, thus, they can be enhanced by blending silk fibroin films with other synthetic or natural polymers, for examples, polysaccharide–sodium alginate.

Furthermore, Katori and Kimura [28] and Lee et al. [29] examined the effect of silk/poly(butylenes succinate) (PBS) bio-composites. They found that the mechanical properties including tensile strength, fracture toughness and impact resistance, and thermal stability of biocomposites would be greatly affected by their manufacturing processes. Moreover, a good adhesion between the silk fibre and PBS matrix was found through the observation and analysis by Scanning Electron Microscope (SEM) imaging.

The mechanical properties of Bombyx mori, twisted Bombyx mori and Tussah silk fibres were also investigated through tensile property tests. It was found that Tussah silk fibre exhibited better tensile strength and extensibility as compared with others, and the stiffness of all samples was almost the same. This may be due to the distinction of silkworm raising process, cocoon producing and spinning conditions. Based on the Weibull analysis, it was shown that the Bombyx mori silk fibre has a better reproducibility in terms of experimental measurement, than that of the Tussah silk fibre.

By using silk fibre as reinforcement for biodegradable polymer, the mechanical properties do have a substantial change. Cheung et al. [30] have demonstrated that the use of silk fibre to reinforce PLA can significantly increase its elastic modulus and ductility to
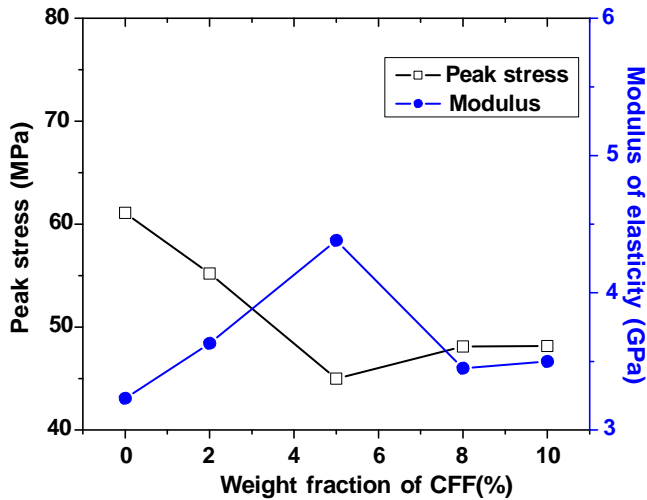
Fig. 7. Relationship between tensile properties and CFF content of CFF/PLA composite.

Fig. 8. Stress–strain curves of (a) pure PLA sample; (b) 5 wt% CFF/PLA composite.

40% and 53%, respectively, as compared with a pristine sample. It was also found that the bio-degradability of silk/PLA biocomposites was altered with the content of the silk fibre in the composites. It reflects that the resorbability of the biocomposites used inside the human body can be controlled, in which this is the key parameter of using this new type of materials for bone plate development.

5.4. CFF/PLA biocomposites

By mixing CFF with biopolymers, like PLA can form a biodegradable composites used for plastic products and implant applications. In preparation of the composites, chicken feather was immersed in alcohol for 24 h, then washed in a water soluble organic solvent, and dried under 60 oC for 24 h [32]. CFF with a diameter of about 5 μm and length of 10–30 mm were separated from the quill and then used. Fig. 5 shows an SEM photograph of a CFF. Fig. 7 also shows the relations between CFF content and peak stress and modulus of elasticity, respectively. The modulus of elasticity of CFF/PLA composite increases with the CFF content and reaches the maximum modulus of 4.38 GPa (increment up to 35.6%) at the CFF content of 5 wt%. These reveal that the incorporation of CFF into the matrix is quite effective for reinforcement. The decrease of modulus for the composite with the CFF content above 5 wt% will be due to the insufficient filling of the matrix resin, designating 5 wt% CFF is the critical content.

It also can be found from the peak stress that the tensile strength of PLA after the addition of CFF is lower than that of pure PLA. This phenomenon, also reported by other researchers [15,32], is an indication of poor adhesion between the CFF and the matrix. Although the CFF surface is rough (Fig. 6a) and the hydrophobic consistency of CFF and PLA, the adhesion between them is a problem to solve. And the stress could not be transferred from the matrix to the stronger fibres. Another possible explanation of this phenomenon can be that the CFFs were randomly oriented inside the composite; the failure of the composite might be initiated by the failure of the matrix and then followed by fibre breakage. Fig. 8 shows the stress–strain curves of the pure PLA and 5 wt% CFF/PLA composite. It is observed that a much longer plateau is located between a strain where the peak stress is reached and the strain at break. It can be concluded that the proper content addition of CFF shows a positive effect on elongation to break for PLA, which was expected because of CFFs acting as bridges to prolong the fracture process of the CFF/PLA composite and that the failure
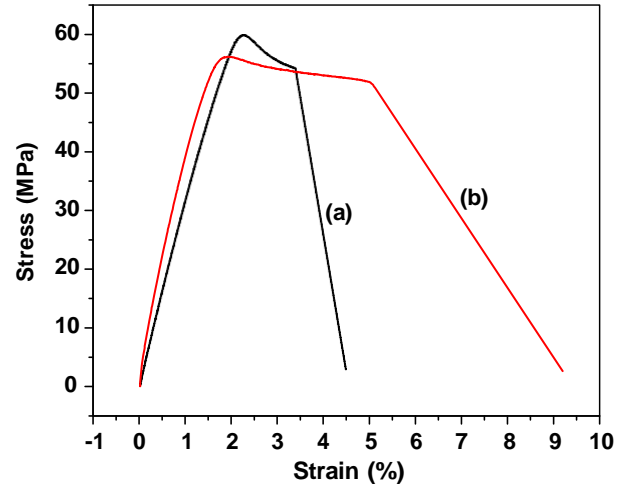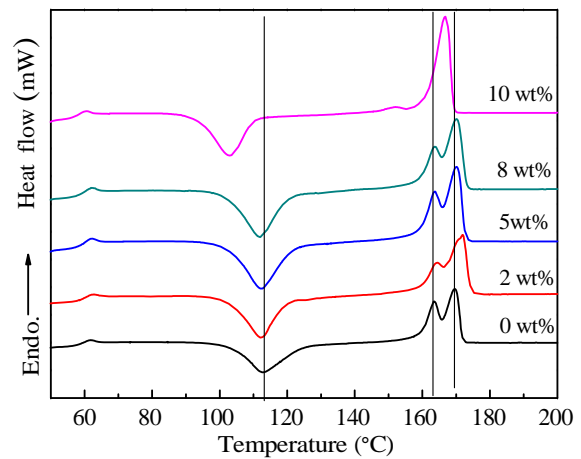

Fig. 9. DSC curves of pure PLA and CFF/PLA composites.

of the composite was controlled by the bridging effect of CFF inside the composite. These conclusions could be proved by the fractured morphology of the microstructures observed by SEM. The thermal properties such as glass transition temperature (T_g), crystallization temperature (T_c), melting temperature (T_m), crystallization enthalpy (ΔH_c) and melting enthalpy (ΔH_m) obtained from the DSC studies are plotted in Fig. 9.

6. Conclusion

The potential use of natural fibre composites is discussed in this paper. Their mechanical and thermal properties have been in depth investigated since the last decade. The mechanical properties in terms of the elastic modulus and ductility of these biocomposites increased substantially compared to the neat polymers. The mechanical properties of most of plant-based fibre composites increased with increasing the amount of fibre into polymer matrix. However, the ultimate strength decreased as expected. From those experimental results, incorporation of the fibres gave rise to a considerable increase of the storage modulus (stiffness) and to a decrease of the tan delta values. These results demonstrate the reinforcing effect of animal-based fibre on PLA matrix. It also reveals that biocomposite with small amount of animal fibre

provided also better thermal properties as compared with pristine polymers.

Although plant- and animal-based fibres were attracted much attention to the product design and engineering, and bioengineering industries and undergone comprehensive researches in the past few years, many works such as their interfacial bonding and stress transfer properties have not yet been solved to date. To wider the applications of these fibres in solving environmental problems, more studies have to be continued in the future.

Acknowledgements

References

[1] Williams DF. Definitions in biomaterials. In: Proceedings of a consensus conference of the European society for biomaterials, vol. 4. Chester, England. New York: Elsevier; 1986.

[2] In: Ratner BD, Hoffman AS, Schoen FJ, Lemons JE. editors. Biomaterials Science. USA: Elsevier Academic Press; 2004.

[3] Wambua P, Ivens J, Verpoest I. Natural fibres: can they replace glass in fibre-reinforced plastics?. Comp Sci Tech 2003;63:1259–64.

[4] Rahman MR, Huque MM, Islam MN, Hasan M. Improvement of physico-mechanical properties of jute fiber reinforced polypropylene composites by post-treatment. Comp Pt A 2008;39:1739–47.

[5] Silva FA, Chawla N, Filho RDT. Tensile behaviour of high performance natural (sisal) fibers. Comp Sci Tech 2008;68:3438–43.

[6] Beg MDH, Pickering KL. Mechanical performance of Kraft fibre-reinforced polypropylene composites: influence of fibre length, fibre beating and hygrothermal ageing. Comp Pt A 2008;39:1748–55.

[7] Wang H, Chang R, Sheng KC, Adl M, Qian XQ. Impact response of bamboo-plastic composites with the properties of bamboo and polyvinylchloride (PVC). J Bionic Eng Suppl 2008;5:28–33.

[8] Shao Z, Vollrath F. Surprising strength of silkworm silk. Nature 2002;418:741.

[9] Zhao HP, Feng XQ, Yu SW, Cui WZ, Zou FZ. Mechanical properties of silkworm cocoons. Polymer 2005;46:9192–201.

[10] Atkins E. Silk's secrets. Nature 2003;424:1010.

[11] Perez-rigueiro J, Viney C, Llorca J, Elices M. Silkworm silk as an engineering material. J Appl Polym Sci 1998;70:2439–47.

[12] Jiang P, Liu H, Wang C, Wu L, Huang J, Guo C. Tensile behavior and morphology of differently degummed silkworm (Bombyx mori) cocoon silk fibers. Mater Lett 2006;60:919–25.

[13] Altman GH, Diaz F, Jakuba C, Calabro T, Horan RL, Chen J, et al. Silk-based biomaterials. Biomaterials 2003;24:401–16.

[14] Kawahara Y, Shioya M. Characterization of microvoids in Mulberry and Tussah silk fibers using stannic acid treatment. J Appl Polym Sci 1999;73:363–7.

[15] Fraser RDB, Parry DAD. The molecular structure of reptilian keratin. Int J Biol Macromol 1996;19:207–11.

[16] Available from: http://www.ornithology.com/lectures/Feathers.html.

[17] Postlethwait RW. Tissue reaction to surgical sutures. In: Dumphy JE, Van Winkle W, editors. Repair and regeneration. New York: McGraw-Hill; 1969. p. 263–85.

[18] Freed LE, Grande DA, Emmanual J, Marquis JC, Lingbin Z, Langer R. Joint resurfacing using allograft chondrocytes and synthetic biodegradable polymer scaffolds. J Biomed Mater Res 1994;28:891–9.

[19] Meinel L, Hofmann S, Karageorgiou V, Zichner L, Langer R, Kaplan D, et al. Engineering cartilage-like tissue using human mesenchymal stem cells and silk protein scaffolds. Biotechnol Bioeng 2004;88:379–91.

[20] Available from: http://www.cs.cmu.edu/people/tissue/tutorial.html.

[21] Annamaria S, Maria R, Tullia M, Silvio S, Orio C. The microbial degradation of silk: a laboratory investigation. Int Biodeterior Biodegrad 1998;42:203–11.

[22] Nomura M, Iwasa Y, Araya H. Moisture absorbing and desorbing polyurethane foam and its production. Japan Patent 07-292240A, 1995.

[23] Hatakeyama H. Biodegradable sericin-containing polyurethane and its production. Japan Patent 08-012738A, 1996.

[24] Ishikawa H, Nagura M, Tsuchiya Y. Fine structure and physical properties of blend film compose of silk sericin and poly(vinyl alcohol). Sen'I Gakkaishi 1987;43:283–7.

[25] Nakamura K, Koga Y. Sericin-containing polymeric hydrous gel and method for producing the same. Japan Patent 2001-106794A, 2001.

[26] Park SJ, Lee KY, Ha WS, Park SY. Structural changes and their effect on mechanical properties of silk fibroin/chitosan blends. J Appl Polym Sci 1999;74:2571–5.

[27] Kweon H, Ha HC, Um IC, Park YH. Physical properties of silk fibroin/chitosan blend films. J Appl Polym Sci 2001;80:928–34.

[28] Katori S, Kimura T. Injection moulding of silk fiber reinforced biodegradable composites. In: Brebbia CA, de Wilde WP, editors. High performance structures and composites. Boston: WIT Press; 2002. p. 97–105. Section 2.

[29] Lee SM, Cho D, Park WH, Lee SG, Han SO, Drzal LT. Novel silk/poly (butylenes succinate) biocomposites: the effect of short fiber content on their mechanical and thermal properties. Compos Sci Technol 2005;65:647–57.

[30] Cheung HY, Lau KT, Tao XM. A Potential Material for Tissue Engineering: Silkworm Silk/PLA. Biocompos Comp Pt B: Eng 2008;36(6):1026–33.

[31] Annual Report. Environment Hong Kong 2005. Environmental Protection Department, The Government of the Hong Kong Special Administrative Region. 2005.

[32] Cheng S, Lau KT, Liu T, Zhao YQ, Lam PM, Yin Y. Mechanical and thermal properties of chicken feather fiber/PLA green composites. Compos Part B. 2009;40:650–4.

Mechanism of reinforcement in a nanoclay/polymer composite

Mo-lin Chan [a], Kin-tak Lau [a,b,⇑], Tsun-tat Wong [a], Mei-po Ho [a], David Hui [c]

[a] Department of Mechanical Engineering, The Hong Kong Polytechnic University Kowloon, Hung Hom, Kowloon, Hong Kong, SAR, China
[b] Centre for Excellence in Engineered Fibre Composites, Faculty of Engineering and Surveying, University of Southern Queensland, Toowoomba, Queensland, Australia
[c] Department of Mechanical Engineering, University of New Orleans, New Orleans, LA 70148, USA

article info

abstract

Using organomodified montmorillonite (MMT) (commonly called ''Nanoclay'') to reinforce polymer-based composites have raised much attention to academic and industrial sectors due to the addition of small amount of nanoclay could substantially enhance the mechanical properties of pristine polymers. However, most of the works done previously have neglected to comprehensively study the basic reinforcing mechanism of the composites, particular the interaction between nanoclay and surrounding matrix even though high tensile strength and modulus were obtained. In this paper, uniformly-dispersed nanoclay/epoxy composite samples, based on our tailor-made experiment setup were fabricated. A tensile property test was conducted to examine the mechanical properties of the samples with different nanoclay content. It was found that the Young's modulus and tensile strength of a composite with 5 wt.% of nanoclay increased up to 34% and 25% respectively, as compared with a pristine sample. Images obtained from scanning electron microscopy (SEM) and results extracted from transmission electron microscope (TEM) proved that interlocking and bridging effects did exist in the composites. Nanoclay clusters with the diameter of 10 nm could enhance the mechanical interlocking inside the composites and thus, breaking up the crack propagation. The formation of boundaries between the nanoclay clusters and epoxy can refine the matrix grains and further improve the flexural strength of the composites.

1. Introduction

Using organomodified montmorillonite (MMT) (commonly called ''Nanoclay'') to reinforce polymer-based composites have raised much attention to academic and industrial sectors due to the addition of small amount of nanoclay could substantially enhance the mechanical properties of pristine polymers. However, most of them have neglected to comprehensively study the basic reinforcing mechanism of the composites, particular the interaction between nanoclay and surrounding matrix even though high tensile strength and modulus were obtained. However, without carefully studying any single step in the production process of the composites, some key parameters that may affect their homogeneity due to the existence of surface tension between stirring materials (like stirrers) and mixture of nanoclay and resin, may be ignored [1,2]. Agglomeration of nanoclay, formation of nanoclay clusters and uncured resin may be resulted if large amount of nanoclay are added into the resin. Changing of resin viscosity and controlling of sonication time may also be the keys to produce

desirable composites with moderate strength and ductility. Extra energy imposed into the mixture under sonication may also cause early curing of the resin, which results in brittling resultant composites.

Many attempts have been reported recently on studying the mechanical, morphological and thermal properties of nanoclay/polymer composites by using mechanical stirring and sonication processes [3,4]. However, most of them can only produce evidences extracted from localized regions of samples and it is hard to achieve homogeneity of the samples as in global scale. These methods are;

(i) Mechanical stirring (at 400 rpm) during the stage of mixing nanoclay/polymer at the temperature of 80 oC for 2 h followed by sonication. Continuously, degassed at 120 oC followed by pre-curing at 170 oC for 5 h and post-curing at 200 oC for 2 h;

(ii) Mixing process was performed in an oil bath at the temperature 50 oC and 70 oC followed by sonication for 8–12 h. Hardener is then added afterward;

(iii) Magnetic stirring (with a magnetic bar) followed by high shear mixer and sonication during the stage of mixing nanoclay/resin at room temperature. Continuously stirring after hardener is added and then followed by vacuum curing at the temperature of 75 oC for 3 h;

⇑ Corresponding author at: Department of Mechanical Engineering, The Hong Kong Polytechnic University Kowloon, Hung Hom, Kowloon, Hong Kong, SAR, China. Tel.: +852 2766 7730; fax: +852 2365 4703.
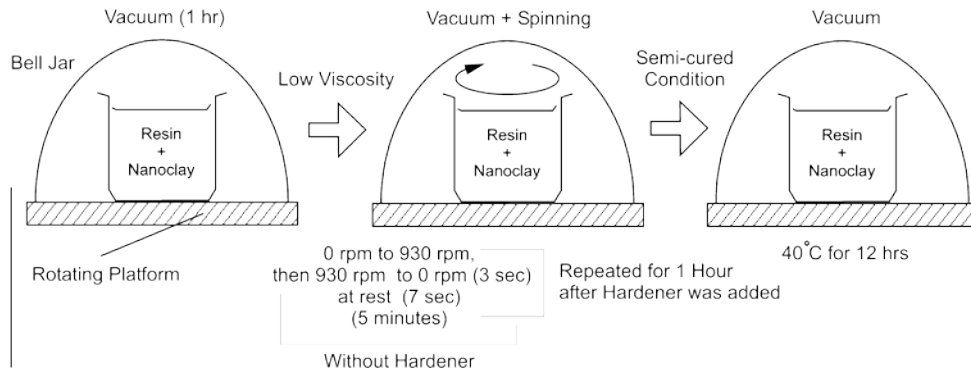E-mail address: Kin-tak.Lau@usq.edu.au (K.-t. Lau).

Fig. 1. Principal of experiment set-up.

(iv) Similar to (i), but the mixing process was controlled at the temperature of 180 oC and 60 rpm to lower down the viscosity [4] and

(v) Similar to (i), but the stirring was at 1500 rpm for an hour and no degassed by pre-curing and post-curing.

Due to the fact that non-uniformly dispersed nanoclay and/or agglomeration of the nanoclay existed inside the composites, large discrepancies of the results were obtained from different tests. Nano-indentation has been appreciated as an excellent tool to exam local properties of nanoclay/polymer composites, however, due to an uneven distribution of nanoclay inside the composites, indented marks being measured after indentation may not provide repeatable readings, which is highly depending on the condition and material properties underneath the indentations. Some works were focused on modeling of nanoclay/polymer composites analytically and computationally, both molecular dynamics (MD) simulations and finite element analysis (FEA). Their results cannot be used directly to explain the physical properties of the composites due to ideal assumptions were used [5,6]. MD can only be used to understand the local bonding properties between the nanoclay (in planar structure scale) and surround matrix molecules. The results cannot be used to further estimate the global properties of the composites. Therefore, a new method should be proposed to produce uniformly-dispersed nanoclay/polymer composites and systematically analyze their mechanical properties at both macro and micro scale levels. The influences due to certain manufacturing parameters such as processing and curing temperatures, stirring type and time, and the curing method should be studied in detail.

This paper is a continuous work of our previous study [7]. A set-up based on the spinning of the mixture of nanoclay and epoxy subject to a controllable curing temperature and pressure environment was used to produce uniformly-dispersed nanoclay/epoxy composite samples with different nanoclay content (see Fig. 1). A tensile property test was then conducted and followed by the investigation on their fracture behavior by using scanning electron microscope (SEM) and transmission electron microscope (TEM).

2. Materials and sample fabrication

Araldite GY251 epoxy resin and hardener HY956 in the ratio of 5:1 were used to produce nanoclay/epoxy composites. Organo-modified nanoclay particles (SiO_2, DK4 series from the Zhejiang FengHong Clay Chemical Co., Ltd. Chain) were then added into the mixture of epoxy resin and hardener to form nanoclay/epoxy composites. All composites with the nanoclay content of 1 wt.%,

3 wt.%, 4 wt.% 5 wt.% and 7 wt.% and four identical samples for each type of composites were made.

In this newly experiment setup, it is comprised of two parts, which are an extracting part and a stirring part. For the extracting part, a pressure pump is connected to a bell jar (Fig. 2a) with a pressure valve and a pressure gauge for controlling and measuring the pressure supply, respectively. The bell jar contains a rotating platform (Fig. 2b), in which the spinning speed can be adjusted by changing the supply voltage. The mixture of nanoclay/epoxy is placed on the platform and spinning at a pre-determined angular speed, x [6].

In the experiment setup, the variable supply voltage is used to provide accelerating and decelerating effects. Centrifugal acceleration and deceleration of the mixture can be calculated by $G_a = x^{2r}$ [7]. Creating the acceleration from zero to maximum velocity on the rotating platform is to ensure that all nanoclay is well mixed together and uniformly-distributed in the through-the-height direction of samples. The effects at acceleration, deceleration and rest conditions will create the movement of the nanoclay to produce uniformly-dispersed samples. The centrifugal acceleration G for nanoclay can be calculated by $G = 9.81 \times 5.5893 \times 10^{-7}(r)^2(D)$, where r is rpm of motor and D is diameter of the container. During the spinning process, the viscosity of the resin increases with time, which ultimately restricts the motion of the nanoclay inside the semi-cured resin. This process can greatly minimize the possibility of sedimentary effect.

However, air bubbles trapped inside nanoclay platelets and between the nanoclay and surrounding matrix may also be another critical factor that may weaken the strength of the composites. During the centrifuging process accompanied with the vacuum environment, all these bubbles will be taken away from the samples. The samples will be remained under vacuum and at spinning condition for 2 h after adding the hardener.

During the process of fabricating the composites, the nanoclay was added into the resin in predetermined weight content. The nanoclay/epoxy resin was placed on a rotating platform and put into a bell jar under vacuum for 55 min to extract gas bubbles. Angular acceleration and deceleration motions were applied through the rotation of the platform from 0 to 930 rpm for 2 s and then returned back to 0 rpm for 1 s. The mixture was then rest for another 7 s. In order to ensure that the nanoclay inside the mixture was uniformly-dispersed, repeated motions by following the previous steps were applied for 5 min. The hardener was then added to the mixture. Spinning of a new mixture was then applied again by using aforementioned procedure for 1 h under vacuum condition till the viscosity increased to avoid any movement of the nanoclay inside the resin. All samples were then removed from the jar. The tensile property test was then conducted after the
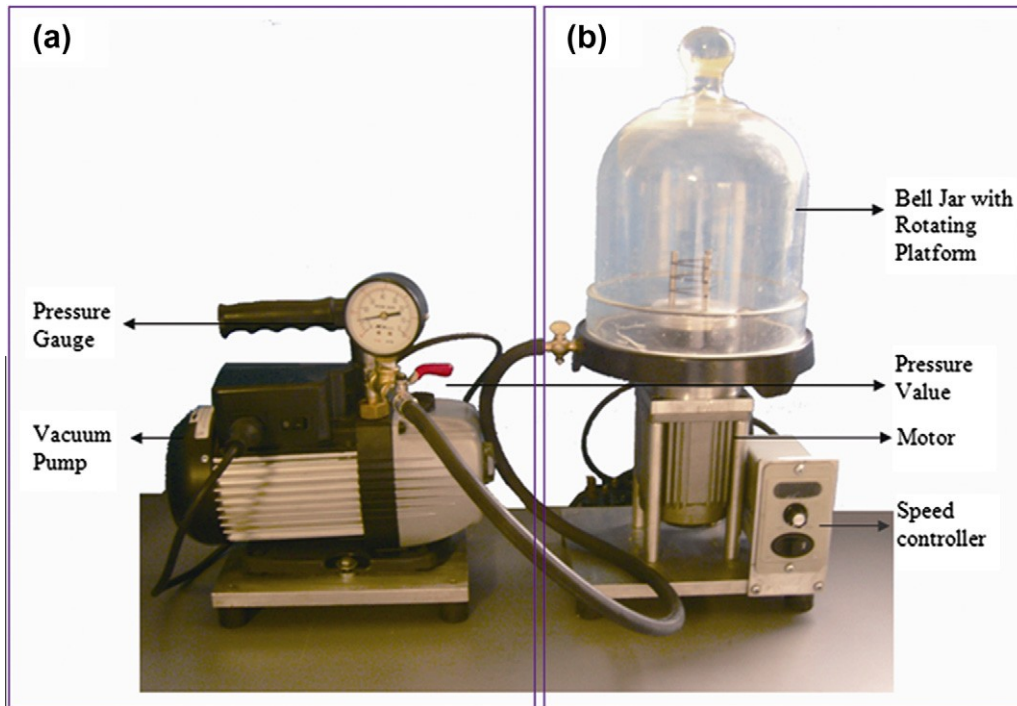
Fig. 2. Experiment set-up.

samples storing inside the chamber for 12 h with the temperature at 40 oC.

3. Experimental results and discussions

3.1. Scanning electron microscope (SEM)

To investigate the homogeneity of the samples with different weight content of nanoclay, the fractographic observation through the use of SEM (Leica Stereo scan 440) was conducted. The SEM was acquired by examining the dispersion condition of nanoclay inside the epoxy matrix.

The samples with 3 wt.% and 4 wt.% of nanoclay are shown in Figs. 3 and 4 respectively, the size of nanoclay clusters were similar with each other. Those particles, indicated by circles, are nanoclay clusters as indicated by EDX. All nano-sized nanoclay clusters (rv<200 nm) were found uniformly dispersed. It proves that the
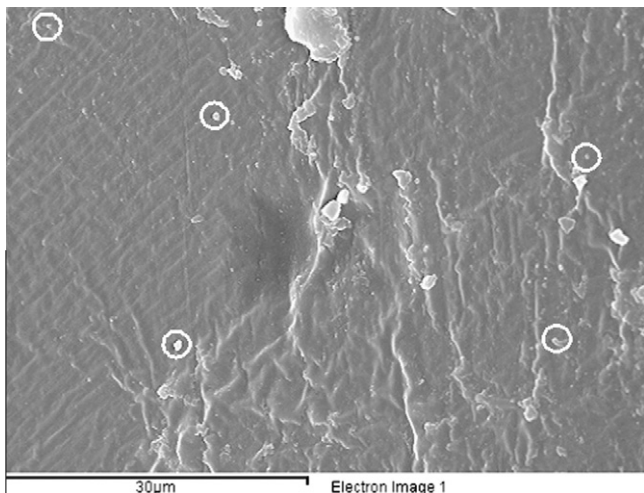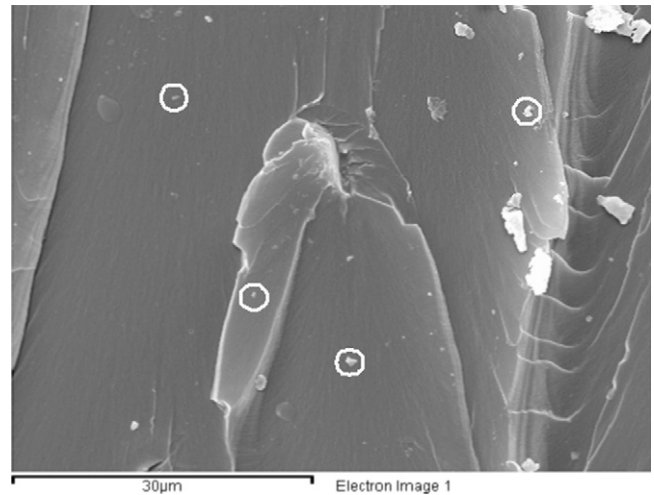

Fig. 4. SEM photograph of the sample 2 (4 wt.% of Manoclay).

fabrication of uniformly-dispersed samples could only be achieved under the following two procedures: (1) Spinning at a condition when the viscosity of resin is low and then (2) mixing the samples when the viscosity of resin start to increase so as the movement of nanoclay is restricted.

During the pouring process of semi-cured nanoclay/epoxy mixture into a dog-bone shape mould for self curing and forming, the viscosity of the composite, at that status, should be high enough to restrict the movement of nanoclay. All samples should be developed in a vacuum environment in order to prevent the formation of air void and moisture.

3.2. Transmission electron microscope (TEM)

TEM can provide direct visualization of the fracture structure morphology. A pristine epoxy and an epoxy with 4 wt.% nanoclay samples are shown in Figs. 5 and 6 respectively, the pattern of
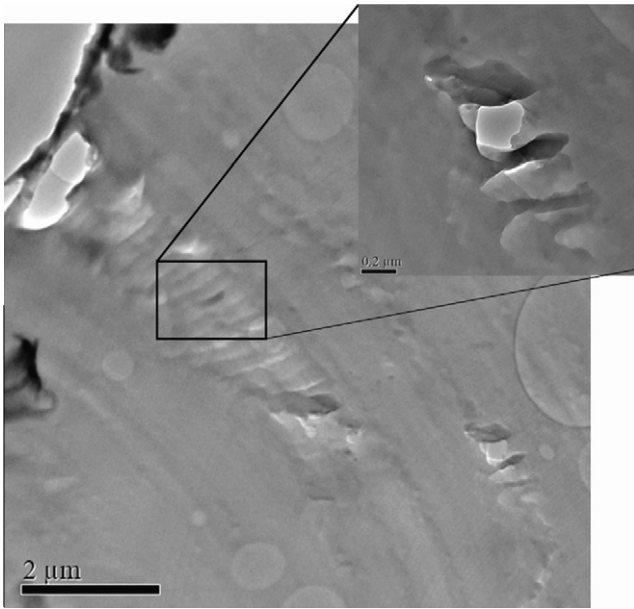

Fig. 3. SEM photograph of the sample 1 (3 wt.% of Manoclay).

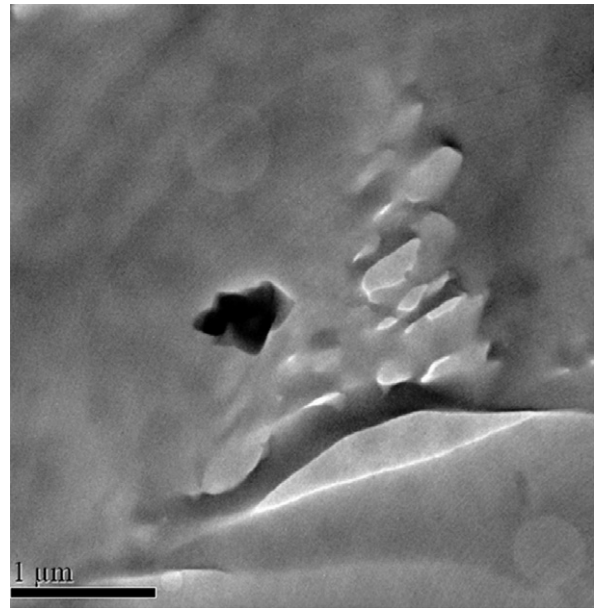Fig. 5. TEM photograph of the sample 3 (pristine epoxy).

Fig. 6. TEM photograph of the sample 2 (4 wt.% of Manoclay).

the cracks along the loading direction of the samples is easily observed. The mode I crack opening was created inside the pristine and 4 wt.% of nanoclay samples. By comparing with these two samples, the pristine sample had more voids that subsequently may form crack easily once it is subject to a tensile load.

For the nanoclay sample, due to the interlocking effect, the addition of the nanoclay can alter the crack formation mechanism. Meanwhile, a bridging effect due to the good bonding between a nanoclay cluster and surrounding matrix could resist the crack, located near the cluster, opening in the sample. The nanoclay clusters can interlock the polymer chains and eventually form strong barriers to stop crack propagation. High residual stress due to the existence of nanoclay clusters inside the micrometer sized polymer matrix grains, would be created at the surface of the nanoclay clusters and polymer matrix interface. According to the Hall–Petch

equation, the formation of the boundaries between the nanoclay clusters and polymer matrix can fine the matrix grains and further improve the flexural strength of nanocomposites. At the same time, this effect causes the nanoclay clusters work as dislocations. Therefore, it results in increasing the fracture energy of the nanocomposites and thus to improve its fracture toughness.

3.2.1. Mechanical properties

As shown in Fig. 7 and Table 1, the increase of Young's Modulus of nanoclay/epoxy samples is dependent on the amount of nanoclay being added. The stiffness of the samples with 3 wt.%, 4 wt.% and 5 wt.% of nanoclay increased by 24%, 31% and 34% respectively.

Table 2 shows that all the nanoclay/epoxy samples achieved higher ultimate tensile strength as compared with the pristine sample. The increase of the strength of the samples with 3 wt.%,
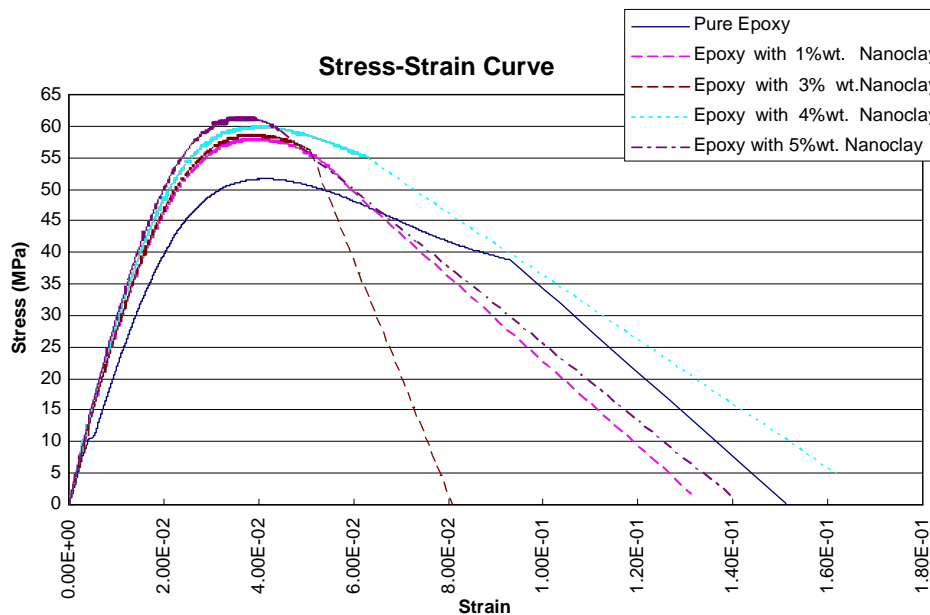

Fig. 7. Stress–Strain curve extracted from tensile test of nanocomposites with different percentage of nanoclay particles.

Table 1
Measured Young's modulus of the samples.

Sample	Young modulus (MPa)	Percentage improvement (%)
Pristine epoxy	2120.30	0
1 wt.% of nanoclay inside epoxy	2474.06	16.68
3 wt.% of nanoclay inside epoxy	2625.09	23.81
4 wt.% of nanoclay inside epoxy	2771.74	30.72
5 wt.% of nanoclay inside epoxy	2841.28	34.00
7 wt.% of nanoclay inside epoxy	3334.00	57.24
9 wt.% of nanoclay inside epoxy	2431.98	14.70

Table 2
Measured ultimate strength of all samples.

Sample	Mean of ultimate strength (MPa)	Percentage improvement (%)
Pristine epoxy	52.4	0
1 wt.% of nanoclay inside epoxy	58.02	10.72
3 wt.% of nanoclay inside epoxy	58.49	11.23
4 wt.% of nanoclay inside epoxy	60.72	15.88
5 wt.% of nanoclay inside epoxy	65.22	24.47
7 wt.% of nanoclay inside epoxy	54.43	3.87
9 wt.% of nanoclay inside epoxy	32.82	−43.43

4 wt.% and 5 wt.% of nanoclay are 12%, 16% and 25% respectively. The results are consistent with our previous studies and the nanoclay provided a mechanical interlocking effect, like micro-pins inside the matrix environment.

4. Conclusion

This paper introduces the use of our newly-proposed experimental set-up to produce homogenous nanoclay/epoxy composites. As in realty, a pure exfoliated nanoclay structure cannot be easily formed by using traditional plastic injection moulding process, our investigation was mainly focused on the nanoclay cluster effect to pristine epoxy. During our test, it was found that the Young modulus and tensile strength of the composites increased with increasing the nanoclay content. The optimal amount of nanoclay should not exceed 5 wt.%. The increases of Young's modulus and tensile strength of a composite sample with 5 wt.% were 28% and 25%, respectively. Further increasing the content of nanoclay would result in decreasing the mechanical properties of resultant composites.

The fracture surface of the sample after the test was then investigated morphologically using SEM and TEM. It was found that the samples with 3 wt.% and 4 wt.% of nanoclay formed nanoclay clusters with uniform size and dispersion. TEM also retrieved that the addition of nanoclay can bridge up the voids to avoid the formation of crack due to the interlocking effect. Nanoclay clusters with the diameter of 10 nm enhanced the mechanical interlocking inside the composites and thus, breaking up the crack propagation. The formation of boundaries between the nanoclay clusters and epoxy can fine the matrix grains and further improve the flexural strength of the composites.

Acknowledgement

References

[1] Dhakal HN, Zhang ZY, Richardson MOW. Nanoindentation behaviour of layered silicate reinforced unsaturated polyester nanocomposites. Polym Test 2006;25:846–52.
[2] Kim BC, Park SW, Lee DG. Fracture toughness of the nano-particle reinforced epoxy composite. Compos Struc 2008;86:69–77.
[3] Subramaniyan AK, Sun CT. Enhancing compressive strength of unidirectional polymeric composites using nanoclay. Composites Part A 2006;37:2257–68.
[4] Iddin MF, Sun CT. Strength of unidirectional glass/epoxy composite with silica nanoparticle-enhanced matrix. Compos Sci Technol 2008;68:1637–43.
[5] Drozdov AD, Christiansen J dec. Cyclic viscoplasticity of high-density polyethylene/montmorillonite clay nanocomposite. Eur Polym J 2007;43:10–25.
[6] Allegra G, Raos G, Vacatello M. Theories and simulations of polymer-based nanocomposites: from chain statistics to reinforcement. Prog Polym Sci 2008;33:683–731.
[7] Chan ML, Lau KT, Ho MP, Cheng A, Wong TT. New equipment and approaches for fabrication of uniformly-dispersed nanoclay cluster/epoxy composites. Polym Polym Compos 2008;16:471–6.